Past, present and future of the nutrients cascade in the Seine, Somme and Scheldt watersheds

Paul Passy

▶ **To cite this version:**

Paul Passy. Past, present and future of the nutrients cascade in the Seine, Somme and Scheldt watersheds. Environment and Society. Université Pierre et Marie Curie - Paris VI, 2012. English. NNT : . tel-00789546

HAL Id: tel-00789546
https://theses.hal.science/tel-00789546

Submitted on 18 Feb 2013

HAL is a multi-disciplinary open access archive for the deposit and dissemination of scientific research documents, whether they are published or not. The documents may come from teaching and research institutions in France or abroad, or from public or private research centers.

L'archive ouverte pluridisciplinaire **HAL**, est destinée au dépôt et à la diffusion de documents scientifiques de niveau recherche, publiés ou non, émanant des établissements d'enseignement et de recherche français ou étrangers, des laboratoires publics ou privés.

UPMC SORBONNE UNIVERSITÉS

THÈSE DE DOCTORAT DE L'UNIVERSITÉ PIERRE ET MARIE CURIE

Spécialité : Biogéochimie spatialisée des hydrosystèmes

École Doctorale 398 Géosciences et Ressources Naturelles

présentée par

Paul Passy

pour obtenir le grade de :

Docteur de l'Université Pierre et Marie Curie

Passé, présent et devenir de la cascade de nutriments dans les bassins de la Seine, de la Somme et de l'Escaut

---

devant le jury composé de :

Mme	Josette Garnier	Co-directrice de thèse
M.	Gilles Billen	Co-directeur de thèse
M.	Damien Cardinal	Examinateur
M.	Patrick Meire	Examinateur
M.	Philippe Cugier	Examinateur
Mme	Chantal Gascuel	Rapporteur
M.	José-Miguel Sanchez-Perez	Rapporteur

(Pour la santé des hydrosystèmes continentaux et marins,) *« il nous faut de l'audace, encore de l'audace, toujours de l'audace »*

Librement inspiré de Danton, 1792

Remerciements

C'est avec une petite appréhension que j'écris cette partie qui sera certainement la plus lue de cette thèse ... Je tiens tout d'abord à remercier Josette Garnier et Gilles Billen pour la confiance qu'ils m'ont accordée il y a trois ans en me confiant ce sujet de thèse. Je pense que vous êtes l'incarnation de l'encadrement idéal aussi bien sur les plans scientifiques que humain. Cependant, votre disponibilité de chaque instant, alors que vous êtes continuellement engagés sur un bon millier de projets différents, me poussent à penser que vous avez un don d'ubiquité qui vous permet de vous retrouver à une bonne douzaine de « Gilles et Josette », sinon je ne vois pas comment vous avez pu être si présents !

Je remercie également l'équipe de Bruxelles, Christiane Lancelot, Nathalie Gypens et Véronique Rousseau pour m'avoir fait participer de façon enthousiaste au programme Timothy. Un grand merci à une autre équipe de « marins », celle de l'Ifremer à qui j'ai fourni mes « sorties » fluviales pour leurs « entrées » marines.

Merci au jury qui a accepté d'évaluer ce travail. Outre mes deux encadrants, je remercie ainsi Chantal Gascuel, Damien Cardinal, Patrick Meire, José-Miguel Sanchez-Perez et Philippe Cugier.

Merci à l'ensemble des participants du programme AWARE avec qui les échanges furent riches et fructueux.

Un immense merci pour les deux meilleures « sigistes » avec qui il est possible de travailler : Marie et Julie. Vos compétences techniques, votre réactivité (et la connaissance de l'Escaut de Julie la wallonne) m'ont plus d'une fois fait gagner plusieurs jours (voire semaines) de travail. C'est extrêmement agréable de travailler avec vous, s'il existe un dieu des SIG, vous êtes ses muses !

Merci à Danièle Valdès Lao de m'avoir permis de participer à l'élaboration et à l'animation de travaux pratiques de SIG. Grâce à toi, la rubrique « enseignements » de mon CV s'en trouve bien étoffée.

Je remercie également l'ensemble des « administratifs » : Nora, Valérie et Dominique. Merci d'avoir toujours répondu à mes interrogations sur les procédures. Merci aussi à Maya, qui vient de quitter Sisyphe. Ta disponibilité et tes compétences vont grandement manquer ! Enfin, merci à Pierre Ribstein de m'avoir accueilli à Sisyphe.

Là où j'ai passé le plus de temps pendant ces trois ans est bien entendu le bureau 410. À mon arrivée il fut très masculin. Vincent, c'est une joie d'avoir passé mes tous premiers mois et mes tous derniers mois de thèse avec toi ! Guillaume Cornichon, le partage de bureau fut très sympathique malgré la quantité phénoménale de bouchons de tubes à essai que tu m'as lancée ainsi que tes ronflements infernaux que j'ai du supportés pendant près de deux semaines de chambre commune. De plus, les deux weekends berlinois, organisés par tes soins, restent inoubliables à de (très) nombreux points de vue ! Alex, bien que tu étais souvent à la plage à l'autre bout du monde, tes conseils et tes avis me furent d'une grande utilité. Je ne t'en veux même pas pour tes nombreux refus lorsque je te proposais un thé en fin d'après midi. Puis le bureau est devenue petit à petit plus féminin avec l'arrivée de Claire puis de Juliette. J'ai troqué des lancers de poubelle contre des odeurs de thé aux jeunes pousses de framboises et vanille. Claire, ta fraîcheur et ta pétillance furent ce qui pouvait m'arriver de mieux pour ma seconde partie de thèse ! Juliette, bien que nous ne partageons pas les mêmes goûts en matière de thé (je suis plus « lardons » que « frisson africain » je reconnais), j'étais très heureux de t'accueillir en 410. La touche non féminine de ce bureau est Wilfried, mais tu n'es jamais là. Tu préfères le cadre forestier de Fontainebleau au cadre « béton et amiante » de Jussieu. Un grand merci à toi pour tous les moments partagés en 410, dans le « tiéquar » ainsi que dans ta patrie orange néerlandaise. Ce petit weekend entre Wageningen et Groninge fut vraiment bon ! Amadou, bien que ton séjour en 410 fut moins long, je te remercie de m'avoir initié au Bambara. Je me souviens également de ton regard triste regardant la neige tomber par la fenêtre !

Cependant, j'étais également souvent à errer dans le couloir et dans les autres bureaux. Notamment dans l'antichambre de Hocine, ce qui m'amène à remercier les doctorants du voyage. Pierre, bien que tu aies tenté de saboter ma thèse à plusieurs reprises en me faisant essayer de mettre des vues 3D dans mes pdf, ou en me vendant ton projet « castors », je te remercie pour ton éternelle bonne humeur. Ma journée commençait bien quand, en arrivant, je te voyais du coin de l'œil assis à ton bureau. Ugo, heureusement que tu es meilleur projectionniste que buveur de mazout ! Ton rire sonore égaille toujours notre couloir. Je suis heureux d'avoir bu un verre de vin avec toi au stand du PC de l'Yonne ! Célestine, tes

moments tricot que tu partages avec les filles du bureau 410 me plaisent toujours. Agnès, les moments fumage à la fenêtre du 410 ont toujours été très agréables. Tu nous manqueras quand tu seras dans tes contrées sauvages outre-Atlantique.

Mes errances me menaient régulièrement en GIS office où, outre Marie et Julie, se trouvait Farès, sans doute le plus grand des cornichons. Farès le mystérieux, qui sous ses aspects cornichonesques et autres cochonneries berlinoises, cache un goût prononcé pour la littérature, la culture et la géopolitique. Je remercie également les voisins du GIS office ; Cyrielle, Sarah et Ppss. Ppss, tes prouesses sur 10 km sont particulièrement bonnes, tu devrais maintenant te confronter à ton chef Nico, que je remercie au passage de m'avoir (longuement) attendu à la fin d'un semi-marathon. Si tu courrais moins vire, tu m'aurais attendu moins longtemps ! Merci également à Aurélien Campoy, Marie Merguez et Chen. Chen, la fin est proche ! Je suis heureux d'avoir partagé ce timing de thèse avec toi.

Ce tour de labo ne serait pas complet, si je ne remerciais pas Aurélien Baro, l'instigateur du thème CFP ! Tu en es arrivé à me faire douter de mon humanité, en m'appelant plus de 237 fois par jour « Poulpe ». Grâce à toi, j'ai un surnom solidement enraciné !

François Moussu, bien que tu sois parti, je te remercie aussi. Notamment pour ce « naked bodies on the couch » ! Bien que mes rapports furent moins intenses, je remercie également Anne, Ludo, Sylvain Clopinette, Camille Contoux et JMM pour son calme à tout épreuve. Merci également à Bruna, Estella et Luis. Luis, je suis très flatté que tu m'appelles à la rescousse dans tes cauchemars.

Merci à mes deux camarades P7 : Sarah et Gabriel. Sarah, merci d'avoir échangé un oreiller avec moi dans les Alpes, d'avoir découvert la gastronomie brésilienne ou afghane du 5$^{\text{ème}}$ et d'avoir su apprécier à sa juste valeur ma coupe de biogéo ! Gabriel, merci pour les après-midis à Ivry avec Horst et pour ton côté rouge post-industriel. Enfin ton déménagement fut la meilleure farce de ces derniers temps.

Guillaume, mon canard, depuis MASS géo on traîne ensemble, à s'échanger le Courrier International ou à partager des carbo devant un programme TV pas toujours top. Tu es maintenant au Togo, mais je ne t'oublie pas. Nico et Yanal, bien que nos contacts soient quelque peu distendus, vous me restez chers. Yanal, je suis fier d'avoir un pote anarcho-rock n'roll comme toi !

Julien, cher Deutéranope, nous nous connaissons depuis la 6$^{\text{ème}}$. Quel beau parcours depuis ces parties de Sim City sur super Nintendo, dans notre beau quartier des Louvrais ainsi que depuis toutes ces séances de ciné à la Pref'. Merci à toi d'avoir été un bon partenaire de tennis et de m'avoir servi de lièvre à la course tous les lundis soirs !

Merci à ma famille de m'avoir soutenu depuis toujours, à tous les moments, dans toutes les circonstances. Fred, Jean, Vasco, merci pour tous ses moments passés à Sagy. Merci Michel, notamment pour m'avoir permis d'animer des formations à Infotique.

Enfin, deux personnes qui ont une place toute spéciale. Ma Lucile, ce que je te dois ne s'écrit pas, ça se vit. Et un immense merci à ma mère, qui est la femme la plus courageuse au monde, qui m'a tout apporté depuis toujours. Avec le recul, je me rends compte que les circonstances ne furent pas toujours faciles, mais je ne m'en suis jamais rendu compte grâce à toi. Tout ce que je suis c'est toi qui l'as fait.

Résumé

Cette thèse s'inscrit dans un projet de science participative financée par l'Union Européenne (AWARE). Le but du projet est de mettre en relation des scientifiques, des citoyens et des gestionnaires afin d'améliorer la qualité des eaux côtières européennes à travers trois cas d'études. Notre cas d'étude est constitué des eaux côtières de la mer du Nord et des trois bassins versants qui les alimentent, la Seine, la Somme et l'Escaut.

Tout au long de ce manuscrit, nous nous attacherons à décrire et comprendre la cascade de nutriments le long du continuum aquatique terre - mer. L'exposé suit une logique amont - aval. Dans un premier temps, nous exposerons la qualité actuelle des hydrosystèmes continentaux et marins au regard de leur évolution passée. Cette reconstitution historique porte sur les trois derniers siècles sur le bassin bien documenté de la Zenne, affluent de l'Escaut traversant Bruxelles et concerne une reconstruction de la qualité de l'eau au cours des s 27 dernières années pour l'ensemble des trois bassins. Dans un deuxième temps, nous explorons le rôle de la topographie et des zones ripariennes sur le cycle de l'azote, d'abord à l'échelle du bassin de l'Orgeval (sous bassin de la Seine), puis à celle de la Seine dans son intégralité. Une troisième partie s'attache à étudier les effets des secteurs stagnants du réseau hydrographique sur les flux d'azote, de phosphore et de silice. Cette étude combine une approche rétrospective, par un travail sur les cartes anciennes, et prospective, par une proposition de scénario de réintroduction d'étangs au sein du chevelu de rivières du bassin de la Seine. Dans un quatrième temps, nous présentons le rôle que jouent les estuaires de l'Escaut et de la Seine sur les flux de nutriments avant leur arrivée en zone côtière. Enfin, une conclusion générale expose les principaux enseignements que nous avons tirés de l'étude de la cascade des nutriments et propose une hiérarchisation de l'efficacité des mesures (préventives ou curatives) qui peuvent être prises pour améliorer la qualité des hydrosystèmes continentaux et marins.

Abstract

This PhD was carried out in the scope of a participative science program (AWARE) granted by the European Union. The aim of this program was to bring together scientists, citizens and stakeholders in order to think about how to improve the quality of European coastal zones, by studying three different cases study. Our case study is focused on the south part of the North Sea and its three contributing watersheds, the Seine, the Somme and the Scheldt basins.

Through this dissertation, we aim to describe and to understand the cascade of nutrients along the land to sea aquatic continuum. The dissertation is organized following an upstream to downstream logic. In a first step, we outline the current quality of the continental and marine hydrosystems according to their past trajectory. This historical reconstruction covers a three centuries period for the well documented basin of the Zenne River, located within the Scheldt watershed. A more precise reconstruction covers the 24 last years for the Seine, Somme and Scheldt basins together. In a second step, we explore the role of the topography and of the riparian zones on the nitrogen cycle. First we explore this role at the scale of the Orgeval basin (sub-basin of the Seine), and then on the whole Seine catchment. In a third step, we explore the role of the stagnant waterbodies of the hydrographic network on the nitrogen, phosphorus and silica fluxes. This survey is composed of a retrospective approach based on the study of old maps, and of a prospective approach by the proposal of scenarios of ponds reintroduction within the hydrographic network. In a fourth step, we present the role played by estuaries of the Scheldt and of the Seine rivers on nutrients fluxes before they discharge into the coastal zone. Finally, a general conclusion summarizes the new knowledge we have gained about the cascade of nutrients. In this part, we also suggest a prioritization of some measures which could be taken in order to improve the quality of the continental and marine ecosystems.

Avant-propos

Cette thèse s'est déroulée au sein de l'UMR Sisyphe d'octobre 2009 à décembre 2012, à l'Université Pierre et Marie Curie, sous la co-directtion de Josette Garnier et de Gilles Billen. Elle a été en grande partie financée par le programme européen AWARE, du 7ème Programme Cadre Européen. Elle a également bénéficié du support scientifique, technique et institutionnel des programmes PIREN-Seine, Nereis, Timothy ainsi que de la FIRE.

Dans la suite de ce manuscrit, afin d'éviter les malentendus entre la *Senne* qui traverse Bruxelles et la *Seine* qui traverse Paris, la première sera toujours nommée par son nom néerlandais *Zenne*.

Enfin, une carte de localisation des trois sous bassins fréquemment étudiés dans cette thèse (*Grand Morin*, *Orgeval* et *Zenne*) se trouve en dernière page.

Table des matières

Introduction : Contexte, problématique, zone d'étude **19**

Contexte **19**
L'eutrophisation des zones côtières européennes . . . 19
Le programme européen AWARE . . . 20
Objectifs . . . 20
Déroulement . . . 21

Problématique : les activités humaines dans la cascade des nutriments **23**
La cascade des nutriments . . . 23
Les fuites de nutriments des activités agricoles . . . 24
Les paysages terrestres et les flux de nutriments . . . 27
Les zones humides ripariennes . . . 28
Les secteurs stagnants du réseau hydrographique . . . 29
Les apports ponctuels urbains et industriels . . . 30
Le filtre estuarien . . . 32
La zone côtière, l'ultime réceptacle . . . 32

Zone d'étude **36**
La mer du Nord et les bassins de la Seine, de la Somme et de l'Escaut . . . 36
Un milieu physique peu contrasté . . . 36
Mais une anthropisation contrastée entre villes et campagnes . . . 38
À la jonction du physique et de l'humain, la qualité de l'eau . . . 39
Méthode : la chaine de modélisation du continuum aquatique terre-mer . . . 40
Le modèle Seneque/Riverstrahler . . . 41
Le modèle MIRO . . . 43
Plan du manuscrit . . . 43

I La situation présente au regard du passé **45**

1 Modelling historical changes in nutrient delivery and water quality of the Zenne river (1790s–2010) : the role of land use, waterscape and urban wastewater management **49**
1.1 Abstract . . . 49
1.2 Introduction . . . 49
1.3 Site description . . . 50
1.4 The modelling approach . . . 51
1.4.1 Geomorphology . . . 52
1.4.2 Hydrology . . . 52
1.5 Exploring the water quality of the Zenne at the end of the 18th and 19th centuries . . . 52
1.5.1 Domestic point sources . . . 55
1.5.2 Industrial point sources . . . 55
1.5.3 Diffuse sources . . . 56
1.5.4 Modelling water quality in the past . . . 58
1.5.5 Nutrient fluxes delivered at the basin outlet . . . 60
1.5.6 Conclusions . . . 60

2 A model reconstruction of riverine nutrient fluxes and eutrophication in the Belgian Coastal Zone since 1984 **61**
2.1 Abstract . . . 61
2.2 Introduction . . . 61
2.3 Study site . . . 63
2.4 Methods . . . 65
2.4.1 The modelling chain, coupling the Seneque/Riverstrahler and MIRO models . . . 65
2.5 Input data to the SR model . . . 66
2.5.1 Point sources . . . 66
2.5.2 Population changes within the 3S basins . . . 67
2.5.3 Improvement of wastewater collection and treatment : the success story of P abatement . . . 67
2.5.4 Diffuse sources . . . 68
2.5.5 Minor land use changes . . . 69
2.5.6 Changes in the N balance of agriculture . . . 69
2.5.7 Diffuse source assessment . . . 71
2.6 Results . . . 72
2.6.1 Validation of the SR model . . . 72
2.6.2 Interannual variations in water quality at the river outlet . . . 73
2.6.3 Water quality in the upstream river network . . . 75
2.6.4 Nutrient fluxes to the coastal zone . . . 76
2.6.5 Effects on the coastal zone . . . 78
2.7 Discussion . . . 80
2.8 Conclusion . . . 81
À retenir sur le passé de la cascade de nutriments . . . 82

II Les zones ripariennes dans le cycle de l'azote **83**

3 Budget of N_2O emissions at the watershed scale : role of land cover and topography (the Orgeval basin, France) **86**
3.1 Abstract . . . 86
3.2 Introduction . . . 86
3.3 Study site . . . 87
3.4 Material and methods . . . 87
3.4.1 Laboratory determination of nitrification, denitrification and nitrous oxide production potentials in batch slurries . . . 87
3.4.2 Soil N_2O flux in situ measurement . . . 88
3.4.3 Digital maps . . . 88
3.4.4 Water sampling . . . 90
3.4.5 Chemical measurement . . . 91
3.4.6 Calculation of indirect emissions by rivers and aquifers . . . 91
3.5 Sources, emissions and transfer of nitrous oxide at the continuum scale . . . 92
3.5.1 Nitrous oxide production by nitrification and denitrification in soils . . . 92
3.5.2 Measured N_2O fluxes in different land-use types . . . 92
3.5.3 Indirect emissions . . . 93
3.6 Orgeval basin scale upscaling of N_2O emissions . . . 94
3.7 Discussion . . . 96
3.7.1 Direct vs. indirect sources of N_2O . . . 96
3.7.2 Catchment nitrous oxide budget . . . 96
3.7.3 Opportunities for nitrous oxide emissions mitigation . . . 97

4 Riparian zones and nitrates elimination **99**
4.1 Introduction . . . 99
4.2 Modeling approach . . . 99
4.3 Exploring various classification of riparian zones with the Seneque/Riverstrahler model : the Grand Morin catchment . . . 100
4.3.1 Test of classification based on land use . . . 100
4.3.2 Test of classification based on the width of the riparian zone . . . 102

4.4 Exploring new classification of riparian zones with the Seneque/Riverstrahler model : the scale of the Seine catchment . . . 102
4.4.1 Test based on the Gaillard's geomorphological classification . . . 102
4.4.2 Test of classification based on homogeneous agricultural areas . . . 103
4.4.3 Test of classification based on the Strahler ordination . . . 104
4.5 Conclusion . . . 105
À retenir sur les zones ripariennes . . . 106

III Le rôle des secteurs stagnants du réseau hydrographique dans les transferts de nutriments 107

5 Restoration of ponds in rural landscapes : modelling the effect on nitrate contamination of surface water (the Seine River Basin, France) 110
5.1 Abstract . . . 110
5.2 Introduction . . . 110
5.3 Study sites and methods . . . 113
5.3.1 The Seine watershed . . . 113
5.3.2 A reference agricultural pond . . . 114
5.3.3 The Seneque/Riverstrahler model and major trends of nutrient fluxes 114
5.4 Results . . . 118
5.4.1 Modelling the agricultural pond case study . . . 118
5.4.2 A census of 18th century ponds in the Seine watershed . . . 119
5.5 Discussion . . . 123
5.6 General conclusion . . . 125

6 Impacts of ponds on nutrients fluxes within the urbanized and industrialized watershed of the Zenne River 126
6.1 Introduction . . . 126
6.2 Hydraulic management in the Zenne : a modeling approach . . . 127
6.3 Hydromorphology . . . 129
6.4 Role of hydromorphology of the drainage network . . . 130
6.5 Conclusion . . . 132
À retenir sur le rôle des étangs . . . 133

IV Le filtre estuarien 134

7 Modelling nutrient transfer along the Scheldt estuary 138
7.1 Modelling phytoplankton succession and nutrient transfer along the Scheldt estuary (Belgium, the Netherlands) . . . 138
7.1.1 The environment of the Scheldt estuary . . . 138
7.1.2 Methods and material available on the Scheldt estuary . . . 139
7.2 Results . . . 142
7.2.1 Discussion . . . 148

8 Modelling nutrient transfer along the Seine estuary 151
8.1 Nutrients transfer through the Seine estuarine zone . . . 151
8.2 Modelling approach . . . 151
8.3 Results . . . 153
8.4 Discussion . . . 154
À retenir sur le filtre estuarien . . . 157

Conclusions générales et perspectives 159

Ce que nous avons appris sur la cascade de nutriments 159

Les scénarios pour le futur co-construits avec les citoyens du programme AWARE 162
Quels scénarios pour la gestion future de la cascade de nutriments ? . . . 162
Sensibilité des leviers d'action . . . 165

Quelques perspectives **167**

Table des figures

1 De gauche à droite : prolifération d'*Ulva armoricana* sur une plage bretonne *(cliché : Thesupermat)*, prolifération de *Phaeocystis* sur une plage de mer du Nord *(cliché : PIREN Seine)*. . . . 19
2 De gauche à droite : interdiction de se baigner lors d'un épisode d'efflorescence d'algues toxiques *(États-Unis, cliché : SEOS)*, poissons morts d'asphyxie échoués sur la plage *(Louisianne, États-Unis, cliché : Thesupermat)*. . 20
3 Les trois schémas d'interactions possibles entre scientifiques, gestionnaires et public. . . . 21
4 Les 30 citoyens du programme AWARE au Jardin des Plantes de Paris en avril 2010, *cliché : Irina Comardicea, Adelphi*. . . . 22
5 La cascade (simplifiée) de nutriments au sein des bassins versants. Seuls sont présentés les transferts de nutriments qui seront étudiés dans cette thèse . . . 24
6 De gauche à droite : Pélican Thage *(cliché : Manuel González)*, Combat naval d'Iquique (guerre de 1879-1884, *Thomas Somerscales, 19ème*) entre Pérou et Chili, et bataille de Callao (guerre hispanno-sud-américaine, *peinture péruvienne anonyme*) entre Espagne et Pérou. . . . 26
7 De gauche à droite : paysage de bocage présentant une mosaïque de forêts et de terres arables traversées par un réseau de haies formant un corridor *(région de Salzbourg, Autriche, cliché : Andrew Bossi)*, paysage d'open-field n'étant qu'une vaste matrice de terres arables *(sud-ouest de l'Angleterre, cliché : Andrew Hill)*. . . . 28
8 De gauche à droite, deux types de zones ripariennes : un cours d'eau bordé d'une ripysylve *(rivière Thredbo, Australie, cliché : Felix Andrews)*, bande enherbée entre des terres arables et la rivière Sturba *(Bosnie-Herzégovine, cliché : Zoran Pravdić)*. . . . 29
9 De gauche à droite : Lac de Pannecière *(cliché : Benchaum)*, lac d'Orient *(cliché : October Ends)*, lac du Der-Chantecoq *(cliché : Klaus Enslin)*. . . . 30
10 De gauche à droite : Vue aérienne de la station d'épuration d'Achères près de la Seine, à 40 km en aval de Paris *(Photo aérienne, IGN 2011)*, bassin d'oxygénation de la station d'Achères favorisant la nitification *(Cliché : SIAAP)*. 31
11 Évolution de la géométrie de l'estuaire de la Seine entre la fin du 18ème siècle et le début du 21ème. . . . 32
12 De gauche à droite : différentes espèces de *Diatomées* au microscope *(corp2365, NOAA Corps Collection)*, efflorescence de *Phaeocystis* à Ambleteuse (Pas-de-Calais) *(Cliché : Lamiot)*, efflorescence de *Diatomées* dans la mer de Barents, Nord de la Norvège *(Image MODIS du 14 août 2011)*. . . . 33
13 De gauche à droite : ICEP-N et ICEP-P calculés pour les bassins européens (état des lieux en 2009). . . . 34
14 Topographie des bassins de la Seine, de la Somme et de l'Escaut. . . . 37
15 a) usage du sol des trois bassins. b) répartition de la population en différence de densité par commune par rapport à la densité moyenne des trois bassins (385 hab.km^{-2}). . . . 39
16 Flux d'azote et de phosphore diffus et ponctuels et de silicium diffus pour l'année 2006 dans le bassin de la Seine. . . . 40
17 Le cycle de l'azote. . . . 41
18 Représentation schématique du modèle RIVE, inspirée de Thouvenot et al. (2007). . . . 42
19 La chaîne de modélisation Seneque/Riverstrahler. . . . 43
20 Postes de la cascade de nutriments traités dans la partie I. . . . 47

1.1 The Hydrographic network of the Zenne river and associated sub-basin units. Main Cities and major stations with observation data used for validation along the Zenne axis are indicated. Dotted line distinguish the major agricultural districts used to differentiate diffuse sources. . . . 51
1.2 Longitudinal variations in 2010, as calculated by the model, of major water quality variables, from Lembeek (km 0) to Heffen (km 56) at the outlet of the river, at four periods in the year (from left to right). From top to bottom discharge ($m^3.sec^{-1}$), oxygen (Oxy), ammonium (NH_4^+-N), total phosphorus (TP), phosphates (PO_4^{3-}-P), and nitrate (NO_3^-N). *Data sources : Vlaamse Milieumaatschappij, Geoloket Waterkwaliteit (http://www.vmm.be/geoview/) and GESZ research project, Impulse Environment initiative from the Brussels Institute for Research and Innovation.* . . . 53
1.3 Longitudinal variations in 2010, as calculated by the model and measured, for variables recently included in the routine survey, silicon, phytoplankton expressed in chlorophyll a concentration, suspended solids, particulate and dissolved organic carbon (POC, DOC). . . . 54
1.4 Distribution of the major sector of industry in 1896 (see text for the data sources and Billen et al. (1999)). . . . 56
1.5 De gauche à droite : carte de Ferraris sur un territoire rural, et sur un territoire urbain (Bruxelles et sa région). Médaillon du Comte Joseph de Ferraris *(Portrait de 1784).* . . . 57
1.6 Extension of the city of Brussels and subsequent changes in land use between Ferraris period and present days (CLC). . . . 58
1.7 Evolution of water quality variable for the periods 1790s and 1890s as calculated by the model. The stations at Lembeek and Eppegem, upstream and downstream Brussels on the main branch are represented. . . . 59

2.1 The Seine, Somme and Scheldt watersheds and the main currents in the English Channel and the North Sea. . . . 64
2.2 Discharges at the outlet of the Seine (Poses), the Somme (Abbeville) and the Scheldt (Doel) rivers for 1984–2007 (no data available for the year 1987 on the Scheldt). Red dots are measurements and blue lines are the SR Model simulations. . . . 65
2.3 Reconstruction of the total N (a) and P (b) loading from domestic wastewater facilities into the Seine and Scheldt drainage network. Data were communicated by Water Agencies from 1999 to 2007 for the Seine and for 2006 and 2007 for the Scheldt, but estimated from information on the population, sewer connection data and WWTP implementation dates for earlier periods. . . . 68
2.4 Agricultural areas within the Seine, Somme and Scheldt watersheds as taken into account in the modelling approach for determination of diffuse sources, together with surplus (see text for explanation). . . . 69
2.5 (a) Historical changes in livestock density (expressed as LU/ha of cultivated area) in the main agricultural regions of the Seine and Scheldt basin during from 1950 to today (LU, livestock unit, represents the amount of livestock equivalent to a modern milking cow, and excreting 85 $kgN.yr^{-1}$). (b) Historical changes in the rate of synthetic nitrogen fertiliser application (expressed as $kgN.ha^{-1}$ of cultivated area and per year) in the main agricultural regions of the Seine and Scheldt basins from 1950 to the present. Sources : National Institute of Statistics (INS) data by agricultural region for Belgium ; Agreste for France, data for one or two departments are used as representative for the whole agricultural area to which they belong. . . . 70
2.6 N crop export vs. total N fertilisation of arable land in the different agricultural areas of the Seine, Somme and Scheldt basins from 1950 to 2005. A fitted curve with equation $Nexport = Ymax \times (1 - \exp(\frac{-fertilisation}{Ymax})$ is also indicated for each data set. . . . 71
2.7 Nitrate concentration in the major aquifers of the Seine, Somme and Scheldt basins (Curie et al., 2011). . . . 72
2.8 Simulation of NO_3^-, NH_4^+, total P, Si, phytoplankton compared to observations at Poses for 1984–2007. . . . 73

2.9 Simulation of NO_3^-, NH_4^+, total P, Si, phytoplankton (compared to observations at Kruibeke and Temse for 1984–2007 (No hydrological constraints available for the year 2007). 74
2.10 P-PO_4^{3-} annual average concentrations within hydrological networks in 1985 (a) and 2007 (b), N-NO_3^- annual average concentrations within hydrological networks in 1985 (c) and 2007 (d) and with 25 % (e) and by 50 % (f) surplus decreases. 76
2.11 SR- simulated N, Si and P annual specific fluxes delivered to the sea at Poses (a,c) and Kruibeke for 1984–2007 (b,d) (no hydrological constraints available for the Scheldt River in 1987). 77
2.12 Abundance of *Phaeocystis* over the 1984–2007 period and for the two scenarios explored in the BCZ in 10^6 cells.l^{-1} (a) ; duration of the *Phaeocystis* blooms for the period studied and for the two scenarios explored, in days (b) and production of *Phaeocystis* expressed in potential biomass in mgC.m^{-3}.yr^{-1} as a function of excess P input over silicon (c). The red line represents the threshold of cells of *Phaeocystis* corresponding to a healthy marine ecosystem (Lancelot et al., 2009). 79
2.13 Poste de la cascade de nutriments traité dans la partie II. 85

3.1 Land use in the Orgeval basin in terms of forest, grassland and cropland. Urban areas are shaded grey. The drainage network is also indicated. 89
3.2 Topographical map of the Orgeval basin. 90
3.3 Nitrous oxide concentrations between January 2007 and December 2008 in rivers at : Mélarchez, first order (a) ; Avenelles, second order (b) and Theil, third order(c). 90
3.4 Results of batch slurries : (a) potential rates of nitrate reduction by denitrification and production by nitrification ; (b) potential N_2O production and (c) ratio of N_2O production to nitrate reduced (denitrification) or produced (nitrification). 93
3.5 Distribution of the daily N_2O emissions of the Orgeval drainage network, as a function of stream order for a winter and a summer period. 94
3.6 Estimation of nitrous oxide emissions as a function of the land cover database and the topography. 95
3.7 Comparison of direct and indirect N_2O emissions at the Orgeval basin scale, based on the « Topo index × (MOS + ECO-MOS) » estimation. 96

4.1 Theoretical maximal extent of riparian zones within the Grand Morin basin. . 100
4.2 Land use within the theoretical riparian zones. 101
4.3 NASH characterizing the goodness of fit of the model for different values of the N riparian transfers rates affected to riparian areas according to their land use,(for arable land (a), forest (b) and grassland (c). 101
4.4 NASH of results of variations of N riparian transfers according the width of the riparian zone, below 100 m (a), from 100 to 300 m (b) and up to 300 m (c).102
4.5 NASH of the results of variations of N riparian transfers according to the geomorphological classification established by Gaillard (2001), for the following classes : Incised in an inorganic substrate (a), Superimposed on an inorganic substrate (b) and Incised in the substratum (c). 103
4.6 Biases of the results of variations of N riparian transfers according homogeneous agricultural area, Brie-Beauce (a), chalky Champagne (b), Yonne depression (c), rich loam (d), Jurassic plateau (e). 104
4.7 Biases of the results of the variations of N riparian transfers according to the Strahler ordination, riparian zones located on order 1 rivers (a), order 2 rivers (b) and order 3 rivers (c). 105
4.8 Postes de la cascade de nutriments traités dans la partie III. 109

5.1 De gauche à droite : César-François Cassini *(Miniature sur ivoire de Jean-Marc Nattier, vers 1750)*, Jean-Dominique Cassini *(Gravure de Conrad Westermayr, 1801)*. 112
5.2 Paris et le bassin de l'Orgeval tels que figurés sur la carte de Cassini. 112
5.3 Location of the Seine basin – Population density, land use, lithology. 113

5.4 Location of the agricultural pond studied within the Orgeval basin in the Brie region, 60 km east of Paris. . . . 115
5.5 Validation of the simulations for the reference years 2003–2006 at the Poses and the Saint Maurice stations for NO_3^- , total phosphorous and dissolved silicon. . . . 116
5.6 Validation of the Seneque/Riverstrahler model applied to the reference agricultural pond for the years 2007–2010. Solid lines are the results of simulation for outflow concentrations of nitrate, total phosphorus and silica. Red dashed lines are the inflows concentrations (measured for NO_3^- and modelled for P and Si). Blue dot line is the discharge. . . . 118
5.7 De gauche à droite : étang agricole artificiel actuel *(Creuse, cliché Paul Passy)*, scène de pêche à la senne sur une gravure ancienne. . . . 120
5.8 Distribution of the 18th century ponds within the Seine watershed, digitised from the Cassini map. . . . 121
5.9 Restoration of ponds within the Seine watershed according to lithology, homogeneous agricultural areas and the historical distribution of ponds. . . . 122
5.10 Comparison of the reference situation with the « Cassini » and « Cassini plus » scenarios at the outlet of the Seine and the Grand Morin sub-basin for the hydrological years 2003–2006. . . . 122
5.11 a) Seasonal variation of nitrate concentration according to the proportion of ponds (in %) within the watershed at the outlet of the Orgeval sub-basin for the hydrological year 2006. b) Annual N flux at the outlet of the Orgeval watershed as a function of the percent watershed area covered by ponds. Calculations are for the hydrological year 2006 (blue bars). The corresponding reduction is also shown (red line). . . . 123

6.1 De gauche à droite : la Zenne à Bruxelles à la fin du 19ème siècle, la Bièvre à Paris au niveau de la manufacture des Gobelins dans l'actuel 13ème arrondissement à la fin du 19ème siècle *(cliché : Charles Marville)*. . . . 127
6.2 The Ferraris map of the Zenne basin, as presented in the Atlas, where the drainage network as considered in the modellling approach is highlighted (left). Distribution of ponds digitalized from the Ferraris map. . . . 128
6.3 Seasonal variation of water quality variable as calculated by the model for the 1890's with and without the ponds (ZOO : zooplankton ; PHY : phytoplankton ; Si : silicon ; PO_4^{3-} : phosphates ; NO_3^- : nitrate). The station at Eppegem downstream Brussels on the main branch is represented. The year 2010 is shown in comparison. . . . 131
6.4 Les postes de la cascade de nutriments traités dans la partie IV. . . . 137

7.1 River network of the 1D RIVE-MIRO model. Km 0 and km 160 are giving the limit of the model domain. . . . 139
7.2 Longitudinal evolution of RIVE-MIRO simulated (solid line) and measured (dots) annual mean of DIN (a), DSi (b), PO_4^{3-} (c) and O_2 (d) along the Scheldt estuary in 2006. The arrows correspond to the localization of the input from lateral tributaries (respectively from the Dender, the Durme and the Rupel from upstream to downstream). Dashed line is the standard deviation of simulated results. . . . 141
7.3 Longitudinal evolution of RIVE-MIRO simulated (solid line) and measured (dots) annual mean of Chl a (a) and freshwater diatoms (b) along the Scheldt estuary in 2006. The arrows correspond to the localization of the input from lateral tributaries (respectively from the Dender, the Durme and the Rupel from upstream to downstream). Dashed line is the standard deviation of simulated results. . . . 142
7.4 Seasonal evolution of RIVE-MIRO simulated (solid line) and measured (dot) DIN, DSi, PO_4^{3-} , O_2 and Chl a concentration at km 150, 120, 78, 64, 36 and 20 of the estuary in 2006. . . . 143
7.5 Seasonal evolution of RIVE-MIRO simulated (solid line) and measured (dot) freshwater diatoms concentration at km 138, 120, 98 and 78 of the estuary in 2006. . . . 146

7.6 Spatio-temporal evolution of marine (diatoms (a) and *Phaeocystis* colonies (c)) and freshwater (diatoms (b) and *Chlorophyceae* (d)) phytoplankton simulated in the Scheldt estuary by the 1D-RIVE-MIRO model in 2006. . . . 147
7.7 Spatio-temporal evolution of marine microzooplankton (a), mesozooplankton (c) and bacteria (e) and freshwater rotifers (b), mesozooplankton (d) and bacteria (f) simulated in the Scheldt estuary by the 1D-RIVE-MIRO model in 2006. . . . 148

8.1 Description du modèle simplifié LIFT de la zone de turbidité maximum de l'estuaire de la Seine. . . . 152
8.2 Interannual variations, in yearly average, of total nitrogen, silicon, phosphorus and organic carbon fluxes entering the Seine saline estuary (Caudebec, in) and leaving the estuary Calculated values by the models (Riverstrahler –in- and LIFT –out-). The difference indicate the retention by the turbidity maximum zone of the Seine estuary. . . . 153
8.4 Relationships between the percentages of total nitrogen, phosphorus and carbon retention and the associated discharges. Average summer values (May to September) for the 24 years. . . . 154
8.3 Seasonal variations for two dry years (1989 and 2005) and one wet year (2001) of total nitrogen (TN), silicon (TSi), phosphorus (TP) and organic carbon (TOC) fluxes entering the Seine saline estuary (Caudebec, in) and leaving the estuary. Calculations by the models (Riverstrahler –in- and LIFT –out-). The difference indicates the retention by the turbidity maximum zone of the Seine estuary. . . . 155
8.5 Comparaison des concentrations en nitrates au sein du réseau hydrographique des 3S pour l'année 2006 et pour un scénario de mise en application de la « DERU » qui devrait être achevée en 2015. L'évolution des *Diatomées* et des *Phaeocystis* est indiquée ainsi que la durée et l'intensité des efflorescences. . . . 163
8.6 Comparaison des concentrations en nitrates au sein du réseau hydrographique des 3S pour le scénario « DERU » (à gauche) et le scénario « Grenelle » (à droite). L'évolution des *Diatomées* et des *Phaeocystis* est indiquée ainsi que la durée et l'intensité des efflorescences. . . . 164
8.7 Comparaison des concentrations en nitrates au sein du réseau hydrographique des 3S pour le scénario « DERU » (à gauche) et le scénario « tout bio » (à droite). L'évolution des *Diatomées* et des *Phaeocystis* est indiquée ainsi que la durée et l'intensité des efflorescences. . . . 165
8.8 Localisation des bassins du Grand Morin, de l'Orgeval et de la Zenne au sein des « 3S ». . . . 192

Liste des tableaux

1.1 Fluxes (Flx) of total nitrogen (N), total phosphorus (P) and silicon (Si) as calculated by the model at the outlet of the Zenne River. ICEP-N and ICEP-P, indicator of potential eutrophication, represent a risk of promoting undesirable algae when positive (e.g. N, P in large excess to silicon). 60

2.1 Main characteristics of the Seine, Somme and Scheldt watersheds. 64
2.2 RMSE, bias and Bravais-Pearson R for the SR Model simulations at Poses, Kruibeke and Temse (** significance between 0.001 and 0.01, * significance between 0.02 and 0.1). 73
2.3 Calculated fluxes ($kg.km^{-2}.yr^{-1}$) of nutrients at the outlet of the Seine, Somme and Scheldt rivers in 1985, 2007 and using the 2007 point and diffuse sources with the hydrology of 1985. 78

3.1 Nitrous oxide fluxes at the water–air interface for the summer and the winter period for different stream orders of the Orgeval basin. 92
3.2 Nitrous oxide emission for the types of land use associated with their respective surface area in the basin and calculations from coefficients including topographic segmentation. 93
3.3 N_2O emission estimations for the Orgeval basin by main land use type and calculated by each upscaling method (in kgN_2O -N yr^{-1}). CLC : Corine Land Cover ; MOS : Mode d'Occupation des Sols ; ECOMOS : land use classification produced by the IAU IDF. 95
3.4 Contribution of the three topographic classes to the total N_2O flux, given for the two upscaling methods based on topography and land use (in kgN_2O -N yr^{-1}). 95

4.1 Land use within theoretical riparian zones (km^2 and %). 101

5.1 Some literature data on N retention in lakes, ponds and reservoirs. (% N retention), and fate of the « retained » N (respective role of denitrification, sediment storage and macrophytes or periphyton uptake in N retention). . . . 111
5.2 N sensitivity test of the model for the sedimentation rate, the benthic remineralisation rate and the N transfer rate of riparian zone. Values are mean annual NO_3^- concentration ($mgN.l^{-1}$) at Poses for the hydrological year 2006. 117
5.3 Fluxes (in $kg.yr^{-1}$) of nitrogen, phosphorus and silicon through the pond as calculated by the model for the 2007 – 2008 and 2009 years. 119

6.1 Changes in the pond surface area (ha) in the various sub-basins of the Zenne river. Ferraris : map of the cabinet (carte de cabinet) 1 :1152, supervised by the Comte de Ferraris 1771-1778 ; DLG : dépôt de la Guerre map 1 :20,000 realized from1865 to 1878 but finished from 1878 to 1880 by the Institut Cartographique Militaire ; present is shown for comparison : map from the pan-european urban atlas, giving information on the urban land use for conurbation > 100 000 inhab, here that for Brussels covers 67 % of the whole Zenne basin (see figure 1.1 for location of sub-basins). 129

7.1 Coefficient of determination (R^2) and the percent bias (Pbias) computed between annual model results and data available at each validation stations along the Scheldt estuary. All of the correlations are significant at the 95 % confidence level. 141

7.2 Coefficient of determination (R^2) and the percent bias (Pbias) computed between daily model results and data available at each validation stations along the Scheldt estuary. All of the correlations are significant at the 95 % confidence level. 142

Liste des encarts

La géopolitique de la déjection du pélican péruvien, *page 26*
Écrêtage et étiage sont les adages des barrages, *page 30*
La carte de Ferraris, du militaire au scientifique, *page 57*
Dans la famille des Directives Européennes, je voudrais . . . , *page 63*
La carte de Cassini, première vision globale de la France, *page 112*
Mais pourquoi tant d'étangs ?, *page 120*
La Zenne et la bièvre, le malheur des rivières urbaines, *page 127*
Le modèle LIFT, un outil simplifié pour la modélisation des transformations biogéochimiques dans les bouchons vaseux estuariens, *page 152*

Introduction : Contexte, problématique, zone d'étude

Contexte

L'eutrophisation des zones côtières européennes

De nombreuses zones côtières d'Union Européenne sont affectées par des efflorescences algales indésirables. Plusieurs types d'algues ont tendance à proliférer à certains mois de l'année le long de certaines côtes. Le type le plus fameux en France est celui communément appelé « algues vertes », regroupant en fait plusieurs espèces d'Ulves. Sur la façade occidentale, il s'agit essentiellement d'*Ulva armoricana* (figure 1) et d'*Ulva rotundata* (Ménesguen, 2003), alors qu'en Méditerranée, c'est *Ulva rigida* qui pose problème. En mer du Nord, ce sont plutôt des algues mucilagineuses comme *Phaeocystis* qui se développent (Lancelot, 1995; Gypens et al., 2007). À la mort de ces colonies algales, bactéries et microbes prolifèrent sur cette matière organique et consomment une grande part de l'oxygène de la colonne d'eau. L'environnement devient ainsi hypoxique voire anoxique dans les cas les plus graves, ce qui entraîne l'asphyxie des poissons et des coquillages.

FIGURE 1 – De gauche à droite : prolifération d'*Ulva armoricana* sur une plage bretonne *(cliché : Thesupermat)*, prolifération de *Phaeocystis* sur une plage de mer du Nord *(cliché : PIREN Seine)*.

Ce phénomène se retrouve le long de très nombreuses côtes dans le monde, principalement le long des pays très urbanisés et/ou dont l'agriculture est intensive. En Europe, hormis la mer du Nord, ces efflorescences se retrouvent en mer Baltique (Howarth and Marino, 2006; Muller-Karulis and Aigars, 2011), en mer Méditerranée (Casabianca et al., 2012; Uitz et al., 2012), en mer Noire (Taylor and Longo, 2010) ou mer Adriatique (Penna et al., 2004; Cozzi and Giani, 2011). Hors d'Europe, le golfe du Mexique (Diaz and Rosenberg, 2008; Rabalais et al., 2010) est une zone particulièrement touchée depuis de nombreuses années. Des « zones mortes » apparaissent régulièrement détériorant les écosystèmes marins et mettant à mal les activités piscicoles. Ce phénomène prend également une ampleur dangereuse au large des pays émergents, notamment au large de la Chine. Les baies de Shangaï ou de Hong-Kong sont particulièrement touchées (Zhu et al., 2011; Shen et al., 2012). Les marées vertes qui s'y produisent posent de plus en plus de problèmes aux activités économiques et aux pouvoirs politiques locaux (Zewei, 2007).

Ces efflorescences algales ont donc un coût important en termes environnemental et économique. En effet, une plage recouverte d'algues en décomposition a tendance à faire fuir le touriste par son aspect inesthétique et les odeurs d'« œuf pourri », dues aux émissions de sulfure d'hydrogène, qui s'en dégagent (Dayssiols, 2009). Dans certains cas d'efflorescences d'algues toxiques, les plages sont mêmes fermées au public (Delattre, 2011) (figure 2 a). Les pouvoirs publics s'efforcent alors de nettoyer ces plages à grand renfort de bulldozers,

tractopelles et camions bennes. Ce qui non seulement coûte très cher, mais est également très destructeur pour la plage et les dunes attenantes. Enfin, lors des épisodes de forte anoxie ou d'hypoxie, les activités de pêche doivent s'arrêter suite à la sur-mortalité des poissons (figure 2 b).

FIGURE 2 – De gauche à droite : interdiction de se baigner lors d'un épisode d'efflorescence d'algues toxiques *(États-Unis, cliché : SEOS)*, poissons morts d'asphyxie échoués sur la plage *(Louisianne, États-Unis, cliché : Thesupermat)*.

Le programme européen AWARE

Objectifs

Le projet AWARE (http://www.aware-eu.net/) est financé par l'Union Européenne et son 7ème Programme-Cadre (Sessa, 2012b). Il se focalise sur la détérioration des écosystèmes marins côtiers. Trois zones côtières européennes ont été étudiées parallèlement : (1) le golfe de Riga (Estonie, Lettonie), (2) le delta du Po et la lagune de Sacca di Goro (Italie) et (3) la partie méridionale de la mer du Nord (Belgique, France). Le golfe de Riga (Stålnacke et al., 2009; Bryhn et al., 2012) tout comme la mer du Nord (Garnier et al., 2009a, 2012) sont fortement pollués et eutrophisés, tandis que le problème de Sacca di Goro concerne plutôt l'élevage intensif de palourdes (Giordani et al., 2009; Viaroli et al., 2012).

Ces trois régions ont été récemment ciblées par plusieurs directives européennes. La Directive Européenne sur les Eaux Résiduaires Urbaines (européen, 1991a), la Directive Nitrate (européen, 1991b), la Directive Cadre sur l'Eau (européen, 2000) et la Directive Marine (européen, 2008) réglementent divers aspects de la gestion des eaux et s'appliquent au cas particulier de ces trois cas d'étude. L'objectif du programme AWARE, pour chaque cas d'étude est d'explorer (Stålnacke et al., 2012) :

1. comment les connaissances scientifiques sont utilisées par les politiques et les gestionnaires ?
2. comment les politiques interagissent avec les citoyens et la société civile ?

Répondre à ces questions permet de définir quel est le schéma (parmi les trois suivants, figure 3) utilisé pour la gestion des zones côtières.

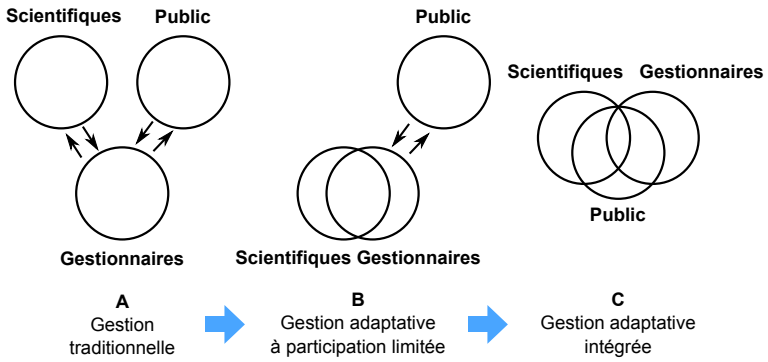

FIGURE 3 – Les trois schémas d'interactions possibles entre scientifiques, gestionnaires et public.

La **gestion traditionnelle** est une approche caractérisée par une distinction nette entre les scientifiques, les gestionnaires et le public. Dans ce modèle, à l'amont, les gestionnaires utilisent les connaissances scientifiques et communiquent les décisions politiques résultantes au public. Il n'y a aucune interaction entre scientifiques et public dans la formulation des problèmes. Dans la **gestion adaptative à participation limitée**, les scientifiques et les gestionnaires travaillent en étroite collaboration, mais le public reste à la fin du processus et se contente de recevoir les informations. Il n'intervient à aucun moment dans la prise de décisions plus à l'amont. La **gestion adaptative intégrée** est le stade le plus avancé en matière d'interaction entre les trois acteurs. Dans ce modèle, les trois groupes interagissent tout au long du processus.

Le programme AWARE est basé sur l'hypothèse que le troisième modèle de gestion adaptative intégrée est le plus abouti en termes de démocratie et de prises de décisions (Sessa, 2012a). Le projet mène donc trois expériences pilotes de gestion intégrée des zones côtières, en vue d'étudier la pertinence et la faisabilité de cette approche à l'échelle de l'Union Européenne.

Déroulement

Dans chaque cas d'étude, le processus a rassemblé des scientifiques, des gestionnaires et 10 citoyens (figure 4). Dans le cas de la mer du Nord, les partenaires scientifiques étaient Sisyphe (http://www.sisyphe.upmc.fr/) de l'Université Pierre et Marie Curie située à Paris et le laboratoire d'Écologie des Systèmes Aquatiques (http://www.ulb.ac.be) de l'Université Libre de Bruxelles, épaulés, pour l'aspect interaction avec les gestionnaires et les citoyens, par le bureau d'études Missions Publiques (http://www.missionspubliques.com/), spécialisé dans l'animation d'ateliers citoyens. Les 10 citoyens participants ont été tirés au sort parmi ceux qui avaient pris connaissance du projet (par voie d'affichage, petites annonces, listes de diffusion ...) et y avaient posé leur candidature. Ces citoyens ne devaient pas avoir d'expériences particulières dans le domaine de l'environnement mais devaient être suffisamment à l'aise en anglais pour prendre part activement aux conférences et aux ateliers (Gleize and Mathieu, 2012).

FIGURE 4 – Les 30 citoyens du programme AWARE au Jardin des Plantes de Paris en avril 2010, *cliché : Irina Comardicea, Adelphi.*

Une première conférence regroupant les citoyens des trois cas d'étude s'est tenue à Paris en avril 2010. À cette occasion, les scientifiques leur ont apporté les connaissances requises concernant les problèmes auxquels sont confrontées les zones côtières. Notamment, le processus menant à l'eutrophisation des eaux côtières et aux efflorescences algales a été expliqué. Ainsi, après cette conférence, les citoyens disposaient des connaissances scientifiques nécessaires pour la suite du projet.

En septembre 2010 s'est tenu dans chaque cas d'étude un atelier local. Dans le cas de la mer du Nord, cet atelier a eu lieu à Bruxelles. Lors de cet événement, les citoyens ont pu interroger et découvrir le point de vue de différents acteurs socio-économiques concernés par la gestion des eaux côtières. Sont intervenus, entre autres, le responsable de l'office de tourisme de Wimereux (station balnéaire du littoral de la Manche), un marin-pêcheur, un cadre de Veolia responsable d'une des stations d'épuration des eaux usées de Bruxelles, le directeur du Service Agriculture de l'Agence de l'Eau Seine Normandie, un élu de la Région Île-de-France chargé des Programmes de Recherche au Conseil Régional.

En janvier 2011, chaque cas d'étude a organisé une conférence locale au cours de laquelle les citoyens ont présenté leurs recommandations aux acteurs locaux. Dans notre cas (mer du Nord), la conférence a été organisée à Dunkerque. Les citoyens, épaulés par les scientifiques, ont ainsi pu présenter leurs recommandations à des représentants des agences de l'eau et des comités de bassin ainsi qu'à toute personne intéressée (riverains, associations, collectivités ...). Une centaine de personnes étaient présentes ainsi que la presse locale (Dufourg, 2011).

Enfin, en juin 2011, les 30 citoyens ont été accueillis au Conseil Économique et Social de la Commission Européenne à Bruxelles pour faire part de leur évaluation du programme et pour présenter leurs recommandations au niveau européen.

Problématique : les activités humaines dans la cascade des nutriments

L'eutrophisation côtière est le plus souvent la conséquence d'apports fluviaux déséquilibrés de nutriments. La charge des fleuves en nutriments résulte des apports diffus et ponctuels dans l'ensemble du bassin versant des fleuves, ainsi que des modifications qu'ils subissent tout au long du continuum aquatique.

La cascade des nutriments

On désigne par cascade des nutriments l'ensemble des transferts et des transformations subies par les nutriments depuis leur introduction sous forme réactive dans la biosphère terrestre jusqu'à leur dissipation finale dans l'atmosphère ou l'océan.

Les activités humaines influencent la totalité de la cascade des nutriments au sein des bassins versants (Billen et al., 2011a; Baron et al., 2012). Elles sont responsables des principaux apports d'azote, de phosphore et dans une moindre mesure de silicium (N, P, Si) (Billen et al., 1998) vers le continuum aquatique. Les fuites de nutriments d'origine agricole (Schott et al., 2009; Di and Cameron, 2002) et les apports ponctuels domestiques et industriels tendent à largement enrichir le milieu en nutriments. Mais certaines activités humaines conduisent aussi à réduire ces flux, comme la restauration et la création de zones humides riveraines ou de bandes enherbées, ou la création de barrages, de retenues ou d'étangs (Mitsch et al., 2005a; Howardwilliams, 1985; Palone and Todd, 1998; Hernandez and Mitsch, 2007). En aval de la cascade, les estuaires peuvent être considérés comme un dernier filtre réduisant les concentrations des sels nutritifs avant leur arrivée en zone côtière, ultime réceptacle et parfait reflet des activités humaines et de leur gestion au sein des bassins versants qui les alimentent. La figure 5 schématise le concept de cascade des nutriments (Billen et al., 2011a).

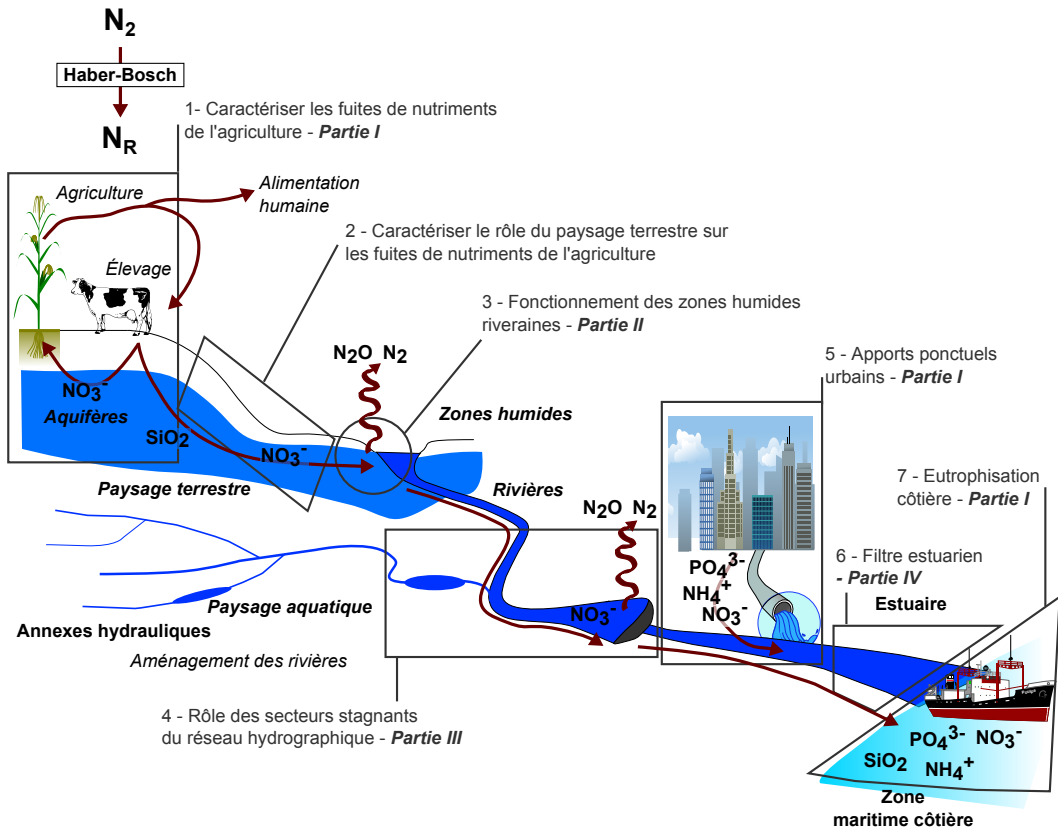

FIGURE 5 – La cascade (simplifiée) de nutriments au sein des bassins versants. Seuls sont présentés les transferts de nutriments qui seront étudiés dans cette thèse

La cascade de nutriments est fortement influencée par le caractère autotrophe ou hétérotrophe du territoire (Billen et al., 2009c). Le concept d'autotrophie et d'hétérotrophie anthropogénique (Billen et al., 2010) des territoires a été particulièrement développé dans le cadre de l'*European Nitrogen Assesment* (Sutton et al., 2011). Un territoire autrophe est un territoire produisant plus de protéines que ce dont sa population (humaine et bétail) a besoin ; alors qu'un territoire hétérotrophe en produit moins que ce dont il a besoin pour subvenir aux besoins de sa population. Classiquement, une région agricole tournée vers la céréaliculture est autotrophe alors qu'une région urbaine ou d'élevage intensif est hétérotrophe (Thieu, 2009).

Les fuites de nutriments des activités agricoles

Les végétaux, quels qu'ils soient, ont besoin d'azote minéral pour alimenter leur croissance (Heller et al., 2004; Meyer et al., 2008). Or, la principale source d'azote à l'échelle planétaire est sous la forme inerte de diazote (N_2) constituant près de 78 % de l'atmosphère (Beltrando and Chémery, 1995). Seules certaines plantes, notamment les légumineuses, sont capables de fixer cet azote via des bactéries azotrophes vivant en symbiose dans les nodules de leurs racines.

Dans la forêt primitive, la végétation pompe l'azote du sol au cours de sa croissance, et le transforme en matière organique végétale. La majeure partie de cette biomasse retombe au sol où les microorganismes de la litière la reminéralisent, la rendant de nouveau disponible. Ainsi, l'azote ne s'accumule pas et son cycle est quasiment fermé. L'azote lessivé par les eaux de pluie n'excède pas 200 $kgN.km^{-2}.yr^{-1}$ (Billen et al., 2011a). Les rivières traversant de tels milieux sont donc peu chargées en azote et peu sujettes aux efflorescences algales (Billen and Garnier, 2009; Garnier et al., 2000a).

Lors du développement de l'agriculture, le principal enjeu a été de transférer la matière azotée issue des écosystèmes capables de fixer l'azote atmosphérique vers les champs de céréales incapables de le fixer. En Europe occidentale, pendant plus de 1000 ans, le bétail a joué le rôle de convoyeur d'azote depuis les pâturages semi-naturels vers les terres arables

où leurs déjections étaient épandues. Élevage et culture étaient ainsi étroitement liés (Pitte, 2012; Billen et al., 2012a).

Du 11ème au 18ème siècle, l'agriculture occidentale était basée sur un système d'assolement triennal (Higounet, 1956; Billen et al., 2009b; Schott et al., 2009). Une parcelle est mise en jachère pendant un an. Le bétail y est parqué la nuit en été, ce qui permet de l'enrichir en éléments nutritifs grâce aux déjections des animaux. En hiver les déjections sont récoltées dans l'étable et épandues sur la parcelle. L'année suivante, il est alors possible de faire une récolte de céréales avec des rendements de l'ordre de 6 q.ha^{-1} et la troisième année de l'ordre de 4 q.ha^{-1}. La densité de population soutenable de ce système est de l'ordre de 50 hab.km^{-2} (Billen et al., 2009a).

Le développement urbain en Europe de l'Ouest s'est accompagné d'un développement des techniques agricoles de leur hinterland (Guerrini et al., 2000). Ainsi, c'est le même territoire qui nourrit les 500 000 parisiens de la fin du 18ème siècle que les 5 millions de franciliens du début du 20ème siècle. Cette évolution a été rendue possible par une gestion plus efficace de la fixation de l'azote par les légumineuses, la systématisation de la culture de fourrage protéagineux, un accroissement du cheptel et une meilleure gestion de ses excréments (Schott et al., 2009). Du début du 19ème au début du 20ème, l'agriculture a abandonné la jachère et l'a remplacée par une culture fourragère fixatrice d'azote. Ce système permet, sans augmenter significativement la taille de l'exploitation, un accroissement de la charge animale et donc des ressources d'éléments fertilisants pour les terres arables. Ce système permet de soutenir une population de l'ordre de 125 hab.km^{-2}.

Mais au début du 20ème siècle, ce système atteint ses limites de productivité vis-à-vis de la population urbaine de plus en plus nombreuse. Dans un premier temps, l'agriculture devient quasiment « minière » en important des substances nutritives de régions éloignées comme le guano sud-américain ou le phosphate de certaines îles du Pacifique.

La géopolitique de la déjection du pélican péruvien

Le *guano* est le nom donné aux excréments des oiseaux marins. Il est très riche en éléments phosphorés mais surtout azotés (Hadas and Rosenberg, 1992), ce qui en fit à la fin du 19ème et au début du 20ème siècle un engrais très convoité, mais surtout une matière première essentielle pour l'industrie chimique (explosifs et colorants). Les deux espèces les plus productives sont le Cormoran de Bougainville (*Leucocarbo bougainvillii*) et le Pélican du Pérou (*Pelecanus thagus*) (figure 6) vivant tous deux le long des côtes Pacifique d'Amérique du Sud. Cette région détient par conséquent le quasi totalité des « gisements » de guano. À la fin du 19ème siècle, les appétits en engrais grandissant des nations européennes et nord-américaines ont fait du guano une substance stratégique. Qui contrôlait ces gisements contrôlait le marché mondial de l'azote et ses bénéfices colossaux.
Cette situation géopolitique a engendré, en grande partie, deux guerres affrontant plusieurs nations dans la région (Kiernan, 1955). La première est connue sous le nom de guerre hispanno-sud-américaine, et s'est déroulée de 1865 à 1866. L'Espagne, soucieuse de mettre la main sur les gisements de guano des Iles Chincha au large du Pérou, a envoyé sa flotte de guerre en prendre possession. Mais le Pérou et les pays voisins, anciennes colonies espagnoles, perçoivent d'un mauvais œil ce retour de la puissance impérialiste. S'ensuit un conflit naval à la fin duquel la flotte espagnole est renvoyée en Europe.
Le second conflit majeur opposa, entre 1879 et 1884, le Chili, le Pérou et la Bolivie. Au 19ème siècle, la région de Tarapacà, le long de la côte Pacifique au nord du désert d'Atacama, appartenait à la Bolivie, ce qui lui donnait un débouché sur la mer. De plus, cette région était riche en guano et en salpêtre, ce qui a attisé la convoitise de ses voisins péruviens et chiliens. Après un conflit de 5 ans, cette région a été annexée par le Chili, privant ainsi la Bolivie d'un accès à la mer et des riches gisements de guano. Selon certains historiens, les marques de ce conflit sont toujours visibles aujourd'hui, la Bolivie étant depuis cette époque un des états les plus pauvres d'Amérique latine.

FIGURE 6 – De gauche à droite : Pélican Thage *(cliché : Manuel González)*, Combat naval d'Iquique (guerre de 1879-1884, *Thomas Somerscales, 19ème*) entre Pérou et Chili, et bataille de Callao (guerre hispanno-sud-américaine, *peinture péruvienne anonyme*) entre Espagne et Pérou.

Enfin, un dernier fait marquant de cette période et de cette région est l'adoption par le Congrès des États-Unis d'Amérique du *Guano Islands Act* le 18 août 1856. Cette loi autorise tout citoyen américain à prendre possession d'une île contenant des gisements de guano. L'île peut être située n'importe où sur la planète, du moment qu'elle est inoccupée ou qu'elle n'est pas soumise à la juridiction d'un autre gouvernement. Elle autorise le président des États-Unis à recourir à la force militaire pour la protéger et les lois fédérales américaines y ont alors cours. Plusieurs îles du Pacifique et des Caraïbes sont toujours sous juridiction étasunienne par application de cette loi (Burnett, 2005), ce qui provoque quelques différends frontaliers avec Haïti notamment.

La situation de l'approvisionnement en azote change radicalement à partir de 1909 et de la découverte par les chimistes allemands Fritz Haber et Carl Bosch du procédé, qui prendra leur nom, permettant la conversion industrielle de l'azote atmosphérique en ammoniaque puis en acide nitrique (Smil, 2004). L'usage des engrais « chimiques », d'abord très chers, ne

se généralisera qu'à partir des années 1950. L'agriculture se transforme alors radicalement et devient dépendante de l'industrie chimique lourde et l'étroite association élevage - culture cesse d'être nécessaire. Certaines régions se spécialisent dans la céréaliculture intensive en utilisant des engrais chimiques, comme le centre du bassin parisien (Billen et al., 2009c). Grâce aux énormes quantités d'intrants, les rendements sont très élevés, atteignant 75 $q.ha^{-1}$ pour le blé tendre et 90 $q.ha^{-1}$ pour le maïs. De tels résultats s'accompagnent de fuites d'azote, essentiellement sous forme de nitrates, très élevées. Les eaux souterraines, ainsi que les cours d'eau drainant ce type de régions agricoles peuvent voir leurs concentrations en nitrates dépasser les 11.3 $mgNO_3^-.l^{-1}$, norme de potabilité selon l'OMS. D'autres régions se spécialisent dans l'élevage intensif, en important des protéines destinées à l'alimentation du bétail de régions lointaines comme l'Amérique du Sud (Billen et al., 2012c; Silvestre et al., 2012). Cette forte concentration de bétail entraîne une grande quantité de déjections, dont une large part fuite vers le réseau hydrographique. Là aussi, eaux souterraines et rivières peuvent être contaminées au-delà des 11.3 $mgNO_3^-.l^{-1}$ (Viennot et al., 2009b).

Bien que l'azote soit l'élément diffus le plus important, le phosphore (Heckrath et al., 1995; Maguire and Sims, 2002) et le silicium (Davis, 1964) sont également présents dans les eaux issues du lessivage des bassins versants. Sur les terres arables, le phosphore est essentiellement présent sous forme de phosphates (PO_4^{3-}). Mais à cause de leur capacité à s'adsorber sur les argiles et les les hydroxydes de fer ainsi qu'à former des composés insolubles avec les carbonates, ils sont peu sujets au lessivage. L'exportation du phosphore des sols vers les cours d'eau est plutôt due aux processus d'érosion qui entraînent les particules de sol chargées en phosphore. Une fois dans la rivière, le phosphore peut s'y désorber. Sous couvert forestier, dans le bassin de la Seine, la teneur en phosphore est de l'ordre de 0.1 $gP.kg^{-1}$ de sol (Billen and Garnier, 2009). Tandis que sur les sols cultivés et fertilisés depuis des décennies, leurs teneurs sont 10 à 15 fois plus fortes. Ainsi, dans les têtes de bassin, les teneurs en phosphore des matières en suspension sont aux alentours de 0.5 $gP.kg^{-1}$, en équilibre avec des concentrations en ortho-phosphates dissous d'environ 0.015 $mg.l^{-1}$.

Le cycle du silicium est sans doute le moins perturbé par les activités humaines (Conley, 2002). Le silicium est un des éléments les plus abondants à la surface du globe (Foucault and Raoult, 2010). Il est en effet un constituant majeur des roches. Leur altération par météorisation et par les agents biologiques (Coque, 2002) libère du silicium. Ce dernier rejoint le réseau hydrographique en concentration plus ou moins grande selon la nature lithologique du bassin versant (Coeur and Gautier, 2008). Un bassin sableux ou granitique présentera des concentrations en silicium plus importantes qu'un bassin marneux ou argileux. Les sols contiennent également de la silice biogénique particulaire sous forme de phytolithes (Bartoli and Souchier, 1978), des concrétions de silicium issues de la décomposition de certains végétaux, comme les *Poacées* (Brochier, 2002) qui les utilisent dans leurs tissus. Ces phytolithes peuvent parvenir aux cours d'eau par les eaux de ruissellement et enrichir la rivière en silicium.

Les paysages terrestres et les flux de nutriments

Les paysages terrestres sont connus pour jouer un rôle important sur les processus biogéochimiques et les transferts de nutriments (Beaujouan et al., 2001; Haag and Kaupenjohann, 2001a), mais ce rôle demande encore à être précisé, d'autant plus que le concept même de *paysage* est difficile à définir. Depuis l'essor de l'écologie du paysage à la fin des années 1970, plusieurs définitions ont été proposées. Une des plus fréquemment retenues est celle formulée par Forman en 1995 (Forman, 1995a) : « *A landscape is a mosaic where the mix of local ecosystems or land uses is repeated in similar form over a kilometre-wide area. Within a landscape several attributes tend to be similar and repeated across the whole area, including geologic land forms, soil types, vegetation types, local faunas, natural disturbance regimes, land uses and human aggregation patterns. Thus a repeated cluster of spatial elements characterises a landscape.* » C'est donc une portion de territoire où une certaine homogénéité des formes d'usage des sols peut être observée (Grataloup, 1998).

Forman et Godron décrivent le paysage selon trois concepts élémentaires (Forman, 1995b; Forman and Godron, 1981) : la tache, le corridor et la matrice. La *tâche* est une surface se différenciant de son voisinage par son apparence (un bosquet, une prairie, un bâtiment ...) ; le *corridor* est un élément linéaire reliant plusieurs tâches (un fossé, une route, une haie ...) ; et la *matrice* est l'élément d'arrière plan englobant tout le reste (les terres arables dans un contexte de grande culture).

En ce qui concerne la cascade de nutriments et notamment celle de l'azote dans un paysage agricole, il est possible de distinguer ces trois éléments (figure 7). Différentes sources d'azote, sous forme de *taches* peuvent être identifiées. Les bâtiments d'élevage ou de stockage d'engrais et de fumures sont des sources d'émissions de N_2O et d'ammoniac (NH_3). Les terres arables sont des sources évidentes de NO_3^- mais aussi de N_2O. Les prairies peuvent l'être aussi dans une certaine mesure. D'autres *taches* sont identifiées comme des réceptacles ou même des « puits » d'azote, en favorisant les processus de dénitrification, comme les forêts ou les zones humides. Mais ces dernières peuvent également être perçues comme des « sources » lorsque du N_2O est émis. Enfin les *corridors*, liant les *tâches* les unes aux autres sont les haies, les fossés ou les drains, permettant la circulation de l'azote réactif entre les différents compartiments.

Une des difficultés d'étude de la cascade d'azote dans le paysage est la variété d'échelles spatiales et temporelles des différents processus (Cellier et al., 2011). Ainsi, un bâtiment d'élevage va émettre vers l'atmosphère du N_2O et du NH_3 qui auront des destins différents (Dragosits et al., 2006). L'ammoniac va se déposer en quelques minutes au bout de quelques mètres à hectomètres préférentiellement sur les zones boisées, tandis que l'oxyde nitreux s'accumule dans l'atmosphère. Les particules fines de nitrates d'ammonium, formées par la réaction de l'ammonium avec les oxydes d'azote (NOx) (Duché and Beltrando, 2010) peuvent être transportées sur des centaines voire des milliers de kilomètres avant de se déposer au bout de plusieurs jours voire plusieurs semaines. Les applications d'engrais, quant à elles, se déroulent sur des parcelles de quelques hectares, s'étalent sur une année et s'intègrent dans une rotation agricole pluri-annuelle. Puis le transfert hydrologique des nitrates peut mettre quelques minutes par transport via les eaux de surface mais plusieurs décennies via les eaux souterraines et seulement quelques secondes ou minutes sont nécessaires à leur dénitrification. Enfin, l'environnement humain dans lequel s'inscrit l'exploitation agricole connait différentes échelles. L'azote des intrants comme des récoltes peut provenir ou être destiné au marché local comme au marché mondial.

FIGURE 7 – De gauche à droite : paysage de bocage présentant une mosaïque de forêts et de terres arables traversées par un réseau de haies formant un corridor *(région de Salzbourg, Autriche, cliché : Andrew Bossi)*, paysage d'open-field n'étant qu'une vaste matrice de terres arables *(sud-ouest de l'Angleterre, cliché : Andrew Hill)*.

Ces nombreux éléments paysagers jouant chacun un rôle sur plusieurs formes d'azote (NO_3^- , N_2O , NH_3 ...) ainsi que cette forte variabilité spatio-temporelle rendent très compliquées les mesures in-situ des processus et des transferts. C'est pourquoi plusieurs équipes ont plutôt orienté leurs recherches vers des modèles paysagers de transfert d'azote (Hatch, 2004; Theobald et al., 2009). Récemment un consortium de groupes de recherche européens a commencé à développer conjointement le modèle intégré à l'échelle du paysage *NitroScape*, qui est un outil couplant des modules déjà existants mais traitant du devenir de l'azote dans des compartiments différents (atmosphère, hydrosystèmes, écosystèmes terrestres ...) (Duretz et al., 2011). À terme, il devrait donc être possible de modéliser de façon intégrée le devenir de l'azote dans un paysage rural.

Les zones humides ripariennes

Les zones humides ripariennes sont connues depuis les années 1970 pour impacter la cascade de nutriments au sein des bassins versants aussi bien s'agissant de l'azote (Pinay and Trémolières, 2002; Fustec et al., 2000) que du phosphore (Fardeau and Dorioz, 2002). De nombreuses études ont mis en évidence leur pouvoir rétentif vis-à-vis de l'azote diffus provenant des activité agricoles (Haycock et al., 1993; Muscutt et al., 1993; Pinay et al., 2002; Durand et al., 2011). À l'aide du modèle Seneque/Riverstrahler, Thieu et al. (2009) ont estimé la rétention riparienne dans le bassin de la Seine à 20.4 % des apports totaux d'azote en année sèche et à 26.0 % en année humide. Cette « rétention » est due pour une très large part au processus de dénitrification.

Selon certains auteurs, les principaux facteurs influençant cette rétention sont le régime hydrologique au sein de la zone riparienne, le lien hydrologique entre cette zone et son bassin amont (McClain et al., 2003) ainsi que sa position dans le bassin versant (Johnston et al., 1990). La dénitrification est maximisée lorsque des conditions anoxiques se mettent en place en présence de carbone facilement assimilable et de nitrates. Un substrat peu perméable et un régime hydraulique lent favorisent ces conditions et par conséquent la dénitrification (Pinay et al., 2000, 1989). Le rôle de l'usage du sol au sein de la zone riparienne n'est pas encore clairement établi (figure 8).

FIGURE 8 – De gauche à droite, deux types de zones ripariennes : un cours d'eau bordé d'une ripysylve *(rivière Thredbo, Australie, cliché : Felix Andrews)*, bande enherbée entre des terres arables et la rivière Sturba *(Bosnie-Herzégovine, cliché : Zoran Pravdić)*.

Certaines études ont également mis en évidence que les taux de dénitrification les plus élevés se trouvaient en bordure haute de la zone riparienne, à l'interface zone riparienne – zone amont immédiatement adjacente. L'abattement d'azote ne semble donc se faire que dans les premiers mètres de la zone, ce qui tendrait à dire que la longueur de l'interface de la zone riparienne aurait plus d'importance que sa largeur (Sabater et al., 2003).

Cependant, il existe des rétroactions négatives (Haag and Kaupenjohann, 2001a). Les zones ripariennes sont sensibles aux dépôts d'azote atmosphérique, qui peuvent porter atteinte à leur biodiversité (Dise et al., 2011). De plus, lors du processus de dénitrification, du N_2O peut être émis, ce qui fait des zones humides des points chauds d'émission de gaz à effet de serre Durand et al. (2011).

D'une manière générale, les zones humides des corridors fluviaux des pays industrialisés ont énormément diminué (Lefeuvre et al., 2002; Prigent et al., 2012). Elles ont souvent été drainées depuis plus d'un siècle pour faire place à des prairies, des terres arables ou des zones d'habitation (Rouillard et al., 2011). Ces modifications anthropiques peuvent accompagner des transformations d'ordre plus naturelles et aboutir dans certains cas à une complète métamorphose fluviale (Bravard et al., 2008).

Les secteurs stagnants du réseau hydrographique

Les secteurs stagnants du réseau hydrographique jouent un rôle non négligeable sur les flux de nutriments au sein des bassins versants. Qu'il s'agisse de lacs, de retenues, de réservoirs, de bras morts ou d'étangs, il est toujours question d'un plan d'eau d'une certaine superficie, conférant aux masses d'eau qui, le traversant, ont un temps de séjour plus long qu'en rivière, ce qui a des répercussions sur les cycles biogéochimiques.

De nombreuses études ont montré le pouvoir rétentif des plans d'eau vis-à-vis de l'azote. Dans les années 1980, de nombreuses études ont été réalisées sur des lacs scandinaves (Henriksen and Wright, 1977; Wright, 1983) ou nord-américains (Hill, 1979; Dillon and Molot, 1990) montrant que les rétentions d'azote au sein de ces milieux pouvaient atteindre plus de 90 % de la charge entrante. Plus tard, des suivis réalisés sur les barrages réservoirs de la Seine (Sanchez and Garnier, 1997; Garnier and Billen, 1994; Garnier et al., 1999), des réservoirs d'eau en Pologne (Tomaszek and Czerwieniec, 2000; Koszelnik et al., 2007; Gruca-Rokosz and Tomaszek, 2007) ou aux États-Unis (David et al., 2006) ont mis en évidence une rétention d'azote atteignant 40 %. Enfin des études orientées vers l'ingénierie écologique dans le bassin du Mississippi ont mesuré un abattement de l'azote allant de 20 à 43 % (Mitsch et al., 2005b; vanOostrom, 1995).

? Écrêtage et étiage sont les adages des barrages

Suite à la crue centennale et catastrophique de 1910 qui ennoya une grande partie de Paris et de sa banlieue, les pouvoirs publics prirent la décision de construire une série de quatre barrages-réservoirs à l'amont de Paris afin d'écrêter les crues hivernales et de maintenir les étiages estivaux à un niveau acceptable pour la navigation (Garnier et al., 1999, 2000b). L'ampleur du chantier fut telle que le premier de ces ouvrages ne fut mis en eau qu'en 1949. Ce premier barrage, sur l'Yonne, forme le lac de Pannecière (figure 9) d'une superficie de 5.2 km^2 et retenant 82.5 millions de m^3 d'eau. Le deuxième, sur la Seine, fut terminé en 1966. Il forme le lac d'Orient, d'une superficie de 23 km^2 et retenant jusqu'à 205 millions de m^3. Le troisième est en dérivation de la Marne et forme le lac du Der-Chantecoq, avec 48 km^2 et 350 millions de m^3, constituant ainsi le plus grand lac artificiel de France métropolitaine. Enfin, en 1990 a été achevé le dernier barrage, sur l'Aube, mettant en eau les lacs Amance et du Temple, d'une superficie totale de 23 km^2 (http://www.seinegrandslacs.fr/).

FIGURE 9 – De gauche à droite : Lac de Pannecière *(cliché : Benchaum)*, lac d'Orient *(cliché : October Ends)*, lac du Der-Chantecoq *(cliché : Klaus Enslin)*.

Ces ouvrages sont gérés par l'EPTB « Seine Grands Lacs », nouveau nom depuis 2011 de l'IIBRBS (Institution Interdépartementale des Barrages-Réservoirs du Bassin de la Seine). Typiquement, ces réservoirs sont remplis entre octobre et avril, afin d'éviter les crues hivernales, et vidangés entre mai et septembre, afin de soutenir les étiages. Le programme PIREN Seine travaille depuis les années 1990 en partenariat avec Seine Grands Lacs pour les aspects quantité et qualité de l'eau.

Cette « rétention » d'azote, peut s'expliquer par trois processus différents : l'assimilation par la végétation, la sédimentation ou la dénitrification. La plupart des études menées sur le devenir de l'azote dans les plans d'eau mettent en évidence le rôle prédominant de la dénitrification. Que ce soit dans des systèmes lacustres, de zones humides naturelles ou artificielles,

ou de réservoirs, la dénitrification est responsable de 40 à plus de 80 % de l'élimination de l'azote (Brinson et al., 1984; Seitzinger, 1988; Hernandez and Mitsch, 2007), soit un rôle 2 à 4 fois plus important que l'assimilation par la végétation ou que la sédimentation (Yan et al., 1997; Kreiling et al., 2011).

L'azote sous forme de nitrate n'est pas le seul élément éliminé dans les secteurs stagnants du réseau hydrographique. La forme ammonium (NH_4^+) ainsi que le phosphore (Braskerud, 2002) peuvent également y être retenus. Certaines agglomérations mettent d'ailleurs à profit cette propriété en construisant des plans d'eau pour traiter leurs eaux usées (Vymazal, 2011; Dalu and Ndamba, 2003). Enfin, le silicium subit également une certaine rétention au sein de ces secteurs stagnants (Koszelnik and Tomaszek, 2008) par suite de la croissance et de la sédimentation des *Diatomées*.

Les apports ponctuels urbains et industriels

Les rivières sont depuis toujours les réceptacles des eaux usées domestiques et industrielles. Jusqu'au 19ème siècle, dans les bassins de la Seine ou de l'Escaut, les pollutions ponctuelles prédominantes étaient liées aux activités de la petite industrie artisanale, située tant en zone rurale qu'urbaine (Billen et al., 1999). Au Moyen-Âge, les industries textile et de tannerie étaient implantées le long des cours d'eau. Le rouissage du lin et du chanvre ainsi que le tannage des peaux étaient responsables d'une pollution ponctuelle difficile à évaluer exactement mais certainement très importante. Néanmoins, étant essentiellement d'origine organique, elle n'a pas laissé de séquelles durables au milieu aquatique (Rouillard et al., 2011).

Les pollutions domestiques et urbaines ne prendront le pas sur ces pollutions de petite industrie qu'au 19ème siècle avec la généralisation du tout-à-l'égout dans les grandes agglomérations. Jusqu'à cette période, le réseau d'égouts de Paris ne dépasse pas les 30 km de long. Les eaux usées sont mal évacuées, stagnent dans les fossés et dans les rigoles creusées dans les rues ou percolent vers la nappe phréatique. Le tout-à-l'égout ne se met en place qu'en 1854 avec l'initiative d'Eugène Belgrand, sous l'impulsion du préfet Haussmann (Favier, 1997). Ce nouveau réseau d'égout débouche d'abord directement dans la Seine à l'aval de Paris au niveau de Clichy. Ces rejets chargés en matière organique, en matières fécales et en urée riche en azote provoque rapidement une déplétion d'oxygène en aval de son exutoire. Par la suite, sont aménagés des champs d'épandage sur lesquels arrivent les eaux usées, fertilisant directement des cultures maraîchères. Finalement, les quantités à épandre augmentant avec le temps, il est décidé de traiter les eaux usées dans des stations d'épuration. La plus importante est construite, toujours à l'aval de Paris, à Achères (figure 10). Cette station est, de nos jours, la plus importante d'Europe, traitant 70 % des eaux usées de l'agglomération parisienne, soit plus de 1 500 000 $m^3.jr^{-1}$ (`http://www.siaap.fr/`).

FIGURE 10 – De gauche à droite : Vue aérienne de la station d'épuration d'Achères près de la Seine, à 40 km en aval de Paris *(Photo aérienne, IGN 2011)*, bassin d'oxygénation de la station d'Achères favorisant la nitification *(Cliché : SIAAP)*.

Les eaux résiduaires urbaines sont chargées d'azote, provenant de l'urée, de matière organique, de bactéries fécales, de silicium en faible quantité provenant des lessives et de phosphore. Ce dernier élément, entre les années 1950 et le milieu des années 1990 était le principal polluant ponctuel (Billen et al., 2011a) car utilisé en abondance dans les poudres à lessiver. À la fin des années 1980, chaque habitant du bassin de la Seine rejetait aux alentours de 4 g de phosphore par jour. Mais grâce à la substitution des poly-phosphates

par les zéolithes dans les lessives durant les années 1990, cette valeur est retombée à moins de 0.5 $gP.jr^{-1}$.

Concernant l'azote rejeté, il peut être sous forme d'ammonium ou de nitrate selon le type de traitement en vigueur dans la station d'épuration (Billen et al., 2011a). Avec un traitement primaire, l'azote rejeté à la rivière est à 70 - 80 % sous forme d'ammonium et les 30 - 20 % restants sont retenus dans les boues. Ce type de traitement a l'inconvénient de favoriser une intense nitrification sur des kilomètres de rivière à l'aval du point de rejet. Ce processus impliquant une consommation d'oxygène, qui s'ajoute à celle liée à la respiration de la matière organique, le cours d'eau peut se retrouver dans un état d'anoxie avancée. Ce fut le cas pendant longtemps à l'aval d'Achères et jusqu'aux environs de Rouen, empêchant le maintien de l'ichtyofaune. L'agglomération bruxelloise, rejetant ses eaux usées dans la Zenne, fut dans ce cas jusqu'à la construction de stations d'épuration dans les années 2000 (Garnier et al., 1991). Du fait du faible débit de la Zenne, la situation était encore plus préoccupante que sur la Seine, atteignant à certaines périodes des stades de complète anoxie. Le paradoxe de ces situations était de permettre dans ces portions de rivière anoxiques des conditions propices à la dénitrification, ce qui aboutissait à l'élimination des nitrates issus des apports diffus de l'agriculture à l'amont du bassin.

Avec un traitement secondaire plus poussé, l'ammonium des eaux usées est soumis à une aération en fin de traitement, permettant sa transformation en nitrate. Ce sont toujours les mêmes proportions de d'azote rejetées à la rivière, mais cette fois sous forme de nitrate, évitant une surconsommation d'oxygène au sein de la rivière.

Enfin, les stations les plus modernes sont aujourd'hui équipées d'un traitement tertiaire permettant de dénitrifier les nitrates précédemment produits. Dans le meilleur des cas, seulement 10 % de l'azote apporté par les eaux usées brutes est rejeté dans le réseau hydrographique.

Le filtre estuarien

Les estuaires sont des milieux de transition entre eaux continentales et marines. Ils présentent des caractéristiques originales, à l'origine de mécanismes physiques, hydrologiques et biogéochimiques complexes (Guézennec, 1999b). La façade atlantique européenne étant soumise à la marée, lors du maximum du flot, l'influence marine peut se faire sentir jusqu'à Rouen sur la Seine et jusqu'à Vilvorde sur l'Escaut. Un bouchon vaseux, formé à la rencontre des eaux douces et salées, descend et remonte ces deux estuaires selon la marée (Brenon and Le Hir, 1999). Les sédiments alternent des phases de sédimentation aux moments des étales de pleine mer ou de basse mer et de remise en circulation lors du jusant et du flot. Les populations zooplanctoniques et algales commencent à changer vers des espèces n'ayant pas les mêmes besoins en nutriments que celles d'eau douce (Pinckney et al., 1999).

La largeur des rivières augmente d'amont en aval, favorisant ainsi les processus de dénitrification benthique (Howarth et al., 2011). Mais les pressions humaines sur ces milieux sont particulièrement fortes et anciennes (Guézennec, 1999a). Depuis l'essor du port de Rouen et particulièrement depuis l'ère industrielle, l'estuaire de la Seine est régulièrement dragué pour faciliter la navigation de navires au tirant d'eau toujours plus important. Ce dragage s'accompagne d'une chenalisation, d'un endiguement et d'un assèchement des slikkes et des schorres au profit de terminaux portuaires, pétroliers et méthaniers. La géométrie de l'exutoire de la Seine a donc été totalement modifiée depuis la fin du $18^{ème}$ siècle. La figure 11 montre que l'estuaire a été comblé sur plus de 6.5 km de section par endroit.

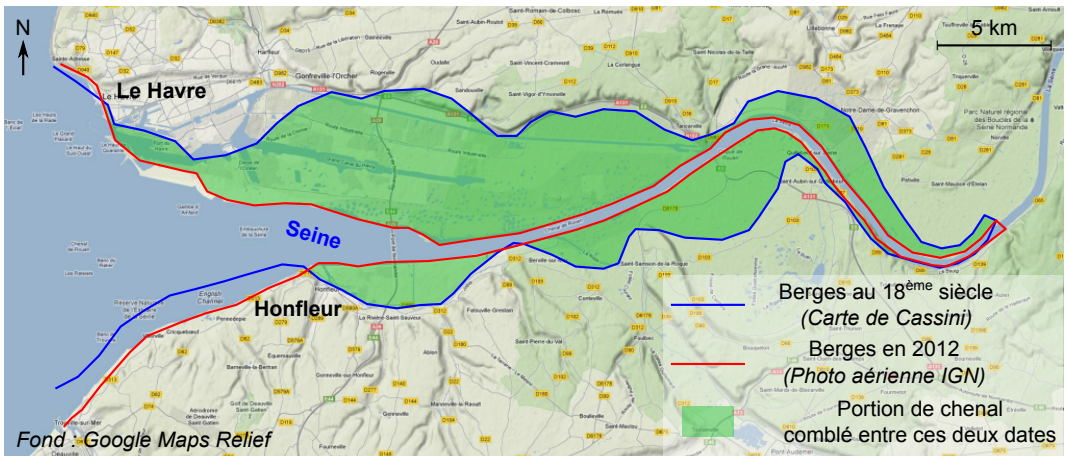

FIGURE 11 – Évolution de la géométrie de l'estuaire de la Seine entre la fin du 18ème siècle et le début du 21ème.

Ce rétrécissement du chenal a profondément transformé les processus biogéochimiques qui s'y déroulent (Avoine et al., 1981), notamment la dénitrification benthique a considérablement diminué limitant ainsi le pouvoir rétentif de l'estuaire.

La zone côtière, l'ultime réceptacle

La zone côtière est l'ultime réceptacle des flux de nutriments provenant des bassins versants contributeurs (Billen et al., 2011a) et reflète donc les activités humaines prenant place dans ces bassins, ainsi que les transformations subies par les nutriments tout au long du continuum aquatique. Grâce aux flux de matières qu'elles reçoivent, les zones côtières sont des régions privilégiées en termes de développement de biomasse par rapport aux eaux ouvertes des océans beaucoup plus pauvres en éléments nutritifs (Nixon and Buckley, 2002).

Deux grands types d'algues sont susceptibles de se développer dans ces eaux côtières (Lancelot et al., 2005). Les premières sont des algues unicellulaires à frustules siliceuses, appelées *Diatomées* (figure 12). Outre de l'azote et du phosphore, leur développement nécessite également du silicium (Martin-Jézéquel et al., 2000). Environ 100 000 espèces de *Diatomées* sont recensées, mais d'autres espèces inconnues sont régulièrement décrites. Ces algues sont en grande partie à la base de la chaîne trophique marine (Humborg et al., 2000), étant préférentiellement broutées par le zooplancton, lui même constituant la principale nourriture des poissons. Le développement de *Diatomées*, à la condition qu'elles ne soient pas toxiques, est donc positif pour l'écosystème marin.

Le second type d'algues à se développer correspond à des algues unicellulaires non siliceuses, notamment les *Dinoflagellées* et les *Haptophycées* comme *Phaeocystis* (Lancelot and Mathot, 1987; Rousseau et al., 1994) dans notre zone d'étude. Ces algues peuvent vivre en solitaire ou en colonies. Lorsqu'elles se regroupent en colonies, elles forment un épais mucilage blanc verdâtre qui flotte à la surface de l'eau et qui peut s'échouer sur les plages. Ce phénomène est surtout visible sur les côtes franco-belges de la mer du Nord (Rousseau et al., 2006; Gypens et al., 2007). Un autre type d'algues non siliceuses très répandues comprend les *Ulves* (Blomster et al., 2002), aussi appelées communément *laitues de mer*, mais qu'on retrouve plus au sud le long du littoral Atlantique. Enfin, en Baie de Seine, ce sont plutôt des *Dinoflagellées (Dinophyta)* (Ménesguen, 2001) qui ont tendance à se développer. D'une manière générale, les algues non siliceuses sont moins appétables que les siliceuses. Elles sont donc moins utilisées par le zooplancton et échappent à la chaîne trophique menant aux poissons, pour être plutôt recyclées par des processus microbiens.

Le développement de ces différents types d'algues est gouverné en grande partie par les rapports molaires de Redfield (Garnier et al., 2010a). Les rapports optimaux sont de 106 : 16 : 1 : 20 en milieu marin, soit 106 moles de carbone pour 16 d'azote, 1 de phosphore et 20 de silicium. Lorsque ces rapports sont respectés, les *Diatomées* profitent des flux des nutriments « stockés » lors de la période hivernale ou apportés au printemps pour se développer courant avril-mai, jusqu'à l'épuisement simultané des trois nutriments dans le milieu. C'est ensuite au tour des algues non siliceuses de se développer fin mai-courant

juin, mais cette croissance ne représente qu'une production de régénération basée sur le recyclage de l'azote et du phosphore dans la colonne d'eau, le silicium étant moins facilement remobilisé.

Cependant, les activités humaines ont grandement perturbé les cycles de l'azote et du phosphore, tandis que celui du silicium a été peu impacté. Il en résulte un net déséquilibre entre azote et phosphore largement en excès par rapport au silicium (Garnier et al., 2010a; Billen and Garnier, 2009). Les rapports de Redfield ne sont plus du tout respectés, pénalisant les espèces siliceuses par rapport aux non siliceuses. Ce déséquilibre entre les trois nutriments entraîne donc des efflorescences d'algues non siliceuses donc non désirables. Les espèces constitutives de ces efflorescences diffèrent selon les côtes, *Phaeocystis* en mer du Nord, *Ulves* au large de la Bretagne et *Dinoflagellées* en baie de Seine.

Dans le cas de la zone côtière franco-belge, les efflorescences algales sont un phénomène qui a toujours eu lieu. Il est probable que même en conditions pristines, certaines années, il ait pu se produire. Cependant, depuis l'ère industrielle et surtout depuis années 1950, ce phénomène a pris une toute autre ampleur (Billen et al., 2001). Jusque dans les années 1990, la conjonction de flux excessifs d'azote et de phosphore parvenant à la mer a entrainé des efflorescences très importantes, pouvant durer jusqu'à 50 jours et compter 60 millions de cellules algales. La spectaculaire diminution des flux de phosphore initiée au milieu des années 1990 a entraîné une certaine baisse de la durée et de l'importance de ces efflorescences. Cependant ce déséquilibre inédit entre un excès toujours très important d'azote par rapport au silicium, couplée à cette relative rareté du phosphore est soupçonnée d'être à l'origine du phénomène relativement nouveau, d'efflorescences de *Diatomées* toxiques comme les *Pseudo-Nitzschia* en baie de Seine.

FIGURE 12 – De gauche à droite : différentes espèces de *Diatomées* au microscope *(corp2365, NOAA Corps Collection)*, efflorescence de *Phaeocystis* à Ambleteuse (Pas-de-Calais) *(Cliché : Lamiot)*, efflorescence de *Diatomées* dans la mer de Barents, Nord de la Norvège *(Image MODIS du 14 août 2011)*.

Ces efflorescences sont le signe d'une eutrophisation du milieu, et sont dommageables pour l'écosystème côtier. La couverture d'algues ou de mucilage a tendance à empêcher la lumière de pénétrer les couches superficielles de la colonne d'eau, ainsi qu'à bloquer les échanges eau - atmosphère (figure 12). De plus, ces populations d'algues meurent rapidement, ce qui engendre un énorme stock de matière organique. Une aubaine pour les bactéries et autres microorganismes qui se repaissent de ce stock, se démultiplient et pompent ainsi la majeure partie, voire la totalité, de l'oxygène dissous de la colonne d'eau. S'en suivent des stades d'hypoxie (Muller-Karulis and Aigars, 2011), voire d'anoxie (Rabalais et al., 2010) dans les cas les plus sévères.

Le risque d'eutrophisation peut être mesuré par l'Indice de Potentiel d'Eutrophisation Côtière (*« Indicator of Coastal Eutrophication Potential, ICEP »*) (Garnier et al., 2010a), basé sur les rapports de Redfield. Cet indicateur représente le potentiel de croissance d'algues non siliceuses, sur les nutriments azotés et phosphorés apportés en excès par rapport au silicium dont ont besoin les seules diatomées. Le risque d'eutrophisation s'exprime donc en termes de production nouvelle de biomasse d'algues non siliceuses, susceptible d'être alimentée en zone marine côtière par les apports fluviaux (Billen and Garnier, 2009). Afin de faire des comparaisons entre bassins, cet indice est souvent exprimé par unité de surface de bassin versant contributeur selon l'équation ci-dessous si l'azote est l'élément limitant :

$$ICEP = \frac{12 \times 106 \times FluxN}{14 \times 16} - \frac{FluxSi}{28}$$

avec $ICEP$ en kgC.km^{-2}.jr^{-1}

$FluxN$ en kgN.km^{-2}.yr^{-1}

$FluxSi$ en kgSi.km^{-2}.yr^{-1}
ou, si le phosphore est l'élément limitant :

$$ICEP = \frac{12 \times 106 \times FluxP}{31} - \frac{FluxSi}{28 \times 20}$$

avec $FluxP$ en kgP.km^{-2}.yr^{-1}

Cet indicateur a été calculé sur l'ensemble des bassins européens (Billen et al., 2011b) et donne ainsi une idée des bassins dont les eaux réceptrices connaissent un risque d'eutrophisation (figure 13) (Garnier et al., 2010a). Il est possible de distinguer les bassins qui ont un risque associé à l'azote, donc aux pollutions diffuses, des bassins qui ont un risque associé au phosphore, i.e. aux pollutions ponctuelles.

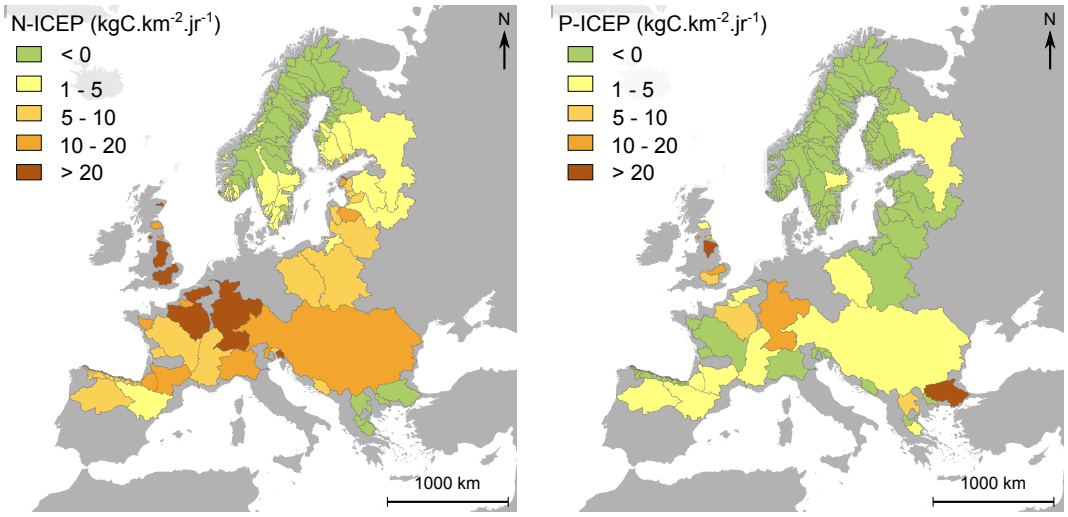

FIGURE 13 – De gauche à droite : ICEP-N et ICEP-P calculés pour les bassins européens (état des lieux en 2009).

Il apparait que la quasi totalité des bassins versants européens présente un risque d'eutrophisation pour leurs eaux côtières à cause d'un surplus d'azote. À part la Fennoscandie, tous les bassins présentent un ICEP-N supérieur à 1. Cette valeur dépasse même les 20 dans les bassins à l'agriculture très intensive du nord ouest de l'Europe (Bénélux, France, Grande-Bretagne et Allemagne). Seuls les bassins les plus septentrionaux, en majeure partie recouvert par la taïga ou la toundra (Norvège, Suède, Finlande) ont un ICEP-N inférieur à 0.

La situation est meilleure concernant l'ICEP-P. La plupart des bassins ont un risque inférieur à 10. Seule la Thrace, partagée par la Bulgarie et la Turquie, présente un ICEP-P supérieur à 20. De nombreux bassins ont un risque inférieur à 0, mais il est possible de distinguer trois groupes différents. Le faible ICEP-P des bassins de la Loire et du Pô peut s'expliquer par des stations d'épuration performantes, tandis que pour la Pologne et les Pays Baltes, il peut s'agir du faible taux de connexion au tout-à-l'égout et enfin, pour les bassins nordiques, c'est leur faible densité de population qui explique leurs bons résultats.

Zone d'étude

La mer du Nord et les bassins de la Seine, de la Somme et de l'Escaut

Un milieu physique peu contrasté

La zone marine étudiée comprend le nord de la Manche et le sud de la mer du Nord. Cette zone maritime, du fait des courants marins dominants est fortement influencée par les apports terrigènes issus des bassins de la Seine, de la Somme et de l'Escaut (les « 3S ») (Turrell et al., 1992). A ce niveau, la mer est peu profonde, ne dépassant pas les 40 m de profondeur (Maes et al., 2005; Ruddick and Lacroix, 2006). Les activités humaines y sont omniprésentes. Il s'agit d'un des chenaux maritimes les plus fréquentés au monde par les navires de commerce, presque 20 % du tonnage mondial y transite en 2005. La pêche est toujours très présente, ainsi Boulogne-sur-Mer est le premier port de pêche français en tonnage débarqué et le premier d'Europe en termes de conditionnement de produits de la mer. Enfin, le tourisme y est également bien développé depuis les stations balnéaires de Wimereux, d'Étretat, d'Ostende ou de Knokke-le-Zoute.

L'ensemble des bassins des 3S couvrent une superficie de plus 100 000 km^2. En terme de taille, le premier bassin est celui de la Seine avec 76 260 km^2 suivi par l'Escaut (19 900 km^2) puis la Somme (6 200 km^2). Les altitudes de ces trois bassins sont relativement faibles (figure 14). Le point culminant du bassin de la Seine est le Haut-Folin (901 m), situé dans le massif du Morvan. Les bassins de la Somme et de l'Escaut sont encore plus plats et culminent respectivement à 223 et 217 m. Au final, les altitudes moyennes sont respectivement de 97, 55 et 26 m pour les bassins de la Seine, de la Somme et de l'Escaut.

FIGURE 14 – Topographie des bassins de la Seine, de la Somme et de l'Escaut.

Ce relief peu accidenté s'explique en partie par la géologie et la lithologie de la région (Soyer and Cailleux, 1964). La majeure partie des bassins de la Seine et de la Somme se situe dans le bassin sédimentaire parisien (Billen et al., 2009b). Cette unité géologique présente une structure en auréoles sédimentaires concentriques (Pomerol, 1986, 2000), s'étageant du Trias au Miocène (Guerrini et al., 2000) et s'appuyant sur le socle cristallin du Morvan à l'extrême sud-est et des Ardennes au nord-est. Les roches sédimentaires affleurantes sont composées de calcaires, craies, marnes, argiles, sables et grès, alternant ainsi terrains perméables et imperméables, et influençant les écoulements de surface (Viennot et al., 2009a; Derruau, 2010). Les régions à substrat imperméable argileux ou marneux présentent une densité de drainage plus importante que celles situées sur substrat perméable crayeux ou sableux. Le bassin de la Somme, situé dans le prolongement du bassin parisien, présente également un substrat sédimentaire.

Le bassin de l'Escaut s'étend en majeure partie sur une région aux unités géologiques alternant, du sud au nord, sables et limons.

Les 3S jouissent d'un climat océanique tempéré (Beltrando, 2004), à amplitudes thermiques faibles et à précipitations abondantes. Paris, dans le centre du bassin de la Seine

a une température moyenne annuelle de 12.4 ° C avec une température minimale moyenne annuelle de 8.8 ° C en janvier et maximale de 16.0 ° en juillet. À Abbeville, dans le bassin de la Somme, ces températures sont respectivement de 9.8, 6.3 et 13.4 ° C. Enfin, à Bruxelles, dans le bassin de l'Escaut, elles sont respectivement de 10.4, 6.8 et 13.9 ° C, dessinant ainsi un gradient décroissant du sud vers le nord. Seules les régions les plus orientales du bassin de la Seine présentent des températures plus contrastées avec des gelées hivernales qui peuvent être assez marquées. Les précipitations suivent ce même gradient sud-nord avec 635.8 mm en cumul annuel moyen à Paris, 731.5 mm à Abbeville et 817.8 à Bruxelles.

L'hydrologie des 3S suit un régime pluvial océanique (Viennot et al., 2009a), marqué par de hautes eaux hivernales et des étiages estivaux. Sur les 25 dernières années, les débits moyens à l'exutoire sont respectivement de 527, 35 et 140 $m^3.s^{-1}$ pour la Seine, la Somme et l'Escaut. Les étiages estivaux peuvent descendre à 145 et 40 $m^3.s^{-1}$ sur la Seine et l'Escaut, comme ce fut le cas en 1996, tandis que les débits ont atteint 2 280 et 555 $m^3.s^{-1}$ en 2001.

Mais une anthropisation contrastée entre villes et campagnes

Les 3S ont subi des influences humaines très fortes depuis des millénaires (Mouchel et al., 2000). Les premières traces d'occupation humaine remontent au Paléolithique, il y a plus de 400 000 ans. Des chasseurs-cueilleurs parcouraient la région et ont laissé des traces de leur présence à l'aval de Paris (Lecolle, 1987), mais leurs impacts sur les milieux restaient modestes. Les premières interventions anthropiques importantes datent des grands défrichements du Néolithique (Girel, 1996). Les Celtes avaient déjà tissé un réseau agricole, de bourgs et de voies de communication. Les Romains ont ensuite développé les centres urbains et aménagé les cours d'eau pour la navigation et l'adduction en eau des cités, dont l'aqueduc captant certaines sources du nord de l'Essonne et approvisionnant Lutèce en eau. Vint ensuite le Moyen-Âge et son développement agricole et urbain. Augmentation de la demande en nourriture des villes et augmentation de la productivité des campagnes se répondent formant une sorte de cercle vertueux (Billen et al., 2009a). Les cours d'eau sont fortement transformés (Rouillard et al., 2011) pour la navigation, faire tourner les moulins ou pour la pisciculture. De nombreuses retenues sont ainsi créées en amont du bassin. La demande en nourriture et donc en engrais se poursuivant, le guano est exploité avant que soit mis au point en 1909 le procédé Haber-Bosch de fixation du diazote atmosphérique. Permettant alors d'apporter de l'azote sous forme minéral aux cultures, les rendements explosent, la population urbaine également (Billen et al., 2012c).

Enfin, aujourd'hui nous nous trouvons dans une situation où les 3S sont à la fois une des régions les plus densément peuplées du monde (Lacoste, 2000), dans laquelle se situent deux agglomérations, Paris (10 300 000 habitants) et Bruxelles (1 950 000 habitants), d'envergure internationale mais aussi dans une des régions agricoles les plus productives de la planète. Les bassins de la Seine et de la Somme non seulement répondent aux besoins de leur population en termes de grains (mais non de viande) mais exportent également céréales, oléagineux ou betteraves vers l'Europe entière et le Maghreb (Billen et al., 2012b), voire au-delà. Le bassin de l'Escaut, quant à lui, importe massivement tourteaux de soja et autres fourrages, ce qui lui permet de fournir sa population en viande et d'en exporter vers les marchés lointains.

Les trois bassins, en 2006, sont dominés par les terres arables (figure 15 a). Relativement, le plus cultivé est le bassin de la Somme, recouvert à 77 % de terres arables, suivi du bassin de la Seine à 52 %, puis celui de l'Escaut à 40 %. Ce dernier est le bassin le plus urbanisé, avec plus de 25 % de sa surface consacrée aux activités urbaines, qui se répartissent assez équitablement sur le bassin. Malgré l'importance de l'agglomération parisienne, le bassin de la Seine n'est pas plus citadin que celui de la Somme, avec 7 % seulement de la superficie occupée par l'urbain. Les principaux foyers de population se situent au centre du bassin, autour de Paris, et le long des principaux axes fluviaux. Sur le bassin de la Seine, les prairies sont reléguées aux marges occidentales, orientales et méridionales et couvrent 10 % du bassin, contre 8 % pour l'Escaut et 4 % pour la Somme. Enfin, les forêts, à peu près bien dispersées sur les bassins de l'Escaut et de la Somme, recouvrant 8 % de leurs superficies, sont reléguées aux marges du bassin dans le cas de la Seine, mais en recouvrent tout de même 25 %.

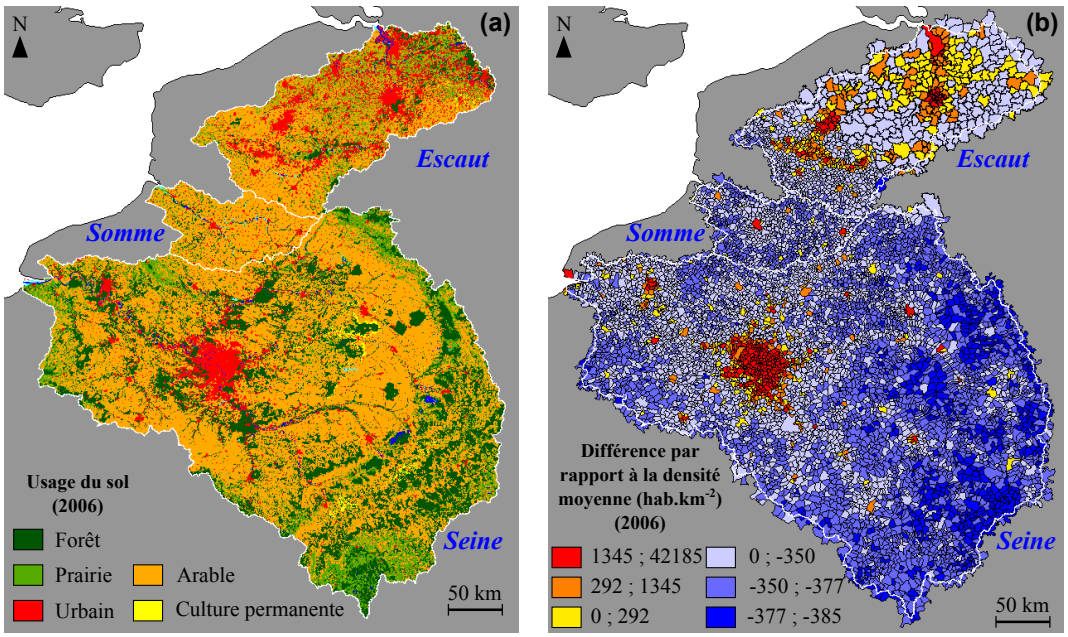

FIGURE 15 – a) usage du sol des trois bassins. b) répartition de la population en différence de densité par commune par rapport à la densité moyenne des trois bassins (385 hab.km^{-2}).

La figure 15 b) montre la répartition de la population au sein des trois bassins. La différence de densité de population à l'échelle communale par rapport à la densité de population moyenne des trois bassins y est représentée. Dans le bassin de l'Escaut, la population a tendance à simplement se regrouper autour des grandes cités de Bruxelles, Anvers, Gand ou Lille. Dans le bassin de la Somme, Amiens et Abbeville sont les deux lieux les plus peuplés. Par contre, pour la Seine, il est intéressant d'observer un clair gradient de population croissante par auréoles de l'amont vers le centre et l'aval du bassin. Cette organisation concentrique n'est perturbée que par les principaux axes fluviaux qui ont tendance à être plus peuplés que les interfluves (Billen et al., 2009b).

À la jonction du physique et de l'humain, la qualité de l'eau

À la jonction du milieu physique et des activités humaines se situe la qualité de l'eau au sein du réseau hydrographique (figure 16). Un bilan du devenir des nutriments a été calculé pour l'année « humide » 2001 par Thieu (2009) pour le bassin de la Seine. Pour cette année, les sources diffuses d'azote ont prédominé par rapport aux sources ponctuelles (3961 kgN.km^{-2}.yr^{-1}) contre (553 kgN.km^{-2}.yr^{-1}). Ce fut également le cas concernant le phosphore (92 kgP.km^{-2}.yr^{-1} contre 72 kgP.km^{-2}.yr^{-1}) et le silicium (1688 kgSi.km^{-2}.yr^{-1} contre 52 kgSi.km^{-2}.yr^{-1}. À l'exutoire du bassin de la Seine, les flux d'azote se sont élevés à 2311 kgN.km^{-2}.yr^{-1}, ceux de phosphore à 100 kgP.km^{-2}.yr^{-1}, et ceux de silicium à 1143 kgSi.km^{-2}.yr^{-1}. Les principaux facteurs d'abattement de l'azote mis en évidence sont la rétention riparienne (1161 kgN.km^{-2}.yr^{-1}, soit 26 % du flux d'azote total) et la dénitrification benthique (65 kgN.km^{-2}.yr^{-1}, soit 1.5 % du flux d'azote total).

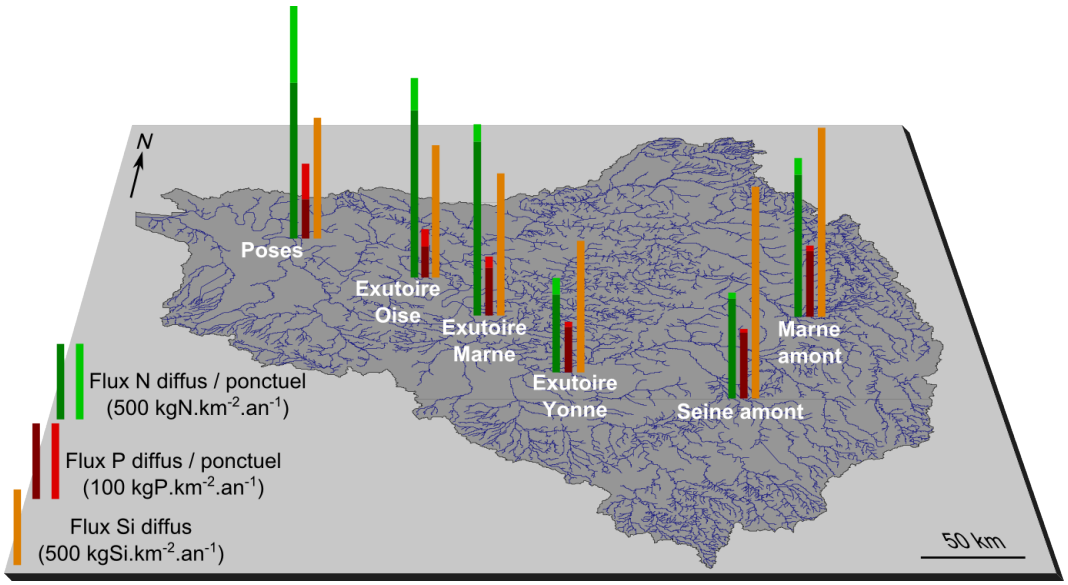

FIGURE 16 – Flux d'azote et de phosphore diffus et ponctuels et de silicium diffus pour l'année 2006 dans le bassin de la Seine.

La figure 16 met en évidence que les têtes de bassin sont essentiellement sujettes aux pollutions diffuses (Penven et al., 2000), aussi bien azotées que phosphorées. Ils présentent également des flux de silicium importants. À l'exutoire des grands axes (Marne et Oise), la part des pollutions ponctuelles tend à augmenter. Mais c'est surtout après l'agglomération parisienne et le rejet de sa principale station d'épuration localisée 40 km en aval de Paris, à Achères, que la part des pollutions ponctuelles prend de l'importance. Cependant, du fait de la modernité des traitements des eaux usées, les pollutions diffuses restent prédominantes surtout en ce qui concerne l'azote.

Méthode : la chaine de modélisation du continuum aquatique terre-mer

Les simulations appliquées au continuum aquatique terre-mer, font intervenir le modèle de rivières *Seneque/Riverstrahler* (Garnier et al., 2000a) et le modèle marin *MIRO*. Ces deux modèles décrivent le cycle du carbone et des trois éléments biogènes qui l'accompagnent (N, P, Si). Le cycle de l'azote (figure 17), est un des plus complexes et un des plus affectés par les activités humaines (Viennot et al., 2009b; Sutton et al., 2011). L'interconversion des formes réduites inorganiques (NH_4^+) et organique (acides aminés) par les métabolismes autotrophes et hétérotrophes constitue l'essentiel du cycle naturel de l'azote (Billen et al., 1998). S'y superposent la réduction des nitrates lors de son absorption autotrophe, ainsi que l'oxydation de l'ammonium en nitrite (NO_2^-, d'état d'oxydation +3) par nitrosation via les bactéries nitrosantes puis en nitrates (NO_3^- , d'état d'oxydation +5) par nitratation par les bactéries nitratantes ; la suite nitrosation - nitatration formant la nitrification. Intervient également la dénitrification des nitrates en diazote par des bactéries anaérobies. Ces deux derniers processus conduisent à l'émission de produits azotés d'état d'oxydation intermédiaire, comme l'oxyde nitreux (N_2O , d'état d'oxydation +1), le monoxyde d'azote (NO, d'état d'oxydation +2) et le dioxyde d'azote (NO_2) (Galloway et al., 2008; Billen et al., 2011a).

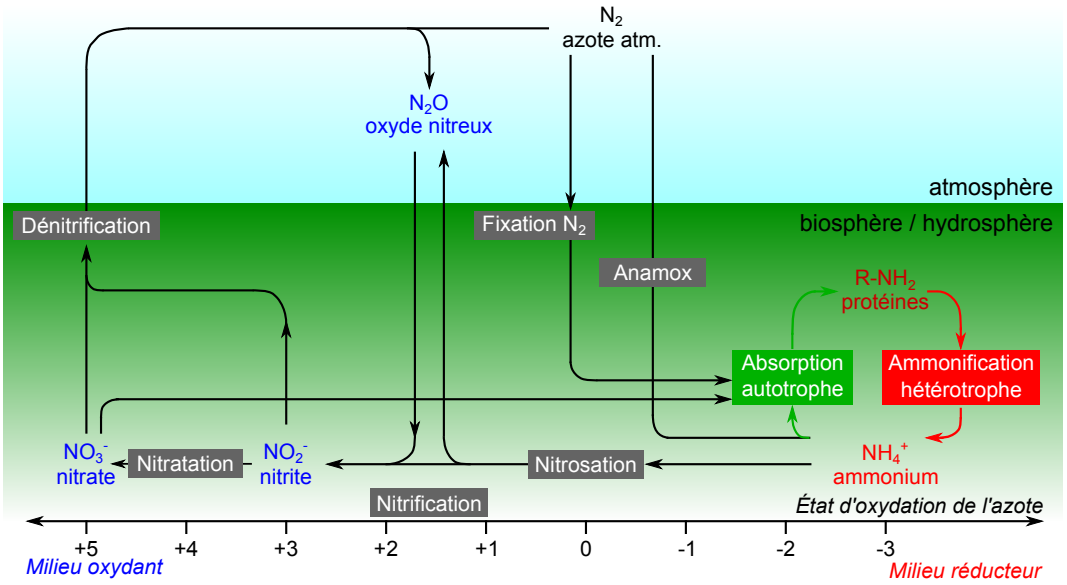

FIGURE 17 – Le cycle de l'azote.

Le modèle Seneque/Riverstrahler

Le modèle Seneque/Riverstrahler est développé au sein de l'UMR Sisyphe et dans le cadre du programme PIREN-Seine depuis plus de 20 ans (http://www.piren-seine.fr/). Il s'agit d'un modèle spatialisé, déterministe et mécanique, décrivant les processus biogéochimiques s'opérant au sein de la colonne d'eau d'un tronçon de rivière. Le modèle décrit le réseau hydrographique de n'importe quel système fluvial comme une combinaison de bassins et d'axes caractérisés par leur morphologie. Le flux d'eau traversant ce réseau correspond au débit spécifique, discrétisé en débit de surface et en débit de base, grâce au filtre récursif de Eckhardt (Eckhardt, 2008).

Le principe est de coupler ces débits transitant au travers du réseau hydrographique à un modèle décrivant les processus biologiques, microbiologiques et physiologiques s'opérant au sein de la colonne d'eau. La cinétique de ces processus est décrite par le modèle RIVE (figure 18) dont une description détaillée est disponible dans Garnier et al. (2002).

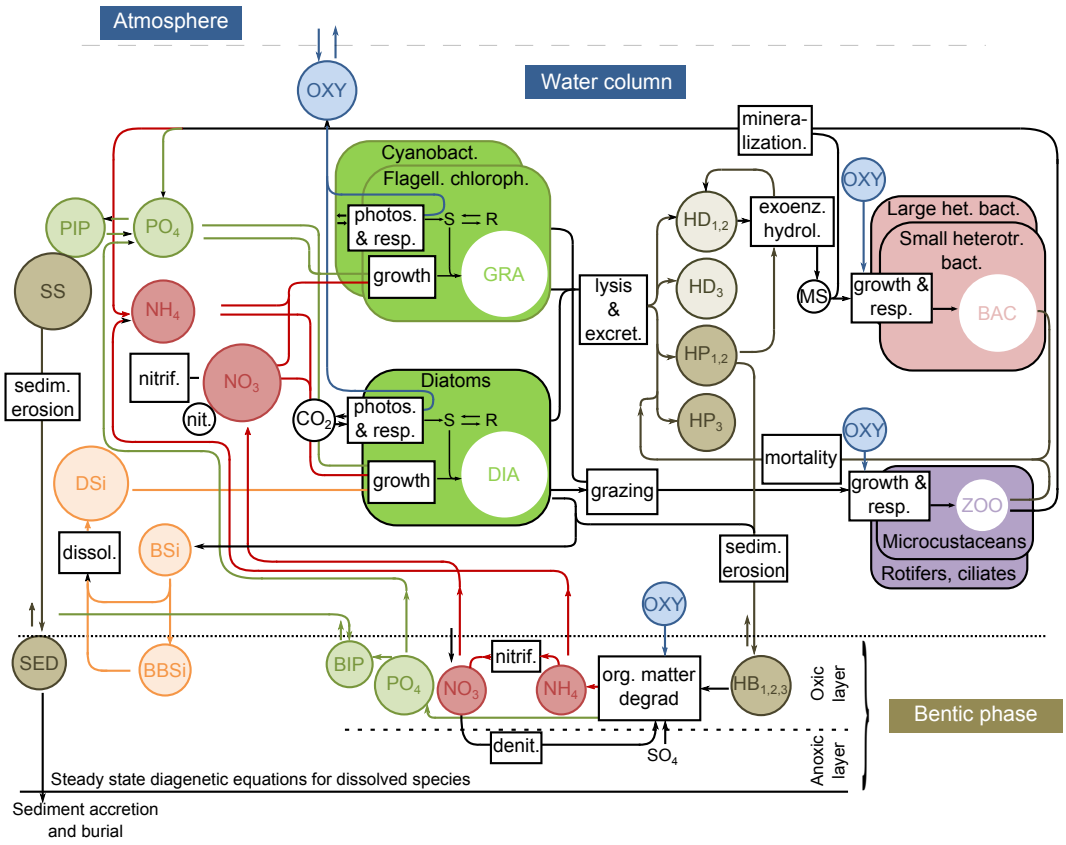

FIGURE 18 – Représentation schématique du modèle RIVE, inspirée de Thouvenot et al. (2007).

Les variables décrites comprennent les nutriments, l'oxygène dissous, les matières en suspension, le carbone organique dissous et particulaire et les biomasses algales, bactériennes et zooplanctoniques. Les principaux processus concernant la transformation, l'élimination ou l'immobilisation des nutriments au cours de leurs transferts au sein du système hydrographique dont la production primaire algale, la dégradation aérobie ou anaérobie de la matière organique par les bactéries planctoniques et benthiques, la nitrification, la dénitrification, l'adsorption et la désorption du phosphore sont explicitement décrits et calculés. À l'amont, le modèle prend en compte les nutriments d'origines diffuse et ponctuelle issus des activités humaines. Aux sources diffuses sont associées des concentrations de surface et sous racinaires d'azote, de phosphore et de silicium. Les sources ponctuelles correspondant aux rejets de stations d'épuration et d'industries précisément localisés sur le réseau hydrographique.

Le modèle Seneque/Riverstrahler a été largement validé sur les 3S (Thieu, 2009; Billen et al., 2005, 2009c), mais aussi sur des systèmes fluviaux plus exotiques comme le Fleuve Rouge au Vietnam (Quynh, 2005; Quynh et al., 2005) et son delta (Luu et al., 2012) (figure 19).

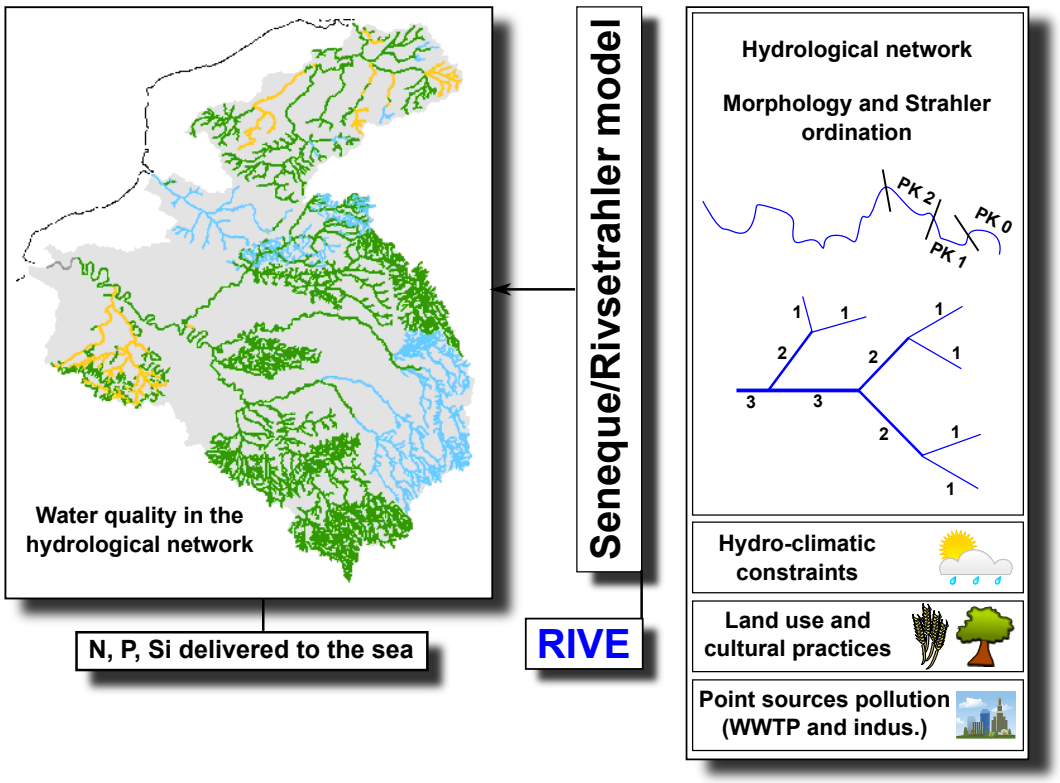

FIGURE 19 – La chaîne de modélisation Seneque/Riverstrahler.

Le modèle MIRO

MIRO est également un modèle biogéochimique déterministe, décrivant les cycles de l'azote, du phosphore et du silicium mais en milieu marin (Lancelot et al., 2005, 2007; Thieu et al., 2010). Sa structure inclut 38 variables d'état assemblées dans quatre modules décrivant les dynamiques du phytoplancton (diatomées, nanoflagellées et *Phaeocystis*), du zooplancton (copépodes et microzooplancton), la dégradation de la matière organique dissoute et particulaire et la régénération des nutriments (NO_3^- , NH_4^+ , PO_4^{3-} , $Si(OH)_4$) par les bactéries au sein de la colonne d'eau et des sédiments. Les équations et les paramètres sont formulés selon les connaissances actuelles sur les cinétiques et les facteurs contrôlant les processus auto et hétérotrophiques s'opérant dans les écosystèmes marins.

Plan du manuscrit

Cette thèse est composée d'une compilation d'articles parus ou à paraître dans des revues scientifiques à comité de lecture ou de chapitres d'ouvrages. Le manuscrit s'ouvre avec une introduction générale présentant les activités humaines et leurs impacts sur la cascade des nutriments au sein des bassins versants, la zone d'étude et les outils de modélisation employés. Suivent quatre parties allant de l'amont à l'aval de la cascade de nutriments. La première partie replace la santé des hydrosystèmes d'aujourd'hui en regard avec le passé. La deuxième partie s'attache à décrire et caractériser le rôle des zones ripariennes dans le cycle des nutriments. La troisième partie présente le rôle que peuvent jouer les secteurs stagnants du réseau hydrographique sur le devenir des nutriments. Enfin, la quatrième partie présente l'effet du filtre estuarien sur les nutriments avant qu'ils ne parviennent à la mer ainsi que quelques scénarios pour la gestion future de la cascade des nutriments ayant pour but l'amélioration de la santé des zones côtières. Dans un dernier temps une conclusion générale récapitule succinctement cette thèse.

Afin de respecter au mieux ce plan et d'éviter les redites, notamment en ce qui concerne les sections des articles « Zone d'étude » et « Méthodes », certains articles ont été tronqués ou découpés. Par exemple, l'article *Modelling historical changes in nutrient delivery and water quality of the Zenne river (1790s–2010) : the role of land use, waterscape and urban wastewater management* traitant d'une part d'un aspect rétrospectif et d'autre part du rôle

des étangs sur les cycles de nutriments, a été découpé en deux parties. Celle portant sur l'étude rétrospective se retrouve ainsi dans la première partie de la thèse, tandis que celle portant sur les étangs se retrouve dans la troisième partie. Ces éventuels découpages seront précisés au début de chaque partie.

Enfin, quelques encarts en français, ne figurant pas dans les articles d'origine, ont été ajoutés au cours du texte. Ces encarts, visuellement indépendants du reste du manuscrit, éclairent certains points intéressants de chaque partie.

Première partie

La situation présente au regard du passé

« Un édifice basé sur des siècles d'histoire ne se détruit pas avec quelques kilos d'explosifs. »

Pierre Kropotkine

Cette partie I met la cascade de nutriments actuelle en perspective avec son évolution historique. Le chapitre 1 est extrait de l'article :

Modelling historical changes in nutrient delivery and water quality of the Zenne river (1790s–2010) : the role of land use, waterscape and urban wastewater management, *Josette Garnier, Natacha Brion, Julie Callens, Paul Passy, Chloé Deligne, Gilles Billen, Pierre Servais, Claire Billen*, accepté dans *Journal of Marine Systems, doi.org/10.1016/j.jmarsys.2012.04.001.*

Cet extrait correspond à la partie de l'article traitant de l'analyse rétrospective des flux de nutriments dans le bassin de la Zenne. Il permet de replacer dans le temps long l'évolution de la qualité de l'eau da la Zenne, intéressante pour sa dualité rurale et urbaine. En retraçant l'évolution de la qualité de l'eau vis-à-vis des principaux nutriments au cours des 18ème et 19ème siècles, nous posons la question du « bon état écologique » des cours d'eau et de leur situation de référence.

Le chapitre 2 est constitué de l'intégralité de l'article :

A model reconstruction of riverine nutrient fluxes and eutrophication in the Belgian Coastal Zone since 1984, *Paul Passy, Nathalie Gypens, Gilles Billen, Josette Garnier, Vincent Thieu, Véronique Rousseau, Julie Callens, Jean-Yves Parent, Christiane Lancelot*, soumis à *Journal of Marine Systems.*

Ce chapitre décrit le chemin parcouru en termes d'abattement des pollutions aquatiques depuis le milieu des années 1980 et met en évidence les secteurs sur lesquels les efforts ont été menés et ceux pour lesquels des efforts restent à fournir. Enfin, il décrit l'évolution de la zone côtière franco-belge en termes d'efflorescences algales et de la qualité des hydrosystèmes continentaux. Les postes de la cascade de nutriments auxquels s'intéressent cete partie sont présentés sur la figure 20.

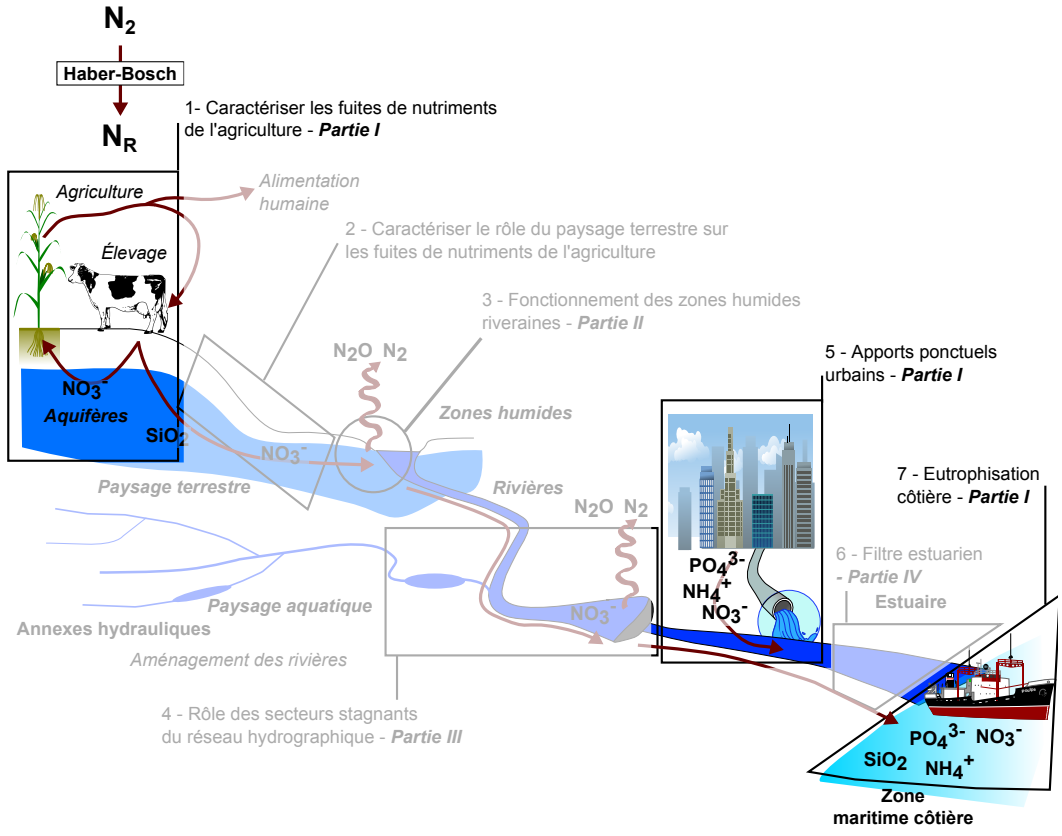

FIGURE 20 – Postes de la cascade de nutriments traités dans la partie I.

Ainsi nous nous intéressons à trois postes différents :

- l'évolution des pratiques agricoles et des fuites associées depuis la fin du 18ème siècle pour la Zenne et depuis 1984 pour les rivières Seine, Somme et Escaut (Scheldt), « les 3S »,
- l'évolution des rejets ponctuels domestiques et industriels en termes de quantité et de traitement,
- l'évolution des efflorescences algales du point de vue de leur durée et intensité en mer du Nord depuis 1984.

Chapitre 1

Modelling historical changes in nutrient delivery and water quality of the Zenne river (1790s–2010) : the role of land use, waterscape and urban wastewater management

1.1 Abstract

The Seneque/Riverstrahler model has been used to explore the effect of human-induced changes in drainage network morphology and land use on organic and nutrient pollutions, for the 1890s and 1790s. With the development of human civilization, past environmental constraints differed compared to nowadays. Research has sought to reconstruct (i) point sources (domestic and industrial), using statistics and archives from these periods, and (ii) diffuse sources via landscape and riverscape analysis based both on maps and agricultural statistics from the periods concerned. This study shows that a maximum of pollution occurred in the 1890s at the height of the industrial period, due more to the industrial load than to the domestic one. This substantial organic and nutrient pollution might have lasted up to very recently, when the Brussels Northern wastewater treatment plant began operation in 2007, significantly reducing the organic and nutrient load of the Zenne River, returning to a background pollution level assessed herein for the 1790s before industrialization exploded.

1.2 Introduction

An increasing population with its urbanization and sanitation needs, as well as changes in industrialization and agricultural practices and structural landscape transformations have considerably modified the natural biogeochemical cycles of essential bio-elements from local to larger scales (Sutton et al., 2011).

The Zenne River, a tributary of the Scheldt River via the Dijle and Rupel Rivers, represents an emblematic case study for understanding and modeling the importance of organic and nutrient loads coming from highly populated watersheds, and the transfer of pollution through the drainage network to the estuarine and coastal marine zones. Despite its small size and modest water contribution (7 %) to the Scheldt and Belgian coastal zone, it contributes today up to 25 % of the total N and P delivered by the Scheldt to the North Sea.

An interesting feature of the Zenne is that since the Middle Ages, the river played a major role in the development of the city of Brussels and consequently its hydromorphology and pollution is inherently linked to the city's development (Billen and Duvosquel, 2000; Deligne, 2003). It is interesting to note that historically, due to the asymmetry of the river bankmorphology in the Brussels area, human activity essentially developed on the flat

left bank, whereas the hilly right bank developed into a residential area for the aristocracy (Billen and Duvosquel, 2000). Early in history, the Zenne River's hydrology was considerably modified (mill operation, navigation, etc.), to such an extent that Brussels was called « Portus » at the beginning of the 11th century (Deligne, 2003). Similar to other famous mediaeval cities of Northern Europe, a prosperous textile craft industry strongly contributed to the demographic, economic and cultural expansion of Brussels, soon supported by the construction of the Willebroeck canal linking Brussels to Antwerp, at the estuary, in the 16th century (Deligne, 2003). In the 19th century, due to (i) the natural increase in alluvium and (ii) water withdrawn by the new Charleroi canal, the Zenne discharge decreased, which further enhanced alluvium and reduced the dilution of pollution coming from craft industries ; as a result, for sanitation purposes, the river was covered in the 19th century, between 1867 and 1871 (Demey, 1990), while most mill ponds had already disappeared a century before (Deligne, 2003, 2012). Since the river disappeared from the perception of riverine inhabitants, the preservation of water quality was no longer a priority for Brussels, even though, in the late 20th century, most other larger cities were equipped with efficient wastewater treatment plants (WWTPs). The implementation of national directives, but most particularly the European directives (EUUrban waste water treatment directive, UWWTD, 1991 ; EU-Water framework directive, WFD, 2000) pushed for the improvement of wastewater treatment plants or construction of new ones. However, despite its status as a European city and the European Union capital, Brussels was paradoxically only very recently equipped with WWTPs (in 2000 and 2007 for the Brussels South and North WWTPs, respectively).

The present study aims at highlighting, over a long historical period of two centuries, the particular role played by Brussels on the Zenne River's ability to transfer pollutants to the Scheldt estuary and North Sea coastal zone. Aware of huge industrial activities in the past (Billen et al., 1999)), we wished to explore the importance of these industrial sources in terms of organic matter and nutrient contamination of surface waters.

After validation on the recent well-documented period, the model was adapted and applied to much earlier historical periods in order to place the present situation within a broader historical perspective. The results of a previous interdisciplinary work (Billen et al., 1999), evaluating the early (circa 1890) industrial and domestic loads, were used for this purpose.

1.3 Site description

The Zenne watershed has a surface area of 1160 km^2 and is a small order 3 tributary of the Rupel, a major basin of the Scheldt. Due to the proximity of the marine coastal zone, the climate is rainy, with annual precipitation amounting to 850 mm, and mild, with a mean temperature of 15 $^\circ$ C ; the topography is flat with an altitude of 140 m at the spring and a mean slope of 0.23 %.

The main branch of the river extends over 58 km between Lembeek and Zennegat at the confluence with the Dijle River and its downstream part belongs to the tidal Scheldt estuary (figure 1.1). For well documented last 20 years, the Zenne River at Lembeek has had an average discharge of 3.8 $m^3.s^{-1}$ and at Eppegem the average discharge was 10 $m^3.s^{-1}$, rather low compared to 62 $m^3.s^{-1}$ and 140 $m^3.s^{-1}$ for the Rupel and Scheldt, respectively.

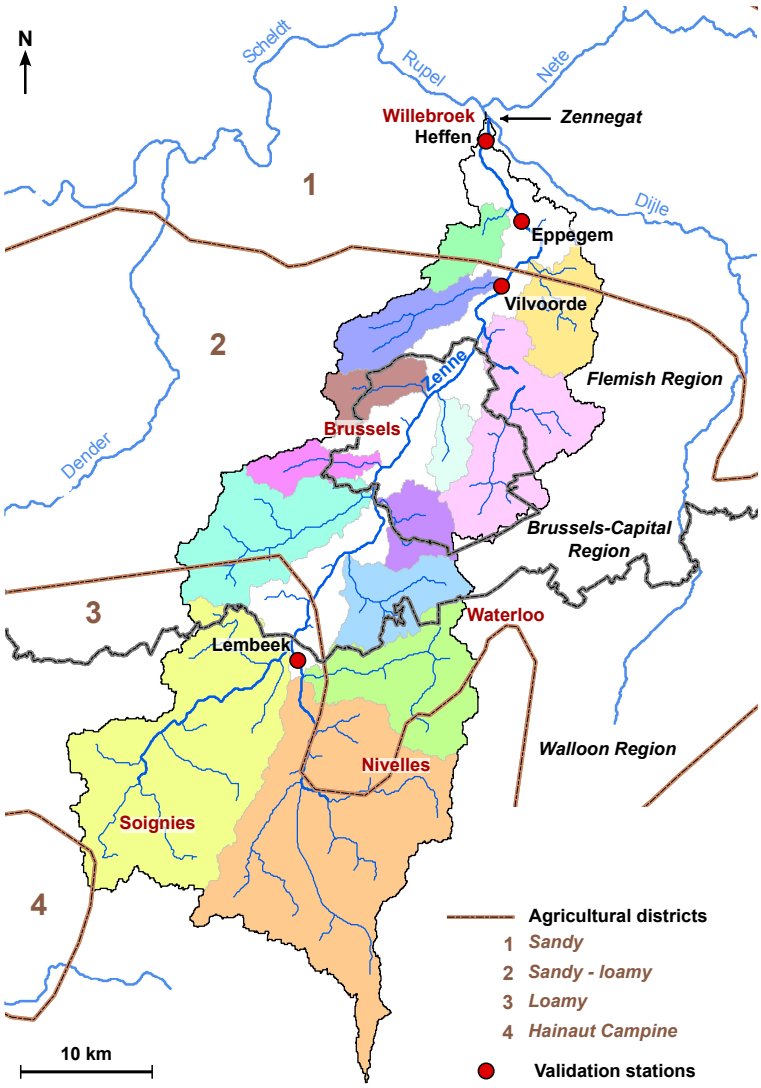

FIGURE 1.1 – The Hydrographic network of the Zenne river and associated sub-basin units. Main Cities and major stations with observation data used for validation along the Zenne axis are indicated. Dotted line distinguish the major agricultural districts used to differentiate diffuse sources.

The Zenne River crosses the Brussels conurbation over a distance of about 20 km starting 19 km after Lembeek. The nowadays proportion of urban area of the Zenne is the highest in the Scheldt basin and presently reaches 40 % of the land use, with forest occupying the lowest proportion. The population density exceeds 1200 inh.km^{-2}, more than twice higher than that of the whole Scheldt basin.

The Zenne basin is characterized by 13 major sub-basins, including the upstream Zenne watershed (Zenne WSH, 1.1) and a main axis from Lembeek to the confluence with the Dijle River, Eppegem being the last measurement station, 41.5 km from Lembeek, where the tidal zone starts (figure 1.1).

1.4 The modelling approach

The modelling approach is based on the Seneque/Riverstrahler model as described in the introduction of this dissertation, with the constraint databases for the Zenne system implemented as follows.

1.4.1 Geomorphology

The drainage network was established from the SRTM DEM (Digital Elevation Model, NASA, 2000) at a resolution of 90 m, and divided into 13 sub-basins and one branch (from Lembeek to the confluence with the Dijle, with a resolution of 1 km (figure 1.1). The slope, length and width of the rivers were evaluated according to Thieu et al. (2009). The model calculates depth from the discharge, width and slope of each river stretch using standard hydraulic relationships, as also described by Thieu et al. (2009).

To take into account the fact that the Zenne was covered from 1867 to 1871, in the city of Brussels, model runs were performed for the last 140 years applying no solar irradiance to the covered river stretch (20 km in Brussels area).

1.4.2 Hydrology

To run the model, the discharge of the hydrological medium year 2010 was chosen. The water fluxes were partitioned into a direct runoff and base flow component, using the recursive digital filter method (Eckhardt, 2005, 2008) based on the observed daily values at Eppegem (data from Hydrologisch Informatie Centrum, Waterbouwkundig Laboratorium, Departement Mobiliteit en Openbare Werken van de Vlaamse Overheid ; `http://www.waterstanden.be/`), the outlet station of the hydrological network.

Distinguishing these two components of the discharge specifically takes the inputs of diffuse sources into account, through runoff and base flow, as well as the surface point sources and their transformation and transfer in the drainage network.

1.5 Exploring the water quality of the Zenne at the end of the 18th and 19th centuries

To validate the model, before exploring much earlier historical periods in order, the hydrological year of 2010, was selected together with the appropriate constraints of points and diffuse sources. When comparing simulated longitudinal profiles with observations for 2010 when many water quality observations exist (figure 1.2), a good agreement between the observations of quality variables and the model's calculations is found for oxygen, nitrogen (ammonia and nitrate), phosphorus (phosphates and total phosphorus). This good agreement can be explained by the constraints, especially those of point sources (Ouattara et al., 2012), that are better documented with the implementation of the Water Framework Directive.

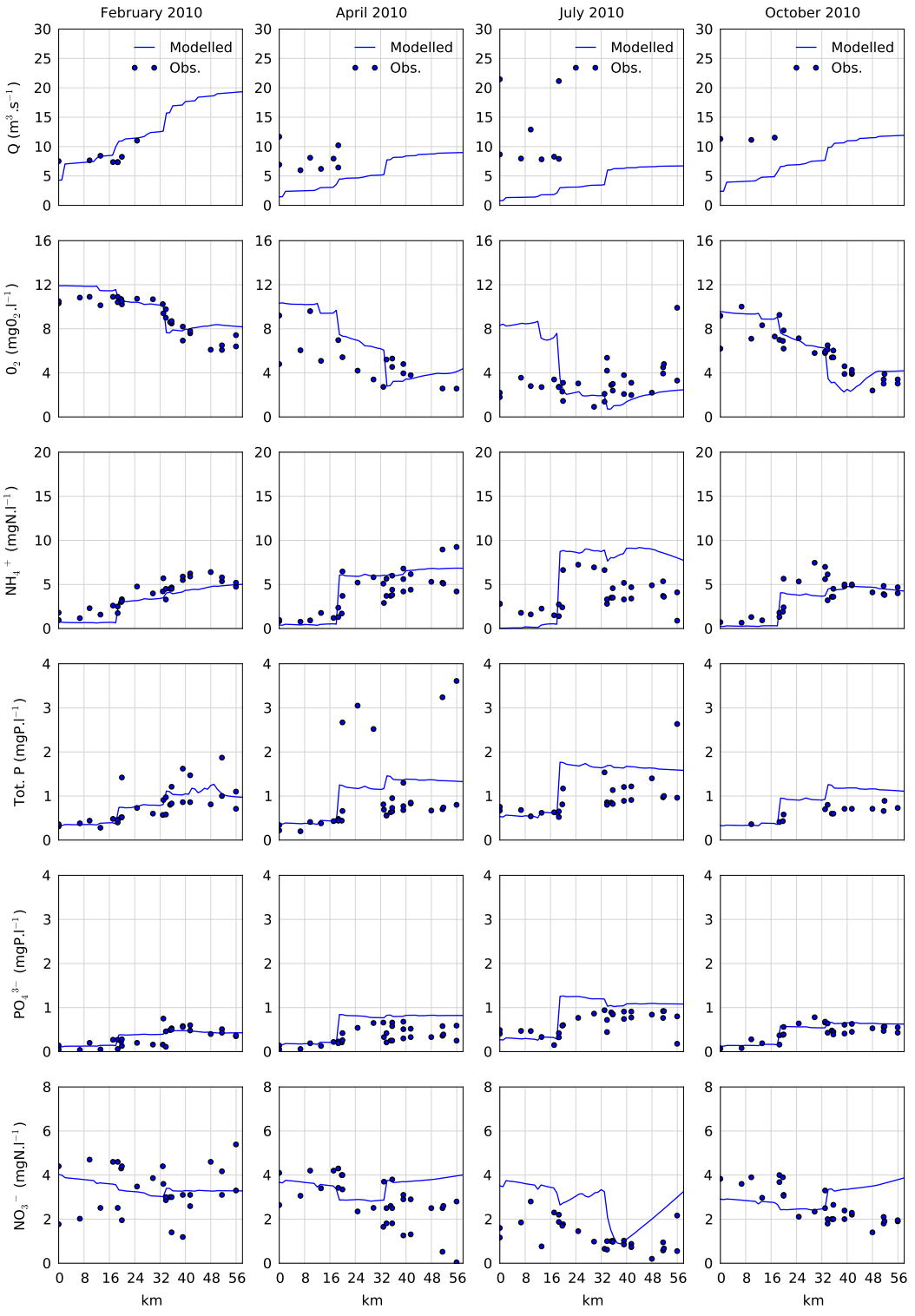

FIGURE 1.2 – Longitudinal variations in 2010, as calculated by the model, of major water quality variables, from Lembeek (km 0) to Heffen (km 56) at the outlet of the river, at four periods in the year (from left to right). From top to bottom discharge ($m^3.sec^{-1}$), oxygen (Oxy), ammonium (NH_4^+-N), total phosphorus (TP), phosphates (PO_4^{3-}-P), and nitrate (NO_3^-N). *Data sources : Vlaamse Milieumaatschappij, Geoloket Waterkwaliteit (http://www.vmm.be/geoview/) and GESZ research project, Impulse Environment initiative from the Brussels Institute for Research and Innovation.*

In addition to the good agreement of the model results with the observations obtained for 2010 for the variables routinely measured to assess organic pollution, others such as dissolved and particulate organic carbon (DOC and POC), phytoplankton biomass (Phy, expressed as chlorophyll a concentrations), silicon (Si), required by the diatoms as a nutrient

complementary to phosphorus and nitrogen, and suspended solids (SS) are also clearly in accordance with the observations (figure 1.3).

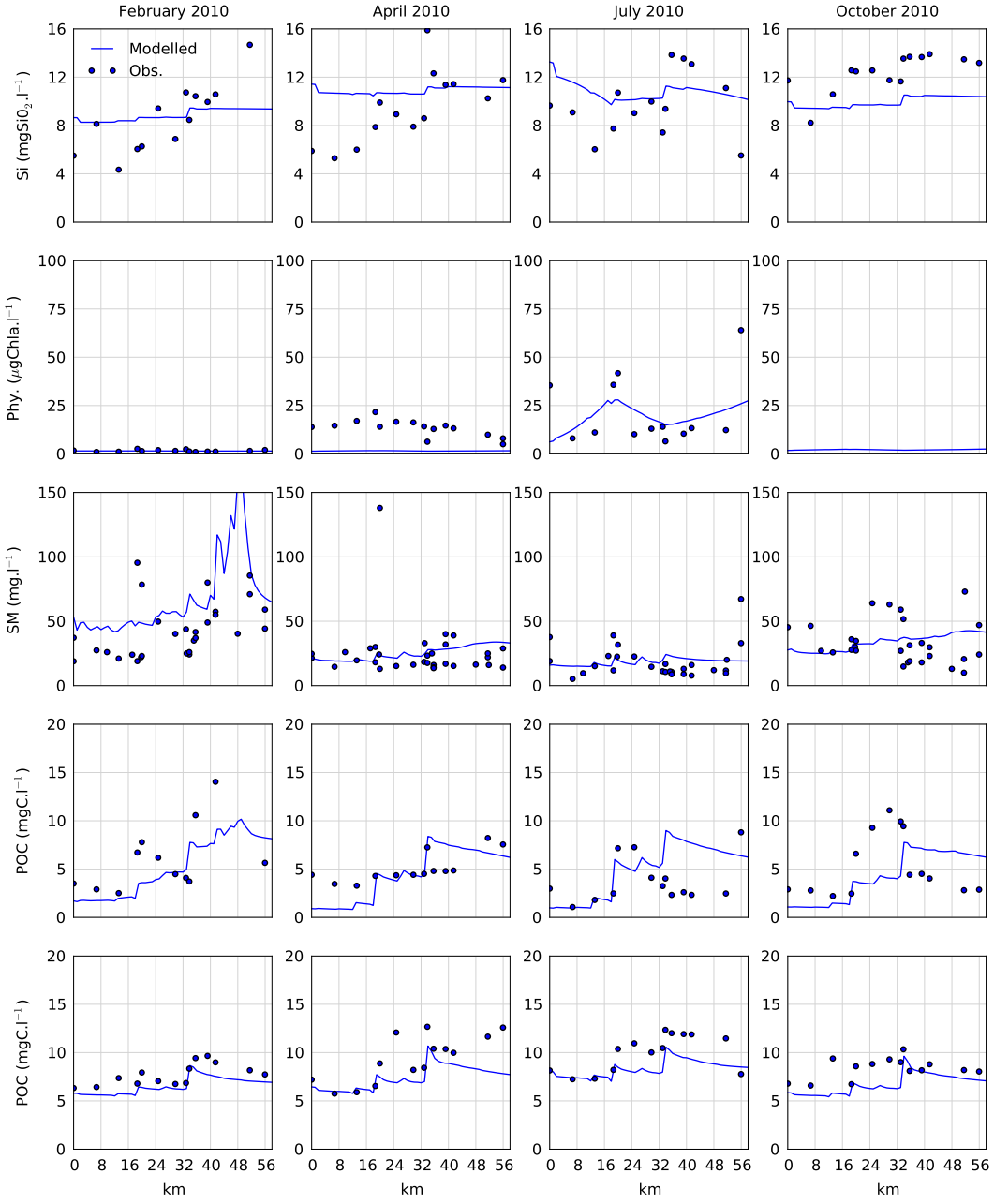

FIGURE 1.3 – Longitudinal variations in 2010, as calculated by the model and measured, for variables recently included in the routine survey, silicon, phytoplankton expressed in chlorophyll a concentration, suspended solids, particulate and dissolved organic carbon (POC, DOC).

To model the Zenne system under historical conditions (1890s and 1790s), we chose to use the discharge of 2010, close to a mean hydrological year so as to explore the role played by global changes in sectors such as agricultural practices and land use, industry and waste water collection/treatment, and hydromorphology.

For modelling approaches constraint specificities for historical simulations require knowledge on (i) the point sources as determined from historical archives for industrial and domestic loads, (ii) the diffuse sources from the land use types from old maps and the agricultural nitrogen budget, and (iii) the historical hydromorphology of the river, which has been considerably modified by human activities. Stagnant systems, deeper and wider than the river itself, increase the residence time of the water flow, subsequently modifying the net growth rate of the biological compartments, and nutrient cycling.

Indeed, human activity has resulted in extensive alteration of the hydraulic regime of rivers beginning in the Middle Ages (10th to 12th centuries). At that time, mills were installed on the smallest streams as well as on the major rivers, and hydraulic energy from water mills played a major role in many activities (Demey, 1990). The construction of embankments along higher-order streams for flood protection also began as early as the 12th century (Décamps et al., 1988). From the middle of the 18th century, development of transport and trade led to large-scale canalization and depth regulation works with construction of locks on the major rivers of Western Europe, and pollution and insanitation of the river due to industrialization led public authorities to cover many small urban rivers in northern Europe, such as the Zenne in Brussels (Deligne, 2003) but also the Bièvre in Paris (Berthier, 2007).

At the same time, many ponds were filled either for public health reasons or because fish breeding or water mill activities ceased after the introduction of the steam engine. In addition, drainage of wetlands, which was widespread in the first half of the 20th century, resulted in complete insulation of the rivers from their flood plain (Amoros and Roux, 1988).

1.5.1 Domestic point sources

The release of domestic wastewater into surface waters is a characteristic of urbanization. In most traditional agricultural life systems, human as well as animal excrement and domestic wastes are recycled onto croplands (Barles, 2007). As early as the Middle Ages in Western Europe, however, a primitive system of wastewater collection, often taking advantage of small streams, was organized in even small urban agglomerations for evacuation of domestic wastes to rivers. Modern-type large sewer systems were installed in most large cities in the mid-19th century. Disposal of part of the collected wastewater onto cropland was often organized, but direct discharge into rivers dominated. Physicochemical and biological treatment of wastewater in centralized purification plants began in the early 20th century but became a general practice only after the 1950s.

The « inhabitant-equivalent » is the current value of the pollution load corresponding to the mean daily per capita production of domestic wastewater. Stated by decree in most industrialized countries for taxation purposes, in Belgium the regulation defines it as follows (per Inh. Equ.) : 90 g day^{-1} suspended solids, 54 g day^{-1} BOD (i.e., 19 g day^{-1} biodegradable organic carbon) and 10 g N day^{-1}. As for N, this value closely corresponds to the physiological level of N excretion (Verbanck et al., 1994). Physiological excretion of P, on the other hand, is evaluated at 1.2 gP day^{-1}, which probably corresponded to the « historical » P Inh. Equ. Note that, it reached 3.5 gP day^{-1} in the 1990s at the maximum use of polyphosphates in washing powders and then decreased to 2 gP day^{-1} from the 2000s when they were banned (Billen et al., 1999; Servais et al., 1999; Garnier et al., 2006). For silicon, the release from domestic wastewater is low with respect to diffuse sources of this element, but not insignificant ; it was evaluated at 0.45–1.12 gSi day^{-1} by (Sferratore et al., 2006).

The population data were gathered within the Zenne basin from census statistics (for the 1890s, from the National Statistics of the year 1890 ; for the 1790s, from the National Statistics of 1800 for Brussels and surrounding towns, and the census from the Napoleonic period in 1801, for the remaining Zenne basin, see Jaumain (2011)). For the 30 cities that were thereby identified for the 1790s and 56 cities for the 1890s, pollution loads were calculated (given the specific pollution load per inhabitant, Inh. Equ.) and were geo-referenced for this study. Whereas the population of the Zenne watershed reached 1.79, 1.82, and 1.91 million inhabitants in 1990, 2000, and 2006, respectively, it was only about 45,000 inhabitants for the 1790s and 300,000 for the 1890s.

We considered that 25 % of the waste load was discharged into the Zenne drainage network, exactly as we did for the traditional rural population in another context (Le et al., 2007). This assumption seems reasonable because application of domestic sewage as fertilizer onto cropland was still significant at that time (Barles, 2007).

1.5.2 Industrial point sources

Evaluation of the pollution load caused by industrial activities is difficult for historical times. The approach adopted in this study consisted in estimating the industrial load and its spatial distribution from the census of workers by industrial sector (INS, 1896 ; INS, 1876–1900) and knowledge of the specific pollution load per worker-day for each sector with the technological conditions of historical periods (Billen et al., 1999). These 1896 industrial statistics provide a census of industrial establishments (3751) and associated workers

(36,792) distributed among 77 industrial locations, which were all geo-referenced for the present modeling purposes. Ten of these locations situated on the major branch of the river totaled more than 60 % of the number of factories and workers. For each of the 12 major sectors known to be a source of pollution (figure 1.4), the loss of organic matter and associated nutrients was estimated from the technical literature of the 18th and 19th centuries (Figuier, 1860; Privat-Deschanel and Focillon, 1880; Puissant and de Beule, 1989; de Beule, 1994). For many of the activity sectors, the fabrication processes used at an already industrial scale in the 1890s were nearly identical to those in use one century before, on a cottage industry scale. At historical times, however, some reduction of organic and nutrient industrial effluents should have occurred through settlement, because wastewater storage basins, allowing easier management of waste discharges into the rivers, were in common use and became mandatory during the second half of the 19th century (Onclincx, 1991). For the 1890s, the total production per sector and the number of workers for each sector made it possible to calculate the pollution load reaching the river throughout the Zenne basin. Among the various sectors considered, the production of glue and gelatin and of paper accounted for 62 % of the pollution, and food and beverages (most notably breweries) represented an additional 21 %, with the remaining 17 % related to a variety of sectors (figure 1.4).

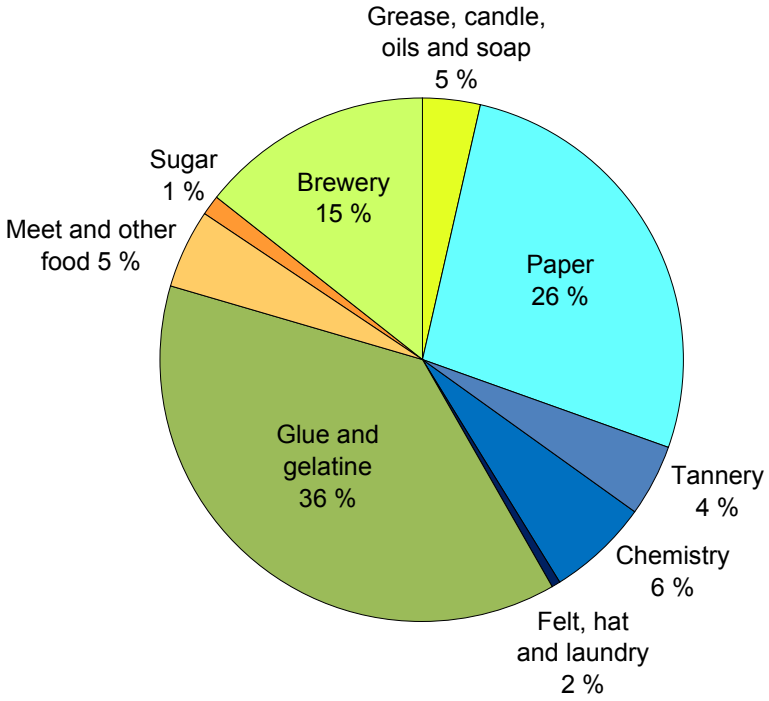

FIGURE 1.4 – Distribution of the major sector of industry in 1896 (see text for the data sources and Billen et al. (1999)).

Uncertainties on former industrial processes are difficult to evaluate and depend on the type of process considered. For example, Turkey red dyeing illustrates the different steps of the pollution generated : washing with lime ; using sheep excrement ; oil baths ; impregnating with gall ; applying alum ; dyeing with madder root ; boiling with soda, oil and soap ; and boiling with tin salts, soap and nitric acid. All these steps also included rinsing and drying phases (Figuier, 1860).

For the 1790s, considering the increase in the population between 1801 and the 1890s, although speculative we applied a ratio on the same order of magnitude, a factor of 10 for a rough estimation of the industrial load, in order to analyze the ecological status of the Zenne basin, immediately before industrialization became widespread.

1.5.3 Diffuse sources

A GIS land use layer was established on the basis of the Ferraris map (de Ferraris, 1770), (figure 1.6). We considered this information representative of the rural landscape over the entire 19th-century period. The most striking difference with the present land use is the

obvious extension of urban areas, from 5 % to 50 %, at the expense of cropland and forest, which decreased from 65 % to 25 % and from 17 % to 8 %, respectively. Pasture and orchards were also quite important in the rural landscape at this time, and today they are restricted to scarce riparian sites along the rivers (figure 1.6).

La carte de Ferraris, du militaire au scientifique

La carte de Ferraris ou carte des Pays-Bas autrichiens est la première carte précise et détaillée couvrant les territoires de l'actuelle Belgique et de l'actuel Luxembourg. Cette région est passée des mains de la Couronne d'Espagne à celles de la Couronne d'Autriche en 1713 par le traité d'Utrecht. Les autrichiens, conscients de la difficulté de défendre ce territoire par manque de frontière naturelle (fleuves ou relief), face aux poussées du Royaume de France, décident de le cartographier précisément à des fins militaires (Vervaeck et al., 1960). Ainsi, le Comte Joseph de Ferraris (figure 1.5), mathématicien et officier général dans l'artillerie est dépêché sur place pour superviser les relevés topographiques.

FIGURE 1.5 – De gauche à droite : carte de Ferraris sur un territoire rural, et sur un territoire urbain (Bruxelles et sa région). Médaillon du Comte Joseph de Ferraris *(Portrait de 1784)*.

Ces relevés sont effectués entre 1770 et 1778. La carte résultante est au 1/11520$^{\text{ème}}$ et est découpée en 275 planches (http://www.kbr.be/collections/cart_plan/ferraris/ferraris_fr.html), sur lesquelles sont représentées toutes les informations de terrain susceptibles d'intéresser l'armée : topographie, cours d'eau, zones humides, routes, dépressions ... (figure 1.5) Cette carte s'avère donc très riche pour étudier les paysages et leurs évolutions de la fin du 18$^{\text{ème}}$ siècle jusqu'à nos jours.

In order to assess the magnitude of nitrate leaching by arable land in historical periods, a complete nitrogen budget was calculated from agricultural statistics available at the town level for 1880 (Ministère de l'Agriculture, 1885), according to the same procedure as for current budgets (see subsection 2.5.6). The results show that the surplus of N total fertilization over crop N uptake was between 5 and 17 kgN.ha^{-1}.yr^{-1} in 1880 in the Loamy, Sand Loamy and Sandy regions, respectively.

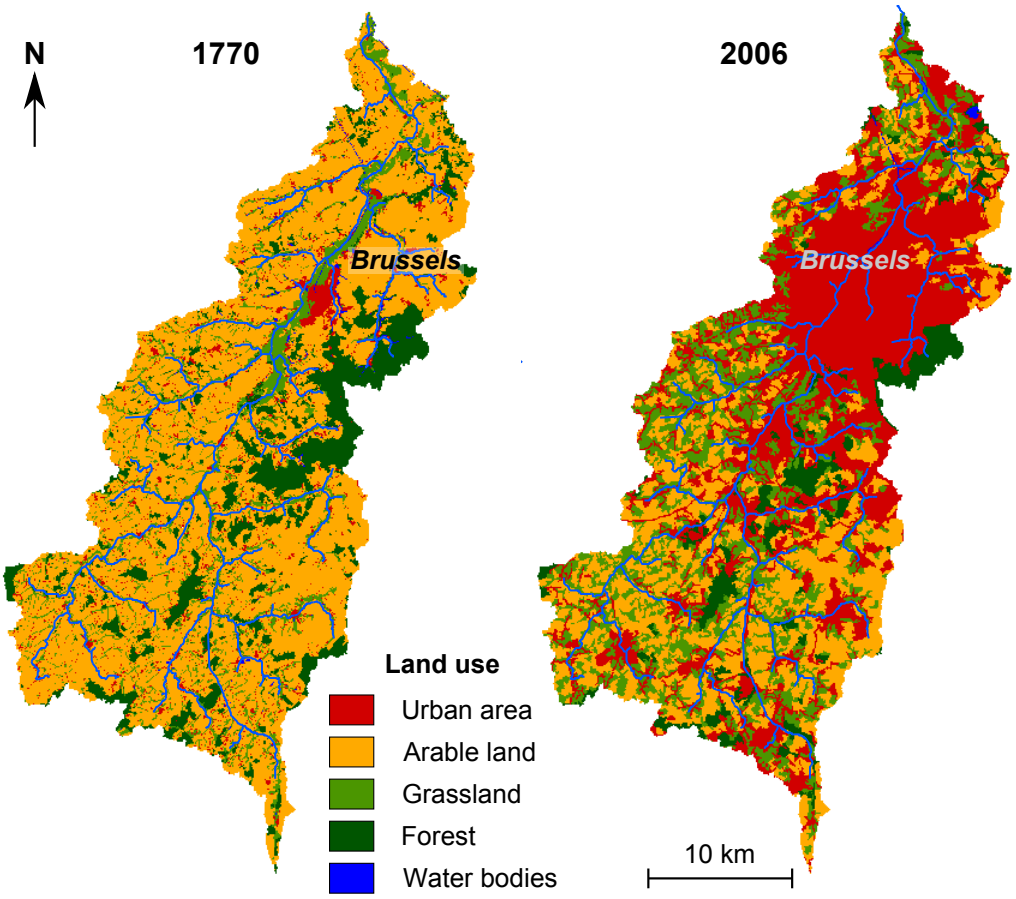

FIGURE 1.6 – Extension of the city of Brussels and subsequent changes in land use between Ferraris period and present days (CLC).

1.5.4 Modelling water quality in the past

Our modeling framework is a powerful tool to quantitatively assess the overall effects of sometimes opposite historical trends in forcing functions as reconstructed above. We calculated the water quality of the Zenne River with the set of constraints corresponding to the end of the 18th (1790) and the end of the 19th (1890) centuries (figure 1.6). The results show that, among the periods explored, the water quality was the worst in the 1890s, essentially due to the organic and ammonium pollution, typically characterizing the impact of industrial effluents, greater than domestic effluents at these times, contrary to what is observed today.

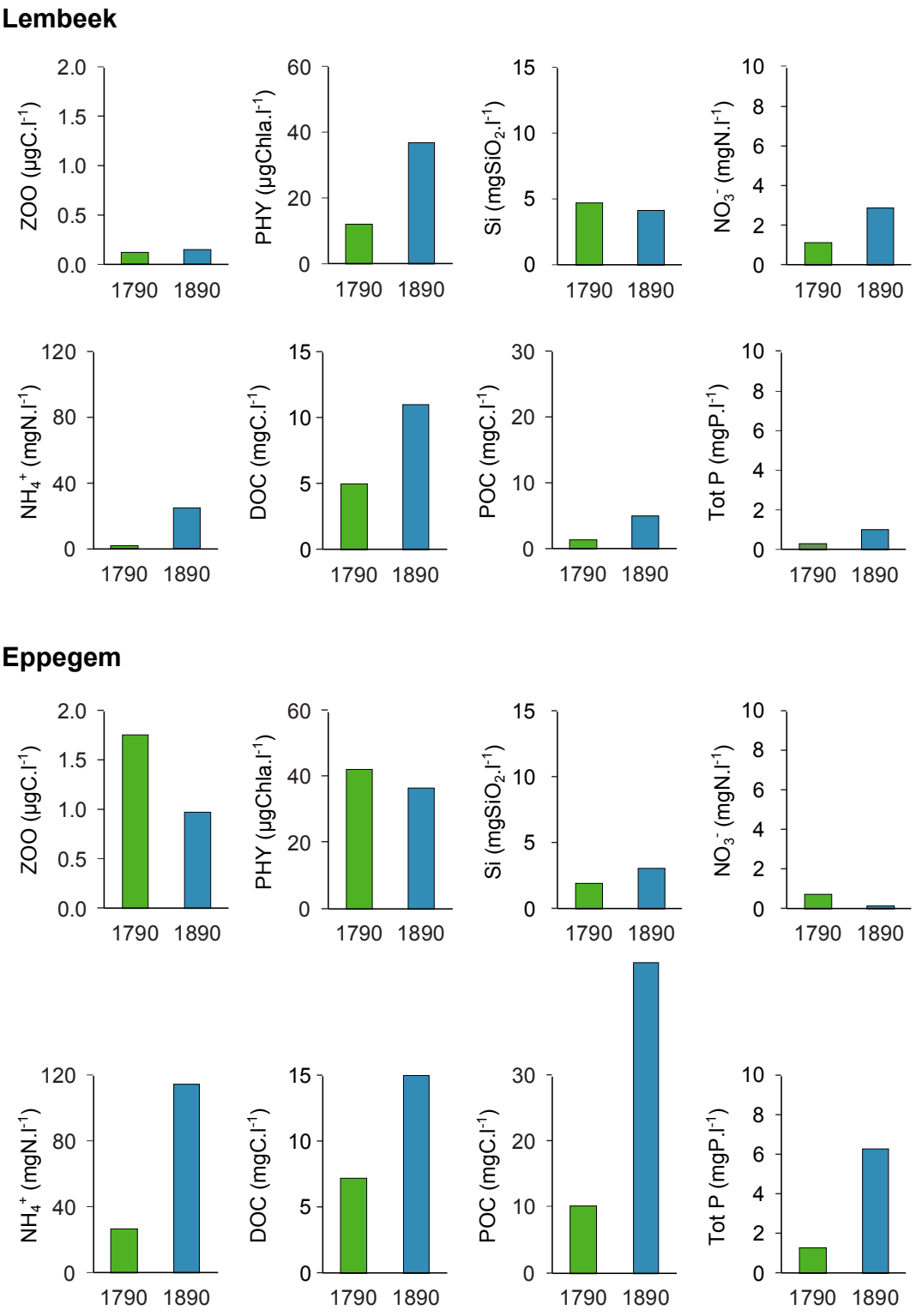

FIGURE 1.7 – Evolution of water quality variable for the periods 1790s and 1890s as calculated by the model. The stations at Lembeek and Eppegem, upstream and downstream Brussels on the main branch are represented.

The results found for the 1790s, despite the speculative assumptions on the industrial loads, show the background water quality of the Zenne River just before the industrial revolution in continental Northern Europe (Belgium and France, followed by Germany) (figure 1.7). Interestingly, after the wastewater purification measures, the present level of pollution returned to a level close to this historical background level in terms of quality.

Typically, the industrial activities of the 1890s were responsible for the pollution of the river more than domestic activities, dating back to the 1850s, taking into consideration the covering of the river in the Brussels district ending in 1871 intended to prevent people from

Year	FlxN, kgN.km^{-2}.d^{-1}	FlxP, kgP.km^{-2}.d^{-1}	FlxSi, kgSi.km^{-2}.d^{-1}	ICEP-N, kgC.km^{-2}.d^{-1}	ICEP-P, kgC.km^{-2}.d^{-1}
2010	8.0	0.8	3.8	36.8	25.9
1890's	50.6	2.3	1.5	284.0	89.9
1790's	6.2	0.3	0.9	33.3	9.1

TABLE 1.1 – Fluxes (Flx) of total nitrogen (N), total phosphorus (P) and silicon (Si) as calculated by the model at the outlet of the Zenne River. ICEP-N and ICEP-P, indicator of potential eutrophication, represent a risk of promoting undesirable algae when positive (e.g. N, P in large excess to silicon).

contracting water-borne diseases.

1.5.5 Nutrient fluxes delivered at the basin outlet

In addition to water quality, applying the Seneque/Riverstrahler model also allows one to compare the nutrient deliveries to the estuarine area corresponding to the historical situations explored, assuming identical hydroclimatic conditions (those of 2010) (table 1.1). In line with the observations made on water quality, the calculated fluxes delivered at the outlet of the Zenne basin indicate a peak for phosphorus and nitrogen loads in the 1890s and a return in 2010 to the baseline situation simulated for the 1790s. This nutrient trajectory shows the Zenne ecosystem's capacity to recover, after a pollution that probably lasted for two centuries, from the early 1800s to the early 2000s. However, the resilience to nutrient and organic load must differ from that for other pollutants such as metals and persistent organic pollutants (POP : dioxins, PCBs, some pesticides and pharmaceuticals, among others ; Meybeck and Helmer, 1989). The behavior of silicon is particularly striking, showing a higher flux in 2010 than in the historical periods. Silicon is typically uptaken by *Diatoms* and trapped in ponds by sedimentation to the bottom, thus more in the 1790s than in the 1890s, due to the loss of thei surface of the ponds. This higher silicon flux for the present period is further accentuated by the fact that the effluents of wastewater treatment plants are significant point sources of silicon, as pointed out by Sferratore et al. (2006).

1.5.6 Conclusions

Whereas the Seneque/Riverstrahler modeling approach has been used, up to now, for retrospective analysis over a period of time for which experimental data were available (from the 1970s Billen et al. (2005, 2007b), this study has shown that the model can be adapted to explore historical periods provided that (i) it has been validated on present well-documented situations and (ii) the past constraint data required can be reconstructed from historical sources.

The results of the detailed investigations carried out within the scope of this project in close collaboration between historians, biogeochemists and ecologists offer new insight into the past trends of nutrient delivery at the outlet of an urban basin. It reveals the importance of organic matter and nutrient contamination of surface waters by industrial activities as early as the middle of the 19th century. Industrial pollution preceded, rather than followed, domestic pollution in West European countries. Our analysis also revealed that, owing to this substantial and early pollution by the industrial sector, point discharge of nutrients into surface waters may have been maximum at the turn of the 19th century, leveling off long before the WFD reversed the trend.

Chapitre 2

A model reconstruction of riverine nutrient fluxes and eutrophication in the Belgian Coastal Zone since 1984

2.1 Abstract

The OSPAR convention signed in 1992 by 15 European states including Belgium and France pledged to reduce the nutrient (nitrogen N and phosphorus P) loads from land-based sources to the Channel and the North Sea to half of what they were in 1985. In this paper, we use a river basin–coastal sea chain model to describe the evolution of nutrient loads to the Belgian Costal Zone originating from the Seine, Somme and Scheldt watersheds from 1984 to 2007 in order to assess the N and P reduction with respect to the OSPAR goals and the resulting effect on coastal eutrophication, especially *Phaeocystis* blooms. Since the early 1990s, most nutrient reduction actions have been devoted to domestic and industrial wastewater treatment, resulting in a sharp P decrease between 1984 and 2007 : from 260 to 90 kgP.km^{-2} for the Seine River and from 215 to 110 kgP.km^{-2} for the Scheldt River. In spite of improved N treatment of wastewater, there is no clear decrease of N loads, which mostly originate from leaching intensively cultivated arable lands. N fluxes at the outlet of the Seine and Scheldt rivers were, respectively, 1990 and 2210 kgN.km^{-2} in 1984 and 1830 and 1390 kgN.km^{-2} in 2007. However, this relatively low decrease appears to be more influenced by hydrological conditions than by better efficiency of N use in agriculture. We conclude from this analysis that the OSPAR objectives for P have been achieved, whereas for N radical changes in agricultural practices are still required. The P reduction achieved allows, for the period of concern, a 50 % decrease of *Phaeocystis* colony blooms in the Belgian Coastal Zone, both in magnitude and duration. However, the simulated decrease, of maximum abundance, i.e., from 60 10^6 in 1984 to 30 10^6 cells.l^{-1} in 2007, is still insufficient when compared to the ecological-quality indicator of 4 10^6 cells.l^{-1}. A further decrease of nutrients is still necessary to decrease undesirable blooms more satisfactorily.

2.2 Introduction

Coastal eutrophication, following that of freshwater lake systems (Vollenweider, 1969), has been one of the most challenging environmental issues since the 1980s and remains so at the beginning of the 21st century. The imbalance in river inputs of nitrogen (N) and phosphorus (P), with respect to those of silicon (Si), reflecting human activities within watersheds (Billen et al., 2007a; Galloway et al., 2008; Lassaletta et al., 2009), is the source of non siliceous algal blooms in rivers and coastal waters (Officer and Ryther, 1980; Billen et al., 2007b; Howarth et al., 2011; Howarth and Marino, 2006; Seitzinger et al., 2010). N originates to a large extent from diffuse agricultural sources resulting from an excessive organic or mineral fertilisation of arable land (annual or permanent crops), which has increased in the last 40 years (De Vries et al., 2011). On the other hand, household and industrial wastewater releases still account for the major P sources despite the progress made in water purification

and the growing importance of diffuse sources from agricultural soil (Némery and Garnier, 2007). However, many coastal zones of developed and emerging countries are experiencing severe eutrophication (Diaz and Rosenberg, 2008; Howarth, 2008). Most damaged zones are at the outlet of watersheds with intensive agriculture (Domingues et al., 2011), high population density and inefficient urban wastewater treatment. Eutrophication can lead to hypoxia and even to anoxia as in the Gulf of Mexico (Turner et al., 2005), the Black Sea (Ludwig et al., 2010), China's coastlines (Zhu et al., 2011) and the Baltic Sea (Conley et al., 2011).

In the European Union, although the problem has been pointed out since the late 1960s, at the national scale, citizens, managers and politicians only began to worry about the damage in the middle of the 1970s for stagnant systems and the 1980s for running waters and coastal zones (Ferreira et al., 2011). In 1991, the European Parliament adopted the « Nitrates Directive » (91/676/CEE, 1991a) targeting N pollution caused by agricultural activities. Each member state had to identify « vulnerable areas », i.e., where nitrate (NO_3^-) concentration in water was above 50 mgN-NO_3.l^{-1} or where undesirable eutrophication may occur. Within these areas, « good agricultural practices » must be applied in order to respect the balance between crop nutrient requirements and fertiliser applications (Ruiz-Ramos et al., 2011). Recently, the European Commission referred France to the Court of Justice of the European Union for an excessively relaxed application of these measures. In 1992, the OSPAR convention was signed by bordering NE Atlantic States, who agreed to reduce nutrient export by 50 % in 2010 compared to 1985, the year taken as a reference (Foden et al., 2010). In 2000, the « Water Framework Directive » (WFD, 2000/60/CE, 2000) was adopted by European legislators (Borja et al., 2010). Each member state had to define « hydrological districts » within its territory, in which measures should be taken in order to reach the « Good Ecological Status » (Ferreira et al., 2011) and the « Good Chemical Status » of water bodies (rivers, lakes, transitional and near-shore coastal waters) by 2015. The WFD was followed up by the adoption in 2008 of the Marine Strategy Directive (MFD, 2008/56/EC, 2008), which extended to all European seas the need to achieve or maintain good environmental status in the marine environment by the year 2020.

In this context, this paper explores how the respective changes that have occurred in the last 24 years (1984–2007) in urban wastewater treatment and in agriculture have modified the quality of surface river waters in the Seine, Somme and Scheldt drainage basins, their nutrient delivery to the coastal zone, and the related coastal eutrophication visible in spring as undesirable blooms of *Phaeocystis* colonies (Lancelot et al., 1987; Rousseau et al., 1994). Previous papers have focused on the same studied zone computing N, P and Si budgets at the watershed scales (Thieu et al., 2009) but for only two or three contrasted hydrological years. Other papers computed fluxes delivered to the coastal zone over a long period on the Seine watershed (Billen et al., 2007b, 2001) or on the Scheldt one (Billen et al., 2005), with a non spatially distributed version of the Riverstrahler model. Some other papers were devoted to the marine ecosystem and their algal developments (MIRO model : (Gypens et al., 2007; Lacroix et al., 2007b,a). Coupling between the Riverstrahler-Model and a marine model Siam 3D was tested on the Seine Bight (Cugier et al., 2005) whereas the coupling of the models Riverstrahler and MIRO was explored over a long period for determining the riverine deliveries at the Belgian coastal zone. The GIS-based spatially distributed version of the Riverstrahler model (Seneque-Riverstrahler, SR, (Ruelland et al., 2007)) and its coupling with MIRO model was made possible for one year (Lancelot et al., 2011) where some measures dealing with the improvement of WWTP or a better management of diffuse pollutions were explored in Thieu et al. (2010). The present paper goes further by modelling nutrients and riverine phytoplankton over 24 years on the Seine, Somme and Scheldt watersheds using this new, improved version of the SR model. The spatial distribution allows us to model the changes which occurred within the hydrological networks in terms of anthropogenic N and P concentrations from 1984 to 2007.

Compared to similar previous coupled river–coastal sea models applied in either the Seine–Eastern Channel and the Scheldt/Seine–Southern North Sea, the new spatially explicit application is well designed to calculate the seasonal and spatial variations of water quality within drainage networks ranging in scale from 10 to over 100 000 km^2. In addition, the method for calculating N diffuse sources release from agricultural practices was revised and now includes estimates of N surplus.

A complete year-to-year reconstruction of the changes in hydrology, agricultural practices and wastewater treatment over the 24-years period was carried out here, describing in detail the evolution of water quality within the drainage network of the three watersheds, mainly in

terms of NO_3^- and PO_4^{3-}, two major threats for freshwater water quality and drinking water production, in comparison with silicon a key essentially diffuse nutrients. Further chaining this new version of the Seneque/Riverstrahler model implemented on the Seine, Somme and Scheldt, with the marine ecological MIRO model (Lancelot et al., 2005), made it possible to quantify the relationship between the changes in human activity in the watersheds and algal development in the adjacent coastal zone over the entire 24-years period. Particular attention is paid to the response of *Phaeocystis* bloom magnitude and duration to the quantitative and qualitative modifications of nutrient loads to the coastal sea.

? Dans la famille des Directives Européennes, je voudrais ...

Sur la zone étudiée, s'appliquent quatre directives européennes principales et une convention régionale :

- La *Directive Cadre sur l'Eau* (2000/60/EC) adoptée en 2000 oblige les États Membres à identifier leurs masses d'eau et leurs caractéristiques au sein de districts de bassins versants. Cette directive a pour objectif, pour chaque masse d'eau, d'atteindre le « bon état écologique » et le « bon état chimique » d'ici 2015. Pour les masses d'eau les plus anthropisées (canaux, secteurs endigués ...) une dérogation est possible, et seul un « bon potentiel écologique » (mais tout de même un bon état chimique) est requis.
- La *Directive Cadre Stratégie pour le milieu marin* (2008/56/EC) est l'extension de la Directive Cadre sur l'Eau au milieu marin. Les États Membres sont tenus de faire le point sur l'état écologique de leurs eaux côtières, d'y évaluer l'impact des activités humaines et de déterminer leur bon statut écologique sur la base de critères comme la biodiversité, la présence d'espèces invasives, le niveau d'eutrophisation ou les changements dans les conditions hydrologiques. Sur cette base, les États Membres doivent définir des objectifs et des indicateurs afin d'atteindre un bon statut environnemental.
- La *Directive Nitrates* (1991/676/EC) est intégrée à la Directive Cadre sur l'Eau. Son but est de protéger les eaux communautaires des nitrates issus des sources diffuses agricoles. Les États Membres ont l'obligation d'identifier les eaux de surface et souterraines polluées ou menacées par l'azote d'origine agricole, avec une attention particulière pour les masses d'eau dont la contamination nitrique dépasse les 50 $mgN.l^{-1}$ (11.3 $mgNO_3^-.l^{-1}$). Les zones vulnérables à la pollution nitrique doivent être délimitées et un code de bonnes pratiques agricoles doit y être mis en place.
- La *Directive sur les Eaux Résiduaires Urbaines* (1991/271/EC) réglemente le développement de la collecte et de l'épuration des eaux usées domestiques. En 2005, chaque État Membre aurait du collecté et traité les eaux usées de toutes les agglomérations supérieures à 2000 équivalents habitants et mettre en place des traitements d'épuration plus poussés pour les agglomérations de plus de 10 000 équivalents habitants. Cependant, seules l'Autriche, le Danemark et l'Allemagne l'ont, à ce jour, pleinement remplie.
- La *Convention OSPAR* a pour objectif de protéger les eaux de l'Atlantique du nord-est. Elle engage les États riverains a prendre les mesures nécessaires, notamment pour réduire l'eutrophisation de ces régions. Un des objectifs est de réduire les flux d'azote et de phosphore de moitiée par rapport à ce qu'ils étaient en 1985.

2.3 Study site

The study focuses on the Seine, Somme and Scheldt (the « 3S ») watersheds located in the north of France, Belgium and The Netherlands (figure 2.1). Due to the dominant mean water circulation pattern (Turrell et al., 1992), nutrient loads cumulate along a SW-NE direction so that waters flowing in the Belgian coastal zone are directly impacted by the Scheldt and indirectly by the Seine and Somme rivers. A total watershed area of 102 380 km^2 is drained by more than 26 300 km of rivers. The relief is smooth, less than 100 m in altitude on average, with a maximum elevation of 910 m in the southeastern part of the Seine basin (Table 2.1).

	Seine	Somme	Scheldt
Area (km^2)	76 270	6 190	19 900
Max alt. (m)	910	223	217
Mean alt (m)	97	55	26
Drain. dens. ($km.km^{-2}$)	0.29	0.11	0.26
Mean disch. ($m^3.s^{-1}$)	527	35	140
Pop. 2006	16 440 175	683 675	10 854 432
Pop. 1990	15 382 830	663 980	10 333 355

TABLE 2.1 – Main characteristics of the Seine, Somme and Scheldt watersheds.

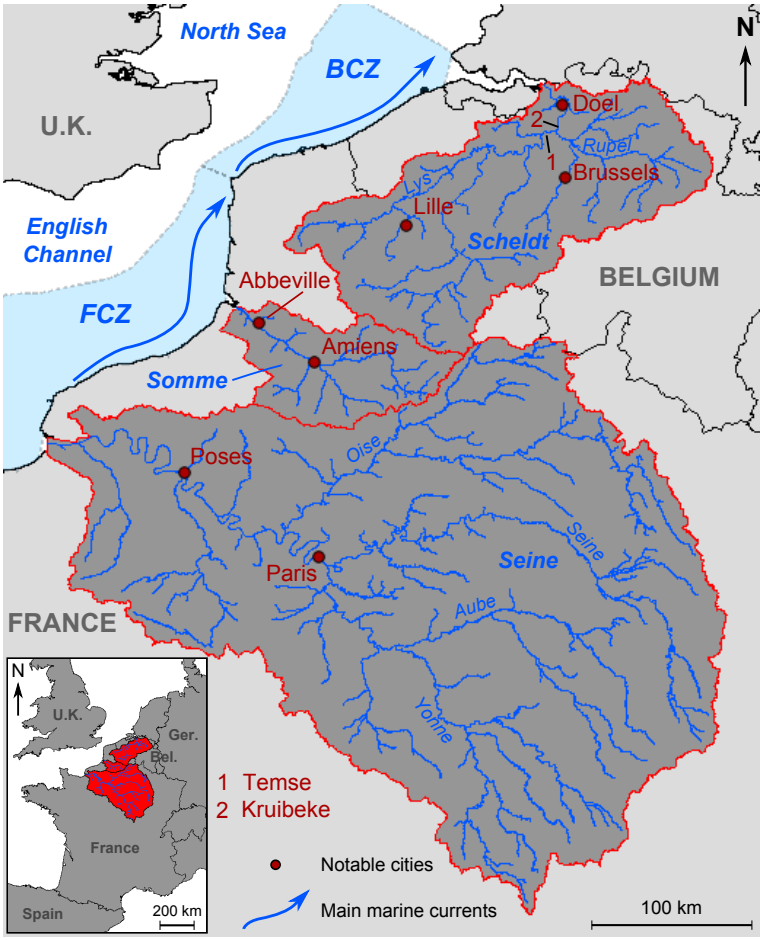

FIGURE 2.1 – The Seine, Somme and Scheldt watersheds and the main currents in the English Channel and the North Sea.

The geology is dominated by sedimentary formations. Limestone, clay and chalk formations of the Somme and Seine watersheds form concentric rings around Paris. Metamorphic formations are only present in the southern part of the Seine basin (Billen et al., 2007a). The Scheldt basin is dominated by loamy, sandy and loamy-sandy formations.

The climate is oceanic temperate with a yearly 630 mm of precipitation with a maximum during winter and a minimum during summer. The mean annual temperature is about 12 °C with a mean annual amplitude of 8 °C. Hydrology follows the climatic constraints of temperate regions, with minimum discharges observed at the end of summer and the maximum ones during winter (figure 2.2). Mean discharges for the 1984–2007 period are 527 $m^3.s^{-1}$, 140 $m^3.s^{-1}$ and 35 $m^3.s^{-1}$ for the Seine at Poses, Scheldt at Doel and Somme at Abbeville, respectively. The hydrology of the three watersheds is well synchronized, as can be observed from to the moving average over 12 months (figure 2.2).

Maximum discharges are observed in 1998, 1995 and 2001 for the three basins, while minimum ones are observed in 1992, 1996 and 2006. Some oscillations are evidenced with

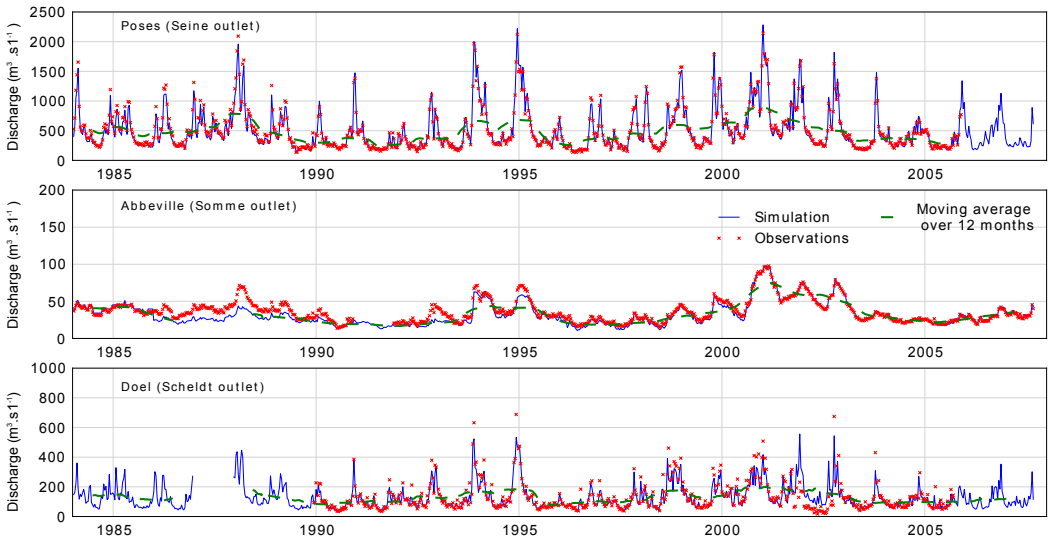

FIGURE 2.2 – Discharges at the outlet of the Seine (Poses), the Somme (Abbeville) and the Scheldt (Doel) rivers for 1984–2007 (no data available for the year 1987 on the Scheldt). Red dots are measurements and blue lines are the SR Model simulations.

discharges increasing over 2 or 4 years and then decreasing over 1 or 4 years. Nevertheless, with a studied period of only 24 years, it is not possible to show any oscillatory phenomenon or a link with the North Atlantic Oscillations (NAO). Massei et al. (2010) showed oscillations of NAO can explain 23 % of total variance of Seine River flow. This kind of observations can be partially verified at the outlet of other watersheds of the region as that of the Rhine River (Ionita et al., 2012) or the Thames Rives (Marsh, 2001). It should be reminded however that the hydrology of the Seine and Scheldt basins are deeply impacted by human activities. Reservoirs have been built in the upstream part of the Seine basin in order to regulate discharges (Garnier et al., 1999) and some flow derivations are present within the Scheldt basin).

In 2006, arable land dominated within the three basins (Corine Land Cover 2006), at 77, 52 and 39 % for the Somme, Seine and Scheldt, respectively. Arable lands are located in the centre of the basin of the Seine while for the Scheldt they are located in the southern part. Grasslands cover less than 10 % of the three basins. The maximum is reached within the Seine basin with 9.8 % of grasslands located on the edges of the basin, essentially in Morvan and in Normandy. Forests are scarce within the Somme and the Scheldt basins, i.e., 7 % in each, but cover a quarter of the Seine basin, essentially at the northern, eastern and southern edges. Despite the weight of the Parisian agglomeration, urban areas only cover 7 % of the Seine basin in the centre and along the main rivers. The Scheldt basin is more densely populated with some 25 % of the basin devoted to urban areas homogeneously distributed within the watershed. The major physical and human characteristics of the three basins are summarised in table 2.1.

2.4 Methods

2.4.1 The modelling chain, coupling the Seneque/Riverstrahler and MIRO models

The Seneque/Riverstrahler model (SR Model), a generic modelling tool coupled to a GIS-interface, was designed to calculate the seasonal and spatial variations of water quality within drainage networks ranging from 10 to over 100 000 km^2 (Ruelland et al., 2007; Thieu et al., 2009). The river network is represented as a combination of sub-basins and branches. Sub-basins are idealised by a regular scheme of confluence of tributaries with mean morphological characteristics by stream order (Strahler, 1957). These sub-basins are connected to branches represented with a higher, kilometric spatial resolution. This representation of the drainage network takes into account the biogeochemical processes occurring in both small first-order streams and large tributaries. The water flows in the hydrological network

are calculated from the specific discharges generated within the watershed of the different sub-basins and branches considered, as calculated from recorded daily discharge at available gauging stations, and separated into surface runoff and base-flow components using the Eckhardt recursive filter (Eckhardt, 2008).

The principle of the SR model is to combine these water flows that are routed through the defined structure of basins and branches with a model describing the biological, microbiological and physical-chemical processes occurring in the planktonic and benthic realms of the water bodies. The module representing the kinetics of the biogeochemical processes is known as the Rive model and contains 30 state variables. These include nutrients (i.e. all inorganic, organic, dissolved and particulate N, P, Si forms), oxygen, suspended matter, dissolved and particulate detrital organic carbon, and phytoplankton as diatoms and non-siliceous algae, bacteria and zooplankton (Garnier et al., 2002). Most processes important to the transformation, elimination and/or immobilisation of nutrients during their transfer within the river network are explicitly calculated, including algal primary production, aerobic and anaerobic organic matter degradation by planktonic as well as benthic bacteria with coupled oxidant consumption, nutrient remineralisation, nitrification and denitrification, and phosphate reversible adsorption onto suspended matter and subsequent sedimentation. The calculation scheme is based on a Lagrangian approach in which water bodies from each headspring are followed along the drainage network structure assuming a steady flow regime. The seasonal variations are described by considering successive steady flows every 10 days over the whole year cycle. A detailed description of the Rive Model equations and parameters is reported in Garnier et al. (2002). Besides morphological and climatic constraints, the SR Model considers diffuse and point sources of nutrients from land-based anthropogenic sources (see below).

SR outputs at the river outlets allow one to quantify nutrient fluxes delivered to the sea as well as the ICEP index, an indicator of the eutrophication potential (Billen et al., 2007b; Garnier et al., 2010a).

MIRO is also a mechanistic biogeochemical model and was designed to asses and understand eutrophication problems associated with *Phaeocystis* blooms in coastal zones (Lancelot et al., 2011, 2007, 2005). Similar to the RIVE model, MIRO includes 38 state variables assembled in four modules describing the dynamics of phytoplankton (diatoms, nanoflagellates and *Phaeocystis*), zooplankton (copepods and micro-zooplankton), the degradation of dissolved and particulate organic matter (each with two classes of biodegradability) and the regeneration of inorganic nutrients (NO_3^-, NH_4^+, PO_4^{3-} and Si(OH)4) by bacteria in the water column and the sediment. Equations and parameters were formulated based on current knowledge of the kinetics and the factors controlling the main auto- and heterotrophic processes involved in the functioning of the coastal marine ecosystem (fully documented by Lancelot et al. (2005) and in http://www.int-res.com/journals/suppl/appendix_lancelot.pdf). For this application, MIRO is implemented in a multi-box system, arranged in successive boxes from the Seine Bight to the Belgian Coastal Zone. Each box receives water from the upstream adjacent box and adjacent rivers and exports water to the downstream adjacent box. The boxes and geographical features are described in Lancelot et al. (2005) and the residence times are calculated based on results of the COHERENS-3D hydrodynamical model (Lacroix et al., 2004), as described in Gypens et al. (2007).

The similar structure of the SR and MIRO models makes it feasible to combine them (Lancelot et al., 2007), so as to calculate the effect of land-based sources of nutrients derived from human activity in the watersheds on coastal eutrophication.

2.5 Input data to the SR model

SR-MIRO simulations were conducted over the 1984 period making use of meteorological conditions and point and diffuse sources of nutrients as constraints.

2.5.1 Point sources

Point sources are industrial and urban wastewater released into the river network via (or not) wastewater treatment plants (WWTPs). Each WWTP is characterised by a number of treated equivalent inhabitants and the type of treatment applied (namely primary, secondary or tertiary treatment, including P removal, nitrification and denitrification). For the years after 2000, these data were obtained from Water/Environmental Agencies in France and

the Walloon and Flemish regions for Belgium. For the 1980s and 1990s, the point sources were reconstructed taking into account population dynamics and the rate of connection to sewer systems within each watershed, the year of the implementation of each WWTP and assumptions on the future improvements in wastewater treatment. Within the Scheldt and the Somme watersheds, industrial releases are assumed to be mainly collected by urban sewers and to reach the rivers via domestic WWTPs. Within the Seine watershed, industrial discharges are treated within their own wastewater treatment.

2.5.2 Population changes within the 3S basins

The French « Institut National de la Statistique et des Sciences Economiques » (INSEE) and the Belgian Federal Government released population census figures for the years 1990 and 2006. In 2006 the total population of the 3S was about 28 million inhabitants (INSEE/ INS), compared to 26.4 in 1990, i.e. an overall increase of 5.7 %. The population is not uniformly distributed within the 3S watersheds. In 2006, the Scheldt basin was the most densely populated with 540 inh.km^{-2}. The highest densities are located in the central part of the basin around Brussels and in the northern part around Antwerp. The density within the Seine basin is 215 inh.km^{-2} on average, but presents a significant disparity. Within the Parisian agglomeration, the fourth in Europe with roughly 12 million inhabitants, the density can reach more than 5000 inh.km^{-2}, while large rural areas have fewer than 20 inh.km^{-2} in the upper parts of the basin. The Somme watershed is less populated and the average density is 110 inh.km^{-2}.

Between 1990 and 2006, the population increased in the three watersheds, by 6.9 %, 3.0 % and 5.0 % for the Seine, Somme and Scheldt basins, respectively. This increase was not uniformly distributed : the density decreased in the upper part of the Seine watershed and increased in the Parisian agglomeration and in the downstream part of the watershed. Population density also increased in the Northern part of the Scheldt basin.

2.5.3 Improvement of wastewater collection and treatment : the success story of P abatement

In the middle of the 1980s, the reduction of urban and industrial point sources of organic matter, phosphorus (P) and ammonium (NH_4^+) pollution was the main challenge for river water quality. In-stream organic matter degradation and nitrification of NH_4^+ released by insufficient WWTPs was indeed leading to severe oxygen depletion in large sectors of the drainage network, especially the Seine downstream from Paris (Billen et al., 2007b) and the Zenne and Rupel downstream from Brussels (Billen et al., 1985). Regarding P, the specific discharge was about 4 mgP.l^{-1}.day^{-1}.inh^{-1} and was not or poorly treated within the WWTPs, so that P was largely in excess in comparison to both Si and N in downstream river sectors (Billen et al., 2005, 2001).

In early 1990, the situation improved for two main reasons. The first one was the banishment of polyphosphates from washing powders, which rapidly reduced the specific P discharge to about to 2 mgP.l^{-1}.day^{-1}.inh^{-1}. This banishment occurred earlier in Belgium, during the late 1980s and the early 1990s, than in France where it occurred during the mid and late 1990s due to the resistance of the French industrial lobbies (Billen et al., 1999)). The specific P discharge is nowadays about 1 mgP.l^{-1}.day^{-1}.inh^{-1}, close to the value of physiological release (Verbanck et al., 1994). The second reason was the gradual implementation of P treatment in WWTPs (Even et al., 2007). In compliance with the urban wastewater treatment directive (91/271/CEE, 1991b), municipalities with more than 2000 inhabitants are obliged to treat their wastewaters before their release into rivers. Cities located within NO_3^--sensitive areas have to implement a tertiary treatment in order to decrease the P discharge by about 85 % and the N discharge by about 70 %. The largest fraction of Parisian treated wastewaters is released into the Seine at Achères, some 50 km downstream from Paris. This WWTP is one of the largest in Europe, treating more than 1 700 000 m^3.day[pleaseinsert\prerenderunicode{âÍš}intopreamble]1 of wastewater, and was equipped with a P tertiary treatment in 2000 ; it was upgraded to nitrify all NH_4^+ beginning in 2007. A 70 % denitrification will be achieved in 2015.

Within the Scheldt watershed, until the beginning of the 21st century Brussels wastewater was not treated at all and was directly released into the Zenne River. In 2000, a first WWTP, « Brussels South », treating about 360 000 equivalent inhabitants, with a rather basic activated sludge process, was implemented a few kilometres upstream from Brussels

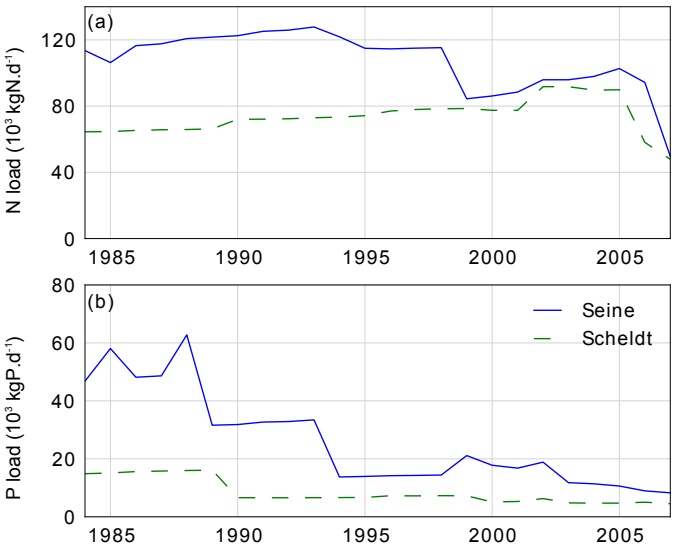

FIGURE 2.3 – Reconstruction of the total N (a) and P (b) loading from domestic wastewater facilities into the Seine and Scheldt drainage network. Data were communicated by Water Agencies from 1999 to 2007 for the Seine and for 2006 and 2007 for the Scheldt, but estimated from information on the population, sewer connection data and WWTP implementation dates for earlier periods.

and was fully operating in 2001. A second one, « Brussels North », treating both P and N of some 1 100 000 equivalent inhabitants, was implemented a few kilometres downstream from Brussels in 2007.

The reconstruction of N and P deliveries of WWTPs over the period (figure 2.3) shows that the release of P in the Seine quickly decreased from 1988 to 1994 and up to 2007 (figure 2.3 a), while for the Scheldt a 50 % decrease is observed in 1989–1990 (figure 2.3 b). N domestic inputs slightly increased in the middle of the 1990s in the Seine, then decreased slightly and quickly in 2007 with the implementation of tertiary treatment (figure 2.3 a). On the Scheldt basin, N gradually increased from 1984 to 2003, stabilised for some years before it quickly decreased in 2006 and 2007 (figure 2.3 a) after the implementation of Brussels North WWTP.

2.5.4 Diffuse sources

Lithology and soil properties, land use, agricultural practices and climatic constraints together determine the diffuse sources of nutrients (N, P, Si) to the hydrosystem. Diffuse sources are determined based on land use (Corine Land Cover 2006) and agricultural practices (official French and Belgian agricultural statistics). Twelve major agricultural regions have been distinguished within the 3S watersheds : these are the Belgian agricultural zones (Campine, sandy region, sand-loamy region, loamy region) for the Scheldt, and groupings of French Small Agricultural Regions as defined by Mignolet et al. (2007) for the Seine and Somme watersheds (figure 2.4).

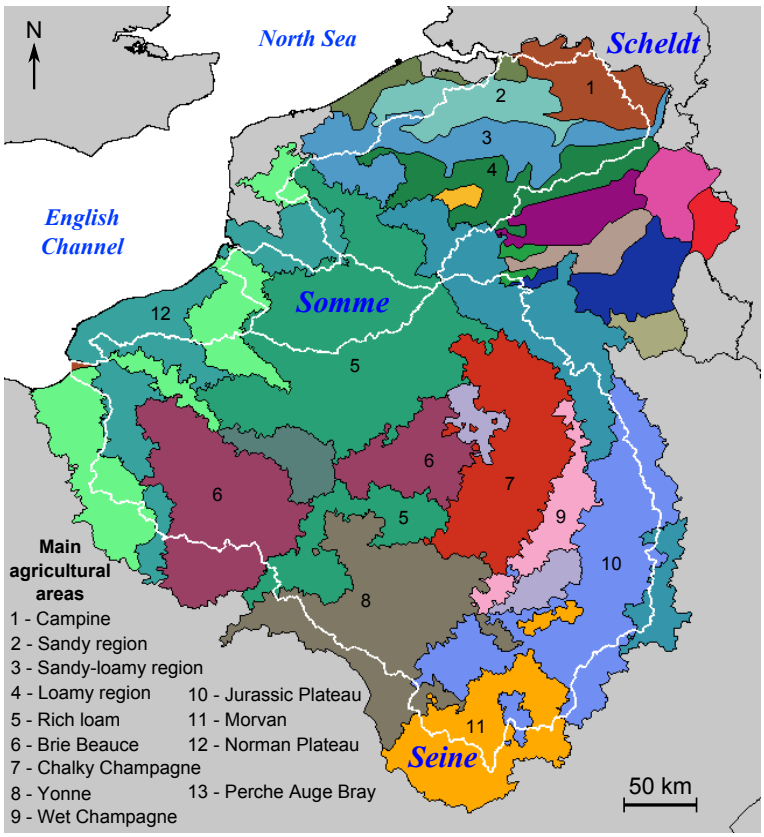

FIGURE 2.4 – Agricultural areas within the Seine, Somme and Scheldt watersheds as taken into account in the modelling approach for determination of diffuse sources, together with surplus (see text for explanation).

For each land use type and each of the 12 agricultural regions, a mean constant concentration is provided for sub-root water and groundwater concentrations, respectively, which are derived as described below. The effect of agriculture on water quality is far from being direct, however, as a significant fraction of the released nutrient finds its way through aquifers with residence time on the order of several decades in the studied area.

2.5.5 Minor land use changes

Changes in land use between 1990 and 2006, as described by the Corine Land Use data base, are minor. The most important trends are a 1.8 % increase in urban areas within the Scheldt basin, and a 0.60 %, 0.43 % and 0.42 % decrease in areas devoted to grasslands for the Seine, Somme and Scheldt basins, respectively. Other land use classes are quite stable spatially. Changes were greater for agricultural practices than land use.

2.5.6 Changes in the N balance of agriculture

The long-term trajectory of agricultural development during the last 50 years greatly differs between the different agricultural regions of the three basins. The regions of the central part of the Seine basin have gradually specialised in cereal and industrial crops and are characterised by very low livestock densities (< 0.3 LU.ha^{-1} of agricultural land, where livestock unit (LU) represents the amount of livestock equivalent to a modern milking cow and excreting 85 kgN.yr^{-1}). By contrast, very intensive livestock farming (> 5 LU.ha^{-1}) has increased in the northern part of the Scheldt basin, whereas livestock densities were maintained or even lowered in the peripheral regions of the Seine basin, e.g. in the Morvan region (figure 2.5 a).

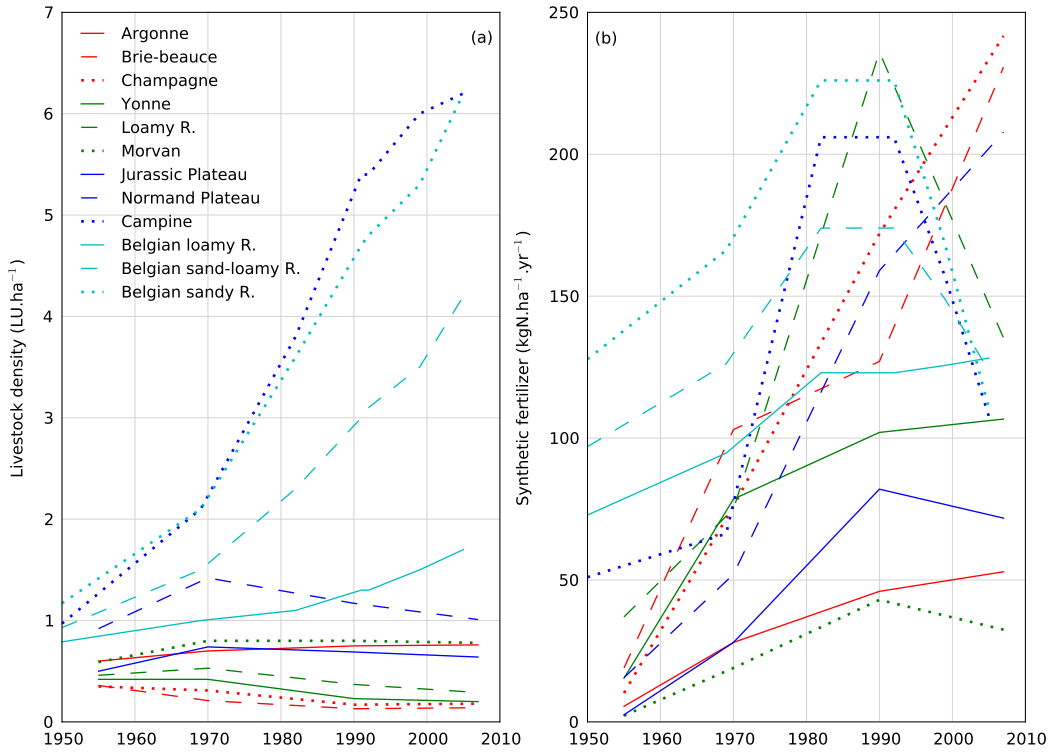

FIGURE 2.5 – (a) Historical changes in livestock density (expressed as LU/ha of cultivated area) in the main agricultural regions of the Seine and Scheldt basin during from 1950 to today (LU, livestock unit, represents the amount of livestock equivalent to a modern milking cow, and excreting 85 kgN.yr^{-1}). (b) Historical changes in the rate of synthetic nitrogen fertiliser application (expressed as kgN.ha^{-1} of cultivated area and per year) in the main agricultural regions of the Seine and Scheldt basins from 1950 to the present. Sources : National Institute of Statistics (INS) data by agricultural region for Belgium ; Agreste for France, data for one or two departments are used as representative for the whole agricultural area to which they belong.

The regions also differ in their use of synthetic fertilisers (figure 2.5 b). While already common in Belgium in the 1950s, the use of industrial N fertilisers increased only in the 1960s and the 1970s in most French areas, where it reached 230 kgN.ha^{-1}.yr^{-1} in the Brie-Beauce and Champagne regions, i.e. close to the current levels in Belgium. In recent years, the rate of synthetic N fertilisation application has stabilised or decreased in all other regions, as for P fertilisers. In order to characterise the past trajectory of each agricultural region since the 1950s in terms of N use, a complete N budget of arable land was calculated from agricultural statistics available at some key periods : urbanisation since the 1950s, industrialisation of agriculture since the 1970s and the European reforms since the 1990s. Total N output by exported crops was calculated from production figures and converted into N content using standard coefficients (Billen et al., 2009a). Total fertilisation was calculated as the sum of synthetic fertiliser and manure application, biological atmospheric N fixation by legumes, and atmospheric deposition. The details of the calculations and hypotheses are provided in the supplementary material section.

For each region, we then plotted the average N crop export per hectare cropland against total N fertilisation (figure 2.6). The data were fitted by a curve with the following equation :

$$Nexport = Ymax \times (1 - \exp(\frac{-fertilisation}{Ymax}) \tag{2.1}$$

where $Ymax$ represents the maximum yield at saturating fertilisation.

For most French agricultural regions, the trend obtained shows a general increase of total fertilisation over the 1950–2005 period, accompanied by a much more limited increase of production, thus a gradual decrease of the N use efficiency (figure 2.6 a, b).

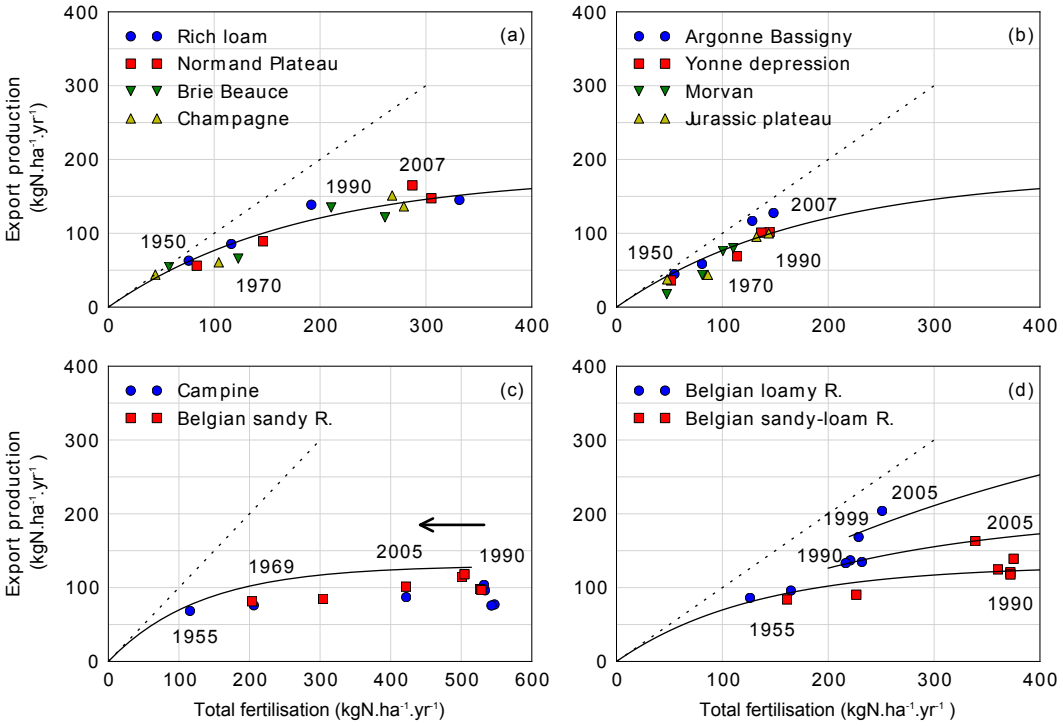

FIGURE 2.6 – N crop export vs. total N fertilisation of arable land in the different agricultural areas of the Seine, Somme and Scheldt basins from 1950 to 2005. A fitted curve with equation $Nexport = Ymax \times (1 - \exp(\frac{-fertilisation}{Ymax})$ is also indicated for each data set.

The same conclusion holds for the agricultural regions of the Scheldt basin until the 1990s, with even higher fertilisation rates and lower efficiency rates. However, changing trends have become apparent in the past few decades. In the Southern regions (figure 2.6 d), an increase in $Ymax$ can be observed, suggesting better N use efficiency and fewer losses. In the Northern regions (figure 2.6 c), the total fertilisation rate, although still quite high, has been decreasing since the 1990s. This last trend corresponds to the implementation of public policies aiming at reducing agricultural N pollution. While these policies are still only incentive in France, they were compulsory in the Walloon region of Belgium, where a public organism (Nitrawal) is in charge of systematic control through cropland soil analysis, and in the Flemish region, where treatment of livestock manure and export of N residue have been strongly encouraged by public financial support. In 2008, the Flemish region has treated and exported, respectively, 20 % and 30 % of the N and P content of its total livestock waste production.

2.5.7 Diffuse source assessment

The difference between N crop export and N fertilisation (the vertical distance between each point and the diagonal line in the diagrams of figure 2.6) represents the N-surplus, i.e. the excess fertilisation over the N taken up by crops. This surplus is available for leaching, gaseous emission or storage as organic N in the soil.

The N concentration of surface runoff characterising the different land use classes and agricultural areas of the three basins were assessed based on the assumption that, for well-drained arable soils, leaching is by far the main fate of the agricultural surplus ; when divided by the runoff depth, it provides a good estimate of NO_3[pleaseinsert\prerenderunicode{âĺš}intopreamble] concentration of sub-root water. This approach cannot be used, however, for hydromorphic soils, like those often found in Northern Belgium, where denitrification as N_2 gas is the major fate of the N surplus. Nor can it be used for permanent grassland soils, which accumulate very large amounts of N in the soil organic pool and are subject to rather limited N leaching compared to arable land. The base-flow concentration was estimated from previous studies (De Becker et al., 1985; Curie et al., 2011; Fritz, 1994; Poitevin, 1997; Roberts and Marsh, 1987; Rousseau et al., 1986; Strebel et al., 1989; Vandenberghe, 2010) on groundwater concentration available for the major aquifers of our study area (figure 2.7) ; in regions

without large aquifers, the same concentration was taken for surface and base-flow components. In the SR model, these values are used to characterise the diffuse sources of nutrients.

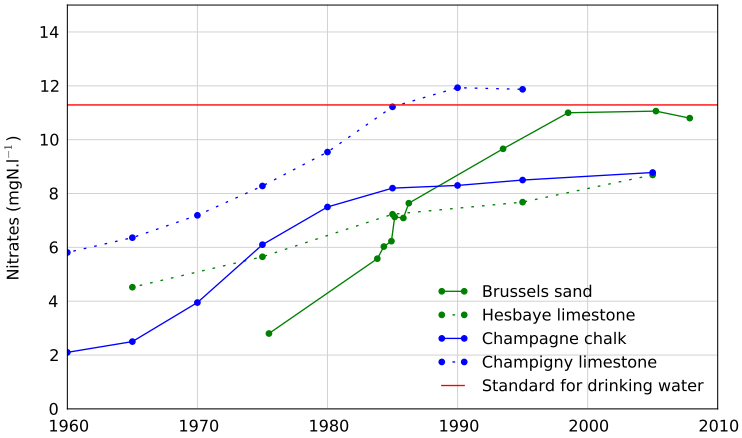

FIGURE 2.7 – Nitrate concentration in the major aquifers of the Seine, Somme and Scheldt basins (Curie et al., 2011).

2.6 Results

2.6.1 Validation of the SR model

Figures 2.8 compares SR simulations of water quality variables (nutrients, phytoplankton) at Poses (the outlet of the basin, upstream from the estuarine zone) with observations for the 1985–2007 period, provided by the Seine Normandy Water Agency (Agence de l'Eau Seine Normandie, Réseau National de Bassin). The discharge during the period varied greatly, with the driest years in 1996 and 2005 and the wettest in 2001 and 1995 (figure 2.2). We calculated three indicators of the goodness of fit of the RS simulations. The (root mean square error) RMSE :

$$RMSE = \sqrt{(\sum (vobs - vcalc)^2}$$

is a measure of the inaccuracy of the model's prediction. The bias :

$$bias = \frac{\sum (y - x)}{\sum (x)}$$

is a measure of the systematic relative over- or underestimation by the model. The Bravais-Pearson R :

$$r = \frac{cov(x, y)}{\sqrt{var(x) \times var(y)}}$$

measures how well a model fits observations (Allen et al., 2007; Krause et al., 2005). Table 2.2 gathers the values of these estimators for the most important variables. Collectively, these indicators show a generally good fit between calculation and observations for most variables, especially for P, with a highly significant Bravais-Pearson R higher than 0.5. The goodness of fit is lower for NO_3^- and NH_4^+ ; this is particularly true for the 1980s and early 1990s, probably in part because of the difficulty of obtaining reliable data on point sources of NO_3^- and NH_4^+ at that time. For phytoplankton, despite a 62 % bias, the seasonal variations are well captured.

For the Scheldt River, simulations were extracted at Kruibeke for the 1996–2007 period and at Temse for the 1984–1995 period and were compared with available data provided by the Vlaamse Milieumaatschappij (VMM), l'Unité de Gestion du Modèle Mathématique de la Mer du Nord (UGMM) and the Administration Sea and Watercourses (AWZ) (figure 2.9). The driest years were 1990 and 1996 and the wettest ones were 2001 and 1988 (figure 2.2). Regarding water quality, whereas simulations did not fit the observations as well at

Criteria	Phyto	SM	NO_3^-	NH_4^+	PO_4^{3-}	Ptot	SiO_2	O_2
Seine : Poses								
RMSE	1.52	1.39	0.06	0.04	0.01	0.01	0.15	0.10
Bias	62.43	-36.41	-8.55	-22.85	-10.90	18.52	8.16	0.92
R	0.24**	0.57**	0.09*	0.50**	0.74**	0.63**	0.38**	0.58**
Scheldt : Kruibeke								
RMSE	7.04	8.43	0.23	0.42	0.02	0.05	0.49	0.56
Bias	27.13	-15.70	-26.23	-121.22	-55.26	13.06	-8.45	-119.73
R	0.35*	0.27*	-0.20	0.35*	0.63**	0.08	0.73	0.65**
Scheldt : Temse								
RMSE			0.59	0.50	0.091	0.21		0.85
Bias			-58.05	20.70	-1.26	35.19		-92.72
R			0.55*	0.60	0.81**	0.16		0.62**

TABLE 2.2 – RMSE, bias and Bravais-Pearson R for the SR Model simulations at Poses, Kruibeke and Temse (** significance between 0.001 and 0.01, * significance between 0.02 and 0.1).

Kruibeke and Temse as at Poses using RMSE indicator, taking into account the Bravais-Pearson R, the agreement is reasonable. Besides the less numerous data for validation, the lower model performance between the two watersheds can be explained by the forcing data that were more difficult to reconstruct over the 24-years period for the Scheldt watershed. The performance of the SR model applied to the Somme could not be assessed due to insufficient observations available.

2.6.2 Interannual variations in water quality at the river outlet

Seine River. The long-term variation of NO_3^- concentrations at the outlet of the Seine River brought out two distinct periods (figure 2.8).

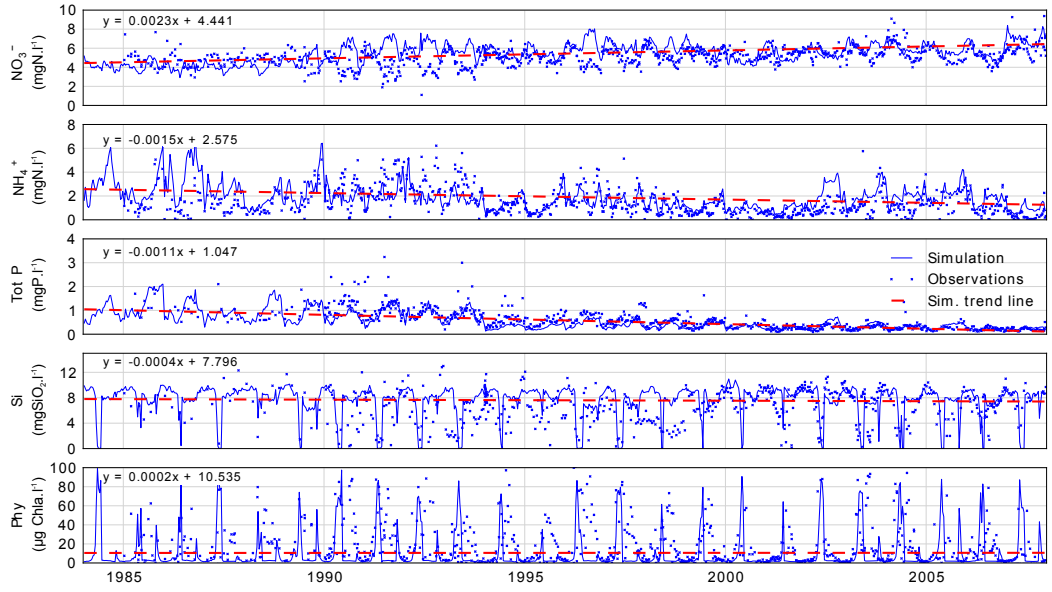

FIGURE 2.8 – Simulation of NO_3^-, NH_4^+, total P, Si, phytoplankton compared to observations at Poses for 1984–2007.

The first one, from 1984 to 1998, showed a slight NO_3^- annual increase, from 4.5 to 6.7 mgN-NO_3.l^{-1}. The period after 1998 was characterised by concentrations stabilising around 6.7 mgN-NO_3.l^{-1}. Over the period, the slope of the simulated concentration trend line in function of time shows an increase of 44.70 %. The seasonal variations follow the hydrological regime with lower NO_3^- concentrations by low discharge. Overall, the interannual variations of NH_4^+ (figure 2.8) concentrations mainly reflect the gradual improvement of wastewater

treatment as well as a trend related to the hydrological regime, with higher values at high discharge. From 1984 to the first half of the 1990s, the maximum concentrations of NH_4^+ reached 5 or 6 mgN-NH_4^+.l^{-1}, while they have not exceeded 3 or 4 mgN-NH_4^+.l^{-1} since the year 2000. From 1987 to 2007, a general decrease of 51%. The spectacular decrease in P concentrations observed (figure 2.8) was well captured by the SR model, closely related to the improvement of wastewater treatment plants. Seasonal variations again follow the hydrological regime, with higher concentrations by low discharge. In the second half of the 1980s, the maximum concentrations of phosphates reached about 2 mgP.l^{-1} with a yearly average around 1 mgP.l^{-1}. Since 2000, the maximum concentrations have been approximately 0.4 mgP.l^{-1} and the yearly average concentration less than 0.2 mgP.l^{-1}. The percentage of decrease is the highest with a value of 90 % from 1984 to 2007. Si follows a clear regular seasonal pattern with a winter maximum of 10 mgSiO_2.l^{-1} and a spring/summer depletion explained by diatom growth (figure 2.8). No clear trend is observed and the slope of the simulated Si trend line is insignificant, showing a decrease of 5 % over the period. As shown by Sferratore et al. (2006), human activities had little impact on the Si cycle, and the interannual variability was dictated by the succession of dry and wet years, which favoured or prevented algal development. Phytoplankton seasonal fluctuations mirrored the Si variations (figure 2.8), indicating that diatoms dominate the freshwater phytoplankton community. Interestingly, the spring maximum reached by phytoplankton showed significant interannual variations (40–80 μgChla.l^{-1}; figure 2.8) with no regular trend related to the long-term P decrease, suggesting that no limitation by this element has yet been reached, at least in the downstream Seine drainage network. Summer phytoplankton development at Poses, of lesser amplitude and generally dominated by green algae (Garnier et al. 1995; and unpublished data) are not well represented by the model. As green algae are very rapidly mineralized once in the salinity gradient, the simulations might not affect per se the total nutrient load delivered to the sea.

Scheldt River. Unlike in the Seine, simulated and observed NO_3^- concentrations at the Scheldt outlet were rather stable during the simulated period, i.e. varying between 4 and 6 mgN-NO_3^-.l^{-1} (figure 2.9). This is indicated by the lower value of the slope of the trend line of simulated NO3- in Kruibeke showing a slight decrease of 8 % over the period. From 1984 to the end of 1990, the simulated maximum concentrations reached 8 mgN-NH_4^+.l^{-1} with a yearly average at 4.1 mgN-NH_4^+.l^{-1}. The simulated trend of NH_4^+ (figure 2.9) showed a marked decrease after 1997, most probably in response to gradual improvement of wastewater treatment in the watershed. After 2000, the maximum simulated concentrations reached 4 and 5 mgN-NH_4^+.l^{-1} in Temse and Kruibeke, respectively, and were slightly overestimated compared to observations. Overall the decease of NH_4^+, from 1984 to 2007, is 30 %. In 2007, thanks to the implementation of the new Brussels North WWTP, the concentration was less than 1 mgN-NH_4^+.l^{-1}, still overestimated compared to observations.

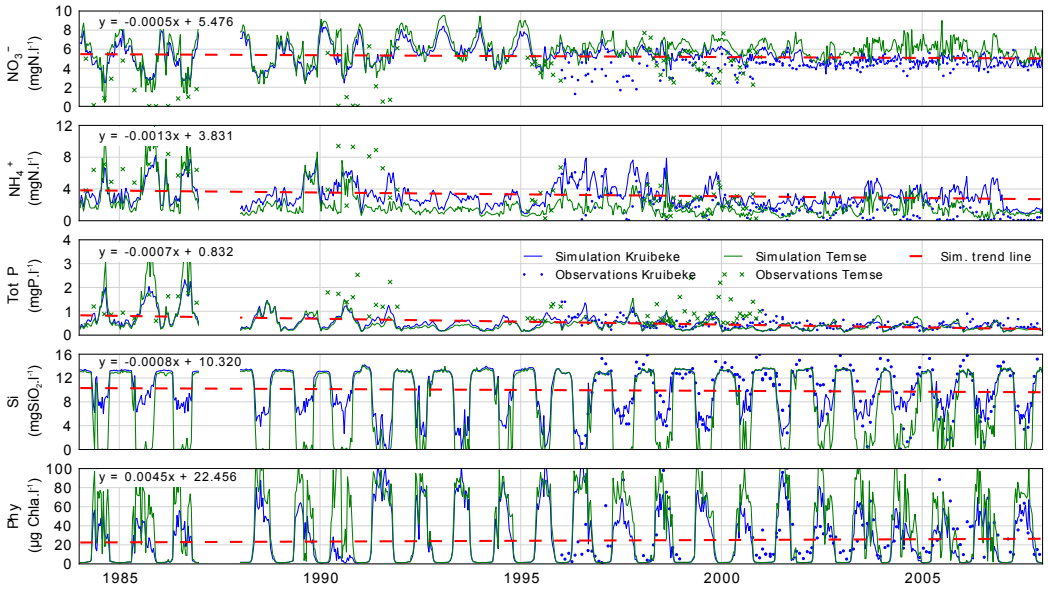

FIGURE 2.9 – Simulation of NO_3^-, NH_4^+, total P, Si, phytoplankton (compared to observations at Kruibeke and Temse for 1984–2007 (No hydrological constraints available for the year 2007).

The simulated P concentration (figure 2.9) was maximum between 1984 and 1987, amounting to 3 mgP.l^{-1} (yearly mean, 1.8 mgP.l^{-1}) but began a sharp decrease in 1989 responding to the P banishment in washing powders, slightly earlier than for the Seine (Billen et al., 1999). A second decrease is visible after 1998, corresponding to the implementation of P treatment in WWTPs (figure 2.9). Note that the purification of the agglomeration of Brussels was efficiently operating in 2007. The maximum concentrations reached in 2000 were about 1 mgP.l^{-1} and the yearly mean was approximately 0.5 mgP.l^{-1}. Consequently, the P decrease at Kruibebeke reaches 70 %.

The simulated interannual variations of Si and phytoplankton were in better agreement with the observation that those obtained in the Seine River. The minimum Si concentration occurred in summer at the time of maximal phytoplankton growth, and maximum values reached in winter (13 mgSiO_2.l^{-1}). The maximum level of phytoplankton was observed in early summer ; concentrations reached 60–100 μgChla.l^{-1} depending on the year as reported by (Kromkamp and Van Engeland, 2010).

Somme River. Concerning the interannual simulation for the Somme basin discharges ranged from 12 to 105 m^3.s^{-1}, respectively, in 1996 and 2001, with a yearly average of 36 m^3.s^{-1} (figure 2.2). Concentrations are not shown due to the lack of validation data over this long term period, see Table 2.3 for changes in simulated fluxes. However, we can mention a mean annual NO_3^- concentration increased from 5 to 7 mgN-NO_3^-.l^{-1} over the simulated period due to the large part of the basin devoted to agriculture. Total P followed the same trend as in the Seine and Scheldt watersheds and decreased from 0.3 to 0.08 mgP.l^{-1} over the simulated period. Si and phytoplankton were quite stable over the period studied, 14 mgSiO_2.l^{-1} and 7 μgChla.l^{-1} with some peaks at 30 μgChla.l^{-1} in the late 1990s.

2.6.3 Water quality in the upstream river network

The SR model provides a comprehensive simulation of water quality at any point of the drainage network of the 3S rivers, which is also of great importance for human activities (Vörösmarty et al., 2010). Figure 2.10 provides a summarising view of these results as maps of average NO3$^-$ and phosphate concentrations in all tributaries. P concentrations within rivers strongly decreased between 1985 and 2007 (figure 2.10 a, b). In 1985, ortho-phosphate concentrations in the low-order rivers of the upper parts of the basins were less than 0.16 mgP.l^{-1}. PO_4^{3-} concentrations in higher-order rivers, such as the Marne, Oise and Somme, ranged from 0.16 to 0.64 mgP.l^{-1}. In the downstream part of the Seine River, values higher than 0.64 mgP.l^{-1} were reached. The situation within the Scheldt basin was the worst due to the higher population density and PO_4^{3-} concentrations reached more than 0.64 mgP.l^{-1} in almost two-thirds of the drainage network (figure 2.10 a). The situation greatly improved in

2007 with PO_4^{3-} concentrations in most of the Seine and the whole Somme watershed less than 0.16 mgP.l^{-1}. Only PO_4^{3-} concentrations in the part of the Seine River downstream of the Parisian agglomeration remain high, ranging from 0.16 to 0.32 mgP.l^{-1}. In the Scheldt watershed, where PO_4^{3-} concentrations were less than 0.16 mgP.l^{-1} upstream, but increase rapidly to 0.32 mgP.l^{-1} or more in intermediate rivers (figure 2.10 b).

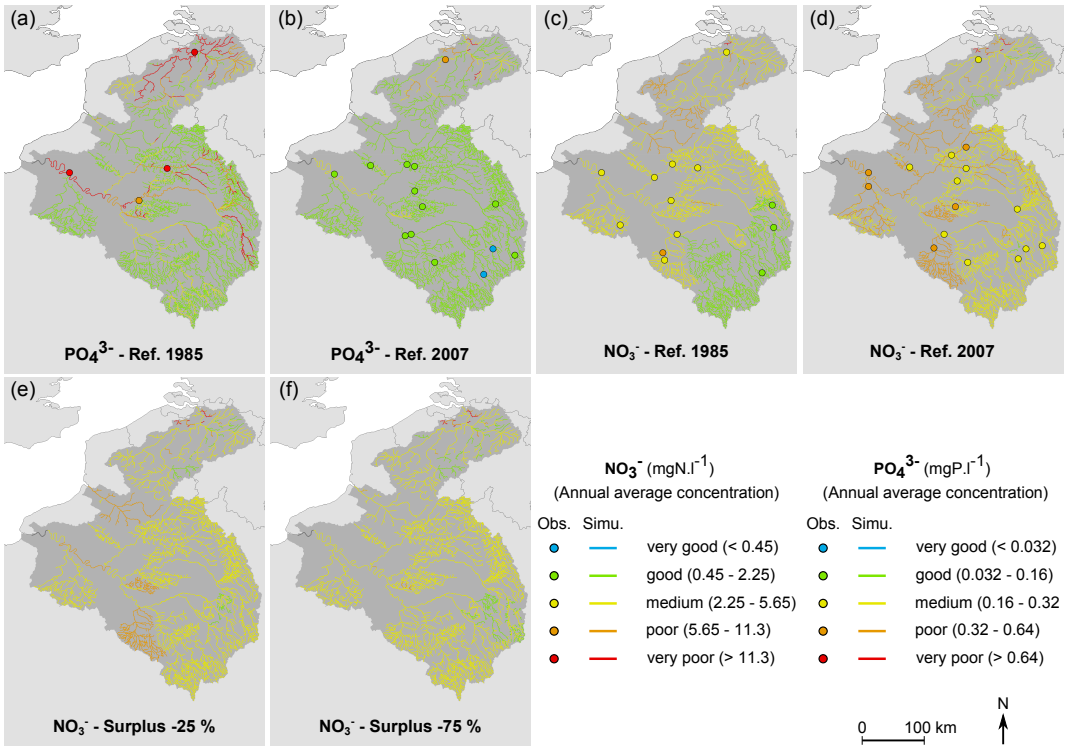

FIGURE 2.10 – P-PO_4^{3-} annual average concentrations within hydrological networks in 1985 (a) and 2007 (b), N-NO_3^- annual average concentrations within hydrological networks in 1985 (c) and 2007 (d) and with 25 % (e) and by 50 % (f) surplus decreases.

NO_3^- concentrations within the three watersheds did not follow the same trend. In 1985 NO_3^- concentrations in the upper parts of the Seine basin (Yonne, Aube, Marne) were less than 2.25 mgN-NO_3^-.l^{-1}. In the major parts of the Seine and Scheldt basins, NO_3^- concentrations were less than 5.65 mgN-NO_3^-.l^{-1}. Only in the Somme basin and in the French upper part of the Scheldt basin, did NO_3^- concentrations reach 11.3 mgN-NO_3^-.l^{-1} (figure 2.10 c). In 2007, NO_3^- concentrations were higher everywhere within the three watersheds and exceeded the value of 2.25 mgN-NO_3^-.l^{-1}. In the southern part of the Scheldt Basin, in the whole Somme basin and in several sub-basins of the Seine, NO_3^- now ranges from 5.65 to 11.3 mgN-NO_3^-.l^{-1} (figure 2.10 d).

2.6.4 Nutrient fluxes to the coastal zone

Annual specific nutrient inputs to the coastal zone are estimated from N, P and Si provided by SR simulations at the outlet of the Seine, Somme and Scheldt rivers, respectively at Poses, Abbeville and Kruibeke for the simulated period (figures 2.11). Obviously, the most striking feature is the strong dependence of these nutrient fluxes on the concomitant interannual variation of discharge, which undergoes, over the period studied, a succession of dry and wet years with a 6 to 7 years periodicity. The reduction of nutrient sources when it occurred is superimposed and somehow masked by this hydrologic trend. Thus, Si fluxes, not significantly affected by human activities, are very much dependent on hydrological conditions. Si reached a maximum in the wettest year in 2001 for the Seine (2050 kgSi.km^{-2}) (figure 2.11 a), the Scheldt (1735 kgSi.km^{-2}) (figure 2.11 b) and the Somme (2800 kgSi.km^{-2}), with annual averages of Si fluxes for the period 1984–2007 of 1005, 1130 and 1215 kgSi.km^{-2}.yr^{-1}, respectively. For the Seine at Poses, maximum N fluxes observed during the wettest years 2001 and 1995 are twice those of dry years, reaching 3175 kgN.km^{-2} and 2760 kgN.km^{-2}, respectively, versus 1415 kgN.km^{-2} and 1440 kgN.km^{-2} in 1989 and 1996 (figure 2.11 a). For

the Scheldt at Kruibeke, maximum N fluxes similarly occurred during the wettest years in 2001 and 1988, reaching 2665 kgN.km^{-2} and 2550 kgN.km^{-2}, respectively, but the minimum N flux, 1390 kgN.km^{-2}, was observed in 2007, not the driest year, reflecting in part the effect of implementation of the Brussels North wastewater treatment plant (figure 2.11 b). Regarding P inputs, a two-thirds decrease was observed at Poses from 290 kgP.km^{-2} in 1985 to 90 kgP.km^{-2} in 2007, i.e. 69 % (figure 2.11 c ; Table 2.3), by 49 % at the outlet of the Scheldt, from 210 to 110 kgP.km^{-2} (figure 2.11 d), and by 33 % at the outlet of the Somme, from 85 to 55 kgP.km^{-2} (see also Table 2.3).

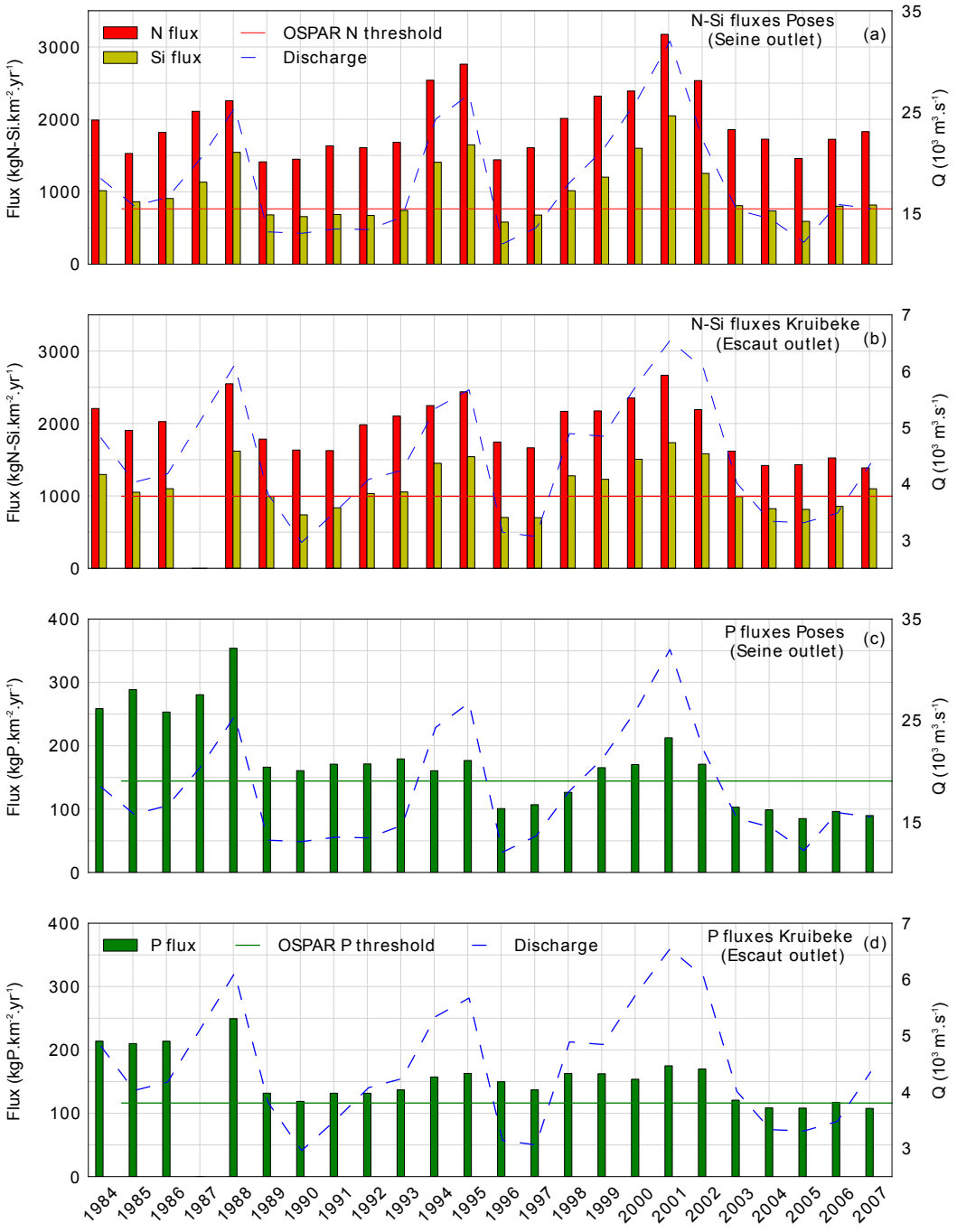

FIGURE 2.11 – SR- simulated N, Si and P annual specific fluxes delivered to the sea at Poses (a,c) and Kruibeke for 1984–2007 (b,d) (no hydrological constraints available for the Scheldt River in 1987).

The OSPAR convention recommended a 50 % reduction of N and P fluxes delivered to the Greater North Sea with respect to the reference year 1985. For rigorously assessing the degree of achievement of this recommendation, the actual fluxes in 2007 cannot be simply

	Basin	N flux	P fluxes	Si fluxes
1985	Seine	1530	290	865
	Somme	1550	85	1600
	Scheldt	1905	210	1050
2007	Seine	1830	90	820
	Somme	1845	55	1320
	Scheldt	1390	110	1100
2007 with hydro 85	Seine	1875	93	710
	Somme	2200	70	1580
	Scheldt	1100	100	970
Evolution (%)	Seine	+19.7	-68.9	-5.3
	Somme	+19.0	-33.3	-17.5
	Scheldt	-27.1	-48.7	+4.6

TABLE 2.3 – Calculated fluxes ($kg.km^{-2}.yr^{-1}$) of nutrients at the outlet of the Seine, Somme and Scheldt rivers in 1985, 2007 and using the 2007 point and diffuse sources with the hydrology of 1985.

compared to those of 1985, because of the difference in hydrological regime for the two years. In our modelling approach, hydrological forcings can be separated from anthropogenic factors (land use and agricultural practices and wastewater management). We therefore calculated the nutrient fluxes at the outlet of the 3S using the point and diffuse nutrient sources of 2007 combined with the hydrology of 1985 (Table 2.3). The differences between the runs in 1985 and in 2007 using the hydrology of 1985 can be explained only by changes in anthropogenic factors. The increase or levelling off of $N\text{-}NO_3^-$ delivered to the coast can be explained by the inefficiency of the measures taken against the agricultural diffuse pollutions. The decrease of $N\text{-}NH_4^+$ and of total P is due to the improvement in terms of urban and industrial waste waters treatment. In the case of the Scheldt basin, due to its dense urbanization, the decrease of $N\text{-}NH_4^+$ explains the decrease observed in terms of N fluxes delivered to the coast. The results (Table 2.3) show that whereas the OSPAR objective was achieved for P, the N flux in 2007 was higher (or still high) than in 1985 (1875 $kgN.km^{-2}$ vs. 1530 $kgN.km^{-2}$ for the Seine and 1845 $kgN.km^{-2}$ vs. 1550 $kgN.km^{-2}$ for the Somme, 1390 $kgN.km^{-2}$ vs. 1905 $kgN.km^{-2}$ for the Scheldt) at the same hydrology.

2.6.5 Effects on the coastal zone

The response of *Phaeocystis* blooms in the Belgian coastal zone (BCZ) to changing river nutrient inputs since 1984 were evaluated with the MIRO multi-box model forced with prevailing meteorological conditions and SR simulations of nutrient fluxes delivered by the Seine, Somme and Scheldt rivers. The results (figure 2.12) are appraised as maximum *Phaeocystis* colony cells reached (10^6 $cells.l^{-1}$) and bloom duration (days), making use of the ecological indicator of 4 10^6 $cells.l^{-1}$ determined by Lancelot et al. (2009) for scaling undesirable *Phaeocystis*. The simulated long-term evolution of *Phaeocystis* maximum abundance (figure 2.12 a) compares reasonably well with observations, although calculated peaks are often higher than observations, due to the weak temporal resolution of observed data. For instance, the observed high values in 1993 only last 8 days, while in average only 9 to 11 observed data are available per year. Nevertheless, simulation shows some 50 % reduction over the period, i.e. from 60 to 30 10^6 $cells.l^{-1}$. Using the conversion factors described in Lancelot et al. (2005), this would correspond to a chlorophyll decrease over the simulated period from 34 to 17 $mg.m^{-3}$. Despite this significant decrease, the maximum *Phaeocystis* abundance still remains well above the threshold value of 4 10^6 $cells.l^{-1}$ corresponding to a healthy ecosystem characterised by an efficient transfer of *Phaeocystis* production to higher trophic levels as defined by Lancelot et al. (2009). Over the period, the duration of undesirable *Phaeocystis* blooming defined as the number of successive days with abundance greater than 4 10^6 $cells.l^{-1}$ (Lancelot et al., 2011) decreased from 51 to 25 days (figure 2.12 b). Overall nutrient reduction measures taken on the 3S watersheds over the last two decades reduced undesirable *Phaeocystis* blooms by 50 %.

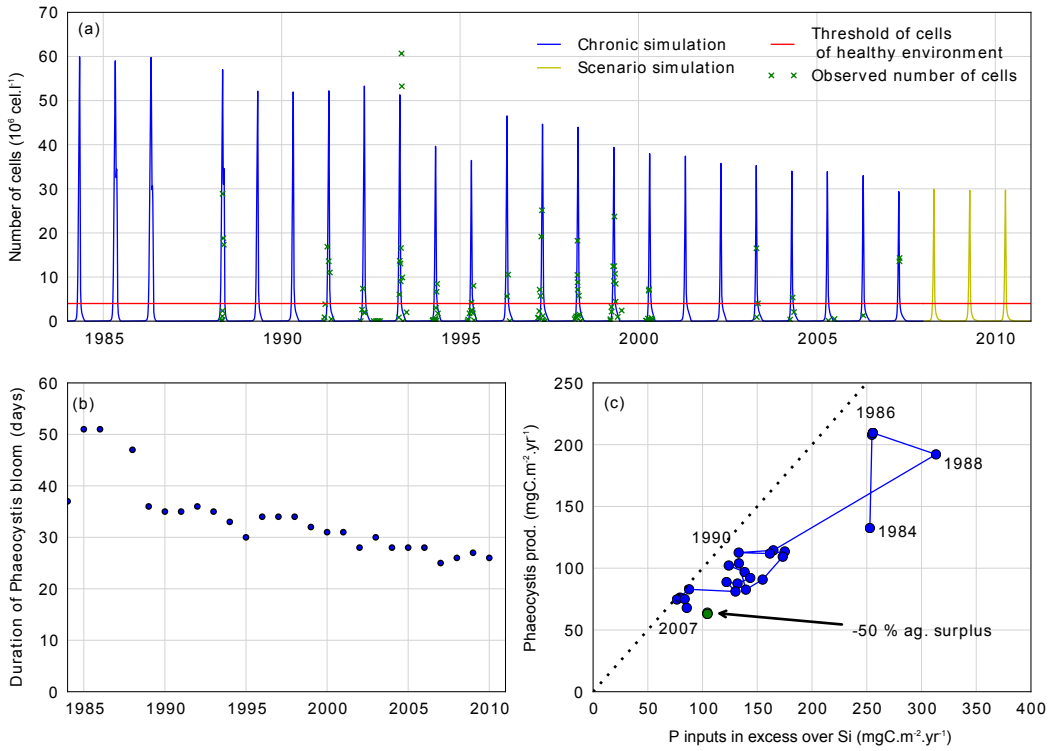

FIGURE 2.12 – Abundance of *Phaeocystis* over the 1984–2007 period and for the two scenarios explored in the BCZ in 10^6 cells.l^{-1} (a) ; duration of the *Phaeocystis* blooms for the period studied and for the two scenarios explored, in days (b) and production of *Phaeocystis* expressed in potential biomass in mgC.m^{-3}.yr^{-1} as a function of excess P input over silicon (c). The red line represents the threshold of cells of *Phaeocystis* corresponding to a healthy marine ecosystem (Lancelot et al., 2009).

The link between nutrient river enrichment and *Phaeocystis* blooms is evidenced in figure 2.12 c. On this figure the SR-MIRO annual production of *Phaeocystis* colonies in the BCZ is plotted against the calculated total annual P fluxes to the zone, directly from the Scheldt, and from Atlantic inflows enriched by the nutrient inputs of the Seine and the Somme rivers, in excess over the corresponding silicon flux, taking into account the Redfield ratios (Lancelot et al., 2011). This excess P is expressed in terms of the potential biomass of non siliceous algae which can be produced on it. This analysis is based on the assumption that diatoms are growing first, up to the exhaustion of silicon, the remaining nutrients being then used for the growth of non siliceous algae (Billen et al., 2007b; Officer and Ryther, 1980). The diagonal represents the situation where all the P in excess over silicon is transformed into *Phaeocystis* biomass, expressed in carbon unit using the Redfield ratio (figure 2.12 c). In the eighties, a large part of the P was not transformed into biomass, suggesting that N was the limiting nutrient. On the contrary in the late 2000's years, almost all the P was transformed into biomass, showing that P becomes the limiting nutrient. The results show that *Phaeocystis* annual production is controlled by P (r^2=0.63 ; figure 2.12 c) loads rather than N, which is always in excess with respect to P or Si. This is further supported when relating the annual *Phaeocystis* production to the potential eutrophication indicator ICEP (Garnier et al., 2010c) estimated from SR-MIRO N, P, Si loads to the BCZ. This indicator is primarily based on nutrient requirements by diatoms (molar C :N :Si :P = 106 :16 :16 :1 ; (Brzezinski and Nelson, 1995; Redfield et al., 1963), the excess N or P being converted to carbon as an estimate of primary production associated with agricultural eutrophication. Due to the P control of *Phaeocystis* production, the ICEP indicator is better expressed based on P excess. As shown in figure 2.12, the long-term trajectory of *Phaeocystis* production closely follows the reduction of P inputs. Moreover, the *Phaeocystis* production quantitatively matches the P excess brought into the zone, leaving only 20–30 % unutilised. No such link between *Phaeocystis* production and N input is observed. N, greatly in excess over P, is not a limiting nutrient for *Phaeocystis* production over the whole period of study. This means that a large part of N input into the BCZ is exported to the North-East, where

it can have further eutrophication effects.

2.7 Discussion

Like many river systems in densely populated and intensively cultivated regions of the world, the Seine, Somme and Scheldt rivers have been considerably enriched in both P and N with respect to the still nearly natural Si level (Howarth et al., 1996). When the OSPAR convention defined its aim of reducing by 50 % (compared to 1985 levels) the P and N delivery from land-based sources to the sea, both nutrients were in excess over Si, which resulted in severe eutrophication problems in the French and Belgian coastal waters such as toxic algal episodes in the Seine Bight (Cugier et al., 2005) and *Phaeocystis* foam accumulation in the Northern French, Belgian, Dutch and German coasts (Lancelot et al., 1987; Skaloud et al., 2006). Severe deterioration of freshwater quality within the drainage network of the 3S rivers was also caused by excess P and N inputs from the watershed, including eutrophication of large river and stagnant areas, oxygen depletion and generalised NO_3^- contamination. The measures taken by water authorities in compliance with the urban wastewater European directives (Council Directive 91/271/EEC) first consisted in increasing the sewer connection rate and improving wastewater treatment. It helped to decrease the NH_4^+ discharge to rivers by 70 % since the early 2000s, thanks to the implementation of a nitrification step (Even et al., 2007). The banishment of poly-phosphates from washing powders and the implementation of specific P removal steps in wastewater treatment led to a considerable reduction of urban P sources. The more recent and still ongoing implementation of denitrification in the largest WWTPs comprises the last phase of these efforts to reduce point sources of nutrients to surface water. Nowadays, point sources of P in the rivers studied here have been reduced to the same level as diffuse sources of this element from erosion of agricultural soils, and roughly 80 % of N originates from diffuse sources (Thieu et al., 2009). The limit of the policies devoted to point sources of nutrients is therefore close to being reached in terms of environmental improvement.

These measures have considerably improved freshwater water quality as far as NH_4^+ and P contamination is concerned. The OSPAR objective of reducing P delivery to the coastal zone by 50 % has been achieved. As a result, while N controlled *Phaeocystis* colony blooms in the 1980s, it is now P that controls eutrophication in the BCZ, and both the intensity and the duration of *Phaeocystis* blooms have been reduced by half. This shift from N to P limitation was also shown in the Adriatic Sea impacted by the nutrient loads from the Po River (Cozzi and Giani, 2011).

On the other hand, as far as N is concerned, the situation has not improved in the past 24 years. NO_3^- contamination of ground and surface freshwater resources is still a matter of great concern. River N flux delivered to the coastal zone has not been significantly reduced in spite of the OSPAR recommendations. A large amount of excess N, not used by algal growth in the BCZ, is exported to adjacent areas to the North. This situation results from the fact that no or insufficient interventions have been devoted to reducing agricultural sources of nutrients, which clearly dominate over urban sources in terms of N inputs. We suggest that the agricultural soil N surplus might be a convenient indicator to assess the efficiency of measures aiming at limiting agricultural NO_3^- losses. Our analysis of N soil surpluses in the different agricultural areas of the 3S watershed shows that these have increased considerably since the middle of the 20th century, and that recent limited reducing trends are only observed in the Walloon and Flemish areas of the Scheldt basin, while the trend is still increasing in most areas of the Seine and Somme basins (figure 2.6). Efforts to reduce N contamination of hydrosystems should aim to reduce N leaching into rivers as managing landscapes (Passy et al., 2012) or reduce agricultural N soil surpluses (Lassaletta et al., 2012), either by precision agriculture techniques (Di and Cameron, 2002; Tilman et al., 2002), good agricultural practices (Thieu et al., 2010) or by organic farming Billen et al. (2012c); Thieu et al. (2011). To illustrate the potential sensitivity of the system to such measures, we ran the SR-MIRO chain model for a scenario representing the 2007 conditions with a 25 % and a 50 % reduction of the agricultural soil surplus of all agricultural land, and assuming an immediate response of aquifers. The results show a significant decrease of NO_3^- contamination of rivers, with most waterbodies of the three watersheds reaching NO_3^- concentrations less than 5.65 mgN-NO_3^-.l^{-1}, half the standard for drinking water quality (figure 2.10 e, f). In the scenario with 50 % reduction of the agricultural surplus, the flux of N delivered to the sea would be reduced to 1215, 1070 and 1200 kgN.km^{-2}.yr^{-1} for the Seine,

Somme and Scheldt, respectively, which would meet the OSPAR target. The simulation shows, however, that no further significant effect on *Phaeocystis* blooms would be achieved, in terms of neither intensity nor duration, because N remains in excess over P, which is still controlling the algal dynamics (figures 2.12). Further limitation of *Phaeocystis* blooms will thus require additional actions to reduce P inputs to the sea, including measures addressing the diffuse sources of this element.

2.8 Conclusion

Nutrients transfers through the watersheds of the Seine, Somme and Scheldt greatly changed from 1984 to 2007. In 1985, the OSPAR reference year, the excess of P was the major problem. Within the hydrological networks, only the upstream parts had P concentrations less than 0.032 mgP.l^{-1}.Fluxes delivered to the coastal zone reached 290 kgP.km^{-2}.yr^{-1}, 85 kgP.km^{-2}.yr^{-1}, and 210 kgP.km^{-2}.yr^{-1} for the Seine, Somme and the Scheldt respectively. The decrease of P fluxes was more than 50 % from 1985 to 2007, so the OSPAR P objective is reached. Concerning N-NO_3^-, the upstream parts of the hydrological networks had N concentrations less than 2.25 mgN-NO_3^-.l^{-1}. But two thirds of the drainage network had N concentrations ranging from 2.25 to 5.65 mgN-NO_3^-.l^{-1}. In terms of fluxes at the coastal zone, 1530 kgN.km^{-2}.yr^{-1}, 1550 kgN.km^{-2}.yr^{-1} and 1905 kgN.km^{-2}.yr^{-1} were delivered by the Seine, Somme and the Scheldt respectively. N was the limiting nutrient for *Phaeocystis* development, and blooms achieved more the 60 10^6 cells per litre and lasted more than 50 days.

From 1985 to 2007, thanks to the improvement of the waste water treatment, point sources pollution greatly decreased. P, mostly originating from point sources, drastically decreased during this period. Almost all the rivers of the three watersheds have now P concentrations below 0.16 mgP.l^{-1}. Only the Seine from Paris to the estuary and sectors from intermediate rivers to main lower branch of the Scheldt Rivers has P concentrations above 0.16 mgP.l^{-1}. P fluxes delivered to the coastal zone also greatly decreased. In 2007, they are 90 kgP.km^{-2}.yr^{-1} 55 kgP.km^{-2}.yr^{-1} and 110 kgP.km^{-2}.yr^{-1} for the Seine, Somme and Scheldt respectively. Per contra, N-NO_3^- concentrations in rivers increased from 1985 to 2007. At this date, the N-NO_3^- concentrations are ranging from 0.16 to 0.32 mgN-NO_3^-.l^{-1}, in almost the two thirds of the rivers of the three watersheds. In the Loing, Somme and Eure basins, these concentrations are above 0.32 mgN-NO_3^-.l^{-1}. It is also the case for some parts of the Scheldt River and the downstream part of the Seine River. In 2007, 1830 kgN.km^{-2}.yr^{-1}, 1845 kgN.km^{-2}.yr^{-1} and 1390 kgN.km^{-2}.yr^{-1} are delivered to the coastal zone by the Seine, Somme and Scheldt respectively, the OSPAR N objective being far from reached. The same trends of P and N fluxes were reported in many places in Europe (Bouraoui and Grizzetti, 2011; Grizzetti et al., 2012).

As a whole, because of its sharp decrease, P is now the limiting nutrient in the coastal marine waters, driving the *Phaeocystis* blooms decrease, in amplitude and duration. On the other hand, the suspected role of excess N in the induction of algal toxicity in marine systems, particularly in the case of domoic acid production, pleads for a reduction of N fluxes delivered to the sea (Klein et al., 2010; Trainer et al., 2012).

This paper has illustrated the potentialities of a modelling approach coupling a watershed model with a coastal sea model to analyse the long-term trends of freshwater quality, river fluxes delivered to the sea and the response of the marine ecosystem. This type of approach is required to better target the future actions aiming at controlling water quality in the aquatic continuum from freshwater to coastal zones.

À retenir sur le passé de la cascade de nutriments

- ⋆ Avant le 20ème siècle, les pollutions ponctuelles d'origine industrielle dominaient largement dans le bassin de la Zenne.
- ⋆ L'usage du sol du bassin de la Zenne a considérablement changé entre 1770 et 2006. L'urbain (agglomération bruxelloise) s'est largement développé au détriment des prairies, des terres arables et des forêts.
- ⋆ En amont de Bruxelles, en 1790, les pollutions du réseau hydrographique restaient faibles, mais en 1890, elles avaient déjà augmenté du fait de l'industrialisation du bassin, notamment en ce qui concerne l'ammonium, le carbone et le phosphore.
- ⋆ Une dynamique similaire s'observe à l'aval de Bruxelles mais, avec une pollution beaucoup plus importante en 1890, où ammonium, carbone et phosphore ont atteint des sommets, respectivement 120 $mgN.l^{-1}$, 75 $mgC.l^{-1}$ et 6 $mgP.l^{-1}$.
- ⋆ Les flux d'azote et de phosphore ont présenté des pics en 1890, respectivement 50.6 $kgN.km^{-2}.jr^{-1}$ et 2.3 $kgP.km^{-2}.jr^{-1}$, résultant dans des ICEP N et P très élevés (284 et 90 $kgC.km^{-2}.jr^{-1}$ respectivement).
- ⋆ À l'échelle des bassins de la Seine, de la Somme et de l'Escaut, depuis 1950 les régions agricoles se sont spécialisées soit en élevage intensif soit en culture intensive.
- ⋆ La fertilisation azotée a augmenté dans toutes les régions, puis a commencé à baisser dans les années 1990 dans certaines (en Belgique par exemple) et à continuer à augmenter dans d'autres (les régions de grande culture du bassin de la Seine).
- ⋆ Les apports azotés ont augmenté plus vite que l'export d'azote par les cultures, engendrant une augmentation des surplus. Seules les régions agricoles belges voient leurs surplus diminuer depuis la fin des années 1990. Les régions plus forestières ou liant élevage et culture présentent des surplus moins importants (Morvan, Yonne, plateau Jurassique).
- ⋆ La contamination des nappes des 3S s'approchent du seuil de 11.3 $mgN.l^{-1}$.
- ⋆ À l'exutoire de la Seine (à Poses), aucune diminution des concentrations de nitrates n'est observée entre 1984 et 2007. Ces concentrations restent aux alentours de 7 $mgN.l^{-1}$ en été. Par contre, du fait de l'amélioration des stations d'épuration, les concentrations en ammonium et en phosphore diminuent. Les premières passent de plus de 5 $mgN.l^{-1}$ en 1984 à moins de 2 en 2007, et les secondes de 2 $mgP.l^{-1}$ en 1984 à moins de 0.5 en 2007.
- ⋆ À l'exutoire de l'Escaut, une dynamique similaire est observable. Cependant, du fait la plus forte densité de population du bassin, la diminution des pollutions ponctuelles est plus marquée. Si les concentrations en nitrates restent aux alentours de 6 $mgN.l^{-1}$, les concentrations en ammonium passent de 8 à moins de 2 $mgN.l^{-1}$ et celles de phosphore de plus de 3 à 0.5 $mgP.l^{-1}$.
- ⋆ Au sein du réseau hydrographique, les concentrations en phosphore ont nettement diminué entre 1984 et 2007. La quasi totalité du réseau est passé de *pauvre* à *bon*. Par contre, les concentrations en nitrates ont eu tendance à augmenter. Les parties amont étaient classées comme *bons* en 1984, alors qu'en 2007, tout le réseau est *moyen* ou *pauvre*. Une réduction des surplus de 25 ou 75 % améliorerait la situation.
- ⋆ Les flux d'azote à l'exutoire de la Seine n'ont pas diminué sur les 24 dernières années. Leurs fluctuations suivent essentiellement les fluctuations hydrologiques. Ils se situent toujours au dessus de 1500 $kgN.km^{-2}.yr^{-1}$, ce qui est largement supérieur à l'objectif OSPAR de 900 $kgN.km^{-2}.yr^{-1}$. Seuls les flux de phosphore ont diminué, passant de 250 $kgP.km^{-2}.yr^{-1}$ en 1984 à 100 $kgP.km^{-2}.yr^{-1}$ en 2007, remplissant l'objectif OSPAR de 145 $kgP.km^{-2}.yr^{-1}$ dès 2003.
- ⋆ Les flux N et P suivent une tendance similaire à l'embouchure de l'Escaut. Les flux d'azote sont passés de 2000 à 1400 $kgN.km^{-2}.yr^{-1}$ (soit, toujours au dessus de l'objectif OSPAR), et ceux de phosphore de 200 à 100 $kgP.km^{-2}.yr^{-1}$, atteignant l'objectif OSPAR en 2004.
- ⋆ La durée des efflorescences algales en zone côtière a diminué, passant de 50 à moins de 30 jours. Leur intensité a également diminué, passant de 60 millions de cellules 30 millions. Cette baisse est avant tout gouvernée par la diminution des apports en phosphore.

Deuxième partie

Les zones ripariennes dans le cycle de l'azote

« Une erreur originale vaut mieux qu'une vérité banale. »

Fiodor Dostoïevski

Cette partie II se focalise sur le rôle que jouent les zones rapariennes sur le cycle de l'azote au sein des bassins versants. Ces zones de transition entre les écosystèmes terrestres et aquatiques sont à l'origine d'un abattement du nitrate mais peuvent également être à l'origine d'une émission d'oxyde nitreux au fort pouvoir de réchauffement atmosphérique.

Le chapitre 3 reprend intégralement l'article :

Budget of N_2O emissions at the watershed scale : role of land cover and topography (the Orgeval basin, France), *Guillaume Vilain, Josette Garnier, Paul Passy, Marie Silvestre, and Gilles Billen*, *Biogeosciences*, mars 2012, *doi 10.5194/bg-9-1085-2012.*

Il met en évidence le rôle de la topographie et notamment des zones de bas de pente et riparienne dans les émissions d'oxyde nitreux, dans le bassin de l'Orgeval en Seine-et-Marne.

Le chapitre 4 n'a pas fait l'objet d'une publication mais s'inscrit dans la continuité du chapitre 3. Il s'intéresse au pouvoir dénitrifiant des zones rapariennes à l'échelle des bassins du Grand Morin et de la Seine. Il tente de mettre en évidence le facteur essentiel à la dénitrification dans les zones rapariennes, en testant le lien entre l'abattement du nitrate et l'usage du sol, la largeur de la zone riparienne ou le substrat géologique.

La position des zones rapariennes dans la cascade de l'azote traité dans cette partie est representé sur la figure 2.13.

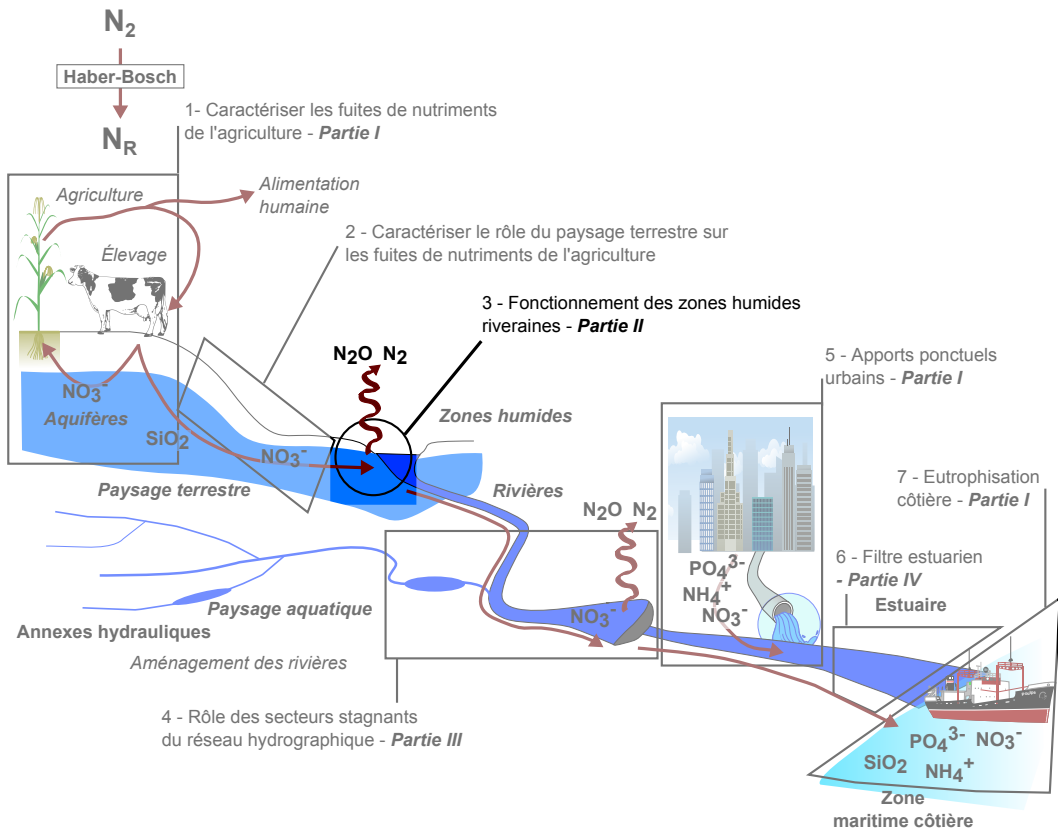

FIGURE 2.13 – Poste de la cascade de nutriments traité dans la partie II.

Chapitre 3

Budget of N_2O emissions at the watershed scale : role of land cover and topography (the Orgeval basin, France)

3.1 Abstract

Agricultural basins are the major source of N_2O emissions, with arable land accounting for half of the biogenic emissions worldwide. Moreover, N_2O emission strongly depends on the position of agricultural land in relation with topographical gradients, as footslope soils are often more prone to denitrification. The estimation of land surface area occupied by agricultural soils depends on the available spatial input information and resolution. Surface areas of grassland, forest and arable lands were estimated for the Orgeval sub-basin using two cover representations : the pan European CORINE Land Cover 2006 database (CLC 2006) and a combination of two databases produced by the IAU IDF (Institut d'Aménagement et d'Urbanisme de la Région d'Ile-de-France), the MOS (Mode d'Occupation des Sols) combined with the ECOMOS 2000 (a land-use classification). In this study, we have analyzed how different landcover representations influence and introduce errors into the results of regional N_2O emissions inventories. A further introduction of the topography concept was used to better identify the critical zones for N_2O emissions, a crucial issue to better adapt the strategies of N_2O emissions mitigation. Overall, we observed that a refinement of the land-cover database led to a 5 % decrease in the estimation of N_2O emissions, while the integration of the topography decreased the estimation of N_2O emissions up to 2 %.

3.2 Introduction

Nitrous oxide (N_2O) is mainly produced by the microbial-mediated processes of nitrification and denitrification in soils. Its formation is influenced by several factors : climate (rainfall, temperature), soils (physical and chemical composition), substrate availability (nitrogen and carbon) as well as land management practices (Vilain et al., 2010; Skiba et al., 1998; Smith et al., 1998).

While the processes of N_2O production occur on a scale of less than one centimeter (i.e. the micro-scale or process scale), N_2O emissions are usually measured at scales of several centimeters to several hundred meters (Schimel and Potter, 1995). For example, a measurement at a single point (the point scale) could either be representative of emissions from a closed chamber with an area of typically 0.1–1 m^2 or a micro-meteorological measurement of typically 105 m^2 (10 ha) area, with the aim of obtaining results at the point scale that would reflect the micro-scale process and to extrapolate these measurements at the regional (possibly global) scale (Bouwman, 1996; Bouwman et al., 2002a,b).

However, the point scale can vary substantially (Rolston and Folorunso, 1984), because of the heterogeneity of denitrification activity or the presence of « hot spots » in soil (Ambus and Christensen, 1994; van den Heuvel et al., 2009). As a result, the N_2O fluxes emitted from soils at the observation scale show a high degree of spatial and temporal variability (Parton

et al., 1998; Rolston and Folorunso, 1984) with coefficients of variation on the order of 500 % (Folorunso and Rolston, 1985). Therefore, the predictive relationships between N_2O fluxes and their associated control variables are very difficult to define (Corre et al., 1996).

A large number of simulation models have been developed to predict N_2O emissions, each one having its own philosophy and performance : STICS-NOE (Brisson et al., 2003; Hénault et al., 2005), DNDC (Li, 1996; Giltrap et al., 2010), CERES-EGC (Jones, 1984; Gabrielle et al., 2006b), NGAS (Parton et al., 1996, 2001) or DAYCENT (Parton et al., 1998; Del Grosso et al., 2001), and Image (Bouwman et al., 2006). The N_2O simulation models can be classified into three main categories : laboratory, field and regional/global levels.

Extrapolated data of N_2O emissions at the local (1–100 km) or regional (100–100 000 km) scale from point-scale measurements can be achieved using an intermediate scale, such as the plot (from 100–1000 m). A first source of error can be introduced by the scale and the accuracy of different land cover maps (DeFries et al., 2004; Bach et al., 2006; Schmit et al., 2006; Verburg et al., 2006). The high relation between land use and N_2O emissions highlights the importance of the land cover data when carrying out N_2O emissions inventories (Plant, 1999; Matthews et al., 2000).

Evidencing the relationship with landscape makes it possible to partition the land into units defined by the relief (topographic attributes) and land use. A significant selection of sampling units (topography) may thus allow the extrapolation of flux measurements collected at points within these units (Corre et al., 1996).

This study aims to establish a nitrous oxide budget at a sub-basin scale of 100 km^2 (taking into account both direct and indirect emissions from groundwater and rivers). One of the objectives was to analyze how different land cover representations potentially introduce errors into the estimations of regional N_2O emissions inventories. A second major challenge was to assess the effect of topography on the estimation of the N_2O emissions at the basin scale. Accordingly, we then discussed agri-environmental measures that can decrease N_2O emissions as well as increase water quality.

3.3 Study site

The Orgeval basin belongs to the Seine basin (France) and is located approximately 70 km east of Paris. The whole study basin covers around 106 km^2. Annual rainfall is about 700 mm and the climate is semi-oceanic. The mean annual temperature is between 10 and 11 ° C ; the coldest month being January (mean temperature, 0.6 ° C) and the warmest August (mean air temperature, 18 ° C). The Orgeval watershed is particular in that it is highly homogenous in terms of pedology, climate and topography (mean altitude, 148 m, with few slopes except in the valleys).

Most of the Orgeval catchment surface is covered with a quaternary loess deposit (up to 10 m thick). The top layer comprises loess silt and the sublayer is enriched in clay, in winter producing a shallow water table and waterlogged soils due to its low permeability. Underneath the loess layer, two tertiary aquifer formations separated by discontinuous grey clay and a loamy gypsum layer interact with the streams (Mégnien, 1979). The shallowest formation is the Brie Limestone Oligocene formation, with a relatively short water residence time. The deepest formation is the Champigny Limestone Eocene, with a longer water residence time. The river incises all layers in its lower course and when the valley cuts through the impermeable green clay layer ; springs located at the bottom of the Brie Limestone formation emerge and join the river. Most of the basin's surface area is artificially drained (about 90 % of the usable agricultural area) and dominated by agricultural land (82 %, i.e. 87 km^2) ; the remaining surface is covered by woods (17 % of the surface, i.e. 19 km^2) and urban zones or roads (1 % of the surface) (figure 3.1). Agriculture is dominated by grain crop rotation (with wheat, maize and barley) and field beans as the main rotation.

3.4 Material and methods

3.4.1 Laboratory determination of nitrification, denitrification and nitrous oxide production potentials in batch slurries

Emissions sources of nitrous oxide were assessed in laboratory experiments. Soils of the transect were placed in ideal optimal conditions for nitrification and denitrification to determine the maximum nitrification and denitrification rates as well as the nitrous oxide

production by the two mechanisms and the ratio of (N_2O produced)/(nitrate reduced or produced). Briefly, five experiments were carried out to determine the mean nitrification and denitrification potentials in 2009 and 2010 at various seasons and cropping conditions. For each experiment, soil samples were collected in two different locations along the slope (i.e. slope and footslope) and incubated for 4 h to 6 h in triplicates, at laboratory temperature (20 °C), in the dark, in oxic or anoxic conditions, and N substrate addition (NO_3^- saturation and anoxia for denitrification ; NH_4^+ saturation and oxic conditions for nitrification) (see Garnier et al. (2010c) for the methodology, results in Vilain et al. (2012), Vilain et al., unpublished data).

3.4.2 Soil N_2O flux in situ measurement

The nitrous oxide flux measurements were conducted weekly to bimonthly using the closed-chamber technique (Hutchinson and Livingston, 1993). This method, fully described in Vilain et al. (2010), consisted in measuring the gas fluxes from series of five aluminum non-vented and hermetically closed chambers (open bases of 50 cm cm cm). Four gas samples were taken from each chamber headspace with a 30 mL Terumo syringe and transferred to a 12.5 mL pre-evacuated glass vial (Labco Exetainer) for transport to the laboratory. N_2O concentrations in gas samples were analyzed in the laboratory using a gas chromatograph (Varian 3800) coupled with an electron capture detector (ECD). The gases were separated on a pre-column and a column packed with a Hayesep Q 80/100 mesh. Concentrations were calculated by comparing peak areas integrated with those obtained with standard N_2O concentrations (0.205, 0.540 and 3.30 ppm). N_2O fluxes were determined by calculating the linear regression slope of the N_2O concentration as a function of the sampling time (Livingston and Hutchinson, 1995) and adjusted for area and chamber volume. A sample set was accepted only when it yielded a statistically significant linear regression R^2 value according to the number of values taken into account.

Measurements (21 dates from May 2008 to August 2009) were taken on two agricultural plots chosen along a north-westward falling slope reaching the Avenelles River with an average inclination of 6 % in five topographical landscape positions from the shoulder to the footslope position. During this time period, plots were successively cropped to wheat/barley, an oat intercrop and corn. The sampled field can be assumed to be representative of the whole Orgeval watershed in terms of agricultural practices and especially fertilizer application.

3.4.3 Digital maps

Land use

The estimation of land-cover-based nitrous oxide emissions from the Orgeval basin is based on land use maps of the basin. Two databases with different resolutions were compared. The first one is the pan-European CORINE Land Cover 2006 database (CLC 2006) produced by the European Environmental Agency (EEA, 2007), which classifies lands into 44 classes. The minimum size of each polygon is 25 hectares. The database homogeneously covers the study area and using high-level aggregation classes (third level), the Orgeval basin is distributed into four CLC 2006 classes : arable land (class codes 211 and 242) with 79.08 %, forests (classes 311 and 324) with 19.57 %, grassland (class 231) with 0.76 % and urban areas (class 112) with 0.59 %. Giving the relatively small scale of the study area (104 km^2), the CLC 2006 database lacks precision and underestimates the area covered by grass and urban lands due to their fragmented nature (often less than 25 ha) (figure 3.1, left panel).

To correct this imprecision, a second database was used : it is a combination of two databases, both produced by the Institut d'Aménagement et d'Urbanisme de la Région d'Ile-de-France (IAU IDF, Urban Planning and Development Agency for the Paris Ile de France Region). The MOS (Mode d'Occupation des Sols, Land use) is a land-use classification in 81 classes covering the Ile-de-France region with a geometric precision of 1/5000 (IAU, 2005a). The 25-m resolution raster, available free of charge on their website (http://www.iau-idf.fr/cartes/cartes-et-donnees-a-telecharger/donnees-a-telecharger.html), was used. It corresponds to the year 2003 and the classes are aggregated into 11 items. The MOS is mainly designed for urban planning ; therefore seven out of the 11 classes detail urban land types and grasslands are aggregated with arable lands. This database was thus combined with the ECOMOS 2000, a land use classification also produced by the IAU IDF and available on their website (IAU, 2005b). It details the « natural » classes from the MOS 1999

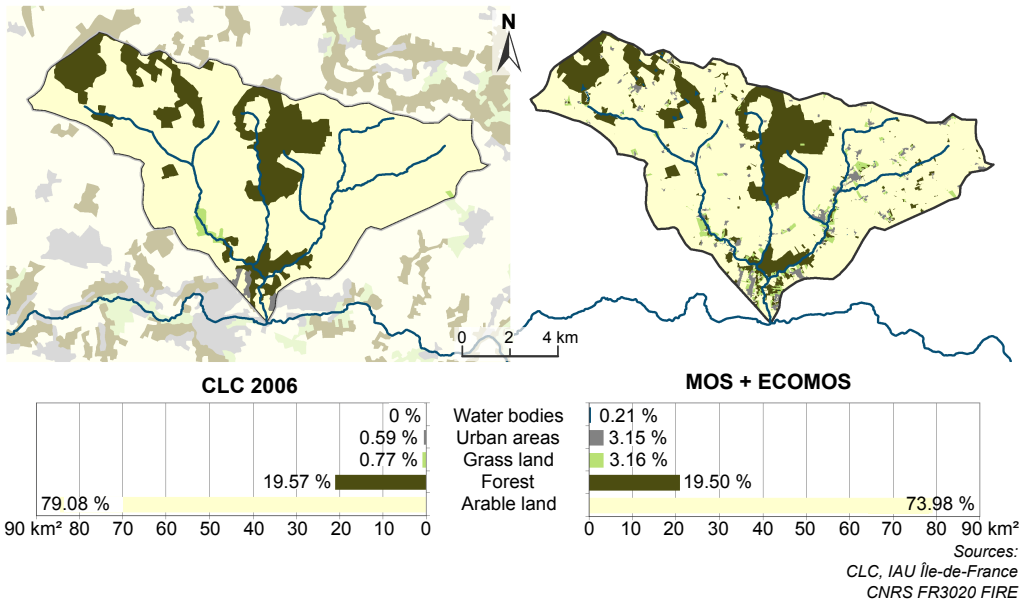

FIGURE 3.1 – Land use in the Orgeval basin in terms of forest, grassland and cropland. Urban areas are shaded grey. The drainage network is also indicated.

(forest and agricultural land) into 146 classes (distributed in six levels), excluding arable lands. The ECOMOS maps 2000 m^2 polygons. The third level was used to extract forests and grasslands that were merged with the vectorized MOS data, thus dividing the « natural » classes into arable land, grassland and forest. For the Orgeval basin, this new combined land-use database (MOS + ECOMOS) gives : 73.98 % arable lands, 19.50 % forests, 3.16 % grasslands, 3.15 % urban areas and 0.21 % water bodies (figure 3.1, right panel).

The use of MOS + ECOMOS instead of CLC 2006 helps to accurately take grassland into account, reducing the part of cropland by almost 6 %.

Topographic index

To extend the analysis even further, we developed an index to differentiate topographical landscape positions on cropland, as this was shown to largely influence the N_2O emissions (Pennock et al., 1992, 1993; Izaurralde et al., 2004; Vilain et al., 2010). The topographical index was first suggested as an indicator for surface runoff contributing areas by Kirkby (1975) and was the basis for the rainfall-runoff model called TOPMODEL (Beven and Kirkby, 1979). The most commonly used form of the index is defined as

$\ln(\alpha / \tan\beta)$

where α is the upslope contributing area to a given point of the catchment and β is a local surface slope angle (Beven, 2001). This index represents the propensity of any point to become saturated. High topographic index values are good general indicators of wetlands (Curie et al., 2007; Merot et al., 2003). In this study, the topographic index was adapted into a Concentration Flux Position index (figure 3.2) (CFP index). Indeed high values of topographic index are a good indicator of wetness, but slope and shoulder positions are not well discriminated by a low value of this topographic index. We then built this CFP index by mixing the topographic index map and the slope map, allowing a clearer distinction between the footslope, slope and shoulder positions. The topographic index map was calculated from a 25-m resolution digital elevation model produced by the Institut Géographique National (IGN) and is divided into three classes following the landscape segmentation approach proposed by Pennock et al. (1987) :

1. The footslope class corresponds to areas where the topographic index is greater than the threshold value of 13 (Curie et al., 2007). These areas with high topographic index values represent areas that are likely to be saturated. This class corresponds to the thalwegs and to areas located immediately at the foot of prominent reliefs such as buttes.

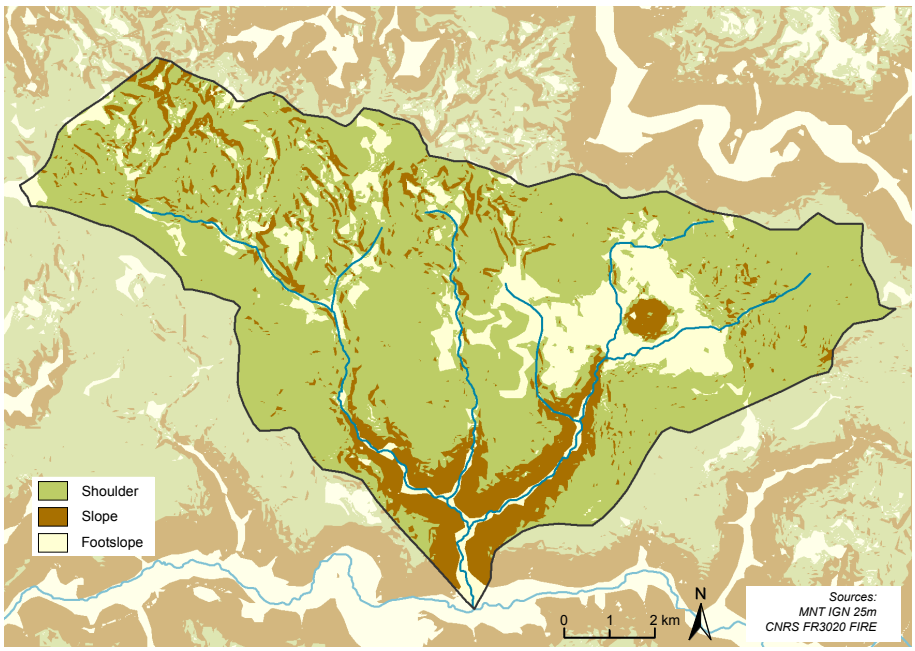

FIGURE 3.2 – Topographical map of the Orgeval basin.

2. The slope class was determined using the slope map without any topographic index threshold. This class corresponds to the areas where the slope is greater than 2 %.
3. The shoulder class corresponds to the areas where the slope is less than 2 % and the altitude higher than 100 m without any topographic index threshold.

Upscaling methods

Applying the three landscape position classes to the cropland class of the land-use databases (CLC 2006 and MOS + ECO-MOS) allowed us to upscale N_2O emissions to the Orgeval basin scale with two new approaches : topography crossed with CLC 2006 and topography crossed with (MOS + ECOMOS).

3.4.4 Water sampling

River

Dissolved N_2O concentrations in river water were monitored monthly in the Orgeval basin from January 2008 to December 2009. First to third-order streams (Strahler stream order are used to define stream size based on a hierarchy of tributaries, first order being the smallest permanent stream) were sampled (figure 3.3) and considered representative of all of the watershed's streams. Water samples from the river were directly taken in the riverbed in a 2 L bottle and transported to the laboratory for further analysis after storage at 4 °C. Water samples for N_2O were directly collected in 100 mL glass flasks, without air bubbles, fixed with HgCl2 6 % in order to stop any biological activity, and sealed with a rubber septum excluding any headspace gas.

Groundwater

Three piezometers were installed along a transect over an elevation gradient (mean slope, 2.2 %) from agricultural fields toward the stream including three slope positions (Vilain et al., 2011) : (i) plateau, (ii) midslope and (iii) river bank. The two piezometers in the plateau and midslope were inserted at a 15 m depth and reached the phreatic groundwater of the Brie. The piezometer situated in the River bank was inserted at a 3 m depth and reached the green clay layer. All were slotted on the bottom 1 m and wrapped with a 250 μm seamless polyester filter sock to prevent coarse sand particles from entering the well. Groundwater was sampled using an immerged pump from April 2008 to April 2010, with the piezometer

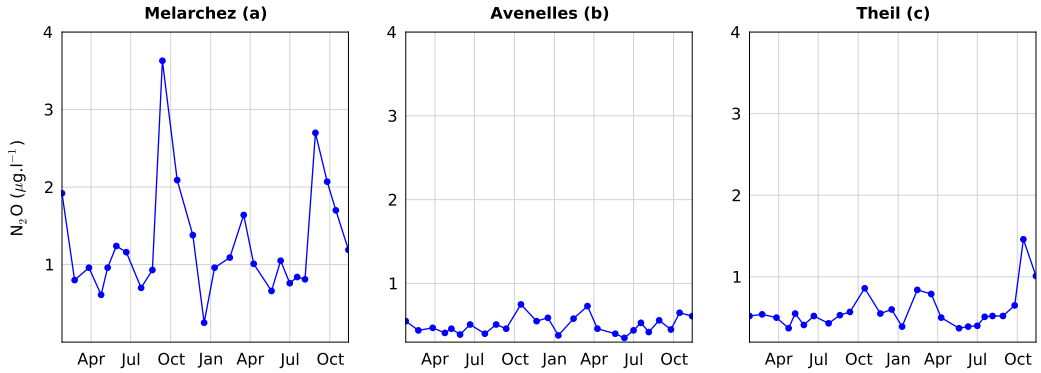

FIGURE 3.3 – Nitrous oxide concentrations between January 2007 and December 2008 in rivers at : Mélarchez, first order (a) ; Avenelles, second order (b) and Theil, third order(c).

emptied by flushing out water prior to collecting the sample in order to remove the standing water. Water samples were treated the same way as river samples.

3.4.5 Chemical measurement

Dissolved inorganic nitrogen

Ammonium was measured on filtered water (GF/F 0.4 μm porosity) with an autoanalyzer (Quaatro, Bran and Luebbe) using the indophenol blue method (Slawyk and MacIsaac, 1972). Nitrate was measured on filtered water, after cadmium reduction to NO_2^- , and NO_2^- was also automatically measured with the sulphanilamide method according to (Jones, 1984) prior to cadmium reduction of NO_3^- .

Dissolved nitrous oxide

Nitrous oxide in water samples was determined with a gas chromatograph (Perichrom PR 2100) equipped with an electron capture detector (ECD). An aliquot (20 mL) of the water sample was degassed with an argon–methane (90/10) mixture, trapped and concentrated in a molecular sieve. After desorption, N_2O concentrations were determined in triplicate.

3.4.6 Calculation of indirect emissions by rivers and aquifers

River

The N_2O flux across the water–atmosphere interface (F) can be calculated for each stream-order river of the Seine drainage network according to the relation :

$$F = K_{N_20} - N_20_{Eq} \tag{3.1}$$

with :
F, (μg m^{-2} h^{-1}) : flux of N_2O from the water column to the atmosphere
[N_2O], (μgN L^{-1}) : is the mean N_2O concentration in river water
[N_2O]$_{Eq}$, (μgN L^{-1}) : is the concentration at saturation for the atmospheric N_2O concentration
K_{N_20}, (m h^{-1}) : is the gas transfer velocity
The saturation concentration of N_2O in water at the present ambient atmospheric concentration (310 ppb) was determined using temperature-dependent values of N_2O solubility in water. This solubility can be expressed by the following polynomial relationship :

$$N_20_{Eq}, (\mu g N L^{-1}) = 0.0002T^2 - 0.0167T + 0.5038 \tag{3.2}$$

where T is the temperature in $^\circ$C.
According to the work by Wanninkhof (1992) and Borges et al. (2004), the gas transfer velocity K_{N_20} (m h^{-1}) in rivers, under conditions where the wind speed can be ignored, can be expressed as :

$$K_{N_20} = 1.719[(600/Sc_{N_20}) \times (v/d)]^{0.5} \tag{3.3}$$

Order	Surface water area (km^2)	Summer flux ($mgN\ m^{-2}\ d^{-1}$)	Winter flux ($mgN\ m^{-2}\ d^{-1}$)
First	0.1709	8.91 ± 7.65	4.67 ± 2.76
Second	0.0654	1.17 ± 0.47	0.84 ± 0.50
Third	0.0171	1.03 ± 0.45	1.05 ± 0.94

TABLE 3.1 – Nitrous oxide fluxes at the water–air interface for the summer and the winter period for different stream orders of the Orgeval basin.

with :
v ($m\ s^{-1}$) : is the water flow rate d (m) : is the depth of the water column
The values were validated by field experiment in the studied area (figure 3.6, (Garnier et al., 2009b).

Sc_{N_2O} : is the Schmidt number, defined as the ratio between kinematic viscosity and mass diffusivity. It expresses the effect of temperature and the specificity of N_2O with respect to other gases on gas transfer properties. The Schmidt number for N_2O can be expressed as (Jähne et al., 1984) :

$$ScN_2O = 2056 - 137T + 4.317T^2 - 0.05435T^3 \tag{3.4}$$

The corresponding surface areas and N_2O fluxes from rivers of each stream order in the Orgeval river drainage network, under typical high-flow and low-flow conditions, are gathered in table 3.1.

Groundwater

Indirect emissions from groundwater can be estimated using hydrogeological data. We assumed that all the N_2O in the groundwater discharge is released into the atmosphere from agricultural drains or directly by diffusion from the water table to the unsaturated zone (Garnier et al., 2009b), and we used the estimated daily groundwater N_2O concentrations based on two-weeks interval measurements (considering a constant concentration rate beginning with the date of each sampling until the next sampling) and the daily water flow, for the Avenelles sub-basin (4570 ha). Then the N_2O flux emerging at springs can be estimated using the relation described by Verhoff et al. (1980) :

$$Flx = \frac{\sum C_i Q_i}{n \times a} \times 365 \tag{3.5}$$

Where Flx = N_2O flux, in $kgN\ ha^{-1}\ yr^{-1}$,
C_i = discrete instantaneous concentration ($kg\ N_2O\text{ -}N\ L^{-1}$),
Q_i = instantaneous discharge ($L.s^{-1}$,
n = study duration (days),
a = sub-basin area (ha)

3.5 Sources, emissions and transfer of nitrous oxide at the continuum scale

3.5.1 Nitrous oxide production by nitrification and denitrification in soils

Although the potential rates of nitrate reduction and production by denitrification and nitrification, respectively, are on the same order of magnitude, a very significant difference occurs when regarding both the nitrous oxide production and the ratio of nitrous oxide produced by the two mechanisms (figure 3.4). In order to determine the main mechanism responsible for the nitrous oxide concentrations in the groundwater, it is interesting to note that the ratio of N_2O produced by nitrification of 0.28 % is close to the mean ratio found in the plateau piezometer (0.26 %; (Vilain et al., 2010)). On the other hand, regarding the seasonal peaks observed either after fertilization or heavy autumn rainfalls, they can be much higher and closer to the 45 % ratio found by denitrification in laboratory. From these measurements and laboratory experiments we can assume that over a year, nitrification

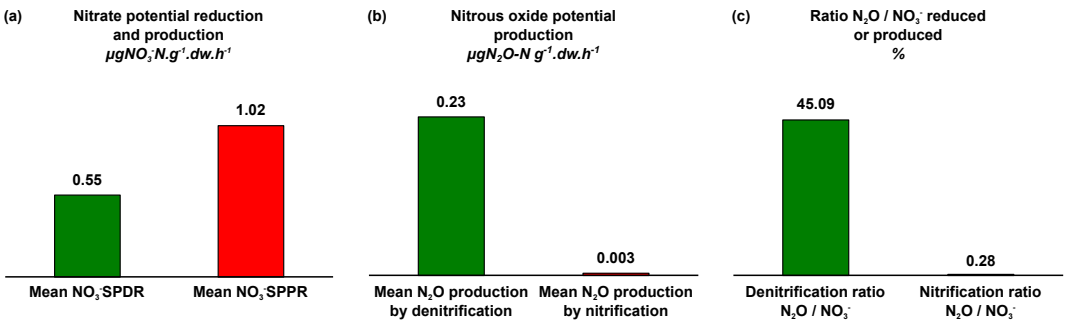

FIGURE 3.4 – Results of batch slurries : (a) potential rates of nitrate reduction by denitrification and production by nitrification ; (b) potential N_2O production and (c) ratio of N_2O production to nitrate reduced (denitrification) or produced (nitrification).

would be the process which occurs most often in soils across the landscape. On the contrary, the denitrification process would occur in fewer occasions and rather in some wet hotspots (such as the footslope positions) during specific conditions such as fertilizer application associated with a higher soil moisture and hypoxia (e.g. high rainfall), conditions necessary for the denitrification process to take place (Bateman and Baggs, 2005; Davidson and Schimel, 1995; Linn and Doran, 1984). However, quantitatively the denitrification contribution can produce a great part of N_2O as the amounts of N_2O produced by denitrification are much greater than by nitrification (see the N_2O / NO_3^- ratios).

3.5.2 Measured N_2O fluxes in different land-use types

Measurements of N_2O emissions from a variety of land uses in agricultural, forest and grassland systems were undertaken in 2008 and 2009. Annual emission rates were then calculated as a function of land use (simple emission factors ; table 3.2) and sub-classified as a function of topography for the agricultural lands, following the landscape segmentation approach proposed by Pennock et al. (1987). The entire landscape was then divided into three segments (shoulder, slope and footslope) and the experimentally determined emission rates were assigned to each of these segments (table 3.2). This procedure highlights the importance of the difference in nitrous oxide emissions between the different topographic positions, with the highest emissions in low topographical positions (emission factor, 4.02 ± 2.20 kg N_2O -N $ha^{-1}yr^{-1}$) with a decrease going up the slope (1.48 ± 0.90 kg N_2O -N $ha^{-1}yr^{-1}$ in the slope position and 1.06 ± 0.50 kg N_2O-N $ha^{-1}yr^{-1}$ in the shoulder position). As shown in Vilain et al. (2010), two main factors drive these highest emissions by footslope soils : (i) a much greater soil moisture which enhances denitrification and then higher N_2O fluxes, and (ii) a higher mineral N availability (NO_3^-) resulting from runoff. For the other land uses (i.e. forest and grassland), we did not consider the influence of topography and applied the same emission rate regardless of topographic position, i.e. 0.55 ± 0.04 and 0.69 ± 0.06 kg N_2O -N $ha^{-1}yr^{-1}$ for forest and grassland, respectively. When not considering the influence of topography for agricultural land, the simple mean emission rate used was 2.01 ± 0.54 kg N_2O-N $ha^{-1}yr^{-1}$ (from Vilain et al. (2010)).

3.5.3 Indirect emissions

By groundwater : EF5g

According to the previously described calculation (see the Materials and Methods section) and taking into account the N_2O concentrations from April 2008 to April 2010 in the plateau piezometer, the indirect N_2O flux from groundwater was estimated at 161.5 kg N_2O -N yr−1 for the entire Orgeval basin (Vilain et al., 2011). This calculation implies that there is no denitrification in the groundwater, assumption based on a previous work in the area which showed the limestone aquifers of the Seine basin have a very limited denitrification capacity (Sebilo, 2003; Sebilo et al., 2003).

	Emission coefficient (kgN_2O -N km^{-2} yr^{-1})	Land area (km^2)	Calculation from emission coefficient (kgN_2O -N yr^{-1})
Mean cropland	200.75 ± 54	78.94	15,847.36 ± 4262.76
Shoulder	105.85 ± 50	58.76	6219.76 ± 2938
Slope	147.83 ± 90	8.00	1182.63 ± 720
Footslope	401.50 ± 22	12.18	4890.57 ± 267.96
Forest	54.75 ± 40	20.81	1139.35 ± 832.4
Grassland	69.35 ± 60	3.37	233.64 ± 202.2

TABLE 3.2 – Nitrous oxide emission for the types of land use associated with their respective surface area in the basin and calculations from coefficients including topographic segmentation.

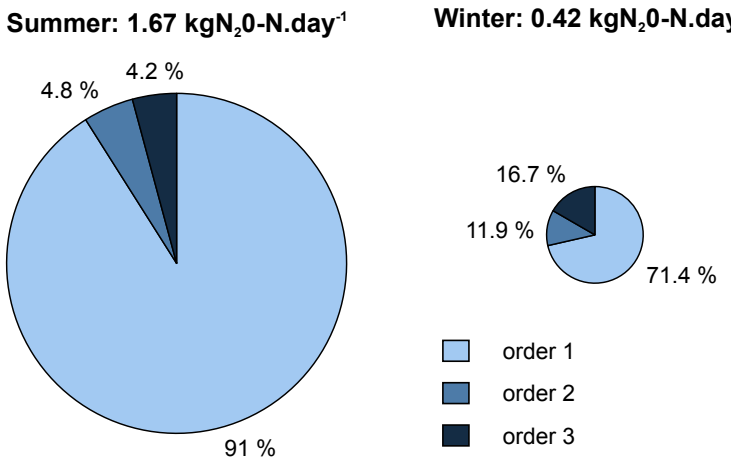

FIGURE 3.5 – Distribution of the daily N_2O emissions of the Orgeval drainage network, as a function of stream order for a winter and a summer period.

By Rivers : EF5r

The methodology proposed by Garnier et al. (2009b) based on the determination of gas transfer velocities for all stream orders was followed. Then the observed supersaturation of dissolved N_2O concentrations in water of all stream orders were multiplied by the corresponding gas transfer rate and by the corresponding water surface area (table 3.1), the result representing the indirect N_2O from drainage network emissions at the Orgeval basin scale (figure 3.2). Dissolved N_2O concentrations were higher in the first-order river (Mélarchez), ranging from 0.25 to 3.63 μgN_2O -N L^{-1} (mean, 1.27 ± 0.36 μgN_2O -N L^{-1}) than in the second-order rivers (Avenelles) and third-order rivers (Theil), with concentrations ranging from 0.35 to 0.75 μgN_2O -N L^{-1} (mean, 0.50 ± 0.05 μgN_2O -N L^{-1}) and from 0.37 to 1.46 μgN_2O -N L^{-1} (mean, 0.59 ± 0.12 μgN_2O-N L^{-1}), respectively (figure 3.2). Temperature varied from 5 to 19 °C and the mean was 10 °C in winter and 15 °C in summer.

The calculated summer emissions for the whole Orgeval basin were four times higher compared to winter emissions (1.67 ± 0.66 kgN_2O -N day^{-1} vs. 0.42 ± 0.09 kgN_2O -N day^{-1} , figure 3.5). This trend confirms the findings of Garnier et al. (2009b) at the larger scale of the entire Seine basin (75 000 km^2) for which summer emissions were twice as high as winter emissions. As also mentioned in Garnier et al. (2009b), N_2O fluxes contribution of first orders was much higher (91 % in summer and 71 % in winter) than the second and third orders together. Taking into account these calculated emission factors, the annual emission from the Orgeval basin drainage network can be estimated at 382 ± 137 kgN_2O -N yr^{-1}.

3.6 Orgeval basin scale upscaling of N_2O emissions

Nitrous oxide emissions were calculated using the four different upscaling methods based on land-cover databases and topography (CLC 2006, MOS+ECOMOS, Topo × CLC 2006,

	CLC 2006	MOS + ECOMOS	Topo + CLC 2006	Topo + MOS + ECOMOS
Arable	16959.80 ± 4562.04	15847.36 ± 4262.80	13201.26 ± 3447.27	12292.95 ± 3269.18
Foret	1144.41 ± 836.10	1139.35 ± 832.40	1144.41 ± 836.10	1139.35 ± 832.40
Grass	56.73 ± 49.08	233.64 ± 202.14	56.73 ± 49.08	233.64 ± 202.14
Total	18161 ± 4638	17220 ± 4348	14402 ± 3548	13666 ± 3380

TABLE 3.3 – N_2O emission estimations for the Orgeval basin by main land use type and calculated by each upscaling method (in kgN_2O -N yr^{-1}). CLC : Corine Land Cover ; MOS : Mode d'Occupation des Sols ; ECOMOS : land use classification produced by the IAU IDF.

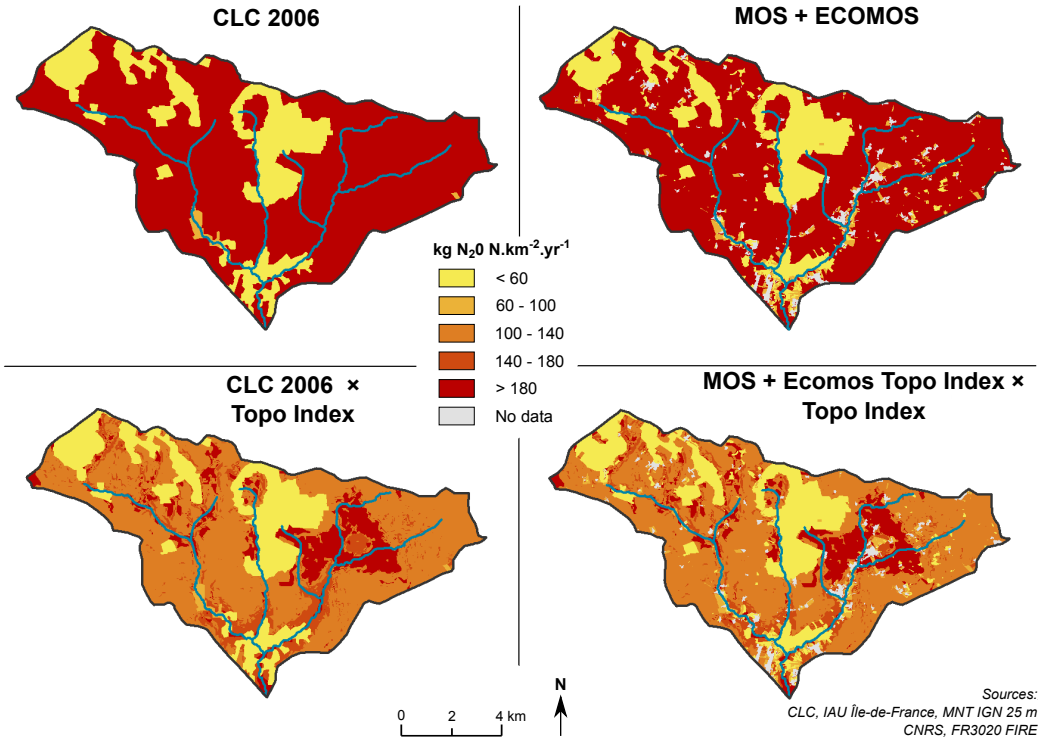

FIGURE 3.6 – Estimation of nitrous oxide emissions as a function of the land cover database and the topography.

Topo × (MOS+ECOMOS)). To each land use and topography class was applied the N_2O emission coefficients detailed in table 3.2. Maps showing the predicted spatial distribution of nitrous oxide emissions rates in the Orgeval basin (expressed per surface area) under the four methods are presented in figure 3.6. Total annual N_2O emissions for the whole Orgeval basin are given in table 3.3 by land-use class and for each upscaling method. Using the highest resolution database (MOS+ECOMOS) reduces the N_2O emissions by more than 5 % compared to CLC 2006-based methods. When considering topography-based methods, the estimations were more than 20 % lower. By combining the added values of both approaches, e.g., a more precise land-cover database and topography classes, N_2O emissions estimations were lowered by almost 25 % (from 18.1 to 13.6 tons of N_2O -N a year for the whole Orgeval basin).

Table 3.4 presents the contribution of each landscape position class to the total budget. Both methods show that 50 % of the N_2O emissions in the Orgeval basin come from soils in the shoulder position, around 38 % from the footslope position and 12 % from the slope.

	Topo × CLC 2006	**Topo × (MOS + ECOMOS)**
Shoulder	7259.93 ± 3333.67	7023.78 ± 3173.05
Slope	1727.33 ± 525.04	1540.48 ± 431.99
Footslope	5415.13 ± 703.32	5101.68 ± 657.76
Total	**14,402 ± 3447.27**	**13,666 ± 3269.18**

TABLE 3.4 – Contribution of the three topographic classes to the total N_2O flux, given for the two upscaling methods based on topography and land use (in kgN_2O -N yr^{-1}).

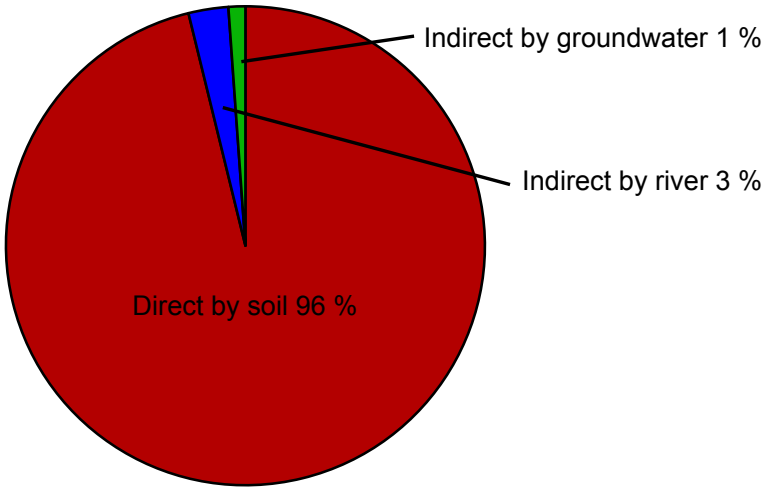

FIGURE 3.7 – Comparison of direct and indirect N_2O emissions at the Orgeval basin scale, based on the « Topo index × (MOS + ECO-MOS) » estimation.

3.7 Discussion

3.7.1 Direct vs. indirect sources of N_2O

Nitrous oxide is produced in soil (and also to a lesser extent in aquifers and river sediments) mainly by the two mechanisms of nitrification and denitrification. Once produced in soil, N_2O can be either directly emitted to the atmosphere (direct emissions, Vilain et al. (2010) or stored in the soil pores and subsequently leached into the aquifer and then transported to the stream, leading to indirect emissions (Vilain et al., 2011; Garnier et al., 2009b). Moreover, besides losses to the atmosphere, further reduction of N_2O might be taken into account as soil microbes can consume N_2O molecules before reaching up the atmosphere (Chapuis-Lardy et al., 2007). Therefore, this expressed indirect flux should be considered as an upper bound flux (Vilain et al., 2011).

The novelty of this study is that it combines direct measurements of both direct and indirect N_2O emissions (N_2O indirect emissions being concentration-based estimates) on the same agricultural sub-basin. Regarding the results of the estimations reported herein, it is clear that the total annual budget of N_2O emissions is driven by the direct emissions by soils, which account for 96 % of the total emissions (figure 3.7). Indirect emissions by rivers and groundwater account for 3 and 1 %, respectively of the total emissions (figure 3.7).

3.7.2 Catchment nitrous oxide budget

At the basin scale, N_2O emissions were the highest in the footslope position on fertilized fields. The 11.4 % of the basin area occupied by this combination of land use and topographic class contributes 35.8 % of the annual N_2O emissions. The lowest emissions were found in forest zones, accounting for 19.5 % of the Orgeval basin and contributing 8.3 % of the annual emissions. On the whole, taking into account the highest resolution direct N_2O estimations from soils (i.e. Topo × (MOS + ECOMOS)) and the indirect emissions from groundwater and rivers, the N_2O budget for the whole Orgeval sub-basin can be estimated at 14.21 × 103 kg N_2O -N yr^{-1}. This estimation, with regard to the sub-basin area, is equivalent to 1.33

kg N_2O-N ha^{-1} yr^{-1} considering both direct and indirect emissions and 1.28 kg N_2O -N ha^{-1} yr^{-1} considering only direct emissions, giving a proportion of 4 % for the indirect emissions. This estimation is well within the range of previous regional estimations in northern France, under similar climatic and pedologic conditions, from 0.84 to 2.0 kg N_2O-N ha^{-1} yr^{-1} , and slightly lower than our previous estimation of 2.0 kg N_2O -N ha^{-1} yr^{-1} for the whole Seine basin (Garnier et al., 2009b). These experimental values are well within the range found with modelling approaches. The CERES-EGC biophysical soil-crop model coupled with the AROPAj economic model gave N_2O emissions in Picardie from 1.07 to 1.97 kg N_2O -N ha^{-1} yr^{-1} (Durandeau et al., 2010) while in the Ile-de-France region, again using the CERES-EGC model, Lehuger (2009) estimated N_2O emissions from 0.84 to 1.29 kg N_2O -N ha^{-1} yr^{-1}. Gabrielle et al. (2006a) used the same model run with geo-referenced input data on soils, weather and land use to map N_2O emissions from wheat-cropped soils and estimated N_2O emissions at 1.37 kg N_2O -N ha^{-1} yr^{-1}.

The nitrous oxide emissions at the regional level can be considered in two ways : as a magnitude of emissions or as a response of N fertilization applied. We have here considered only emissions, based on both topography and land use, even though the information on fertilizer use at the basin scale can be found and could improve this modelling exercise.

However, Freibauer (2003) modelled N_2O emissions at the European scale and showed a poor relationship between these emissions and fertilizer dose (0.4 % of the variability explained by the fertilizer dose). The « fertilizer dose » factor seems to lose influence as the spatial area considered increases (Gabrielle et al., 2006a), confirmed by the study reported by Kaiser et al. (1998), who found that 0.8 % of the variability was explained by the fertilizer dose. Thus, not incorporating the fertilizer dose into our extrapolation may not have produced a significant error in the nitrous oxide flux estimation in the end. Especially since the sampled field is considered as representative of the whole Orgeval basin in terms of fertilization practices, the incorporation of the fertilization rates as a spatial variable was not crucial when upscaling from fields to landscape, as N_2O emissions are assumed to be proportional to applied fertilizer. One of the strengths of the methodology used herein is that it integrates the concept of topography into the estimation of N_2O emissions. Although this method can be refined, especially with regard to nitrogen rates applied on the field, this concept may be further used in subsequent coupling with the process-based models mentioned above (STICS-NOE, DNDC, CERES-EGC, NGAS, DAYCENT, etc.).

3.7.3 Opportunities for nitrous oxide emissions mitigation

A promising direction for nitrous oxide emissions mitigation is the enlargement of buffer strip zones, particularly in low topographical positions. Schultz et al. (2009) reported that the riparian buffer zones have to be adjusted to fit the site. Indeed, all adjacent upland arable lands have different characteristics and then each one requires individual consideration in order to achieve the objectives in terms of nitrate reduction minimizing N_2O emissions. Landscape features can vary along the same water body such as presence or absence of wetlands, width of the floodplain, slope and soil type (Palone and Todd, 1998). In terms of ecological engineering, a conversion to agroforestry seems to be promising both in terms of nitrogen retention and removal, carbon sequestration, biodiversity conservation and soil enrichment (Jose, 2009; Montagnini and Nair, 2004). Moreover, employing agroforestry practices can provide food and fiber while maintaining habitats for threatened species and maintaining local biodiversity and associated ecosystem services such as pollination and pest control (Foley et al., 2005). Agroforestry systems such as riparian buffers have been proposed to control non-point source pollution coming from agricultural fields as they reduce the velocity of runoff by mechanisms such as infiltration, sediment deposition and nutrient retention (Jose, 2009). The effectiveness of these measures has been proved by several studies such as those reported by Udawatta et al. (2002), Anderson et al. (2009) and Lee et al. (2003), the latter showing a 20 % increase in nutrient retention in woody stem buffer compared to a switchgrass buffer. Trees with deep roots in agroforestry systems can even improve groundwater quality by taking up leached nutrient by tree roots. These nutrients are then recycled back into the system through root turnover and litterfall, increasing the nutrient use efficiency of the system (Van Noordwijk et al., 1996; Allen et al., 2004).

A further alternative is to develop buffer strip biomass by harvesting (Spinelli et al., 2006). A conversion of buffer strip to biofuel products (such as switchgrass or miscanthus) could facilitate the expansion of buffer strips suggested above, because the loss of farmer income would be reduced by promoting the products of the riparian buffer zone (Isenhart et al.,

2000; Lee et al., 2003). In a modelling exercise, Gopalakrishnan et al. (2011) investigated such an alternative cropping system where bioenergy crops are grown in buffer strips adjacent to current agricultural crops in the buffer strips. Their results indicated that growing bioenergy crops in buffer strips mitigated nutrient runoff, reduced nitrate concentrations in leachate by 60 – 70 % as well as resulted in a reduction of 50 – 90 % of nitrous oxide emissions compared with traditional cropping systems. However, water consumption by these deep root trees should be simultaneously considered in a perspective of water availability reduction due to climate change.

We tested an extreme hypothetical scenario where agriculture was excluded from the low topographical positions. For this purpose, we simply replaced the value of the emission coefficient corresponding to the agricultural footslope position (401.50 kgN_2O-N km^2 yr^{-1}) with the emission coefficient corresponding to grassland, (69.35 kgN_2O -N km^2 yr^{-1}), which can be assumed a value comparable to the ones found for bioenergy crops without fertilization. Considering this scenario, with a 15.4 % loss of arable land, N_2O emissions of the whole watershed would decreased by 29 % (i.e. 9620 vs. 13 666 kgN_2O-N yr^{-1}).

In conclusion, we have shown that the spatial resolution of the land-use data, as well as the integration of the topography are two important criteria for estimating N_2O emissions at the basin scale. A major challenge for precision conservation in greenhouse gas mitigation can be a variable rate application of N fertilizer in lower slope segments to ensure the highest possible fertilizer use efficiency and hence reduce N_2O emissions from these segments (Pennock, 2005)). *Acknowledgements.* This study was undertaken within the framework of the

European AWARE programme, a project of the Seventh European Framework programme. The FIRE-FR3020 is also greatly acknowledged for its interdisciplinary research framework and for funding the site's equipment. We extend our thanks to the PIREN-Seine program for providing funding for the analysis. Francois Gilloots is sincerely acknowledged for having allowed us to conduct this research in his fields and for his willingness to contribute to scientific knowledge. Many thanks are due to the Cemagref (Patrick Ansart in particular for his help in the field). We also sincerely thank Benjamin Mercier and Olivier Tronquart for their kind laboratory and/or field assistance.

Chapitre 4

Riparian zones and nitrates elimination

4.1 Introduction

Riparian zones are known to eliminate a large part of nitrates issued from diffuse pollution before they reach the hydrosystem. By a modeling approach using the Seneque/Riverstrahler model, Thieu et al. (2009) showed riparian zones are responsible for the retention of 25 - 30 % of diffuse nitrogen sources in dry and wet years respectively (Thieu et al., 2009). There are two different mechanisms affecting nitrates during their transfer through riparian zones : denitrification and uptake by vegetation (Groffman et al., 1992; Haycock and Burt, 1993; Haycock et al., 1993). The first one necessitates easily available organic carbon, anoxic conditions, an favorable temperature of about 20 degrees and nitrate as the major substrate. The second one is due to the uptake by plants for their growth, and does not really represent an elimination but rather a retention of nitrogen in their structure. Denitrification is recognized the main mechanism at the origin of N removal in riparian zones, accounting for 50 - 90 % of the total N elimination under temperate climate where riparian soils are usually saturated in water (Haycock and Burt, 1993; Nelson et al., 1995). Field studies showed N retention reaching 5 to 30 % of the inflowing nitrogen fluxes in a pool of European riparian zones (Sabater et al., 2003). Similar results were found in the Po basin in Italy (Balestrini et al., 2011). But the links between denitrification in these buffer zones and environmental variables are not yet well known. Land use could play a major role, but also the local lithology and geomorphology, as well as the hydrological and hydro-geological conditions. Until now, there is no clear consensus about which is the major driver for denitrification in riparian zones (Sabater et al., 2003). Sabater et al. (2003) pointed out the predominant role of geomorphology and hydraulic gradient, but others pointed out the role of vegetation (Haycock et al., 1993). Is there one unique driver or a combination of drivers depending of the environmental context ?

In this perspective, as the local conditions determining the intensity of riparian retention are not yet correctly understood at small scale, it is a real challenge to introduce a spatialized representation of riparian denitrification within a model of a large watershed with different lithological, hydro-geological and land use conditions such as the Seine basin. The mechanistic description of denitrification within riparian zones still is very hard to formalize due to the difficulty to model the water circulation in these critical zones (Haycock and Burt, 1993). Our objective in this section is merely to discuss how to better parameterize riparian retention in the Seneque/Riverstrahler model.

4.2 Modeling approach

In the Seneque/Riverstrahler model, a value of riparian transfer at optimal temperature is assign to each river stretch based on a typology of river corridors (Billen and Garnier, 1999). The retention is subject to temperature dependence with a formulation and parameters similar to those of benthic denitrification. When the catchment is tile-drained, the retention is reduced in proportion of the area subject to tile drainage, thus by-passing the riparian zones. The same retention factor similarly affects surface runoff and base flow (Thieu et al., 2009).

Gaillard et al. (2006) have proposed a geomorphological typology of river corridors, allowing distinguishing 10 classes of riparian zones. This typology was used in the previous version of the model to define the riparian transfer of nitrate in the Seine watershed. Here, we explore other possible typologies of riparian zones based on land use, geometry or Strahler ordination (Strahler, 1957) coupled with a range of new possible values of N transfers. For each typology tested, the Seneque/Riverstrahler model was run in a loop testing a combination of N riparian transfer coefficients. At the end of these runs, the results were compared with observed nitrate concentration values at all stations using the Nash or the bias criteria.

4.3 Exploring various classification of riparian zones with the Seneque/Riverstrahler model : the Grand Morin catchment

Our first explorations were conducted on the Grand Morin watershed, a sub-basin of the Seine watershed, 1200 km^2 wide, with a total length of river of 515 km, a drainage density of 43 km.km^{-2} and a Strahler order at its outlet of 4. The Grand Morin basin is located in the Brie region, on a quite permeable marl and limestone substrate, with some patches of clay in the thalwegs and a cover of clayey loam on the plateaus. The land use is dominated by arable lands (73 %), whose a significant proportion is tile-drained, forest (17 %) and urban area (5 %). Very few meadows (5 %) are located along the thalwegs. The population, in 2006, is 114130 inhabitants, mainly located in the downstream part of the basin, which corresponds to a density of 95 inh.km^{-2}.

4.3.1 Test of classification based on land use

First, the theoretical maximum extent of riparian zone was delimited, based on a geomorphological criteria. The topographic index was calculated for the Grand Morin watershed using the DEM provided by IGN with a horizontal resolution of 25 m by 25 m according t. Topographic indexes were calculated. Potential riparian zones were defined as the areas with a topographic index lower than 13 (empirically determined values) and crossing a river. Because of the resolution of 25 m, along the order 1 rivers, no riparian zones were detected by this method. So to this geomorphological criteria was added a 25 m buffer criteria around each river of the Grand Morin watershed. The size of the buffer (12.5 m on each side of the rivers) was chosen to keep a spatial coherence with the resolution of the DEM. Finally, the theoretical maximum extent of riparian zones corresponds to the addition of these two criteria. Riparian zones that we delimited cover 119 km^2 (10 %) of the Grand Morin basin (figure 4.1).

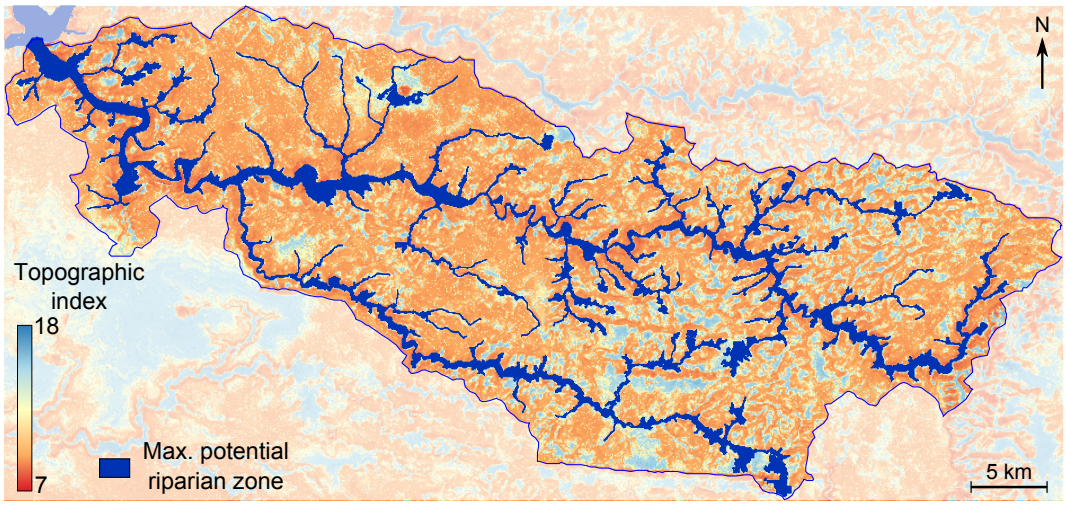

FIGURE 4.1 – Theoretical maximal extent of riparian zones within the Grand Morin basin.

This surface area of riparian zones was intersected with the elementary watersheds of

Land use	Sup. km²	Prop. (%)
Arable land	69.20	62.7
Forest	18.34	16.6
Grassland	5.47	5.0
Urban area	12.19	11.0
Agr. het. area	4.87	4.4
Wetland	0.26	0.2

TABLE 4.1 – Land use within theoretical riparian zones (km² and %).

the Seneque data base, to get the extent of the riparian zones for each sub-basin. Then, it was intersected with the land use, derived from CLC, classified into 8 classes, in order to get the proportion of each land use within the theoretical riparian zones of each elementary basin (figure 4.2).

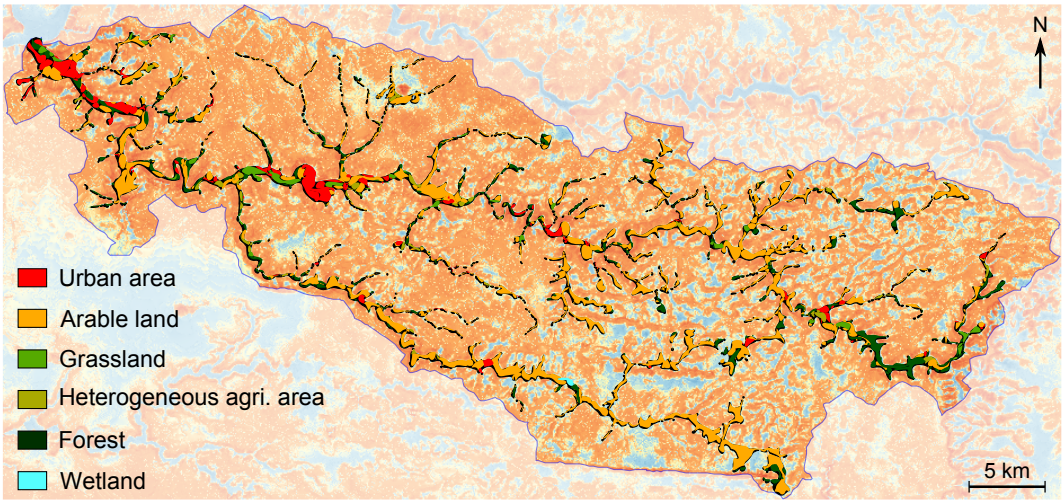

FIGURE 4.2 – Land use within the theoretical riparian zones.

Land use within the riparian zones of the Grand Morin sub-basin is shown in table 4.1. The majority of riparian zones are occupied by arable lands (62 %), following by forests (17 %) and by urban areas (11 %). Interestingly, wetlands as defined by CLC (2006) are almost totally absent. This is due to the relatively coarse resolution of CLC data. We added to the grasslands, a buffer of 10 m (2 m) around each river crossing an arable land, allowing us to take into account the grassed buffer strips between arable lands and rivers which are nowadays compulsory since 2007.

Due to a time calculation limitation, only classes concerning arable lands, grasslands and forests were tested. For each of these classes, transfer coefficients ranging from 0.1 to 0.9 with a step of 0.2 were tested.

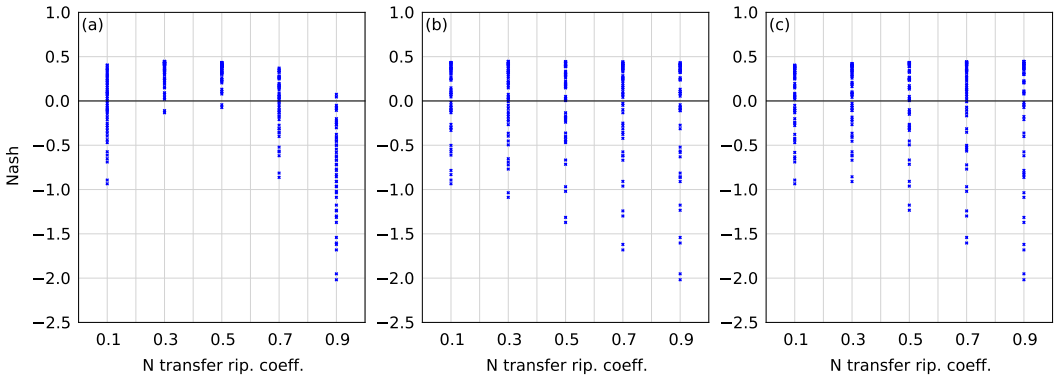

FIGURE 4.3 – NASH characterizing the goodness of fit of the model for different values of the N riparian transfers rates affected to riparian areas according to their land use,(for arable land (a), forest (b) and grassland (c).

Figure 4.3 shows the variations of NASH resulting from the different values of transfer rate assigned to a given riparian land use class. For instance, concerning riparian zones devoted to arable lands (figure 4.3 a), when the N transfer riparian coefficient is set to 0.1, whatever the values of the N transfer for the other classes, the results range from a NASH of -0.95 to 0.45. For a N riparian transfer set to 0.3, the Nash of the results are less scattered. So, the best results (in average) are reached when the N riparian transfer of this class is set to 0.3, whatever the values for the two other classes. The quality of the simulations is very sensitive to the transfer coefficient value assigned to riparian zones covered by arable land (making up 62 % of the total riparian zone in this basin). The best results are obtained when the transfer coefficient is set to 0.3 or 0.5, in combination with riparian transfers for both forest and grassland set to 0.1 (figure 4.3 b, c).

This would indicate that riparian wetlands covered by arable land are less « retentive » than when forested or covered by grassland.

4.3.2 Test of classification based on the width of the riparian zone

In order to go further in the understanding of the riparian zones, the next question was : is denitrification occurring only in few meters at the interface between riparian zone and upper land or does the width of the riparian zone matter ? To answer this question, a classification based on the mean width of the riparian zones of each elementary river was again performed on the Grand Morin basin. Three classes of equal population size were delimited. The first one corresponds to the riparian zones with a width below 100 m, the second one with a width ranging between 100 m and 300 m, and the last one over 300 m. Results in terms of NASH are shown on figure 4.4.

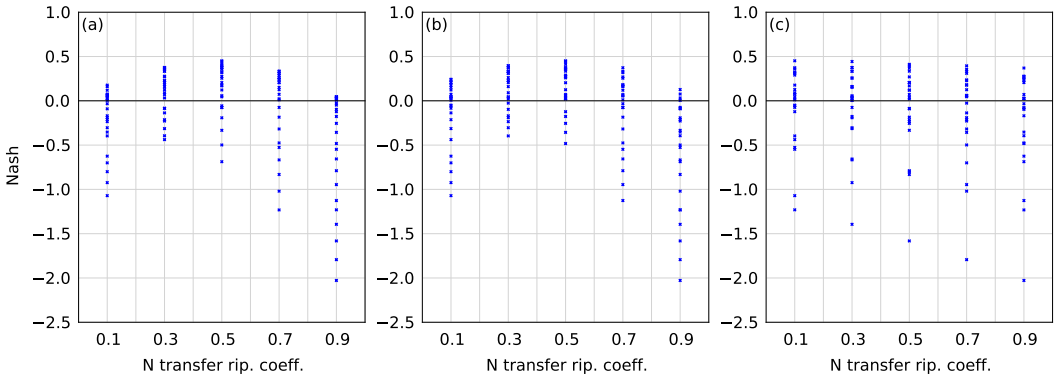

FIGURE 4.4 – NASH of results of variations of N riparian transfers according the width of the riparian zone, below 100 m (a), from 100 to 300 m (b) and up to 300 m (c).

The best results are obtained with a N riparian transfer fixed to 0.3 or 0.5 for the classes of narrow (figure 4.4 a) and intermediate riparian zones (figure 4.4 b). Results are not

affected by the riparian transfer of the class corresponding to the riparian zones up to 300 m large (figure 4.4 c). Indeed, regardless N riparian transfer set for this class, NASH can reach a value of 0.5. So, denitrification doesn't seem to be affected by the width of the riparian zone.

4.4 Exploring new classification of riparian zones with the Seneque/Riverstrahler model : the scale of the Seine catchment

In order to explore more criteria at a more large scale, some simulation were performed at the scale of the whole Seine basin.

4.4.1 Test based on the Gaillard's geomorphological classification

First of all, our methodology based on sensibility tests, was performed on the geomorphological classification of riparian zones, as established by Stéphane Gaillard in 2001 (Gaillard et al., 2006). Only the most three representative classes were tested. These three kinds of riparian zones are « Incised in an inorganic substrate », « Superimposed on an inorganic substrate »and « Incised in the substratum ». Results according this classification are shown on figure 4.5.

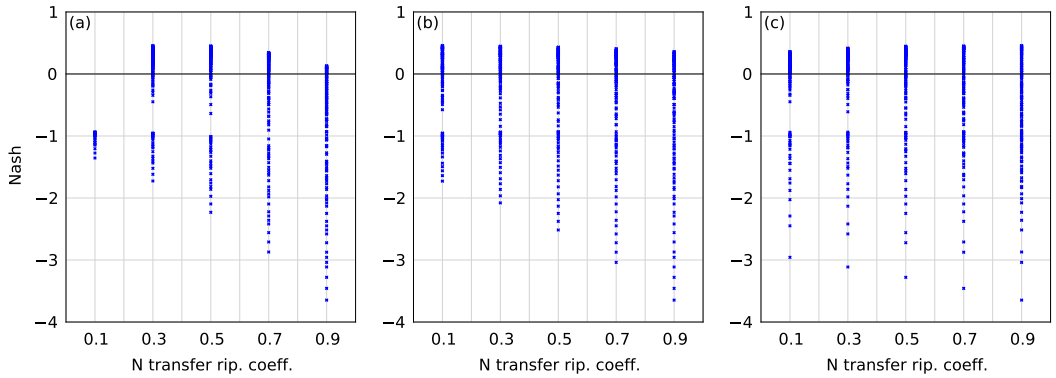

FIGURE 4.5 – NASH of the results of variations of N riparian transfers according to the geomorphological classification established by Gaillard (2001), for the following classes : Incised in an inorganic substrate (a), Superimposed on an inorganic substrate (b) and Incised in the substratum (c).

Concerning the first class (figure 4.5 a) , best results are obtained when the N transfer riparian coefficient is set to 0.3 or to 0.5. Other values of this coefficient lead to unsatisfactory results. For the second class, good results can be achieved with any N riparian transfer coefficient (figure 4.5 b). Nevertheless, with a transfer coefficient set to 0.1, results are better in average. In addition, results are not sensitive to the transfer set for the third class (figure 4.5 c). As a whole, only the first two classes play a role in the riparian retention at the scale of the whole Seine catchment.

4.4.2 Test of classification based on homogeneous agricultural areas

At the scale of the Seine basin, 5 major homogeneous agricultural areas can be distinguished : Brie-Beauce, Rich Loam area (Picardy), Yonne depression, Chalky Champagne and Jurassic plateaus. These represent major the geographical units with distinct landscape features. Tests were performed based on the hypothesis according to which riparian zones have different comportment depending on the agricultural area where they are located. Results according to this classification are shown on figure 4.6.

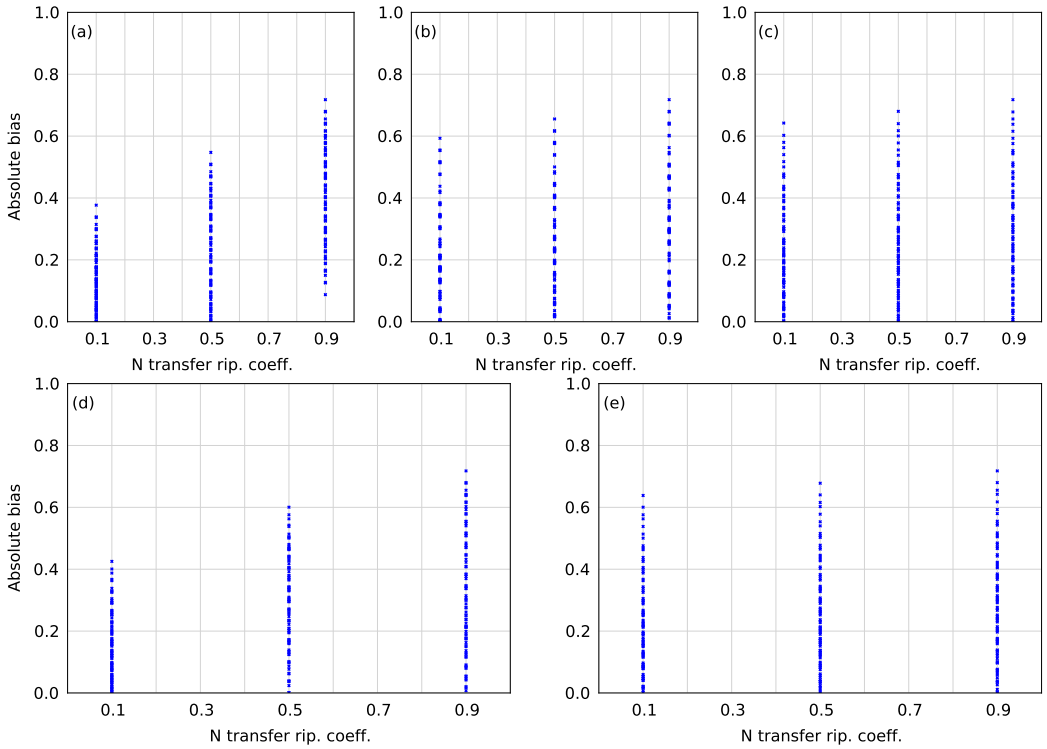

FIGURE 4.6 – Biases of the results of variations of N riparian transfers according homogeneous agricultural area, Brie-Beauce (a), chalky Champagne (b), Yonne depression (c), rich loam (d), Jurassic plateau (e).

Due to a time calculation limitation, for each class of riparian zone, a range from 0.1 to 0.9 with a step of 0.3 was only tested for each N riparian transfer. Due to this coarse resolution in the transfer coefficient, NASH coefficients are weaker than are those calculated at the Grand Morin scale. Therefore, we focused the results via the study of biases, which are less affected by this artifact.

Only agricultural areas of Brie-Beauce (4.6 a) and rich loam (4.6 c) seem to be affected by the variation of the N riparian transfer coefficients. In average, best biases are obtained when N riparian transfer coefficients are set to 0.1. Nevertheless, the dispersion of the biases and the fact, that coefficients of 0.5 or even 0.9 can provide good biases, tend to temperate the relation between agricultural areas and N riparian transfers. Moreover no clear trend can be observed for other agricultural areas. For chalky Champagne (4.6 b), Yonne depression (4.6 c) or Jurassic plateau (4.6 e), good biases can be reached with any N riparian transfer.

4.4.3 Test of classification based on the Strahler ordination

Finally, a trivial classification of riparian zones based on their location in the hydrosystem according the Strahler ordination (Strahler, 1957) was tested. Only N riparian transfers of riparian zones located on orders 1, 2 and 3 rivers were tested. Results, in terms of biases, are shown on figure 4.7.

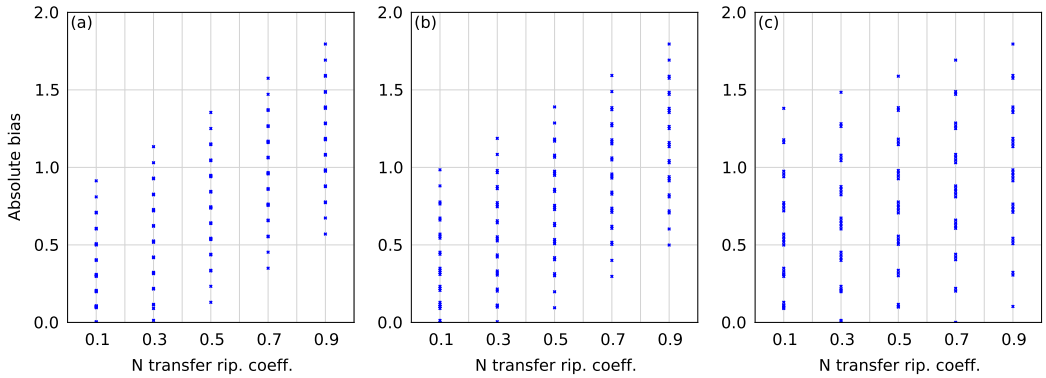

FIGURE 4.7 – Biases of the results of the variations of N riparian transfers according to the Strahler ordination, riparian zones located on order 1 rivers (a), order 2 rivers (b) and order 3 rivers (c).

Concerning the riparian zones located on order 1 rivers (figure 4.7 a), the best results are obtained with a N riparian transfer set to 0.1 or 0.3. With 0.1, in average, results are better. The same conclusion can be formulated for riparian zones located on order 2 rivers (figure 4.7 b). However, concerning riparian zones located on order 3 rivers, no trend can be observed (figure 4.7 c). So, only riparian zones located on order 1 or order 2 rivers seem to be sensitive to the assigned transfer coefficient from watershed to the hydrosystem. This can be explained by the fact that order 1 rivers represent 49 % of the total length of the hydrographic network of the Seine and 51 % of the drained surface.

4.5 Conclusion

The tests carried out here did not allow us to conclude about the links between environmental constraints and N riparian retention. The only conclusive result shows the major role played by riparian zones located on order 1 and order 2 rivers, which is the obvious consequence of the fact that rivers of first and second orders drain more than 50 % of the total basin and represent more than 50 % of the total length of the hydrographic network. Their important role is not so surprising, although mathematically demonstrated here, but it means that, if landscape ecological engineering on riparian zones becomes a measure to reduce nitrates (Allen et al., 2003), it has to be implemented on the low order of rivers. Designing a riparian zone on a large river of order 3 or more, like in the wide wetlands of the Bassée (at the confluence of the Seine and the Yonne rivers) would only have a minor impact on nitrate concentration, although other functions such as biodiversity conservation, water retention during flood event can be beneficial. Field surveys showed that land use seems to play a role on nitrate decrease within riparian zones (Haycock et al., 1993). Riparian zones covered by forests or grasslands are assumed to better denitrify than those covered by arable lands. However to understand the role of land use using a modeling approach, we showed that more precise data are needed. Indeed, some riparian zones are only covered by a very narrow line of trees or grasslands, which were not taken into account in our study, because of the coarse resolution of CLC data. A more precise classification of land use, e.g. based on aerial photographs, should be performed. This kind of approach could lead to interesting results, but needs further studies to be implemented, due to the difficulty to automatically discretize land use from aerial photographs.

À retenir sur les zones ripariennes

- ⋆ Le N_2O est surtout émis par les rivières d'ordre 1 et en période estivale.
- ⋆ Les proportions d'usage du sol varient sensiblement selon la source utilisée, ce qui implique des différences dans les calculs d'émission de N_2O par type de surface.
- ⋆ Les bas de pente sont des lieux de plus grande émission de N_2O. Il est donc important de croiser la topographie avec l'usage du sol afin d'établir un bilan de ces émissions à l'échelle d'un bassin versant.
- ⋆ À l'échelle du paysage, les lieux privilégiés d'émission de N_2O sont les zones de terres arables situées en bas de pente.
- ⋆ À l'échelle du bassin de la Seine, il est difficile de mettre en relation la rétention riparienne avec les facteurs environnementaux via une démarche liant approche statistiques et modélisation déterministe.
- ⋆ Ni l'usage du sol, ni la largeur des zones ripariennes, ni le paysage au sens des petites régions agricoles n'ont été détectées comme influençant la rétention riparienne.
- ⋆ La position de la zone riparienne au sein du réseau hydrographique semble être le facteur explicatif dominant à l'échelle du bassin de la Seine.
- ⋆ La majeure partie de la rétention riparienne a lieu sur les ordres 1 et 2, qui drainent plus de 50 % du bassin.

Troisième partie

Le rôle des secteurs stagnants du réseau hydrographique dans les transferts de nutriments

« L'eau n'oublie pas son chemin. »

Proverbe oriental

Cette partie III s'attache à explorer le rôle des secteurs stagnants du réseau hydrographique sur les flux de nutriments et spécialemnet sur celui de l'azote. De nombreuses études menées sur des étangs ou des réservoirs ont mis en évidence un abattement significatif du nitrate des masses d'eau les traversant.

Le chapitre 5 correspond à l'intégralité de l'article :

Restoration of ponds in rural landscapes : modelling the effect on nitrate contamination of surface water (the Seine watershed, France), *Paul Passy, Josette Garnier, Gilles Billen, Corinne Fesneau, Julien Tournebize, Science of the Total Environment*, juin 2012, *DOI : 10.1016/j.scitotenv.2012.04.035.*

Dans un premier temps, l'application du modèle Seneque/Riverstrahler à un étang agricole dont la concentration en nitrates a été suivie sur trois ans est présentée. Dans un second temps, plusieurs scénarios de réintroduction d'étangs à l'échelle du bassin de la Seine ont été testés mais en conservant l'esprit de « terroir » des régions agricoles en se basant sur la carte de Cassini décrivant les paysages de la fin du 18$^{\text{ème}}$ siècle.

Enfin, le chapitre 6 est un extrait de l'article :

Modelling historical changes in nutrient delivery and water quality of the Zenne river (1790s–2010) : the role of land use, waterscape and urban wastewater management, *Josette Garnier, Natacha Brion, Julie Callens, Paul Passy, Chloé Deligne, Gilles Billen, Pierre Servais, Claire Billen.*

Cet extrait correspond à la partie de l'article traitant de la modélisation des étangs historiques du bassin de la Zenne. En plus des flux d'azote, le devenir des flux de phosphore et de silicium et du développement du phytoplancton y sont présentés. Les secteurs de la cascade de nutriments auxquels s'intéressent cette partie sont présentés sur la figure 4.8.

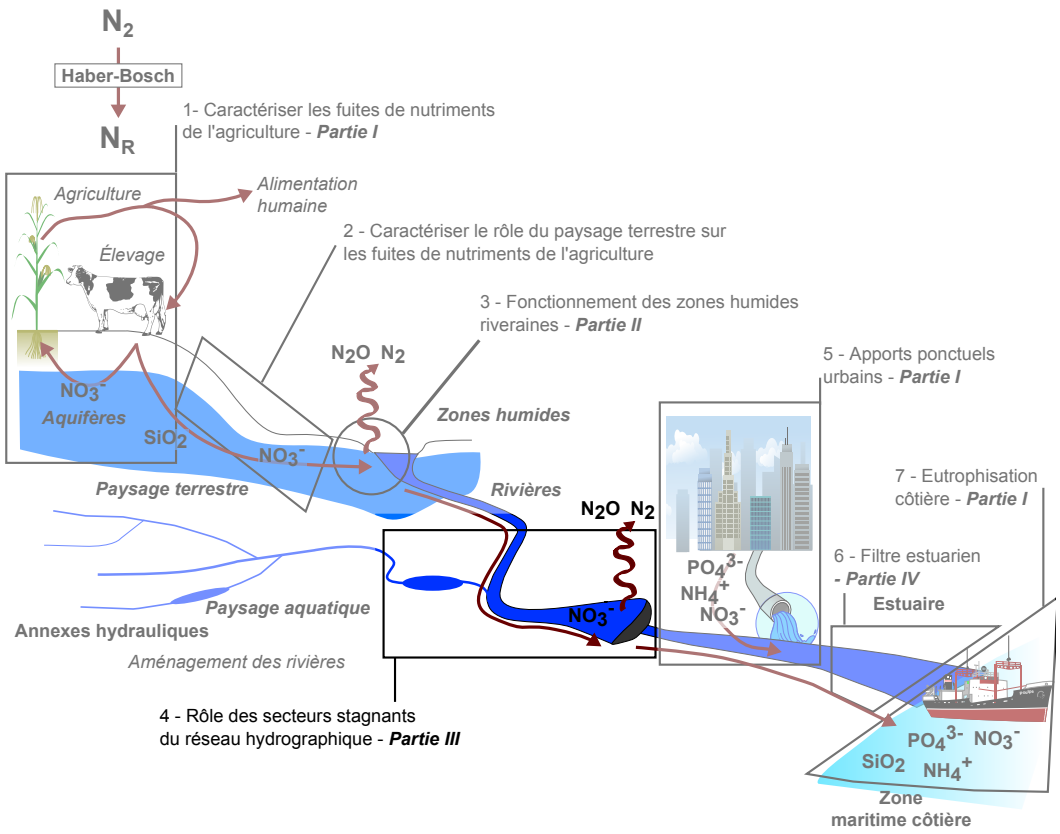

FIGURE 4.8 – Postes de la cascade de nutriments traités dans la partie III.

Chapitre 5

Restoration of ponds in rural landscapes : modelling the effect on nitrate contamination of surface water (the Seine River Basin, France)

5.1 Abstract

Ponds were ubiquitous features of the traditional rural waterscape in the Seine watershed, as shown by the 18th century Cassini map. Using the result of a water quality survey at the entrance and the outlet of a small pond receiving agricultural drainage water, the Seneque/Riverstrahler biogeochemical model was shown to accurately simulate the observed 30 % reduction in nitrogen fluxes crossing this pond. The model was then used to simulate the effect of various scenarios of pond restoration (inspired by their 18th century geographical distribution as revealed by the Cassini map) on surface water nitrate contamination at different spatial scales. In regions with an impermeable lithological substrate, the restoration of ponds at a density of 5 % of the agricultural area would reduce the riverine nitrogen export by up to 25 % on an annual basis. It is suggested that such waterscape management, used in conjunction with more preventive measures, can be a useful means to reduce nitrate contamination of water resources.

5.2 Introduction

Reducing nitrate contamination of ground and surface water is one of the most important challenges faced by environmental policies in developed countries with intensive agriculture (Erisman et al., 2007). Besides being a threat to producing drinking water (Manassaram et al., 2006; Grizzetti et al., 2011) and achieving good ecological status of waterbodies (Water Framework Directive, 2000), nitrogen pollution is the source of imbalanced nutrient loads at the river outlet, leading to coastal eutrophication (Thieu et al., 2009; Lancelot et al., 2011). In the Seine river basin, as in many other European watersheds, considerable improvements have recently been achieved in reducing urban point sources of nutrients including nitrogen to surface water (Hirt et al., 2008), so that diffuse sources from agriculture now overwhelmingly dominate nitrate contamination (Thieu et al., 2010).

Two types of complementary strategies can be applied to control diffuse nitrogen pollution from agricultural activities. Preventive measures act on farming practices, with the objective of either reducing the rate of fertilisation or excess fertilisation over crop uptake (Thieu et al., 2010). Curative measures aim at enhancing nitrate retention or elimination through natural processes occurring in the drainage network, wetlands, riparian strips and reservoirs. In particular, ponds and reservoirs are known to be quite efficient nitrogen retention sites. Three major processes may be involved in nitrogen retention within these sites : uptake by vegetation, sedimentation and denitrification. Water quality surveys on reservoirs

System	N ret. (%)	Fate of N	Reference
Lake, Scandinavia	96 %		(Henriksen and Wright, 1977)
Lake, Ontario (Canada)		Uptake (15 %)	(Hill, 1979)
Lake, Scandinavia	85 %		(Wright, 1983)
Lake, North-eastern USA	97 %		(Hemond and Eshleman, 1984)
Six lakes in North America and Western Europe		Denit. up to 36 %	(Seitzinger, 1988)
Two lakes in Ontario (Canada)	79 - 85 %		(Dillon and Molot, 1990)
Lakes, Denmark		Denit 77 %	(Jensen et al., 1990)
Backwater lake, Mississippi basin (USA)		Denit 82 % Uptake 11.5 %	(Kreiling et al., 2011)
Reservoirs in the Seine basin (France)	40 %	Denit > 40 %	(Garnier et al., 1999)
Reservoir, Illinois (USA)	58 %		(David et al., 2006)
Ponds, Liuchahe watershed (South-eastern (China)	65 %	Denit. 44.1 %	(Yan et al., 1997)
Wetlands within the Tar River basin, NC (USA)		Denit. 13 %	(Brinson et al., 1984)
Lakes and wetlands, Southern Sweden	15 %		(Jansson et al., 1994)
Constructed wetlands	75 %	Denit. 87 % Sedim. 13 %	(vanOostrom, 1995)
Wetlands and lakes in North America and Western Europe		Denit. 63 % Sedim. 37 %	(Saunders and Kalff, 2001)
Constructed wetlands in Mississippi basin (USA)	20 - 43 %		(Mitsch et al., 2005a,b)

TABLE 5.1 – Some literature data on N retention in lakes, ponds and reservoirs. (% N retention), and fate of the « retained » N (respective role of denitrification, sediment storage and macrophytes or periphyton uptake in N retention).

(Garnier and Billen, 1994; Garnier et al., 1999; Tomaszek and Czerwieniec, 2000; David et al., 2006; Koszelnik et al., 2007; Gruca-Rokosz and Tomaszek, 2007) and constructed wetlands (Mitsch and Gosselink, 2000; Mitsch et al., 2005a,b) in Europe and North America showed their N retentive power. Denitrification was shown as the dominant process of this retention/elimination (Brinson et al., 1984; Seitzinger, 1988; Jansson et al., 1994; Hernandez and Mitsch, 2007), as occurring within the river networks (Billen et al., 1998; Alexander et al., 2000; Laursen and Seitzinger, 2002; Thouvenot et al., 2006). Denitrification has been observed to be an order of magnitude higher than sedimentation in both experimental and natural wetlands (Brinson et al., 1984; vanOostrom, 1995). Table 5.1 summarizes results about N retention within ponds and wetlands as well as the fate of nitrogen when available.

Before the industrial revolution, ponds were ubiquitous components of the west European rural landscape (Benoit et al., 2002; Touzery, 1998). The Cassini map (Cassini and Cassini, 1756), the first precise and detailed map of France, drawn mainly for military purposes by César-François de Cassini and Jean-Dominique Cassini between 1756 and 1789, offers a way to quantitatively assess the presence of ponds in the traditional landscape. The Cassini map offers a unique opportunity to take inventory of the numerous ponds which once existed in the rural landscape of the Seine watershed. This 18t century map was constructed by triangulation, allowing georeferencing in the modern Lambert 93 coordinate system (EHESS, 2007). In the Orgeval watershed, for instance, the localisation error is about 60 m. Most often, ponds were the result of a water level increase after building a dam across a river. They were used for many purposes. At this time, large areas of the Seine basin were managed

by abbeys, which built ponds in order to produce fish, sea fish supply being very expensive at the time. Ponds were also used to drive flour or smithy mills. In the upper part of the Seine basin, especially in the woody area of Morvan, ponds were used as water storage reservoirs for accelerating wood floating (Corvol, 2007), massively used to supply Paris in fire wood until the end of the 19th century. Most of these ponds were filled (Derex, 2001) or ceased to be maintained after steam and gas engines came into widespread use. Nowadays there are no more ponds on small order 1 rivers. Only some small ponds (less than 10 000 m^2) remain on the plateaus but not connected to the hydrosystem. In recent years, new ponds or holding tanks have sometimes been established on headstreams or at the outlet of drainage collectors to store water for irrigation.

La carte de Cassini, première vision globale de la France

La carte de Cassini, aussi appelée carte de l'Académie, est la première carte représentant la France dans sa totalité (à l'exception de la Corse, la Savoie et l'Île d'Yeu) (Pelletier, 1990). Cette carte est également une première parce que sa réalisation reposant sur la triangulation géodésique permet d'estimer très précisément les distances. L'échelle adoptée correspond à une ligne pour cent toises, soit une échelle au 1/86 400ème. La carte localise précisément les routes mais pas forcément les villes, les marais ou les forêts. Par contre la quasi totalité des lieux habités y est représentée, ce qui est très utile pour lever l'impôt. La levée de la carte répond à un désir du pouvoir royal d'avoir une vue d'ensemble du royaume (Lascoumes, 2007), de ses voies de commnunications et des éléments « immuables » du paysage, informations primordiales en cas de conflit. Cette carte a donc un but géographique, politique et stratégique (Claval, 2011). « La géographie, ça sert d'abord à faire la guerre » dit Yves Lacoste. Les relevés ont été effectués entre 1756 et 1789 sous la direction de César-François dit Cassini III et Jean-Dominique dit Cassini IV (figure 5.1). Les 180 feuilles composant la carte ont été publiées entre 1756 et 1815.

FIGURE 5.1 – De gauche à droite : César-François Cassini *(Miniature sur ivoire de Jean-Marc Nattier, vers 1750)*, Jean-Dominique Cassini *(Gravure de Conrad Westermayr, 1801)*.

Le résultat est une carte très riche donnant de nombreuses informations sur les paysages terrestres et hydrauliques de la fin du 18ème siècle. Cependant, au regard de l'ampleur de la tâche, les 180 feuilles ne sont pas d'une qualité homogène, si la feuille de Paris est excessivement détaillée (figure 5.2), les régions rurales les plus reculées le sont beaucoup moins. Elle servit cependant de référence pendant près d'un siècle puisque la carte d'État Major qui l'a remplacée n'arrivera que dans la seconde moitiée du 19ème siècle.

FIGURE 5.2 – Paris et le bassin de l'Orgeval tels que figurés sur la carte de Cassini.

In order to quantify the possible effect of pond restoration, we have implemented the Seneque/Riverstrahler biogeochemical model of the Seine watershed to calculate their effect on surface water nitrate contamination at different spatial scales, ranging from a small first-order sub-basin to the whole Seine watershed. The first objective was to develop a routine for using the model to explore the behaviour of a single pond and to validate the results by comparison with data collected over 3 years in an artificial pool established on a

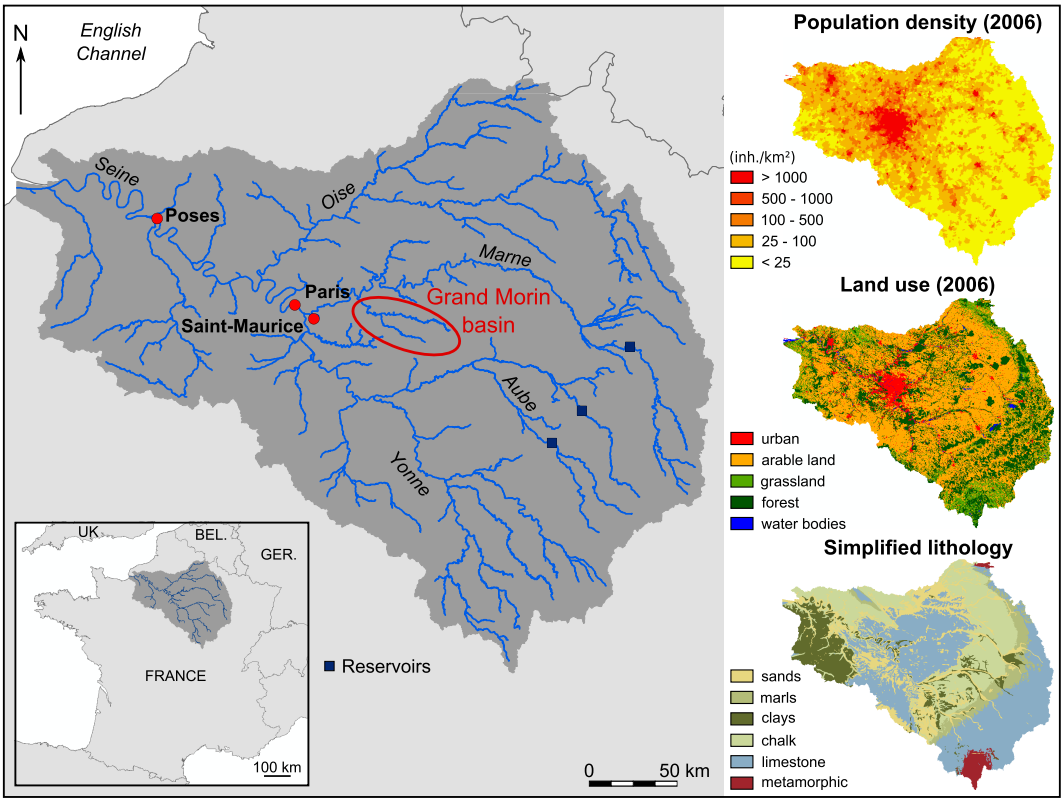

FIGURE 5.3 – Location of the Seine basin – Population density, land use, lithology.

rural stream. The second aim, after having established a census of historical ponds in the entire Seine watershed in the 18th century, based on the Cassini map, was to reconstruct the Seine drainage basin by including all these ponds to explore their effect in the present nitrate contamination context. Finally, to extend the exploration of the nitric contamination reduction potential of ponds, we established various pond restoration scenarios and evaluated their impacts at different sectors of the drainage network.

5.3 Study sites and methods

5.3.1 The Seine watershed

The Seine watershed is located in northern France (figure 5.3). The basin is 71 700 km^2 wide upstream from the last gauging station before the estuarine zone located at the Poses dam. The highest point is Haut Folin – 901 m – located in the south-east in the Morvan Massif. The mean altitude is less than 100 m and the mean slope of the rivers is low, averaging 0.0098 m.m^{-1}.

Limestone, clay and chalk sedimentary formations arranged in concentric rings around Paris dominate the geology of the basin, with an alternation of permeable and impermeable substrates. Only the southern part is made of Palaeozoic metamorphic and magmatic rocks. In the western part and the central part of the basin, a thick layer of fine eolian loam covers the geologic formations.

The climate is oceanic with a regular distribution of precipitations throughout the year but higher evapotranspiration in summer, resulting in high water discharge in winter and low in summer. From 1966 to 1991 three major reservoirs were built in the upper part of the basin. The first one on the Seine River in 1966, the second one on the Marne River in 1974 and the last one on the Aube River in 1991. Both these three reservoirs are holding a total of 750.10^6 m^3. Their management aims at reducing the intensity of winter floods and sustaining summer discharge (Garnier et al., 1999). The annual mean temperature is 12 $^\circ$ C.

The population of the Seine basin was 16 440 175 inhabitants in 2006 (INSEE, 2006). A large part lives in the Parisian conurbation (12 600 000 inh.), the third largest European agglomeration in terms of population. Most of the cities are located in the centre of the basin

around Paris and on the main river corridors. Population density is a mean 215 inh.km^{-2}, but less than 30 inh.km^{-2} in the upstream part of the basin.

Land use is largely dominated by arable land, which covers 53 % of the watershed (Corine Land Cover, 2006). The proportion of urban areas (7 %) is relatively low in comparison with the population. Grasslands, covering 9.8 % of the basin, are located in the periphery of the basin in the Normandy and Morvan regions. Forests, mainly located on the northern, eastern and southern edges of the basin,

Diffuse sources of N represent 78 % of total N input to the hydrosystem, reaching 3960 kgN.km^{-2}.yr^{-1} in wet years, while point sources of N amount to 550 kgN.km^{-2}.yr^{-1}. On the contrary phosphorous originates for 61 % from point sources equalling 70 kgP.km^{-2}.yr^{-1}, while diffuse phosphorus makes up 90 kgP.km^{-2}.yr^{-1} during wet years. Silicon, mainly originating from rock weathering, is essentially (at 94 %) a diffuse source accounting for 1690 kgSi.km^{-2}.yr^{-1} during wet years. From these nutrient fluxes emitted by the watershed to the drainage network, the part effectively delivered to the coastal zone is evaluated to 2310 kgN.km^{-2}.yr^{-1}, 100 kgP.km^{-2}.yr^{-1} and 1143 kgSi.km^{-2}.yr^{-1} (Billen et al., 2009c) cover almost a quarter of the total area.

Part of our results is dedicated to the smaller scales of the Grand Morin and Orgeval watersheds. The former is 4$^{\text{th}}$ order a sub-basin of the Marne River located 30 km east of Paris, and covering an area of 1200 km^2. The substrate is dominated by limestones and marls, covered by a deep layer of loam. The downstream part of the Grand Morin River is essentially urban, while the upstream part is devoted to intensive cereal production. The Orgeval watershed is a 104 km^2 wide, third-order sub-basin of the Grand Morin. Its land use is largely dominated by intensive crop production (Tournebize et al., 2008).

5.3.2 A reference agricultural pond

From 2007 to 2010, a survey was conducted on an agricultural pond located in the Orgeval watershed, 30 km east of Paris (figure 5.4). The surface area of the pond is 3700 m^2, with a depth of about 2 m. Its maximal storage capacity is approximately 8000 m^3. This pond was built to collect and store water coming from a spring and from drain collector receiving water from 35 ha of arable land cultivated with a rotation involving winter wheat/barley, beans or corn, and sugar beetroot, according to conventional practices. Plot nitrate leaching has been evaluated at 3700 kgN km^{-2} year^{-1} (Tournebize et al., 2008).

Less than ten percent of the pond surface is occupied by macrophytes, mainly *Agrostis stolonifera*, *Nasturtium officinale*, *Veronica beccabunga*, and *Lysimachia nummularia*. The rest is free surface water.

Discharge of the two inflows and the outlet, and the water level of the pond were continuously monitored. Calibrated 90 ° V-notch weirs were installed and equipped with water level measurement devices (SE-200 OTT), providing 15-min time step records at the drainage outfall and permanent spring. The outlet discharge of the basin was derived from the water level monitoring of the basin (SE-200 OTT), the recorded input and output discharge and the pluviometric and evaporation data collected daily by a meteorological station belonging to a national network, located at 4 km from the pond. Nitrate concentration monitoring was based on manual sampling every two weeks. The spring was sampled bimonthly due to its low variability.

5.3.3 The Seneque/Riverstrahler model and major trends of nutrient fluxes

The Seneque/Riverstrahler model (SR model) (Billen et al., 1994) is a generic and mechanistic modelling tool to calculate the seasonal and spatial variations of water quality within drainage networks ranging in scale from 10 to 100 000 km^2. The river network is represented as a combination of sub-basins and branches. Sub-basins are idealised by a regular scheme of confluence of tributaries with mean morphological characteristics by stream order (Strahler, 1957). These sub-basins are connected to branches represented with a higher spatial resolution (every kilometre). This representation of the drainage network takes into account both the processes occurring in small first-order streams and those occurring in large tributaries. The waterflows in the hydrological network are calculated from the specific discharges generated within the watershed of the different sub-basins and branches considered. These specific discharges are provided as a constraint to the model : they are calculated using the Eckhardt recursive filter (Eckhardt, 2008) applied to daily discharges

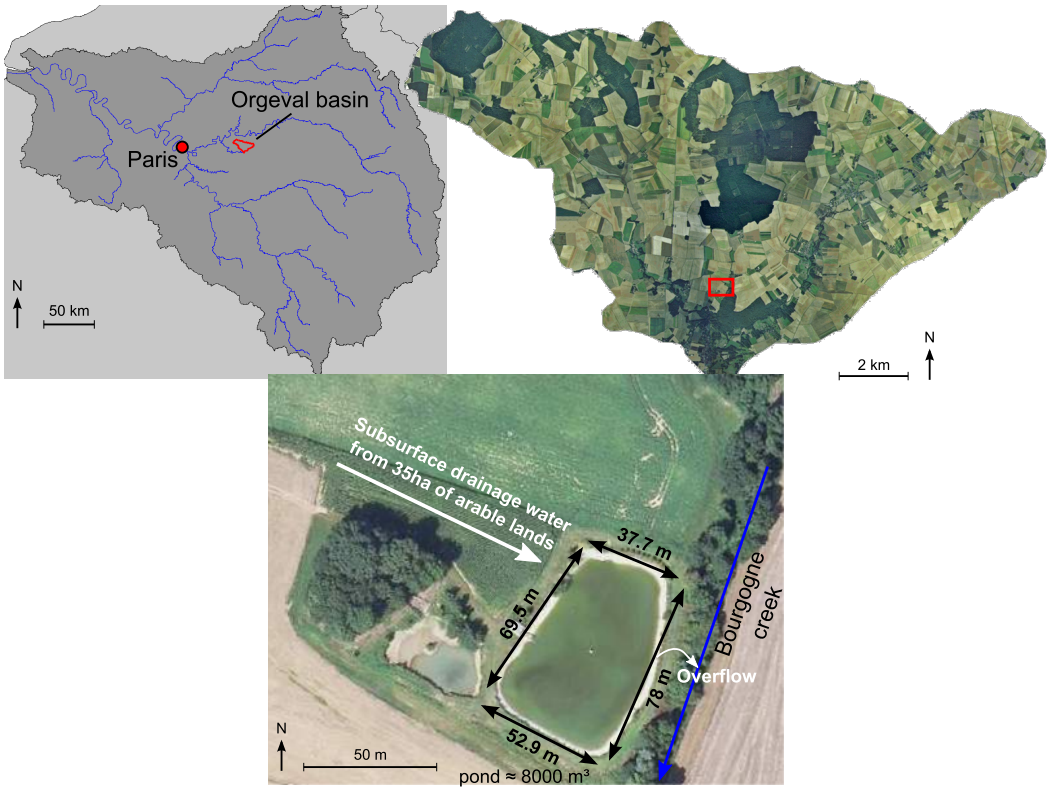

FIGURE 5.4 – Location of the agricultural pond studied within the Orgeval basin in the Brie region, 60 km east of Paris.

measurements at available gauging stations distributed over the watershed. The Eckardt filter permits to distinguish surface or sub-surface runoff and groundwater baseflow without using a rain-discharge model, allowing to almost perfectly reconstructing total discharge of the hydrosystem.

The principle of the model is to combine these water flows that are routed through the defined structure of basins and branches with a model describing the biological, microbiological, and physiochemical processes that occur within the waterbodies, in both planktonic and benthic phases. These processes are described according to the state of art of our knowledge about biogeochemical kinetics, with determined values of the associated parameters, either experimentally or from literature, thus without calibration, and only minimal adjustments of the parameters within the range of their determination. The module representing the kinetics of the processes is known as the Rive model. The state variables comprise nutrients (including all inorganic, organic, dissolved and particulate N, P, Si forms), oxygen, suspended matter, dissolved and particulate non-living organic carbon, and algal, bacterial, and zooplanktonic biomasses. Most processes important in the transformation, elimination, and/or immobilisation of nutrients during their transfer within the river network are explicitly calculated, including algal primary production, aerobic and anaerobic organic matter degradation by planktonic as well as benthic bacteria with coupled oxidant consumption, nutrient remineralisation, nitrification and denitrification, and phosphate reversible adsorption onto suspended matter and subsequent sedimentation. The time resolution of 10 days allowed us to take into account seasonal variations. A detailed description of the Rive Model and the physiological parameters used is provided in (Garnier et al., 2002) and in (Thouvenot et al., 2006, 2007) when the benthic denitrification processes are concerned.

Besides morphological and climatic constraints, Riverstrahler considers diffuse and point sources of nutrients from land-based anthropogenic sources. Diffuse sources are defined according to land use and agricultural practices (Thieu et al., 2010), more specifically from the agricultural surplus calculated as the difference between total N inputs to soils (fertilizers, manure, atmospheric deposition and legume crop N_2 fixation) and N export by the harvest. For each sector of the drainage basin considered, a mean and constant concentration of each nutrient taken into account in the modelling process is provided for sub-root water and

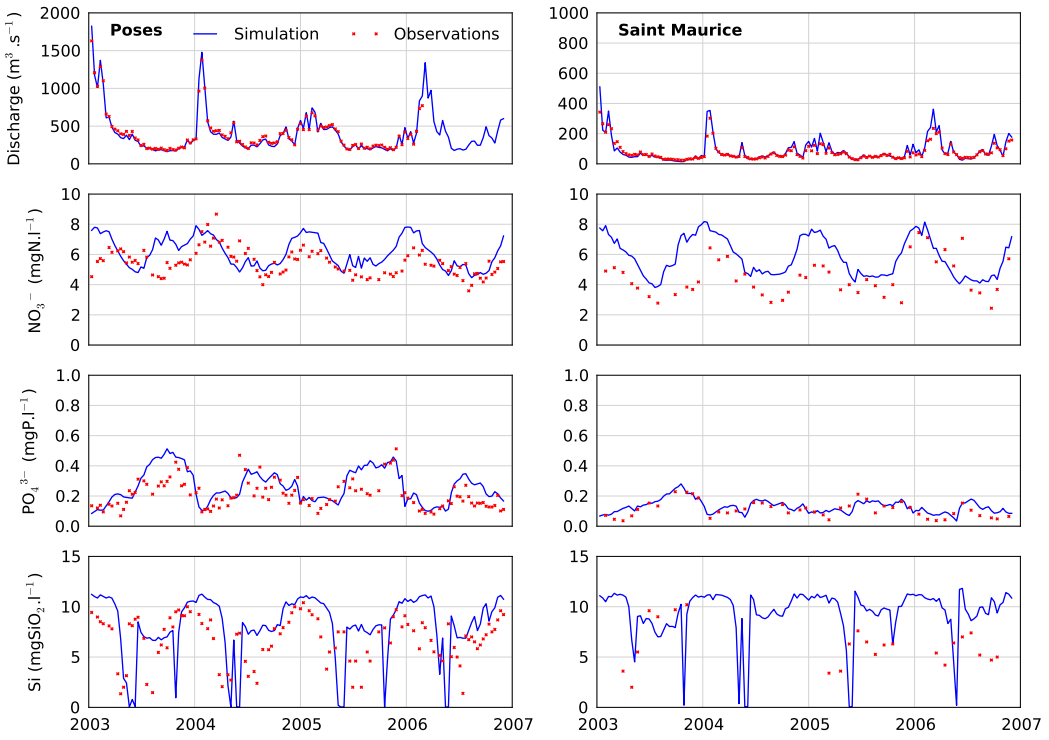

FIGURE 5.5 – Validation of the simulations for the reference years 2003–2006 at the Poses and the Saint Maurice stations for NO_3^- , total phosphorous and dissolved silicon.

groundwater concentrations, respectively. These concentrations are ascribed to the corresponding seasonally variable discharge components, e.g. surface runoff and base flow. These two components are used to calculate diffuse fluxes of nutrients transferred to the river network, taking into account a temperature dependent riparian retention factor assigned to each class of riparian zone. Point source pollution includes household and industrial wastewater. The modelling process takes into account the precise location of the effluents discharged in the river network, the type of treatment applied, especially the nitrogen, phosphorus and organic matter abatement, and the volume of wastewater treated related to the number of inhabitants connected to the wastewater treatment plant.

The model has been widely validated since the 1990s on the Seine river system to respond to various scientific questions. Here, the simulations were compared for NO_3, total phosphorus and silicon with the data provided by the Agence de l'Eau Seine Normandie for the reference years from 2003 to 2006 at Poses, the most downstream gauging station before the estuary, as well as at the Saint Maurice station on the Marne River upstream from Paris (figure 5.5). For each nutrient, different good fit criteria have been calculated (Root Mean Square Error (RMSE), Bias, Bravais and Pearson's r correlation coefficient) (Krause et al., 2005), see below.

- RMSE : $\sqrt{(\sum(vobs - vcalc)^2}$
  should tend to 0.
- Bias : $\frac{\sum(y-x)}{\sum(x)}$
  should tend to 0 and good if < 40 (Allen et al., 2007)
- Bravais-Pearson r : $r = \frac{cov(x,y)}{\sqrt{var(x) \times var(y)}}$
  significance is established according to the Bravais and Pearson's r table

Concerning nitrate, biases are less than 10 for both Poses and Saint Maurice, RMSE values are around 1 and r coefficient are significant at the threshold value of 0.01. Concerning phosphorus RMSE tend to 0, biases are around 10 and r values are also significantly differing

	Reference	-10 %	+10 %	+100 %
Sedimentation rate	4.545	4.549 (+0.09 %)	4.542 (-0.16 %)	4.529 (-0.29 %)
Benthic remineralisation rate	4.54	4.538 (-0.15 %)	4.552 (+0.29 %)	4.606 (+1.6 %)
Riparian transfer	4.54	4.305 (-558 %)	4.785 (+10.1 %)	6.949 (+31.1 %)

TABLE 5.2 – N sensitivity test of the model for the sedimentation rate, the benthic remineralisation rate and the N transfer rate of riparian zone. Values are mean annual NO_3^- concentration ($mgN.l^{-1}$) at Poses for the hydrological year 2006.

from zero at the threshold value of 0.01. Agreement between simulation and observation for silica is less satisfactory, r is not significantly different from zero at Saint Maurice. Nevertheless the overall trends and levels of nutrient concentrations are well captured by the model. This permits us to consider that the description of the processes is correct. Discrepancies can be explained on the one hand by the poor amount of data available concerning the spatial variability of N sub-root water concentration within agricultural areas, and on the other hand by the lack of knowledge about the N retentive power of riparian zones. This term has been empirically calibrated. Besides, the sensitivity of two other parameters, assumed to be central in the conceptual scheme of benthic nutrient transformation processes, namely the sedimentation rate of particulate organic matter and the rate constant of organic matter degradation in the sediments, have been explored (table 5.2) by the method One-Factor-at-a-Time (Czitrom, 1999). The model appears to be reasonably robust with respect to variations of these two parameters.

At Poses, for the 2003–2006 studied period, the maximum discharge occurred at the end of winter and reached more than 1600 $m^3.s^{-1}$ in January 2003. The lowest discharge, nearly 170 $m^3.s^{-1}$, was observed at the end of summer. The annual average was 405 $m^3.s^{-1}$ for the period. The minimum concentration of nitrate was observed in July (around 4.5 $mgN.l^{-1}$), the maximum in January (around 7.8 $mgN.l^{-1}$) and the mean annual fluxes of nitrate were, respectively, 1430, 1320, 1140 and 1290 $kgN.km^{-2}.yr^{-1}$ for the years 2003, 2004, 2005 and 2006. Nitrate concentration is strongly affected by discharge : it decreases at low discharge, and increases with increasing discharges. The major part of the short temporal variations in nitrate concentrations was due to short temporal variation of the discharge, the inter-annual variations of nitrate concentrations are also reflecting the hydrological conditions of the year. Total phosphorous concentrations averaged 0.30 $mgP.l^{-1}$ and the annual fluxes in total phosphorus were, respectively, 45, 44, 42 and 39 $kgP.km^{-2}.yr^{-1}$ for 2003, 2004, 2005 and 2006. Silicon decreased to 0.02 $mgSi.l^{-1}$ in late April and reached 11.17 $mgSi.l^{-1}$ in March. The annual fluxes of silicon were, respectively, 590, 550, 460 and 630 $kgSi.km^{-2}.yr^{-1}$ for the years 2003, 2004, 2005 and 2006. The maximum of phytoplankton generally occurred in June and reached about 100 $\mu gChla.l^{-1}$.

At Saint Maurice, for the 2003-2006 studied period, mean discharge was around 80 $m^3.s^{-1}$. Maximum discharges occurred in winter and reached more than 450 $m^3.s^{-1}$ in January 2003. The lowest discharges were observed in summer and can be less than 30 $m^3.s^{-1}$ during the driest summers. The minimum concentration of nitrate was also observed in July (around 2.5 $mgN.l^{-1}$), the maximum in January (around 7.5 $mgN.l^{-1}$) and the mean nitrate concentration over the four years was around 4.5 $mgN.l^{-1}$. Total phosphorus concentrations averaged 0.25 $mgP.l^{-1}$ with minimum values occurring in winter and maximum values in the late summer. The trend of silicon was almost constant to 8 $mgSi.l^{-1}$ throughout the 4 years, with abrupt falls to less than 2 $mgSi.l^{-1}$ during early summer in some of the years.

5.4 Results

5.4.1 Modelling the agricultural pond case study

The 3-years survey of inflowing and outflowing water quality of the agricultural pond in Brie showed a high retention capacity of this system (figure 5.6). While the mean nitrate

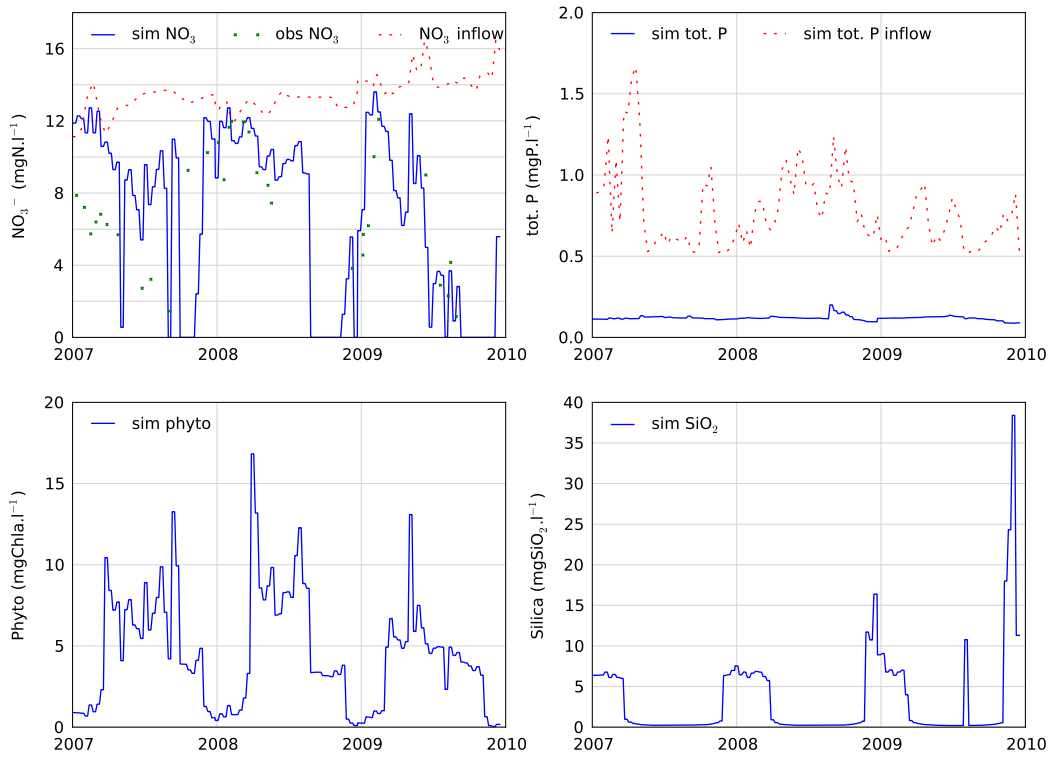

FIGURE 5.6 – Validation of the Seneque/Riverstrahler model applied to the reference agricultural pond for the years 2007–2010. Solid lines are the results of simulation for outflow concentrations of nitrate, total phosphorus and silica. Red dashed lines are the inflows concentrations (measured for NO_3^- and modelled for P and Si). Blue dot line is the discharge.

concentrations in the influent water were seasonally constant and increased slightly from 11 to 13 mgN.ll^{-1} from 2007 to 2010, the outflowing concentrations were much lower and seasonally variable, with a minimum at each late summer of 1.5 mgN-NO_3^- .l^{-1}, 4 mgN-NO_3^- .l^{-1} and 1.2 mgN-NO_3^- .l^{-1} in 2007, 2008 and 2009, respectively. Yearly nitrate retention was 54 %, 27 % and 56 % in 2007, 2008 and 2009, respectively. Phytoplankton, total phosphorus and silicon are also shown on figure 5.6 . The levels of each nutrient are in the same range of order of those measured in summer 2010, 23 μgChla.l^{-1}, 0.02 mgP.l^{-1} and 1.7 mgSi.l^{-1}. Silicon is taken up by phytoplankton in summer. The high value of silicon at the end of 2009 corresponds to a loss of sediment by the pond. Variations of total phosphorus are quite low but the system is phosphorus retentive.

The biogeochemical functioning of this pond was simulated with the Seneque/Riverstrahler model by considering a single stream branch fed with the water flow and the measured nitrate concentrations at the inlet of the pond. Two morphologies of this elementary branch were considered : one representative of first-order streams in the Brie region, the other adjusted to represent a total volume and a residence time similar to the pond (e.g. 1000 m long, 8 m wide, 1 m deep). The simulation of the seasonal dynamics of nitrate reproduces the high concentrations during winter and a decrease in summer (figure 5.6). The bias over the three years is 13 with a rather high Bravais-Pearson's r of 0.73 (significant at 0.01). Although the Seneque/Riverstrahler model was designed for describing large watershed, these results show that the model is able to accurately simulate the biogeochemistry of small ponds or reservoirs in upstream river waters.

The model allows to construct a complete budget of the fate of nitrogen in the pond system, thus to assess the respective role of various processes in nutrient retention (uptake by phytoplankton, storage in the benthos, denitrification) (table 5.3).

The calculations show that within the pond, NO_3^- decreases by 28 % and denitrification is the major process of nitrate elimination. Besides, organic matter decreases by sedimentation and is stored in the benthos, while ammonium is produced and shows higher concentration in the outlet than in the inlet. Silicon and total phosphorus are also retained by sedimentation in the pond, by respectively 68 % and 70 %.

	Input	Output	Balance
NO_3^- ($kgN.yr^{-1}$)	825	607	-218
NH_4 ($kgN.yr^{-1}$)	3	112	+109
Phyto ($kgN.yr^{-1}$)	0	1	+1
Org. mat. ($kgN.yr^{-1}$)	74	26	-48
Tot. N ($kgN.yr^{-1}$)	910	754	-156
Sediment storage ($kgN.yr^{-1}$)			7
Denitrification ($kgN.yr^{-1}$)			217
Tot. P ($kgP.yr^{-1}$)	31	9	22
Sediment storage ($kgP.yr^{-1}$)			19
Tot. Si ($kgSi.yr^{-1}$)	370	128	242
Sediment storage ($kgSi.yr^{-1}$)			286

TABLE 5.3 – Fluxes (in $kg.yr^{-1}$) of nitrogen, phosphorus and silicon through the pond as calculated by the model for the 2007 – 2008 and 2009 years.

5.4.2 A census of 18th century ponds in the Seine watershed

All ponds appearing on the Cassini map over the whole Seine basin were digitised manually. Although the representation of the ponds in this map is not accurate according to modern standards, it is precise enough to provide a general idea of the ponds' distribution in the 18th century landscape. More than 2550 ponds were counted in the Seine watershed area. The largest pond was evaluated to be 420 ha in size, and the mean area was 8.22 ha. A total of 0.24 % of the area of the Seine basin was covered by ponds (figure 5.8). Concerning the depth of these water bodies, medievalist historians agree on a mean value of 1.50 m, as reported for instance in the Diderot and d'Alembert Encyclopedia (Diderot, 1781). Most ponds were located on small headwater rivers on an impermeable substrate, with 69 % of the ponds located on first-order streams. The relationship between the pond densities and lithological characteristics makes it easy to correlate their presence to the distribution of present agricultural regions of the Seine basin. Agricultural regions are defined according to the General Agricultural Census as areas sharing similar cultivation practices and a comparable past (Mignolet et al., 2007). These similarities are conditioned, in large part, by their lithology. Regions such as Champagne Humide, Argonne, Brie, Morvan, Nivernais, Perche, with rather impermeable substrates, were characterised by high pond density, while Champagne Crayeuse, Beauce and Bourgogne Plateau, characterised by infiltrating permeable soils, were devoid of ponds. The total pond area in this scenario was set at 0.24 % of the watershed area, similarly to the Cassini period and 40 % of order 1 streams cross a pond.

Mais pourquoi tant d'étangs ?

Tous les étangs recensés à la fin du 18ème siècle sont artificiels (figure 5.7). Ils sont presque tous au fil de l'eau et suivent le même schéma : une digue est construite en travers de la rivière ce qui créé un « étang » de retenue. Souvent, la digue peut également servir de passage à une route. Nous ne savons pas exactement de quand datent les premiers étangs mais sûrement de l'époque d'installation des grands domaines monastiques et seigneuriaux aux alentours de l'an 1000. En effet, de tels aménagements hydrauliques demandent une certaine organisation centralisée du territoire, assurée à l'époque par la noblesse ou par le clergé (Rouillard et al., 2011).
Dans un contexte de foi chrétienne très marquée, il était prohibée de manger de la viande le vendredi ainsi que pendant le carême, ce qui rendait obligatoire la consommation de poissons pendant plus de 100 jours par an. Or à l'époque il n'était pas possible de s'approvisionner en poisson de mer, il était donc nécessaire de produire le poisson localement (Benoit et al., 2002). Une partie était pêchée en eaux vives, tandis que le reste était élevé en étangs. De ce fait la majorité des étangs étaient destinés à la pisciculture (figure 5.7) (Benoit, 2002).
À cet usage piscicole pouvait être associés des usages artisanaux et de petite industrie. Un moulin pouvait être bâti à l'exutoire de l'étang et actionner une meule destinée à moudre le grain. Des ateliers de tannage ou de rouissage pouvaient également profiter de cette force hydraulique.
Les étangs du bassin de l'Yonne ont eu un autre usage au cours de l'histoire. Ce bassin a la caractéristique d'être à l'amont de Paris, dans le massif du Morvan, dont les forêts ont été épargnées par les grands défrichements historiques. Cette situation en faisait une place de choix pour approvisionner Paris en bois de chauffage (Benoit et al., 2010), destiné à la chauffe mais aussi à la cuisson du pain. Le bois était coupé dans les forêts du Morvan puis jeté dans les petits cours d'eau. Régulièrement les étangs de ces rivières étaient alors vidangés brutalement afin d'entraîner le bois vers l'aval par effet « chasse d'eau », jusqu'à ce que ces « trains de bois » parveiennent à Paris. Le premier train de bois est arrivé à Paris en 1547 et le dernier en 1924, ce qui a durablement affecté les paysages, la faune, la flore et la qualité de l'eau de l'Yonne amont. Paris a conommé jusqu'à 2 000 000 de stères par an pendant cette période.

FIGURE 5.7 – De gauche à droite : étang agricole artificiel actuel *(Creuse, cliché Paul Passy)*, scène de pêche à la senne sur une gravure ancienne.

Enfin, certains étangs étaient destinés à alimenter en eau des canaux de navigation entre plusieurs bassins. C'est notamment le cas des étangs du Loing qui alimentaient les canaux de Briare et d'Orléans, construits au 17ème siècle et permettant une liaison fluviale entre les bassins de la Seine et de la Loire.
Finalement ces étangs ont commencé à disparaître au tournant des 17ème et 18ème siècles, époque à laquelle il devenait économiquement plus rentable de produire du blé que du poisson. Ainsi le recensement fait à partir de la carte de Cassini n'est sûrement pas le maximum historique de l'extension des étangs. Enfin, la Révolution Industrielle du 19ème, en permettant l'importation rapide du poisson marin ou le chauffage de Paris au charbon, a porté le coup de grâce aux étangs restants.

The total pond area in this scenario was set at 0.24 % of the watershed area, similarly

to the Cassini period and 40 % of order 1 streams cross a pond.

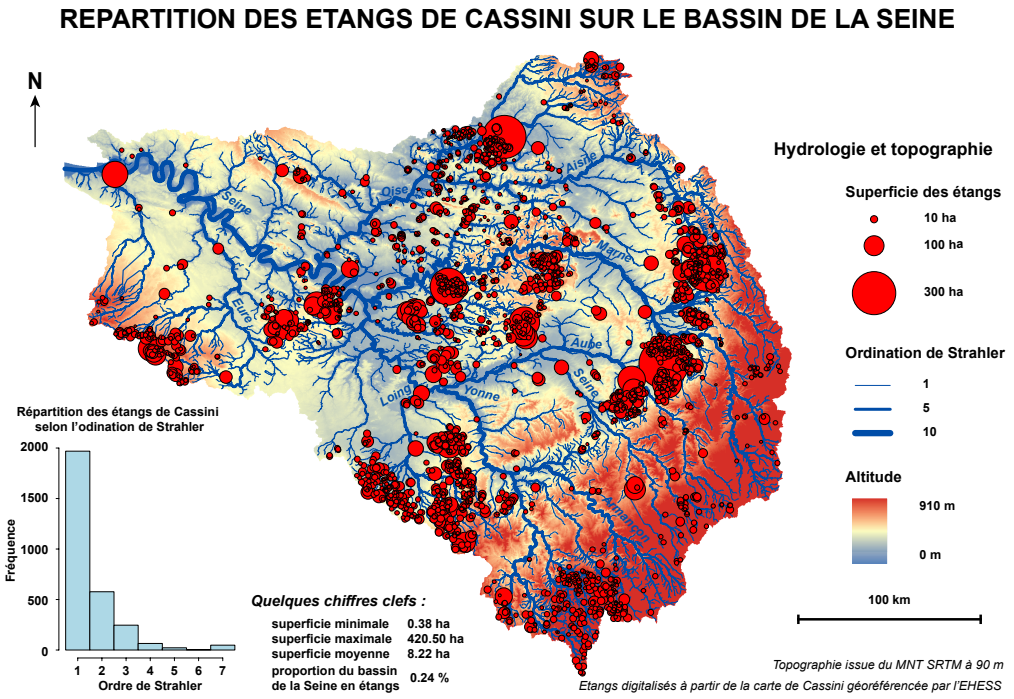

FIGURE 5.8 – Distribution of the 18th century ponds within the Seine watershed, digitised from the Cassini map.

In a second scenario (« Cassini plus »), we increased the proportion of ponds in some sub-basins. The historical pond distribution was clearly determined by the lithology of the Seine River basin (figure 5.3), which coincides with the distribution of current homogeneous agricultural areas. Two kinds of sub-basins have thus been distinguished : those located within homogeneous agricultural areas on impermeable substrate on which ponds were present in the 18th century and those on permeable substrate on which there were no historical ponds. In the former sub-basins, we calculated the mean size of ponds located on 1st order streams. Then on each 1st order stream of these sub-basins a pond was introduced, equivalent to the mean size previously calculated. The same procedure was followed for the ponds located on the 2nd order streams of these sub-basins (figure 5.9). Finally on each 1st and 2nd order streams within impermeable sub-basin one pond was reintroduced in this Cassini plus scenario. Within permeable sub-basins, no ponds were reintroduced. At total, a proportion of 0.76 % of ponds is reached on the whole Seine River Basin and 69 % of 1st order streams cross a pond.

Finally, focusing on the Orgeval sub-basin, ten other scenarios were considered based on the preceding one, with increasing pond area covering 1 – 10 % of the Orgeval watershed.

All these scenarios were run with the Seneque/Riverstrahler model using the hydrological conditions in 2003–2006 for the scenarios at the Seine River scale and only the year 2006 for the last ten scenarios on the Orgeval basin. Land use and point sources pollution are those of 2006. Only the geometry of the elementary river stretches between two confluences varied depending on the scenario : the elementary rivers being 're-shaped' according to the size of the ponds introduced. The results of the « Cassini » and the « Cassini plus » scenarios are shown in figure 5.10.

At the scale of the whole Seine watershed, pond restoration has only a very small impact. According to the hydrological conditions, nitrogen fluxes at Poses over the studied period range from 1140 kgN.km^{-2}.y^{-1} in 2005 to 1430 kgN.km^{-2}.y^{-1} in 2003 for the reference scenario. Only a decrease of 3 % of N flux in average for the 4 years could be achieved with the Cassini Plus scenario. Ponds also have a Si retentive influence. In the reference scenario the yearly mean flux of silicon is 560 kgSi. km^{-2}.y^{-1} at Poses and 480 kgSi.km^{-2}.y^{-1} in the Cassini Plus scenario corresponding to a 14 % decrease.

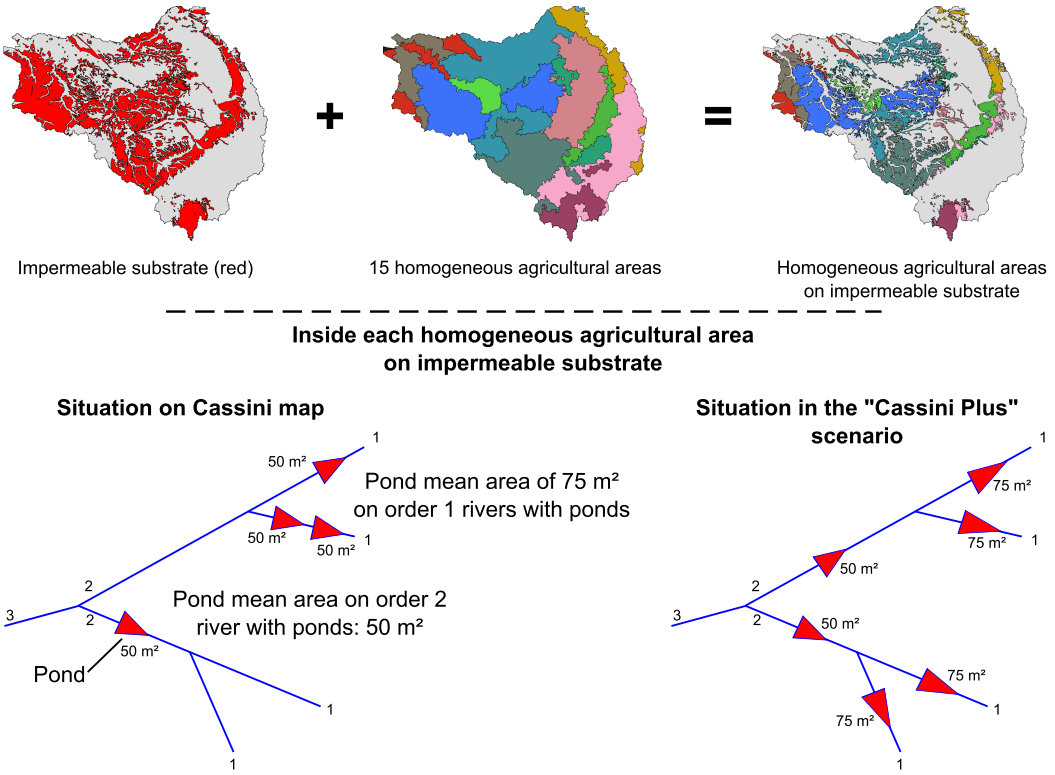

FIGURE 5.9 – Restoration of ponds within the Seine watershed according to lithology, homogeneous agricultural areas and the historical distribution of ponds.

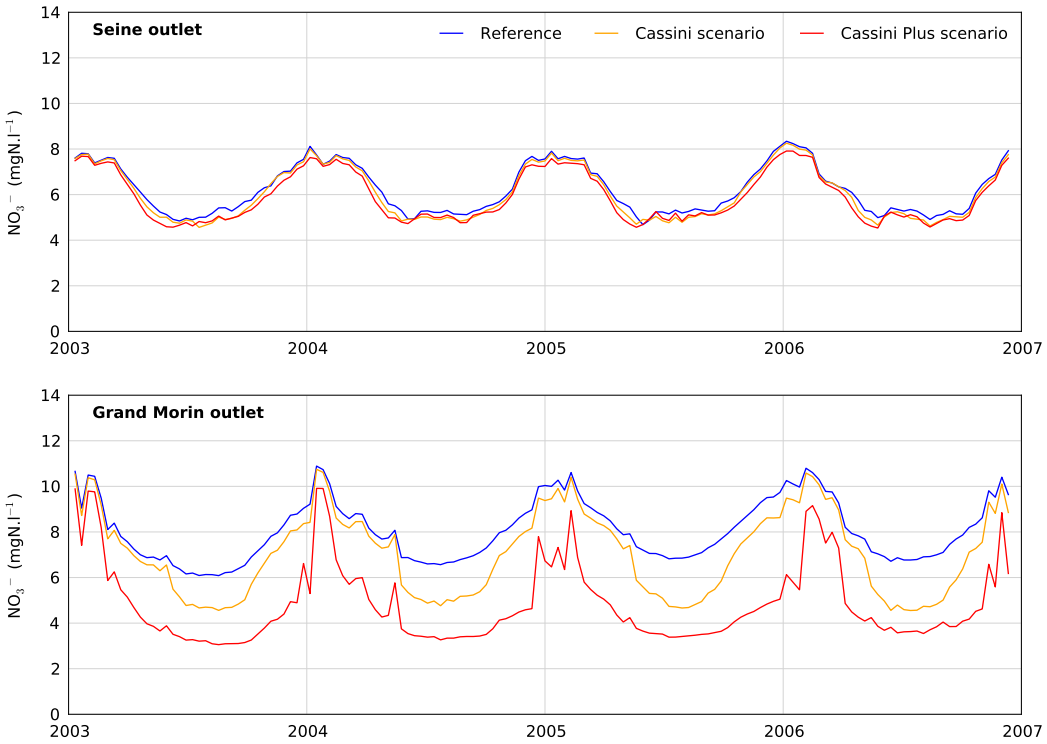

FIGURE 5.10 – Comparison of the reference situation with the « Cassini » and « Cassini plus » scenarios at the outlet of the Seine and the Grand Morin sub-basin for the hydrological years 2003–2006.

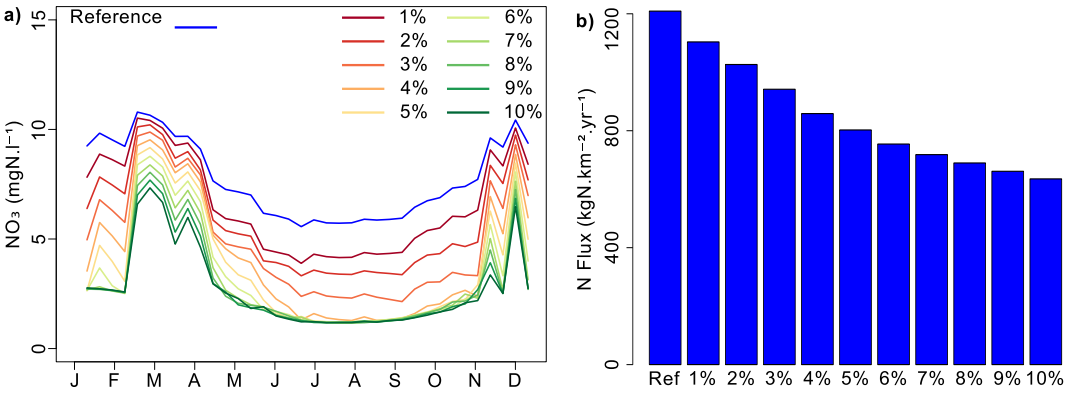

FIGURE 5.11 – a) Seasonal variation of nitrate concentration according to the proportion of ponds (in %) within the watershed at the outlet of the Orgeval sub-basin for the hydrological year 2006. b) Annual N flux at the outlet of the Orgeval watershed as a function of the percent watershed area covered by ponds. Calculations are for the hydrological year 2006 (blue bars). The corresponding reduction is also shown (red line).

In order to highlight the impact of pond restoration, at a smaller scale, we also analyse here the results at the outlet of the Grand Morin sub-basin (1200 km^2). The Grand Morin, located on impermeable substrate, was covered with 1 % of ponds at the end of 18th century and with 2.7 % in the "Cassini Plus" scenario. For the reference situation, N fluxes ranges from 920 kgN.km^{-2}.y^{-1} in 2005 to 1470 kgN.km^{-2}.y^{-1} in 2003. With the Cassini scenario a mean decrease of 2 % can be reached and with the Cassini Plus scenario a mean decrease of 20 % could be achieved at the outlet of the Grand Morin River.

In each of the ten scenarios focusing on the Orgeval sub-basin (104 km^2), the size of the reintroduced pond area was increased from 1 % to 10 % of the total area of each 1st order sub-basin. Figure 5.11a shows the seasonal variations of nitrate concentrations for these ten scenarios compared to the reference 2006 situation. More contrasts between scenarios are logically observed during summer at optimum microbiological activity (i.e. denitrification). Even with a pond density of 1 %, a substantial decrease in nitrate concentrations was observed in summer (from 5.1 mgN.l^{-1} to 4.3 mgN.l^{-1}). Between June and November, a plateau of approximately 1.5 mgN.l^{-1} was reached from a 5 % pond coverage. The effect of ponds was more linear during spring and late autumn. During these periods, each additional percent area of ponds decreased the nitrate concentration by about 0.3 mgN.l^{-1}.

On an annual basis, a 1 % watershed area devoted to ponds already reduced the nitrogen flux at the outlet of the Orgeval basin by approximately 9 % (figure 5.11b). An N decrease of one-third can be reached by 5 % pond cover. Over 5 % pond cover area, no additional reduction was found in the biologically active period (figure 5.11a).

5.5 Discussion

The Seneque/Riverstrahler model, fed with available data on meteorological and hydrological constraints and point and diffuse inputs, was shown to capture most of the trends and levels of nutrient concentration in the Seine drainage network. It was also shown to be able to reproduce the behaviour of nitrate in a small pond established on a head water stream. It is therefore suitable as a tool for testing different scenarios of watershed management, including ecological engineering (Allen et al., 2003). The results obtained in this study show the great potential of ponds implemented on headwater streams to effectively reduce agricultural nitrate contamination in rural regions where the lithological substrate allows their impoundment at densities of a 1 – 5 % of the agricultural area. Such ponds were already present in the traditional landscape of these regions prior to the industrial revolution. The scenario investigations clearly show that the rehabilitation of ponds can be very useful for reducing nitrogen in the headwaters of the Seine basin.

In view of the small ponds areas required to obtain a significant nitrogen reduction, the effect on the water balance by increasing evaporation would be quite minor. Pond restoration however would inevitably have an impact on aquatic biodiversity. Ponds or constructed wetlands could become sites for hygrophilous biodiversity (Oertli et al., 2002). A survey com-

paring streams and ponds biodiversity in an agricultural landscape of the southern part of England led to a twofold higher number of invertebrates in ponds than in streams (Williams et al., 2004). As reported by (Hansson et al., 2005), others studies have shown it is possible to optimize both nutrients retention and biodiversity, for instance by working on geometry and shoreline complexity of ponds. Ponds are stagnant water bodies and their rehabilitation modifies the morphology of channels (Smith et al., 2002) and, may increase water temperature, changes the oxygen diurnal cycle, etc., which all play an important role for fish habitat (Pichon et al., 2006; Pedersen et al., 2009). The fish population could shift from river species such as trout (*Salmo trutta*) to pond species such as carp (*Cyprinus Carpio*). However, reintroducing ponds in 1st order streams would not greatly disturb migratory species such as salmon or eel, contrary to dams located on downstream parts of rivers, which have strong effects on fish populations (Im et al., 2011). Ponds could also have an impact at the scale of the whole surrounding ecosystem. In an English survey, species of macroinvertebrates and macrophytes were enriched next to a pond compared to a nearby stream (Davies et al., 2007). Regarding results issued from our simulations impacts of ponds on silicon fluxes and phytoplankton development, although significant at the outlet of the pond itself (table 5.3), is limited downstream. In average on the three years of the studied period reintroduction of ponds would lead to a decrease by 1.0 mgSiO_2.l^{-1} and by 2.12 μgChla.l^{-1} at the outlet of the Seine basin.

However, besides a possible neutral impact on fish and positive impacts on biological richness, ponds could play a negative role on greenhouse gas emissions (GHG) (Bartlett and Harriss, 1993). Emissions of methane ranging from 6 to more than 60 gCH_4-C.m^{-2}.y^{-1} were measured in a constructed marsh wetlands in central Ohio (Nahlik and Mitsch, 2010; Sha et al., 2010). Emissions of CH_4 were also measured in three ponds of the southern part of Sweden during the years 2003 – 2004. Maximums are observed at the end of summer reaching 9 to 17 mgCH_4.m^{-2}.h^{-1} (Stadmark and Leonardson 2005). The denitrification in the ponds might be at the origin of N_2O emissions, an intermediate product of the process, as already observed in stream sediments (Garnier et al., 2010c). During summer, an average N_2O emission of 26 μmol N_2O-N.m^{-2}.d^{-1} was measured in a reservoir located in Washington State (USA) (Deemer et al., 2011). Garnier et al. (2009b) estimated N_2O emissions for the whole water surface area of the Seine drainage network to 100 – 200 $\times$ 10^3 kgN_2O.yr^{-1}, corresponding to 3 – 6 $\times$ 10^{-4} kgN-N_2O.m^{-2}.yr^{-1}. In the « Cassini Plus » scenario, total area of ponds is 584 $\times$ 10^6 m^2. Thus N_2O emissions by ponds can be estimated to 176 $\times$ 10^3 kgN-N_2O.yr^{-1} to 353 $\times$ 10^3 kgN-N_2O.yr^{-1}, which remains low regarding the total emissions by the soils of the basin reaching 10400 $\times$ 10^3 kgN-N_2O.yr^{-1} (Garnier et al., 2009b).

At the scale of the whole Seine watershed, the lithological conditions of many intensive agricultural areas are not suitable for easy introduction of ponds because of the permeability of the substrate. For this reason, the scenarios tested do not result in a significant reduction in the total nitrogen flux delivered at the outlet of the Seine watershed as a whole. This limitation implies that artificial pond creation can only be one of several other measures to reduce nitrate contamination of water resources. Preventive actions based on fertilising reduction aiming at reducing nitrogen leaching losses from agricultural land should be preferred over curative solutions (Haag and Kaupenjohann, 2001b). Different practices may decrease nitrate leaching. A current one is the introduction of catch crops during winter in order to avoid bare soil during the rainy period. Several studies show that this practice can decrease N leaching by 20 – 30 % (Engstrom et al., 2011). A more drastic solution could be a wide conversion to organic farming. Sub-root water nitrate concentration could shift from 9–13 mgN.l^{-1} in conventional agriculture (Korsaeth and Eltun, 2000) to 4.5–6.5 mgN.l^{-1} in organic farming (Honisch et al., 2002). A modelling exercise of a widespread application of organic farming throughout the Seine watershed decreases the nitrogen surface runoff fluxes by 54 – 73 % (Thieu et al., 2011). Another more technological and possibly more costly way to reduce N leaching could be the implementation of precision farming (Tilman et al., 2002). The aim is to synchronise fertiliser application with plant demand (Di and Cameron, 2002) or to better distribute fertiliser application spatially according to N storage in the soil (Guerif et al., 2007).

Other landscape engineering practices can also reduce nitrate contamination of the hydrosystem. The denitrification power of riparian wetlands is well known (Hill, 1996; Mitsch and Gosselink, 2000; Vidon and Hill, 2004). A riparian buffer zone 460 m long, in an undrained area decreases nitrates by 2200–2640 kgN.yr^{-1} (Kuusemets and Mander, 2002). The floristic composition of the riparian wetland has an impact on nitrogen removal and some species with negative mycorrhiza responsiveness and high root lateral spread have

been shown to be more efficient in terms of nitrogen uptake (Bingham and Biondini, 2010). In the northern region of China, a combination of stone dams, roadside grassed ditches, a vegetated buffer strip, ponds and a riparian buffer zone have provided a 66 % N decrease (Wang et al., 2005). Within the Seine watershed, the denitrification rate by riparian wetlands has been estimated at 35 % (Billen and Garnier, 1999; Curie et al., 2011), but similar to ponds, many of these buffer zones were destroyed when straightening rivers and streams. Preservation, rehabilitation, or even construction of wetlands might be an effective, economical, and ecologically sustainable method to treat N-contaminated waters (Beutel et al., 2009; Arheimer et al., 2004). More generally, the organisation of the landscape within the watershed has an impact on nitrogen cycling (Burt and Pinay, 2005), as landscapes are more or less N-retentive depending on their mosaic of elementary patches (Li et al., 2005).

5.6 General conclusion

The data and simulations presented in this paper show that ponds reintroduction could be an effective way to decrease nitrate concentration in the upstream sectors of watersheds. At the scale of a large catchment like the Seine basin however, the density of ponds would never be high enough to get notable decreases of nitrate delivered to the coastal zone. Indeed ponds implementation would only be possible in areas with impermeable substrate. Managing the spatial organisation of patches within the watershed landscape and the drainage network, by taking advantages of the retentive capacity of a variety of buffer zones including ponds, however offer promising curative means to reduce nitrogen contamination of water resources, but they must be accompanied by preventive methods aiming at reducing the release of nitrate by agriculture.

Chapitre 6

Impacts of ponds on nutrients fluxes within the urbanized and industrialized watershed of the Zenne River

6.1 Introduction

Due to the location of Brussels, in the center of the basin of the Zenne River, its history is quiet well documented, by both detailed cartographic sources and written archives. Thanks to these we have been able to determine the number of ponds present within the watershed at the end of the 19th century. Differently from the Seine basin, the Zenne basin started its urbanization and industrialization earlier by the end of the 18th century. Using the modelling approach as exposed in chapitre 1, its application to the small well documented Zenne basin for historical period in comparaison to the year 2010 allows to go further in this chapter where we hilight the role of ponds on nutrients (N, P and Si) and on the trophic-chain (phyto and zooplankton).

La Zenne et la bièvre, le malheur des rivières urbaines

La Zenne comme la Bièvre sont deux rivières urbaines. Leurs bassins sont respectivement de 1100 et 203 km^2, et leur longueur de 103 et 33 km. Si Les bassins amont sont historiquement ruraux ou périurbain, leur portion aval traverse Bruxelles pour la première et Paris pour la seconde. Elles ont donc été très tôt impactées par le développement de ces agglomérations.
Ces deux rivières ont été utilisées comme égouts pendant très longtemps et de nombreuses industries (tanneries, blanchisseries, brasseries ...) se sont installées le long de leurs berges dès le Moyen-Âge (figure 6.1). Une de ces installations la plus célèbre est la teinturerie des Gobelins, construite au sud de Paris au bord de la Bièvre, et qui a exporté ses tapisseries à travers toute l'Europe entre les 17ème et 19ème siècles. Ces activités industrielles ont profondément modifié le milieu aquatique (Billen et al., 1999). Au tournant des 19ème et 20ème siècles, vu l'état déplorable de ces rivières et leurs émanations pestilentielles, les pouvoirs publics ont décidé de les couvrir et de les convertir ainsi officiellement en égouts.

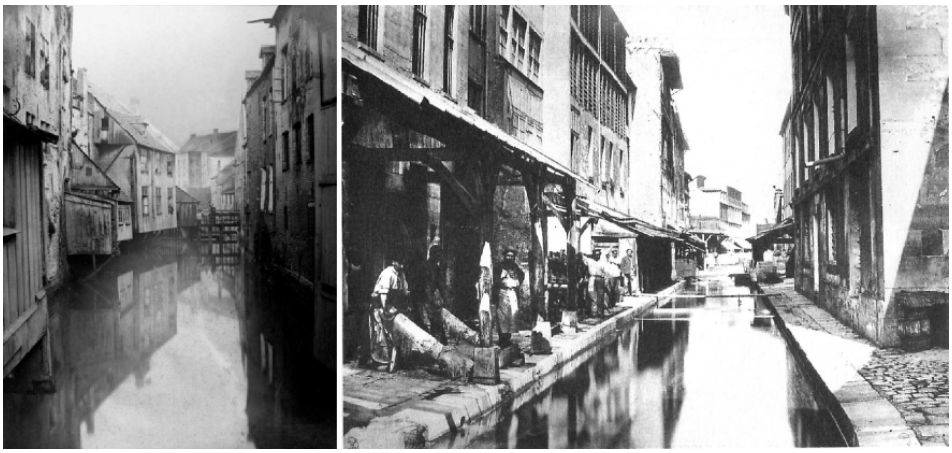

FIGURE 6.1 – De gauche à droite : la Zenne à Bruxelles à la fin du 19ème siècle, la Bièvre à Paris au niveau de la manufacture des Gobelins dans l'actuel 13ème arrondissement à la fin du 19ème siècle *(cliché : Charles Marville)*.

Aujourd'hui les secteurs amont de ces deux rivières ont été réaménagés et servent de lieux de détente et de promenades aux riverains (Carré et al., 2011). La partie aval de la Bièvre est totalement recouverte et passe dans le réseau d'égout de la ville de Paris géré par le SIIAP (Syndicat Interdépartemental de l'Assainissement de l'Agglomération Parisienne). Quant à la Zenne, jusqu'en 2007, elle recueillait la totalité des eaux usées de l'agglomération bruxelloise sans aucun traitement. Son cours inférieur était donc concentré en phosphore, azote et quasiment dépourvu d'oxygène. Elle pouvait être considérée comme une rivière morte. Mais c'est surtout depuis la mise en place en 2007 de la seconde station d'épuration que sa charge en phosphore et azote a considérablement diminué, et que son taux d'oxygène a grandement augmenté. L'état de la Zenne tend donc à s'améliorer depuis quelques années.

6.2 Hydraulic management in the Zenne : a modeling approach

The Zenne watershed has a surface area of 1160 km^2. Whereas we can consider that the drainage network of rivers and streams of the Zenne has not changed when comparing ancient map with present ones, hydraulic annexes, such as stagnant system have deeply changed in their function. A majority of the ponds are today sand-pit lake used for extracting

building material and as recreational area, having lost their connectivity with the drainage network, differently from those in the historical period when they were directly impounded within the river bed. At that time, hydraulic energy from water mills played a major role in many activities. Mills were installed on the smallest streams as well as on the major rivers. Installation of these mills along with the construction of dikes and the creation of ponds all along the smallest stream orders (figure 6.2). This hydraulical management resulted in a succession of fast- and slow-flowing stretches in the most populated areas. Many of these ponds were filled after introduction of the steam engine.

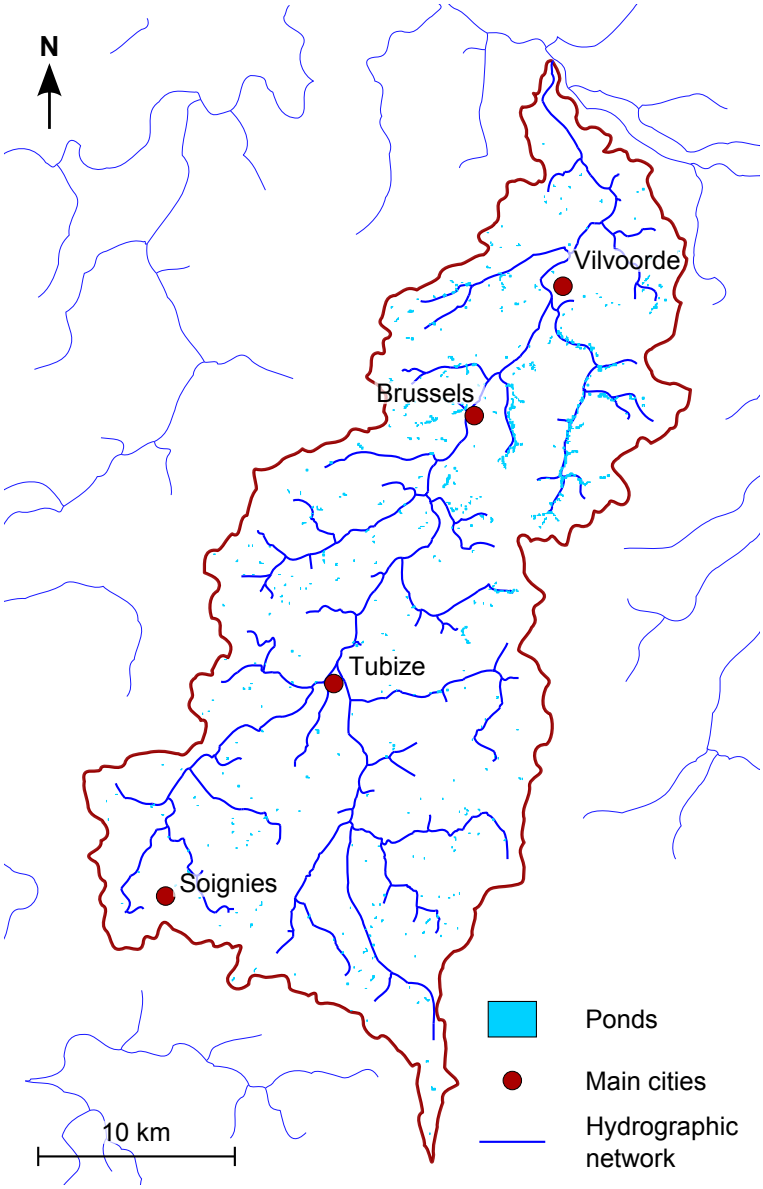

FIGURE 6.2 – The Ferraris map of the Zenne basin, as presented in the Atlas, where the drainage network as considered in the modellling approach is highlighted (left). Distribution of ponds digitalized from the Ferraris map.

For the present period (see chapter 1), we made the assumption of a complete lack of connectivity of ponds, so that no hydraulic annexes where taken into account in the modeling approach. For the historical periods, beside counting and georeferencing the ponds, we also estimated their surface area (see in the following section), and with the expertise of our historian colleagues considered an average depth of 1.5 m according to the orders. Stagnant systems, deeper and wider than the river itself, increase the residence time of the water, subsequently modifying the net growth rate of the biological compartments, and nutrient cycling.

Basins	Basin area (km²)	Ponds surface area (ha)		
		Ferraris	DLG	Present
Zenne axe	192	69	48	97
Zenne WSH	236	22	17	5
Sennette	272	33	36	24
Hain	85	5	4	7
Zuunbeek	91	21	11	12
Linkebeek	28	13	7	0
Pedebeek	22	7	7	10
Molenbeek	25	20	5	4
Maelbeek	17	50	15	7
Woluwe	103	138	55	64
Maalbek	42	28	16	13
Kesterbek	23	4	4	9
Barebeek	47	10	12	12
Meerbek	48	20	18	16
Total Zenne	**1231**	**440**	**255**	**280**

TABLE 6.1 – Changes in the pond surface area (ha) in the various sub-basins of the Zenne river. Ferraris : map of the cabinet (carte de cabinet) 1 :1152, supervised by the Comte de Ferraris 1771-1778 ; DLG : dépôt de la Guerre map 1 :20,000 realized from1865 to 1878 but finished from 1878 to 1880 by the Institut Cartographique Militaire ; present is shown for comparison : map from the pan-european urban atlas, giving information on the urban land use for conurbation > 100 000 inhab, here that for Brussels covers 67 % of the whole Zenne basin (see figure 1.1 for location of sub-basins).

6.3 Hydromorphology

Ponds were inventoried and geo-referenced for the 1890s from the « Dépôt de la Guerre » and « Institut Cartographique Militaire » maps (1865 to 1880, 1 :20,000) (hereafter called DLG maps), (table 6.1) for the whole Zenne basin. The inventory for the present situation is based on the pan-European urban Atlas (2005), giving information on urban land use for conurbations with more than 100,000 inhabitants (here, Brussels), covering only 67 % of the Zenne basin (table 6.1). Although no striking differences appear between the two periods, in terms of pond surface area, the shift in their functions, namely from industrial power generation to recreational or ornamental purposes, led to deep changes in their functionality, from closely connected to the river courses in the past to highly disconnected in the present situation, where sand-pit ponds form a large share of the stagnant systems. For these reasons, the results for the present period shown above were considered without taking into account any stagnant annexes in the hydrological network (ponds were not mentioned above for the present times).

To illustrate the long-term historical changes in ponds, we also geo-referenced the map supervised by the Comte de Ferraris (1771–1778, Carte de Cabinet, 1 :1152) and inventoried the ponds. The data clearly show a nearly 50 % decrease over one century (from the 1780s to the 1880s). As a whole, the surface area of the ponds relative to the surface area of the watershed decreased from 0.36 % in the 1790s to 0.21 % in the 1890s (table 6.1), without a clear further reduction in surface area today, the major feature being their lack of connectivity.

Geo-referencing the ponds for the 1790s (de Ferraris, 1770) and 1890s (DLG map) at the scale of the Zenne basin and estimating their size provides more information on the historical features. Similar to the Zenne, the extensive alteration of the hydraulic regime of rivers by human activity since the Middle Ages (10th to 12th centuries, (Deligne, 2003), is reported for the Paris basin by Guillerme (1983). These stagnant systems were constructed for a variety of functions early in the history of the area (fish ponds : (Benoit and Mattéoni, 2005), fish ponds and mills : (Deligne, 2003) ; wood floating for transportation : (Benoit and Berthier, 2005)) and they were well connected to the rivers, contrary to today's stagnant systems (i) coming from material extraction for construction (building, roads, etc.), such as sand-pit lakes that were then rehabilitated for recreational use ((Garnier and Billen, 1994; Davies et al., 2007; Völker and Kistemann, 2011) or (ii) created in the landscape at the

outlet of an agricultural drainage system for fertilizer (nitrate) removal.

6.4 Role of hydromorphology of the drainage network

For a better understanding of the role of ponds and the covering of the Zenne River in Brussels, seasonal variations of the main impacted variables are shown in figure 6.3 for the downstream station (Eppegem) and for the two historical periods, the 1790s and 1890s, the former being characterized by ten times less pollution, more ponds and the main branch flowing uncovered along its entire course. The present situation (2010) is also shown for comparison.

Whereas in both periods phytoplankton reached a higher level than today owing to the presence of connected ponds, especially in spring and late summer, the level was similar for the two historical periods. However, much higher consumer biomass (zooplankton) at the river's outlet is calculated by the model in the 1790s, supporting the assumption of a much higher phytoplankton production, which was maintained at a similar algal biomass level owing to much higher grazing in the 1790s than in the 1890s (figure 6.3). Note that it is advantageous to focus on zooplankton here which generally does grow much in rivers, because the residence time of the water is lower than its growth rate (Garnier et al., 1995), except when connected to stagnant systems. The higher silicon depletion with ponds, although accentuated in the 1790s, corroborates this interpretation. The higher primary production can be clearly associated with the 20 km of the river receiving light in the 1790s but not in the 1890s (river covered). Therefore, running the model for the two periods with and without ponds brings out the effect of ponds (e.g., residence time) and the effects of covering the river (e.g., light limitation). The presence of ponds, which favored the development of algae and zooplankton, subsequently must have driven freshwater fish production, whose consumption was promoted by the Catholic church, which imposed lent for 166 days per year (Bérard, 1988; Levasseur, 2004).

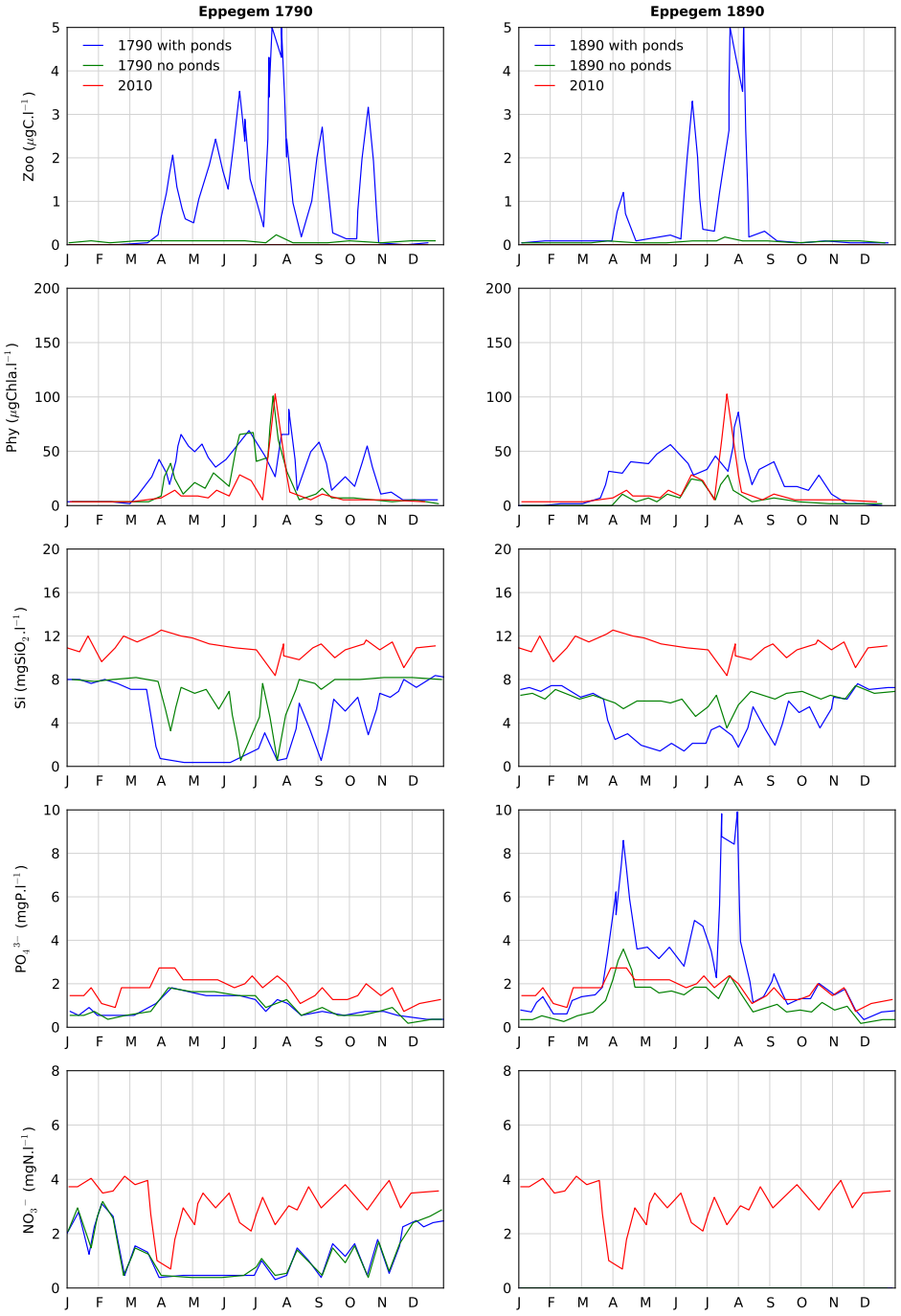

FIGURE 6.3 – Seasonal variation of water quality variable as calculated by the model for the 1890's with and without the ponds (ZOO : zooplankton ; PHY : phytoplankton ; Si : silicon ; PO_4^{3-} : phosphates ; NO_3^- : nitrate). The station at Eppegem downstream Brussels on the main branch is represented. The year 2010 is shown in comparison.

Regarding the other nutrients, differences obtained among the two periods for phosphates are linked to the point source constraints, which ranged within a factor of 10, while at high P loads in the 1890s, higher phosphate may be attributed to higher recycling in ponds (figure 6.3). It should again be mentioned that by comparison with the reference in 2010, phosphates were somewhat lower in the 1790s but much higher in the 1890s. Nitrate of diffuse origin logically shows a much higher level today, due to the recent use of synthetic fertilizers in agriculture (figure 6.3). Particularly striking is the disappearance of nitrate in the 1890s, mostly linked to denitrification, a microbial process associated with organic pollution at the origin of anoxic conditions, favorable to the reduction of nitrate into N_2, i.e., elimination into the atmosphere. Denitrification and nitrate elimination are currently observed in aquatic systems where organic pollution is high, even in the 2000s in the Zenne,

before the implementation of the Brussels wastewater treatment plants, and more generally in the Scheldt estuary up to the 1980 (see Billen et al. (1985) for the 1970s and Soetaert et al. (2006) for a long trend).

6.5 Conclusion

In order to better understand the role of the ponds, phytoplankton and zooplankton -a major phytoplankton consumer- are analysed together. Indeed whereas phytoplankton can blooms with a residence time of only a few days in the river, zooplankton requires at least 3 to 4 weeks, a condition found in summer period when the lower discharge and the ponds increase the water residence time in the drainage network. Whereas in both periods phytoplankton reached a higher level than today owing to the presence of connected ponds, especially in spring and late summer, the level was similar for the two historical periods. However, much higher zooplankton biomass at the river's outlet is calculated by the model in the 1790s (see chapter 1), supporting the assumption of a much higher phytoplankton production, which was maintained at a similar algal biomass level owing to much higher grazing in the 1790s than in the 1890s (figure 1.7). Note that it is advantageous to focus on zooplankton here which generally does not grow much in rivers, because the renewal rate of the water is higher than its growth rate (Garnier et al., 1995), except when connected to stagnant systems. The higher silicon depletion with ponds, although accentuated in the 1790s, corroborates this interpretation. The higher primary production can be clearly associated with the 20 km of the river receiving light in the 1790s but not in the 1890s (river covered). Therefore, running the model for the two periods with and without ponds brings out the effect of ponds (e.g., residence time) and the effects of covering the river (e.g. light limitation). The presence of ponds, which favored the development of algae and zooplankton, subsequently must have driven freshwater fish production, whose consumption was promoted by the Catholic church, which imposed lent for 166 days per year (Bérard, 1988; Levasseur, 2004).

As for the Seine basin, many ponds were built along the Zenne River, for similar purposes. At the end of the 18th century, their effects on NO_3^- were quiet low. On the one hand, pollution by nitrates was low due to the traditionnal cultural practices, on the other hand, the density of ponds within the basin was too weak to get a real impact on nitric pollution. Concerning silicon, ponds were responsible of a depletion especially during Summer. It could be explained by two factors. The first one, silicon was used by phytoplankton, favored by the long residence time of water within pondsn to grow up. The second one, silicon was trapped into the benthic sediments. Finally, for historical periods, silicon was much more sensible to ponds than nitrate.

À retenir sur le rôle des étangs

- ⋆ Les étangs, comme tous les secteurs stagnants du réseau hydrographique, sont des lieux favorisant la dénitrification benthique, éliminant ainsi une proportion non négligeable des nitrates en transit.
- ⋆ Le suivi d'un étang en contexte agricole a permis de quantifier une rétention d'azote dépassant les 50 % en été. Le modèle Seneque/Riverstrahler s'est révélé capable de bien rendre la dynamique saisonnière de l'azote de ce plan d'eau.
- ⋆ À la fin du 18$^{\text{ème}}$ siècle, plus de 2500 étangs étaient présents dans le bassin de la Seine, pour la grande majorité au fil de l'eau sur les ordres 1 coulant sur un substrat imperméable. Ainsi, les étangs représentaient 0.24 % de la superficie du bassin.
- ⋆ À l'exutoire de la Seine, une proportion de 0.24 % ou de 0.76 % d'étangs (selon le scénario construit) n'entraîne pas de diminution des concentrations de nitrates.
- ⋆ À l'exutoire du Grand Morin, 1 % d'étangs entraine une diminution des concentrations en nitrates de 2 % en moyenne annuelle, et une proportion de 2.7 % entraine une diminution de 20 %.
- ⋆ Une série de tests centrés sur le bassin de l'Orgeval a montré que 5 % d'étangs permettait de réduire d'un tiers les concentrations en nitrates à l'exutoire. Au delà de 5 %, peu de gains sont obtenus.
- ⋆ Sur le bassin de la Zenne, 240 étangs étaient présents à la fin du 18$^{\text{ème}}$ siècle.
- ⋆ Ces étangs favorisaient le développement du phytoplancton et du zooplancton, et étaient responsables d'une diminution estivale des concentrations en silicium. L'influence de ces étangs sur les nitrates était faible, vu la faible densité qu'ils représentaient.

Quatrième partie

Le filtre estuarien

« En suivant le fleuve, on parvient à la mer. »

Plaute

Cette partie IV explore le rôle du filtre estuarien sur les flux de nutriments et les développements algaux associés.

Les estuaires, réceptacles de l'ensemble des nutriments transportés par les réseaux hydrographiques, constituent bien souvent des milieux particulièrement actifs sur le plan biogéochimique, susceptibles d'affecter, par transformations, élimination ou stockage, l'importance des flux transférés aux zones marines côtières adjacentes. Ceci est particulièrement vrai dans le cas des estuaires macro-tidaux, tels que ceux de la Seine, de la Somme et de l'Escaut, où les courants de marée conduisent à l'établissement d'une zone de forte turbidité au début de la zone de mélange de l'eau douce et de l'eau de mer. Ce *bouchon vaseux* joue un rôle majeur dans les processus biogéochimiques estuariens. Mais les estuaires sont aussi, dans les pays industrialisés, des zones d'intérêt économique majeur, et les aménagements destinés à implanter des grandes infrastructures portuaires ou à faciliter la navigation on souvent été considérables. Elles peuvent avoir abouti à restreindre fortement l'extension des vasières intertidales et à réduire considérablement le temps de résidence des masses d'eau dans l'estuaire.

Nous présentons dans cette partie deux approches très différentes de modélisation des processus biogéochimiques dans les estuaires. L'une met en œuvre un modèle très détaillé du comportement hydrodynamique et biogéochimique de l'Estuaire de l'Escaut développé à l'Université de Bruxelles. Les conditions limites amont y sont définies par le modèle Seneque/Riverstrahler appliqué à l'Escaut. Dans cette approche, une description déterministe des processus biologiques est associée à une description hydrodynamique précise et spatialement explicite des processus hydrologiques. Un bilan des transferts de nutriments peut en être déduit.

L'autre approche, développée ici pour le cas de l'estuaire de la Seine, consiste dans une modélisation plus simplifiée et générique du rôle du bouchon vaseux, assimilé à un réacteur à lit fluidisé. Si la description des processus biogéochimiques se fait avec une finesse analogue à celle du modèle précédent, la représentation des processus hydrologiques et hydrosédimentaires est beaucoup plus frustre. Le modèle a néanmoins pu être validé avec succès sur le cas de l'estuaire de la Seine. Il est utilisé ici pour étudier le rôle du filtre estuarien sur l'ensemble de la chronique 1985-2007 du fonctionnement du réseau hydrographique de la Seine que nous avons reconstituée .

Le premier chapitre de cette partie (chapitre 7) synthétise l'article :

Modelling phytoplankton succession and nutrient transfer along the Scheldt estuary (Belgium, The Netherlands), *Nathalie Gypens, Eric Delhez, Alice Vanhoutte-Brunier, Sebastien Burton, Vincent Thieu, Paul Passy, Yuhong Liu, Julie Callens, Veronique Rousseau, Christiane Lancelot* accepté dans *Journal of Marine Systems.*

Le second chapitre (chapitre 8) est un extrait de :

C/N/P/Si cycling in the Land-to-Sea Continuum of the Seine River : Modelling the Impacts of Future Human Activity Changes in the Watershed, chapitre de l'ouvrage *Biogeochemical Dynamics at Large River-Coastal Interfaces : Linkages with Global Climate Change*, Editors : T. S. Bianchi, M.A. Allison, & W.-J. Cai. Cambridge University Press, signé par *Josette Garnier, Paul Passy, Vincent Thieu, Julie Callens, Marie Silvestre, Gilles Billen.*

Il présente la demarche générique du modèle LIFT et son application à la chronique de résultats obtenus à l'exutoire fluvial de la Seine depuis 1984. Il en découle une quantification de l'effet filtre de l'estuaire de la Seine sur les nutriments N, P et Si.

Une discussion générale de l'effet des estuaires sur les flux de nutriments issus de leurs bassins versant amont clôture ce chapitre.

Le poste de la cascade de nutriments traité dans cette partie est représenté sur la figure 6.4.

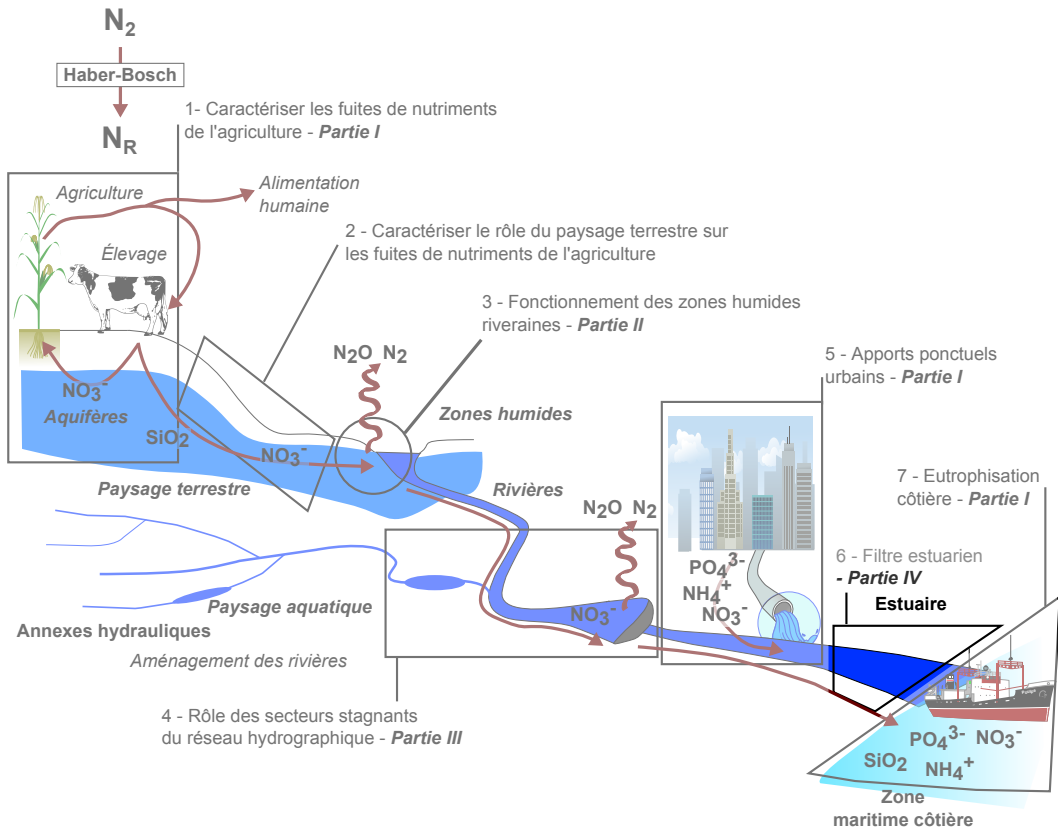

FIGURE 6.4 – Les postes de la cascade de nutriments traités dans la partie IV.

Chapitre 7

Modelling nutrient transfer along the Scheldt estuary

7.1 Modelling phytoplankton succession and nutrient transfer along the Scheldt estuary (Belgium, the Netherlands)

7.1.1 The environment of the Scheldt estuary

Estuaries are shallow open systems strongly influenced by river inputs, mixing with the coastal ocean and exchanges across the sediment-water and atmosphere-water interfaces. These transitional zones between the freshwater and the marine systems are characterized by important salinity (SAL) gradients and receive large amounts of dissolved and particulate carbon (C), nitrogen (N), phosphorus (P) and silicon (Si) of natural and anthropogenic origin from rivers. This riverine material undergoes profound transformations in estuaries before being transferred to the adjacent coastal zone (Wollast, 1983). Under the dual influence of climate and anthropogenic changes (Paerl et al., 2006), estuaries are characterized by a large variability of physical and chemical properties that affect directly planktonic communities and indirectly the biogeochemical role of estuaries, in terms of e.g. transformation, retention or removal of nutrients.

At the interface between freshwater and marine ecosystems, estuaries are characterized by distinct phytoplankton assemblages along the salinity gradient (Attrill and Rundle, 2002; Quinlan and Phlips, 2007; Muylaert et al., 2009). While freshwater phytoplankton is adapted to low salinity and marine species to high salinity, some species are resistant to small salinity fluctuations and grow at intermediate salinity (Muylaert et al., 2009; Roubeix and Lancelot, 2008). In addition to the impact of salinity, the mixing of fresh and marine waters creates unique hydrodynamic and hydro-sedimentary conditions (in particular water residence time and turbidity) that structure the estuarine ecosystem and impact the associated carbon and nutrient cycles (Lancelot and Muylaert, 2012). Understanding the effect of these physico-chemical conditions on phytoplankton organisms and describing the phytoplankton succession is a pre-requisite to assessing the ecological and biogeochemical function of estuaries.

The Scheldt estuary, located in the southwest Netherlands and northern Belgium (figure 7.1), is a shallow, well-mixed, and relatively turbid macrotidal estuary. It is one of the mostnutrient-rich and polluted systems in the world (Wollast, 1988) where human activities on the watershed have deeply altered the quality of surface waters since the second half of the 20th century (Billen et al., 2005; Meire et al., 2005; Van Damme et al., 2005; Soetaert et al., 2006). Increased river nutrient and organic matter inputs have changed the estuarine biological activities and biogeochemical cycles (Soetaert et al., 2006; Billen et al., 2005) and have contributed to the eutrophication of the coastal waters of the Southern North Sea (Lancelot et al., 2007). Since the 1990's the implementation of wastewater treatment led to a marked improvement in the water quality in the estuary (Soetaert and Herman, 1995; Soetaert et al., 2006). In particular, the largest wastewater treatment plant of the city of Brussels (1.4 M inhabitant equivalent IE) is operating since March 2007. Phytoplankton communities are spatially structured in the Scheldt estuary with marked shifts between fre-

shwater, euryhaline and marine species (Muylaert et al., 2000; Lancelot and Muylaert, 2012). Despite important changes in nutrient concentration, primary production in the Scheldt estuary does not seem to have changed significantly with nutrient load modification (Gazeau et al., 2005; Kromkamp and Peene, 2005). Although the recent improvement of dissolved oxygen concentrations in the estuary had modified the importance and the composition of zooplankton organisms (Appeltans et al., 2003; Mialet et al., 2011) with an impact on the phytoplankton biomass (Kromkamp and Van Engeland, 2010).

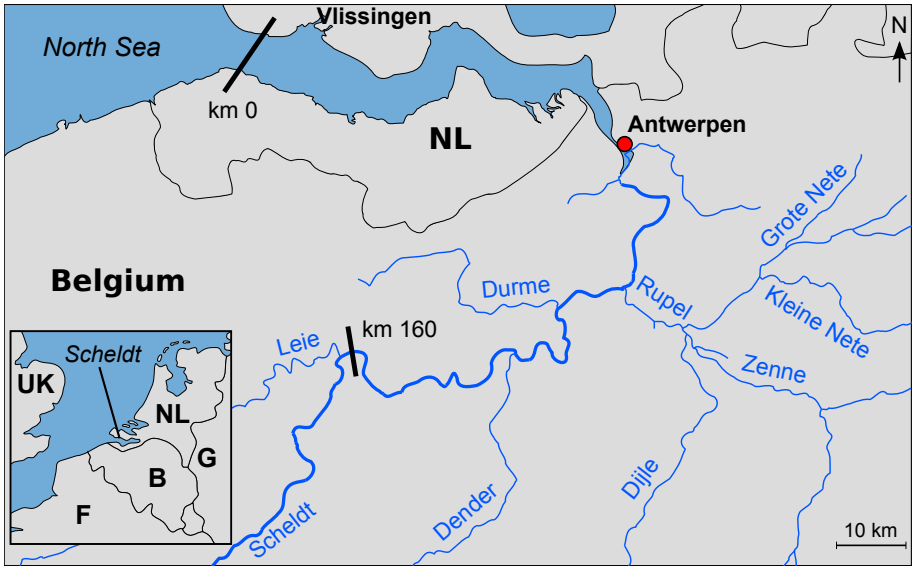

FIGURE 7.1 – River network of the 1D RIVE-MIRO model. Km 0 and km 160 are giving the limit of the model domain.

In this study, we coupled the river (RIVE) and the marine (MIRO) ecologically-based biogeochemical models to describe contemporary plankton succession and the associated nutrient transformation, retention and removal in the Scheldt estuary and to estimate the nutrient export to the coastal zone. For this application the resulting RIVE-MIRO model is coupled with a one-dimensional hydrodynamic model of the Scheldt estuary that includes a suspended sediment module. The offline coupling with the marine 3D-MIRO & CO model (Lacroix et al., 2007b) of the Southern North Sea and the Seneque-Riverstrahler, a biogeochemical model of the Scheldt river system associated to a geographical information system (GIS) description of the watershed (Ruelland et al., 2007), provides respectively the marine, upper estuary and lateral tributary boundary conditions. To the best of our knowledge, this paper is the first attempt to use a river-estuary-coastal sea model that describes explicitly the fate of both freshwater and marine plankton species in the Scheldt estuary and their impact on the nutrient cycling and delivery to the sea. The ability of the model to reproduce biogeochemical trends in the Scheldt estuary is statistically appraised based on a comparison of model simulations with available observations in 2006. Sensitivity tests are further conducted to understand how changing conditions (salinity, turbidity and nutrients) along the estuary drive the spatial distribution of phytoplankton assemblages. Due to the high pressure of human activity on the Scheldt watershed, the coupled model is also used to test the effect of nutrient reduction options (upgrading of waste water, change in agricultural practices) on the nutrient export and eutrophication status of the coastal zone.

7.1.2 Methods and material available on the Scheldt estuary

As previously stated, the coupling RIVE-MIRO models was used for this study. The biological structure of the RIVE-MIRO model assembles fourteen plankton functional types (PFTs) including six phytoplankton groups, four zooplankton and four bacterioplankton groups. The phytoplankton module considers 6 phytoplankton groups : marine diatoms (DAm), marine nanoflagellates (NFm), the *Haptophycea Phaeocystis* (OPm), freshwater diatoms (DAr), *Chlorophyceae* (GRr) and cyanobacteria (Cyr). Phytoplankton growth is described considering 3 intracellular constituents (small metabolites (S), reserve material (R,

[OPM]), functional and structural metabolites (F)) and distinguishes different processes : photosynthesis, reserve synthesis and catabolism, growth and associated nutrient uptake, respiration and lysis (Lancelot et al., 1991, 2005). The zooplankton module details the dynamics of 4 groups of zooplankton : marine microzooplankton (Mzm), rotifers (MZr) and marine (CPm) and freshwater (CPr) mesozooplankton. Trophic relations were established to link freshwater and marine preys and predators. As a first step, freshwater and marine preys are assumed to be available to all classes of zooplankton that however keep their specific prey preferences. Hence, marine nanoflagellates and *Chlorophyceae* are grazed by marine microzooplankton and freshwater rotifers, then marine and freshwater diatoms are grazed by marine and freshwater copepods. Similarly, marine and freshwater bacteria are consumed by marine microzooplankton and rotifers, themselves under the grazing pressure of marine and freshwater copepods. Exception is for large marine *Phaeocystis* colonies and freshwater filamentous cyanobacteria that are reported as unpalatable. *Phaeocystis* colonies escape grazing, but are submitted to colony disruption which releases nanoflagellates cells and organic matter in the water. To account for the osmotic stress caused by salinity changes, the mortality of PFTs is modulated by a function of salinity (limS). This parameter is specific to marine and freshwater PFT and was derived from existing experiments testing the effect of salinity on *Phaeocystis* colonies (Peperzak, 2002) and stenohaline and marine euryhaline diatoms (Roubeix and Lancelot, 2008; Roubeix et al., 2008). Similarly to phytoplankton, zooplankton (Cervetto et al., 1999; Nielsen et al., 2003) and bacteria (Bouvier and Giorgio, 2002) (e.g. Schultz and Ducklow, 2000 ; Bouvier and del Giorgio, 2002) are reported as sensible to osmotic chock. However, in the absence of observations to quantify the effect of osmotic stress on heterotrophic organisms, the relationships to salinity developed for euryhaline marine and freshwater diatoms were respectively applied to marine and freshwater zooplankton and bacteria.

The degradation of organic matter by planktonic bacteria is described considering three classes of biodegradability for both dissolved and particulate polymers distinguished on basis of their biodegradability (labile, semi-labile and refractory) and biogenic silicon (BSi). These pools are each expressed in C (DC1, DC2, DC3, PC1, PC2, PC3), N (DN1, DN2, DN3, PN1, PN2, PN3) and P (DP1, DP2, DP3, PP1, PP2, PP3). The hydrolysis of these polymers produces dissolved monomers (BSC, BSN) that can be taken up by bacteria. Inorganic nutrients include NO_3^- , NH_4^+ , $Si(OH)_4$ and PO_4^{3-} , the latter being involved in adsorption and desorption on/from SPM. Hence inorganic P is described by two state variables : the total inorganic P (PIT) and PO_4^{3-} . At each time step, the model considers that PO_4^{3-} is in rapid adsorption-desorption equilibrium with inorganic particulate phosphorus (PIP), according to an hyperbolic relationship proposed by Billen et al. (2007b). Benthic organic matter degradation and nutrient recycling are calculated using the algorithms developed by Thouvenot et al. (2007).

Model implementation

Model simulations were performed for the year 2006. At the upstream boundaries (Ghent and lateral tributaries ; figure 7.1), 10-day mean values for river discharges and SPM concentrations are imposed using the results of the Seneque-Riverstrahler model. The biogeochemical marine boundary conditions (km 275) are provided by daily values of the state variables at Vlissingen simulated by 3D MIRO & CO model for the year 2006 (Gypens et al., 2011). At this downstream boundary, the freshwater phytoplankton, zooplankton and bacteria are set to zero. At the upstream boundaries (Ghent and lateral tributaries ; figure 7.1), marine phytoplankton, zooplankton and bacteria are set to zero and the model uses 10-day mean values for biogeochemical state variables extracted from the results of the Seneque-Riverstrahler model applied to the whole watershed of the Scheldt. In addition, the model takes into account the inputs from point and diffuse sources along the simulated Scheldt estuary. The point loads, i.e. urban and industrial effluents (SPM, nutrients, organic matters and bacteria) are estimated from (i) the effective volume delivered (depending on the effectiveness of the treatment plant), (ii) the type of treatment applied and (iii) their exact location in the Scheldt estuary. Diffuse sources (SPM, nutrients and organic matters) are calculated from rainfall and a constant average composition of nutrients (determined on the basis of empirical data or results of agronomic and hydrogeological models) allocated according to land use and lithological classes in the watershed.

The time evolution of the state variables is calculated by solving the different equations expressing mass conservation according to the Euler procedure. A time step of 15 min is

	DIN	PO_4^{3-}	DSi	O_2	Chl a	SPM	SAL
R^2	0.88	0.83	0.83	0.47	0.83	0.33	0.94
	$p <$ 0.0001	$p <$ 0.0001	$p <$ 0.0001	$p <$ 0.0007	$p <$ 0.0001	$p <$ 0.0069	$p <$ 0.0001
Pbias	-43	11.1	23	-36.9	21.9	23.7	1.8

TABLE 7.1 – Coefficient of determination (R^2) and the percent bias (Pbias) computed between annual model results and data available at each validation stations along the Scheldt estuary. All of the correlations are significant at the 95 % confidence level.

used for the numerical integration.

Validation data

The observations (O_2, nutrients, Chl a, phytoplankton, organic carbon) available in the Scheldt estuary were downloaded from four national (RIKZ (http://www.waterbase.nl), BMDC (http://www.mumm.ac.be/datacentre/) and regional (VMM(http://www.vmm.be/geoview/), OMES project (http://www.vliz.be/projects/omes/data.php) databases. Freshwater diatom data were provided by Van Burm, Vyverman et al. (unpubl.; http://www.vliz.be/projects/omes/downloads.php).

Statistical analysis

In addition to the visual qualitative assessment of the model results, the coefficient of determination (R^2) and the percent bias (Pbias) computed between model results and data were used to assess and rate the model performance. The statistics were estimated based on annual (Figures 7.2, 7.3; table 7.1) and daily (figure 7.4, table 7.2) values available at each validation stations along the Scheldt estuary. The coefficient of determination describes the degree of collinearity between simulated and measured data and expresses the proportion of the variability in the data set that can be explained by the model. Overall, R^2 ranges from 0 to 1 (perfect fit) and values larger than 0.5 are considered acceptable (Moriasi et al., 2007). The percentage model bias (Pbias, the sum of model errors normalized by the data) measures the average tendency of the simulated values to under- (positive values) or over- (negative values) estimate the observations. The optimal value of Pbias is 0, with low-magnitude values indicating accurate model simulation. Performance levels based on Pbias are rating excellent (|Pbias| < 10 %), very good (10 - 20 %), good (20 - 40 %) or poor (> 40 %) (Allen et al., 2007; Maréchal, 2004). Pbias computed for N and P can however be judged as satisfactory if values are = |70 %| (Moriasi et al., 2007).

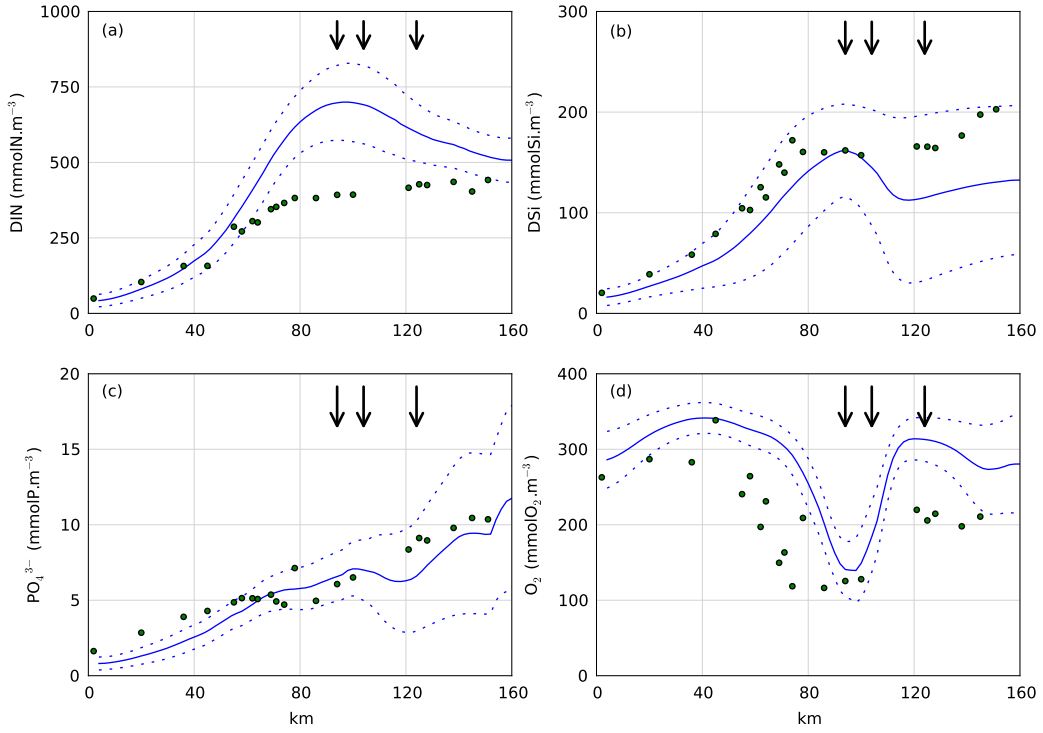

FIGURE 7.2 – Longitudinal evolution of RIVE-MIRO simulated (solid line) and measured (dots) annual mean of DIN (a), DSi (b), PO_4^{3-} (c) and O_2 (d) along the Scheldt estuary in 2006. The arrows correspond to the localization of the input from lateral tributaries (respectively from the Dender, the Durme and the Rupel from upstream to downstream). Dashed line is the standard deviation of simulated results.

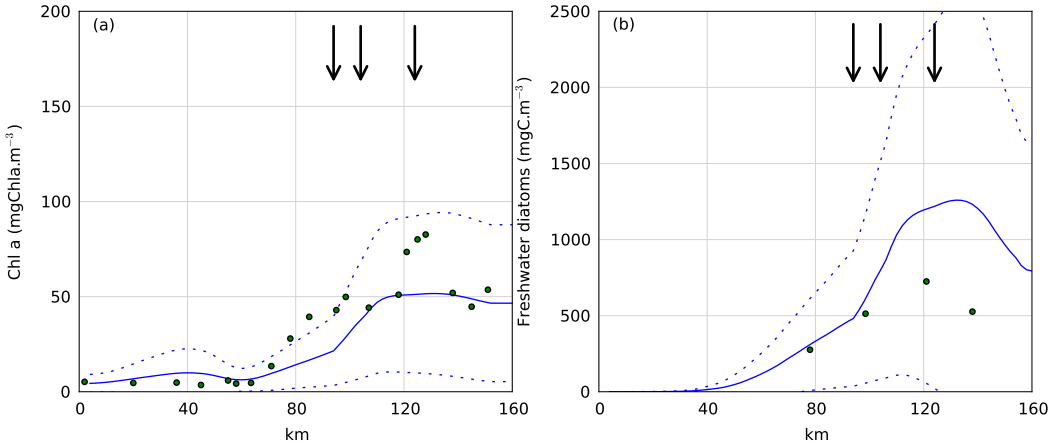

FIGURE 7.3 – Longitudinal evolution of RIVE-MIRO simulated (solid line) and measured (dots) annual mean of Chl a (a) and freshwater diatoms (b) along the Scheldt estuary in 2006. The arrows correspond to the localization of the input from lateral tributaries (respectively from the Dender, the Durme and the Rupel from upstream to downstream). Dashed line is the standard deviation of simulated results.

7.2 Results

The ability of the 1D-RIVE-MIRO biogeochemical model to reproduce physico chemical and phytoplankton trends in the Scheldt estuary is evaluated by visual and statistical comparison of model simulations with available observations for the year 2006. Statistical

	DIN	**PO_4^{3-}**	**DSi**	**O_2**	**Chl a**
R^2	0.54	0.47	0.74	0.33	0.32
	$p < 0.0001$	$p < 0.0001$	$p < 0.0001$	$p < 0.0001$	$p < 0.0001$
Pbias	-38.7	11.3	16.3	-29	19

TABLE 7.2 – Coefficient of determination (R^2) and the percent bias (Pbias) computed between daily model results and data available at each validation stations along the Scheldt estuary. All of the correlations are significant at the 95 % confidence level.

comparisons were performed by averaging model results and observations by geographical location and for the same time period, i.e. yearly (table 7.1) or daily (table 7.2).

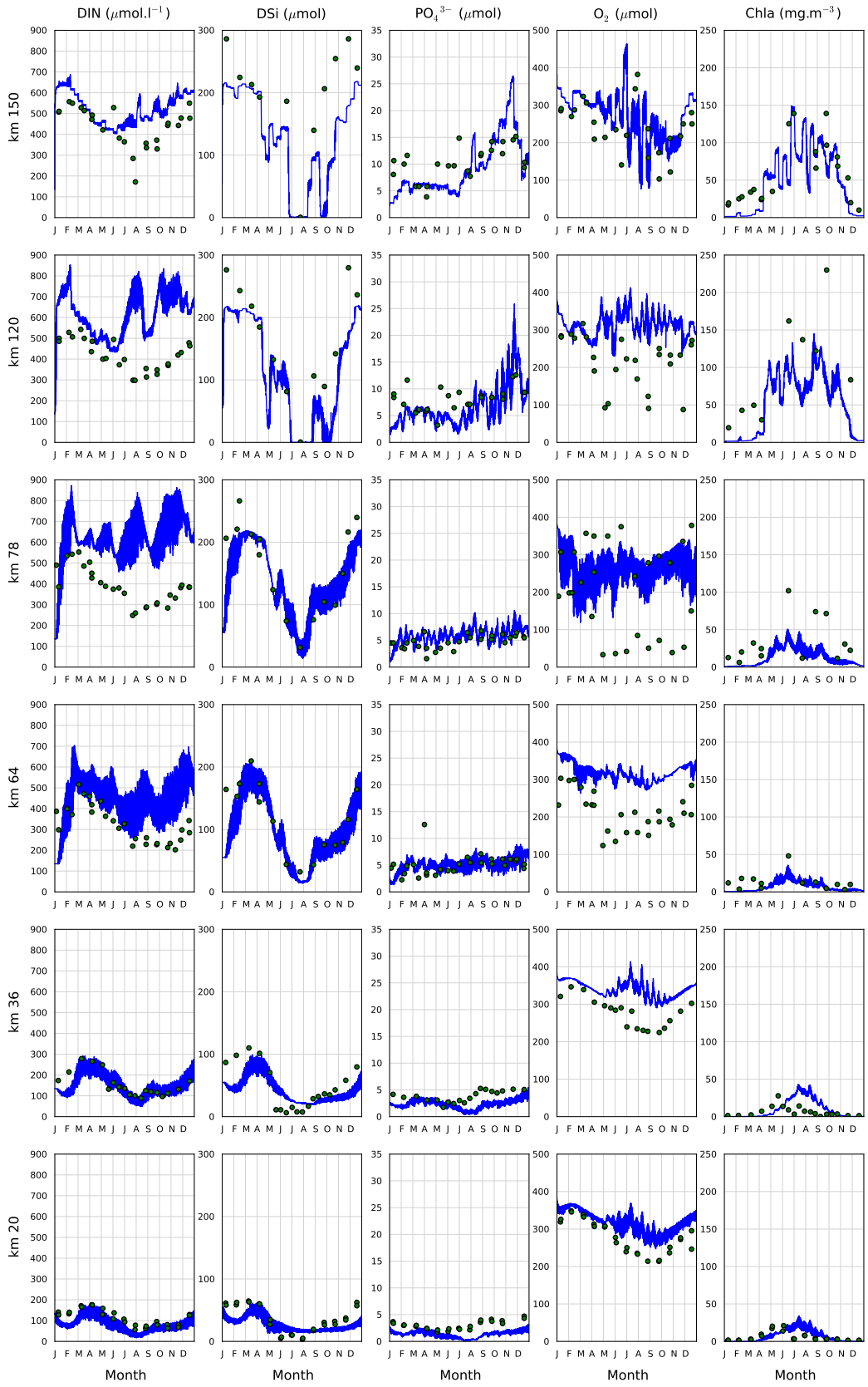

FIGURE 7.4 – Seasonal evolution of RIVE-MIRO simulated (solid line) and measured (dot) DIN, DSi, PO_4^{3-} , O_2 and Chl a concentration at km 150, 120, 78, 64, 36 and 20 of the estuary in 2006.

Annual estuarine profiles of biogeochemical variables

Figure 7.2 compares the modelled estuarine longitudinal profiles with available observations in 2006. Both observations and modelled data were annually averaged and their range of variability is shown by the standard deviation (SD). The coefficient of determination R^2 (table 7.1) rates the model performance with respect to the spatial variability of both physical and biogeochemical variables (Sal, SPM, DIN, DSi, PO_4^{3-} , O_2 and Chl a). R^2 is good (higher than 0.5) for salinity, DIN, PO_4^{3-} , DSi and Chl a, near acceptable for O_2 but low ($\approx$ 0.3) for SPM. The lower value obtained for SPM is mainly associated with the underestimation of the mean concentration in the upstream part of the model. Note also that the actual variability of SPM is very large because of the complex and highly non-linear deposition/resuspension dynamics. Overall the model is thus able to capture the observed upstream-downstream variability. The calculated bias is rated excellent for salinity, very good for PO_4^{3-} , good for DSi, Chl a, SPM and O_2. However, the Pbias values (higher than |40 %|) obtained for DIN suggests that the simulated values are overestimated (table 7.1 ; figure 7.2 a). These values are however still acceptable considering the value of $\pm$ 70 % proposed by Moriasi et al. (2007).

As a general pattern, annual mean concentrations of inorganic nutrients (DIN (NH_4^+ , NO_3^-), DSi and PO_4^{3-} ; figure 7.2) decrease along the salinity gradient due to the important dilution of the upstream input by seawater. The increased concentration simulated between km 110 and 90 coincides with the tributary discharges (figure 7.1). At this location, the annual DIN (figure 7.2 a) and DSi (figure 7.2 b) concentration can reach respectively 700 and 160 mmol.m^{-3}. The observed evolution of DIN (figure 7.2 a) and DSi (figure 7.2 b) in the salt gradient is well reproduced. This is not the case in the upstream estuary where the model overestimates the DIN annual concentration and underestimates the DSi levels, as also shown by the respective Pbias (table 7.1). This discrepancy between model results and observations is partly explained by the upstream boundary conditions (km 160 and tributaries) simulated by the Seneque-Riverstrahler model that propagates in the upstream part of the estuary. Annual mean simulated DSi still remain in data SD envelope along the estuary in agreement with « good » computed Pbias (table 7.1). As pointed by the statistical analysis, the magnitude and longitudinal pattern of annual PO_4^{3-} is well simulated along the estuary with, however, simulated concentrations being in the lower range of observation (table 7.1, figure 7.2 c). Comparison with SPM suggests that the simulated decrease of PO_4^{3-} at km 80 and 120 (figure 7.2 c) are due to its absorption on SPM. The mean annual O_2 concentration (figure 7.2 d) simulated along the estuary is maintained around 300 μmol L-1 except between km 80 and 100 where the concentration decreases down to 150 μmol L-1 due to the important bacterial biomass and organic matter imported by the tributaries (mainly the Zenne) that increase the nitrification and respiration processes (not shown). In general, the simulated dissolved oxygen concentrations slightly overestimate the averaged observations (table 7.1, figure 7.2 d).

The Chl a concentration is calculated from the total (freshwater and marine) phytoplankton biomass simulated by the model making use of a C :Chl a ratio (25 mg :mg ; Lancelot et al. (2005)). Supported by observations, the model suggests the development of two phytoplankton blooms along the estuary, one very modest in the marine area, downstream the MTZ, and the other, more important, in the freshwater tidal section (figure 7.3 a). The slight underestimation of Chl a (figure 7.3 a) in the freshwater estuary (between km 120 and 80) could be explained by the use of an inappropriate C :Chl a ratio for freshwater phytoplankton. Indeed, C :Chl a ratio measured in the Scheldt estuary highly varies with values between 1 and 70 (Lionard et al., 2008a). Sensitivity tests suggest that the model-data fit can be improved by modifying the C :Chl a ratio (not shown). In parallel, the simulated freshwater diatom biomass that dominates the phytoplankton bloom in the upstream part of the estuary (Muylaert et al., 2000) agrees well with available observations in particular in the middle part of the estuary (figure 7.3 b).

Seasonal biogeochemical trends along the estuary

The ability of the 1D-RIVE-MIRO model to capture the seasonal fluctuations can be appraised by comparing seasonal variations of simulated and observed inorganic nutrients (DIN, PO_4^{3-} , DSi), oxygen concentration and Chl a in different key zones of the Scheldt estuary (figure 7.4 ; table 7.2). Overall, the seasonal signals are reasonably well represented in timing and amplitude for most of the selected variables and locations in the estuary

(figure 7.4, table 7.2). The coefficient of determination R^2 computed between daily model results and available data at each validation station rates the model capacity to reproduce the seasonal variability of DSi, DIN and PO_4^{3-} as good (with value > 0.5). R^2 is lower ($\approx$ 0.3) for O_2 and Chl a (table 7.2). The performance level of Pbias value is from very good (PO_4^{3-} , DSi) to good (DIN, O_2 and Chl a) (table 7.2).

In agreement with observations, the simulated inorganic nutrient concentrations show a clear seasonal pattern characterized by higher values in winter, a progressive decrease during spring and summer as a response to phytoplankton growth, and an increase of nutrient concentrations in late summer and autumn (figure 7.4). The observed spring/summer decrease of DIN is however not properly captured by the model between km 78 and 120 where the simulated concentrations are overestimated. This results from the overestimation of DIN inputs by the Scheldt tributaries already pointed out in the analysis of the longitudinal profiles (figure 7.2 a). For all sampled locations, the maximum DIN concentrations are simulated at the end of winter (heterotrophic regeneration and high river discharge) while minima are shown in late spring (phytoplankton uptake and low flow rate). In general the simulated DSi are in good agreement with observations but slightly underestimate observed summer values in the upstream part of the estuary (figure 7.2 b). Despite this underestimation, the seasonal signal of DSi is correctly captured at every location along the estuary. The seasonal evolution of PO_4^{3-} is well reproduced in amplitude and timing for upstream stations and in the vicinity of the MTZs (figure 7.4). The high variability of modelled concentration results from absorption / desorption of PIT on particles and is related to the simulated SPM dynamics. The maximum concentration of PIT is simulated upstream (km 150) in late summer and autumn (with concentrations above 15 μmol.l^{-1}) when the river flow decreases. In the downstream part (km 36 and 20), the simulated seasonal signal is less pronounced than observed and the model fails to catch the amplitude of the observed summer-fall increase. The seasonal variation of O_2 is less well represented and model results tend to overestimate observations (table 7.2 ; figure 7.4). The phytoplankton blooming period is reasonably well captured by the model at the different locations. The timing and amplitude of the Chl a maximum are consistent with the observations, except in the maximum turbidity zone (km 78), where model results underestimate observations.

The comparison of simulated freshwater diatom biomass with available data at 4 stations along the Scheldt estuary (figure 7.5) demonstrates the model capacity to reproduce the amplitude and the seasonal evolution of freshwater diatoms concentrations along the Scheldt estuary. In the upper part of the estuary, observed and simulated freshwater diatoms show a series of blooms between late spring and end-summer that reach biomass higher than 1000 mgC.m^{-3} (figure 7.5 a, b). The magnitude of freshwater diatoms bloom decreases downstream mainly during the spring period (figure 7.5 c,d).

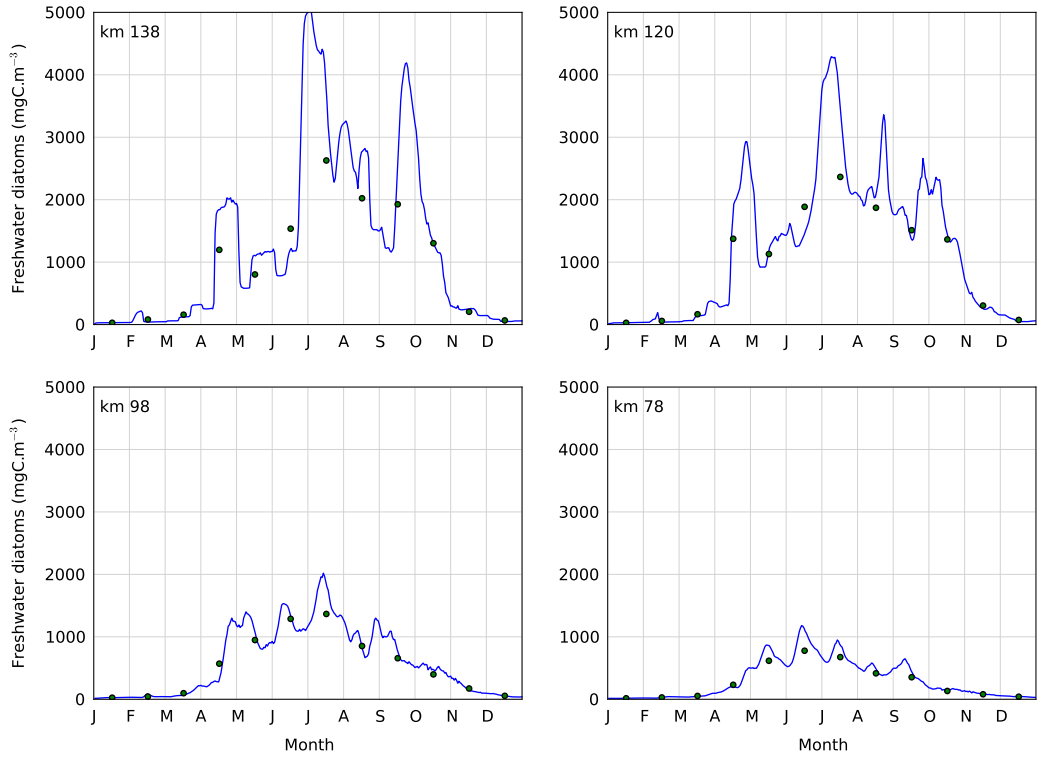

FIGURE 7.5 – Seasonal evolution of RIVE-MIRO simulated (solid line) and measured (dot) freshwater diatoms concentration at km 138, 120, 98 and 78 of the estuary in 2006.

Spatio-temporal evolution of PFTs

Figure 7.6 compares the geographical extent and the magnitude of freshwater and marine phytoplankton blooms. The spatial distribution of phytoplankton simulated in the Scheldt estuary suggests the occurrence of two distinct blooms, one in the freshwater and the other in the marine section of the estuary (figure 7.6). Such a distribution of riverine and coastal communities in the estuary has been reported by Muylaert et al. (2009). The absence of phytoplankton bloom between km 60 and 80 suggests that neither the freshwater nor the marine phytoplankton cross the MTZ at the saline transition. Overall the phytoplankton blooms between mid-April and late October (days 100 and 300) starting earlier in the marine section but extending longer in the upper estuary. The biomass reaches impressive levels upstream and corresponds with a series of blooms simulated between late spring and end summer (figure 7.6). In agreement with observations (Muylaert et al., 2000; Lionard et al., 2005, 2008a), the upstream phytoplankton blooms are dominated by freshwater diatoms and *Chlorophyceae* with biomass as high as 4000 and 2500 mgC m-3, respectively (figure 7.6 b,d), with the *Chlorophyceae* contributing significantly (> 50 %) to phytoplankton in summer between km 140 and 160. On an annual mean basis, other algal groups represent less than 10 % (Lionard et al., 2008b) and simulated cyanobacteria (not shown) represent a negligible biomass (< 2 mgC.m^{-3}). As observed (Lionard et al., 2008a,b), freshwater phytoplankton is present from spring to early autumn. Overall the simulated freshwater diatoms penetrate further downstream than *Chlorophyceae* and reach their maximum in summer between km 140 and 120 (figure 7.6 b). *Chlorophyceae* show their maximum biomass at km 140 and generally disappear downstream km 100 (figure 7.6 d). As a result of different light adaptation (or adaptation to turbulence), diatoms were found to be the dominant phytoplankton species in the freshwater tidal reaches of the Scheldt while *Chlorophyceae* were found to be more successful in the tributaries rivers, especially in summer (Lionard et al., 2005). Throughout the year, simulated and observed (Lionard et al., 2008a) Chl a and phytoplankton biomass declined in the brachish reaches. Nutrient limitation only impacts freshwater diatoms in late summer between km 150 and 110.

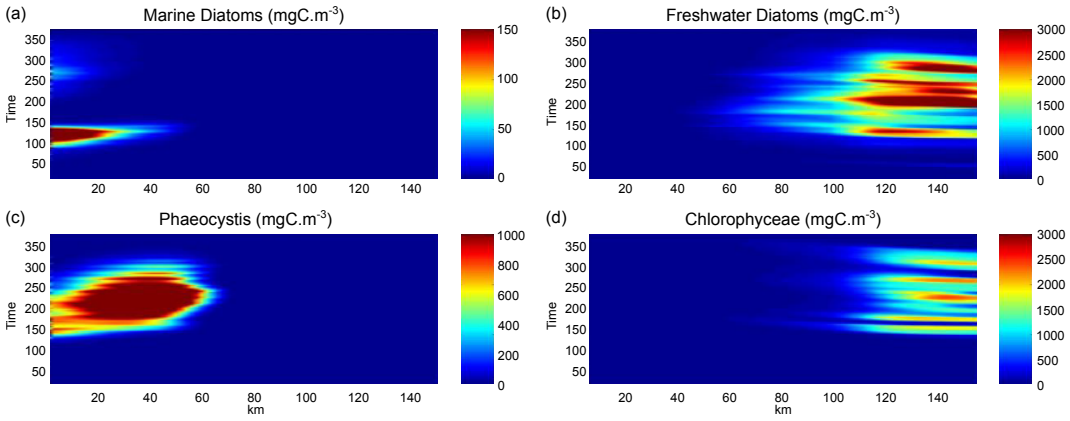

FIGURE 7.6 – Spatio-temporal evolution of marine (diatoms (a) and *Phaeocystis* colonies (c)) and freshwater (diatoms (b) and *Chlorophyceae* (d)) phytoplankton simulated in the Scheldt estuary by the 1D-RIVE-MIRO model in 2006.

In the marine part of the estuary, the simulated phytoplankton bloom is maximum in summer and extends to 50 km upstream. It is characterized by the marine *diatom-Phaeocystis* diatom succession (figure 7.6 a,c), typical of coastal waters (Rousseau et al., 2002). *Phaeocystis* colonies dominate the marine phytoplankton biomass with maxima reaching 2000 mgC.m^{-3} between km 20 and 50 (figure 7.6 c). The simulated marine diatoms biomass is very modest except in the first 30 km between late March and late April, with biomass up to 150 mgC.m^{-3} (figure 7.6 a). In the marine part, nutrients only limit diatoms growth and can partly explain their low biomass. The marine nanoflagellates (not shown) are present in small amounts with biomass always < 10 mgC.m^{-3}. The lack of blooming in spite of a supply of nanoflagellates cells after *Phaeocystis* colony disruption (Lancelot et al., 2005) is explained by the grazing pressure of marine microzooplankton (see below).

Figure 7.7 shows the simulated spatio-temporal variations of freshwater and marine heterotrophic plankton. As expected from the spatio-temporal distribution of their prey, freshwater and marine microzooplankton and copepod distributions show distinct spatial distributions. The time slot and spatial occurrence of marine microzooplankton and copepods are between mid-April and late July and extends to the first 60 km (figure 7.7 a, c) with a biomass of up to 100 and 30 mgC.m^{-3} respectively, i.e. negligible compared to their prey. The success of microzooplankton can be related to the release of nanoflagellates in the ambient water after the disruption of ungrazed *Phaeocystis* colonies and the low significance of mesozooplankton that could control their development (figure 7.6 c, 9a,c). Similarly, the biomass of freshwater copepods and microzooplankton (figure 7.7 b, d) are not significant, excepted between late June and early October, when microzooplankton biomass increases up to 400 mgC.m^{-3} due to the presence of a large amount of *Chlorophyceae* (figure 7.6 d, 9b).

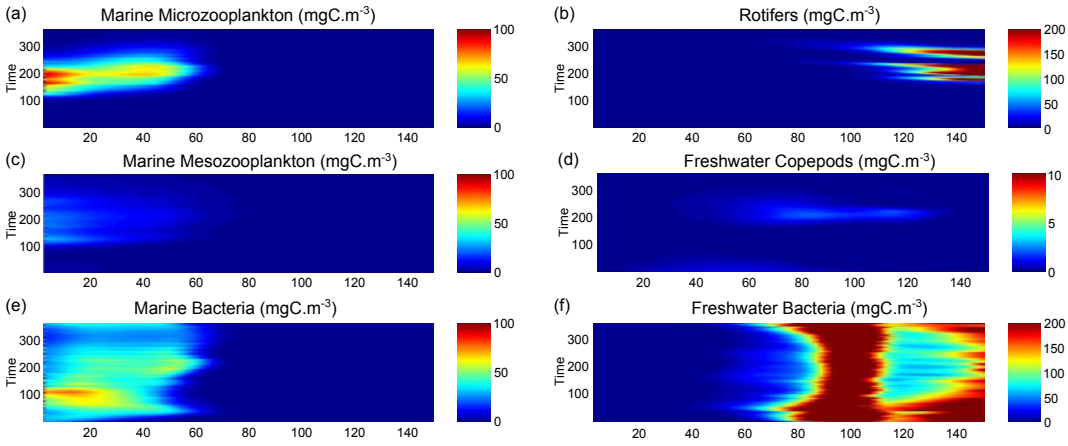

FIGURE 7.7 – Spatio-temporal evolution of marine microzooplankton (a), mesozooplankton (c) and bacteria (e) and freshwater rotifers (b), mesozooplankton (d) and bacteria (f) simulated in the Scheldt estuary by the 1D-RIVE-MIRO model in 2006.

Our model shows the presence of marine bacteria in the first 40 km between mid-February and mid-April with a maximum concentration of 60 mgC.m^{-3} 506 (figure 7.7 e). They remain nevertheless present in lower amounts during the rest of the year with concentrations below 40 mgC.m^{-3}. Contrasting with marine bacteria, whose development corresponds with the release of authochtonous organic matter, extremely high biomass of freshwater bacteria (> 200 mgC.m^{-3}; figure 7.7 f) are shown in the upper Scheldt and at the confluence of the Scheldt with the tributaries due to the discharge of large quantities of both bacteria and organic matter.

7.2.1 Discussion

Model assessment

Model validation shows the model capacity to reproduce seasonal and longitudinal evolution of the physical and biogeochemical variable in the Scheldt estuary with however a significant overestimation of DIN concentration at the confluence with the lateral tributaries. This N overestimation mainly results from uncertainties on determining inputs from point sources, in particular, in the Dyle and the Nete rivers. The effect of DIN overestimation on estuarine phytoplankton dynamics was investigated by decreasing DIN river inputs by a factor 2. Modifying N loads has no impact on freshwater phytoplankton but decreases maximum *Phaeocystis* biomass of about 200 mgC.m^{-3} ($\approx$ 10 % of the reference simulation) around km 40. In absence of important nutrient limitation of phytoplankton growth in the estuary, this discrepancy will only marginally affect the analysis of phytoplankton dynamics in the Scheldt. However, nutrient exports to the coastal zone are largely controlled by river inputs and annual flows of nutrients, N in particular, must be carefully considered and will be only discussed in a comparative and qualitative way.

Several physical-biogeochemical 1D (Soetaert and Herman, 1995; Regnier et al., 1997; Vanderborght et al., 2002; Hofmann et al., 2008) or 2D (Vanderborght et al., 2007; Arndt et al., 2007, 2011) models were previously implemented in the Scheldt estuary to study C, nutrients and/or O_2 biogeochemical transformations and fluxes. In these estuarine models, phytoplankton process formulations are generally based on total primary production (generally associated to diatoms growth) without distinction between phytoplankton groups (Hofmann et al., 2008) or only simulate a limited period of time e.g. summer time; Arndt et al. (2007); Vanderborght et al. (2007). These models are appropriate to reproduce the annual or decadal evolution of biogeochemical processes and concentration along the Scheldt estuary with sometimes a better result than those obtained with our complex model (for N and O_2 in particular). In particular, Hofmann et al. (2008) present estuarine annual C and N budgets and fluxes and describe the spatial patterns of nutrient concentrations and fluxes in the Scheldt estuary for average conditions representing the 2001-2004 period. Arndt et al. (2011) estimate seasonal N and Si transformations and fluxes along the entire continuum of the Scheldt estuary over a period of one year. However, none of these models can be used to understand the dynamics of phytoplankton in the estuary because they do not describe ex-

plicitly the processes associated with the mixing of the marine and freshwater communities as tempted in the here described RIVE-MIRO model.

In addition, most of the previous modelling studies were limited to the saline estuary (from Vlissingen to Rupelmonde) (Soetaert and Herman, 1995; Regnier et al., 1997; Vanderborght et al., 2002) and ignored the role of the tidal river where nutrient transformation processes are particularly intense (figure 7.4). Yet the extension of the model domain to the tidal river was considered by Vanderborght et al. (2007) and Arndt et al. (2011). One step further, our application that couples an explicit description of the watershed with the estuarine model permits to estimate the impact on the Scheldt estuary of the modification of human activity on the watershed and the export to the coastal waters. The off line coupling of a watershed, an estuarine and a coastal model avoids the need for providing boundary conditions at the boundaries of the different models.

Control of phytoplankton succession in the estuary

At the interface between freshwater and marine ecosystems, estuaries provide complex and fluctuating habitats for freshwater and marine phytoplankton where salinity gradient, light availability and water residence time control phytoplankton dynamics (Lancelot and Muylaert, 2012). In the Scheldt estuary, our model results suggest the development of distinct blooms in the freshwater and the marine sections of the estuary (figure 7.6).

After some sensitivity tests, we can suggest that freshwater diatoms and *Phaeocystis* develop in the estuary while *Chlorophyceae* and marine diatoms are mainly transported from the river and marine boundaries respectively. Grazing pressure is negligible and can not explain the bulk phytoplankton distribution although it is partly responsible for the relative importance of diatom vs non diatom patterns. In the absence of salinity-induced mortality, freshwater diatoms would cross the MTZ and grow in the downstream part of the estuary where they could compete for nutrients with marine phytoplankton. Similarly, the presence or absence of euryhaline freshwater species has a significant impact on the distribution and magnitude of freshwater and marine species. When accounting for more than 50 % of the total freshwater diatom biomass, euryhaline species bloom further downstream the MTZ and prevent the penetration and growth of marine species in the estuary. More than salinity or phytoplankton composition at the boundaries, light availability – strongly dependent on SPM concentration -, appears as the main factor controlling the phytoplankton distribution in the Scheldt estuary in 2006 and explain the sharp decrease of freshwater phytoplankton simulated between the km 100 and 70.

Estuarine biological control of nutrient export to the coastal zone

A budget based on the 1D-RIVE-MIRO daily simulations of nutrient fluxes estimates to 1.84 GmolN, 0.063 GmolP and 0.47 GmolSi the annual export of nutrients to the coastal zone in 2006. Nitrogen export is similar to that estimated by Hofmann et al. (2008) for the period 2001-2004 (2.2 GmolN.y^{-1}). The comparison between simulated annual loads and those based on available discharge and nutrient concentrations (RIKZ) show an good correspondence for N (2. 08 GmolN.y^{-1}), P (0.05 GmolP.y^{-1}) and Si (0.045 GmolSi.y^{-1}). Biological activities transform nutrients during the estuarine transfer and modify the proportion of inorganic and organic forms (N, P and Si) exported to the coastal zone compared to the river inputs to the favour of the inorganic ones. Interestingly, as shown by Arndt et al. (2011), part of the biogenic Si (BSi) mineralised in the estuary is from marine origin and corresponds to the mineralisation of marine diatom frustules that have penetrated the estuary (-0.06 GmolSi.y^{-1}, table 7.2). In agreement with Hofmann et al. (2008), our results show that nitrification remains the main process governing the N cycle in the Scheldt estuary and the relative proportion of NO_3^- and NH_4^+ with a net production of NO_3^- . About 4 % of the total N inputs are denitrified in the estuary and similar amount of N are retained in the sediment.

Running the model with having eliminated biological activity from the equations allows estimating the importance of physical processes (transport of dissolved and particulate matter, adsorption/desorption and sedimentation/resuspension, dilution) controlling the export of nutrients to the coastal zone. Comparing the budget calculated with this run with the reference demonstrates the minor role played by the biological activity on the magnitude of the exported nutrients and its major influence on their chemical forms. The increased relative contribution of inorganic vs organic nutrients suggests the dominance of bacterial

organic matter mineralisation and nitrification over phytoplankton uptake in the Scheldt estuary. This is confirmed by analysing the nutrients budget obtained when phytoplankton growth is prevented and biological transformations are due to heterotrophic processes only. In addition, this simulation suggests that the export of inorganic nutrients available for coastal phytoplankton yet relies on the ability of phytoplankton to grow (or not) in the estuary. This is demonstrated by calculating the nutrient budget obtained when maximizing the phytoplankton growth in the estuary.

Chapitre 8

Modelling nutrient transfer along the Seine estuary

8.1 Nutrients transfer through the Seine estuarine zone

As seen in the preceding parts of this work, the drainage network as a whole can be seen as a very active reactor transferring, transforming, retaining or eliminating a large fraction of the elements brought in from the watershed before they reach the river outlet. The estuarine zone similarly represents a second reactor through which the river loading have to transit before reaching the sea. The Seine estuary is a typical macrotidal estuary, characterized by the presence, outside winter periods of high discharge, of a distinct turbidity maximum zone (TMZ). Such estuaries are known to be biogeochemically very active areas (Deborde et al., 2007; Etcheber et al., 2007; Garnier et al., 2008, 2010b).

8.2 Modelling approach

A detailed modelling approach of the processes occurring in the Seine estuary has been developed by coupling the RIVE module, briefly described above, to a detailed 1D-hydro-sedimentary model (Hir et al., 2001) : the SiAM-1D/Rive (Even et al., 2007). A 3D version is under development. In parallel, a more simplified and generic approach, named LIFT (Lumped Idealisation of the ecological Functioning in estuarine Turbitidy maximum, Garnier et al. (2008, 2010b)) has been conducted to assess the nutrient behaviour in the turbidity maximum zone (TMZ) and salinity gradient of the Seine estuary. LIFT is a 0 D-model describing the turbidity maximum zone as a reactor with homogeneously distributed particulate material and where freshwater flowing through it progressively mixes with seawater, while dissolved species react with particulate material.

? Le modèle LIFT, un outil simplifié pour la modélisation des transformations biogéochimiques dans les bouchons vaseux estuariens

LIFT est un modèle simplifié, non spatialisé, des cycles biogéochimiques s'opérant au sein des estuaires (figure 8.1). Il analyse ces processus à l'échelle saisonnière, dans la zone de turbidité maximale (TMZ). La TMZ y est décrite comme un réacteur à lit fluidisé, situé entre l'extême amont de l'estuaire et la zone côtière proprement dite. Un réacteur à lit fluidisé possède la propriété que les échanges réactifs entre les particules et le fluide qui les traverse sont maximisés par l'état de fluidisation et de mélange dans lequel les particules sont maintenues par le flux ascendant de ce fluide. La TMZ y est donc vue comme traversée par un flux d'eau douce se mélangeant progressivement à l'eau salée, tandis que les éléments dissous interagissent avec la matière particulaire supposée homogène dans l'ensemble du domaine.

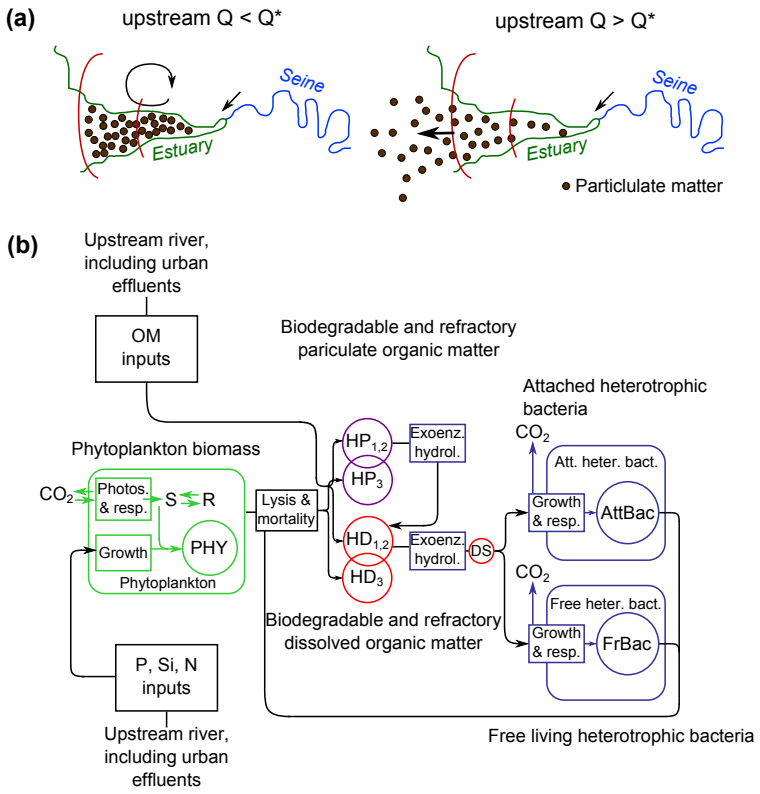

FIGURE 8.1 – Description du modèle simplifié LIFT de la zone de turbidité maximum de l'estuaire de la Seine.

Lorsque le débit est inférieur à un certain seuil, la matière particulaire s'accumule au sein de la TMZ, où sa concentration dépend des apports et des processus biologiques qui s'y opèrent. Quand le débit dépasse le seuil critique, la matière particulaire est expulsée vers la zone côtière (figure 8.1). Les processus biogéochimiques pris en compte dans LIFT sont les mêmes que ceux décrits dans le modèle RIVE. Ainsi, outre les flux de nutriments, le modèle calcule aussi les biomasses algales et bactériennes.

The limit conditions of the LIFT model are given by the calculated value of the water quality variables provided by the SENEQUE/Riverstrahler model at the head of the salinity gradient (here Caudebec, 310 km downstream from Paris). The total volume of the TMZ is estimated to 5.3.108 m^{-3} and the surface area to 7.3.107 m^2 corresponding to the domain of the TMZ extension along the season (Garnier et al., 2008). The initial suspended solid stock, i.e. the total amount of particles within the TMZ was calculated from experimentally determined average concentrations, multiplied by the volume (Garnier et al., 2008, 2010b). When the upstream discharge (Q) is below a critical flow rate (Q*, calibrated to 400 $m^3.s^{-1}$),

particulate matter from the upstream watershed accumulates in the TMZ, while above the critical flow rate, particles are washed out and evacuated to the sea (Garnier et al., 2008).

8.3 Results

The results of the LIFT calculations, when averaged at the annual scale over the last 25 years (figure 8.2) do not show significant retention in the TMZ, neither for total nitrogen and silicon (about 1 %) nor for phosphorus (5 %). 10 % retention is found for total organic carbon (figure 8.2). This is consistent with previous observations that the mixing diagrams of the Seine estuary indicated more conservative mixing than major transformations (Garnier et al., 2010b)). Therefore, at an annual scale, the role of the Seine estuary in possibly eliminating a fraction of nutrients which could reduce eutrophication problem at the marine coastal zone is limited. Estuaries are receptacles of all materials transferred from upstream rivers and estuarine retention was shown to be inversely correlated with the mean residence time of water (Nixon et al., 1996).

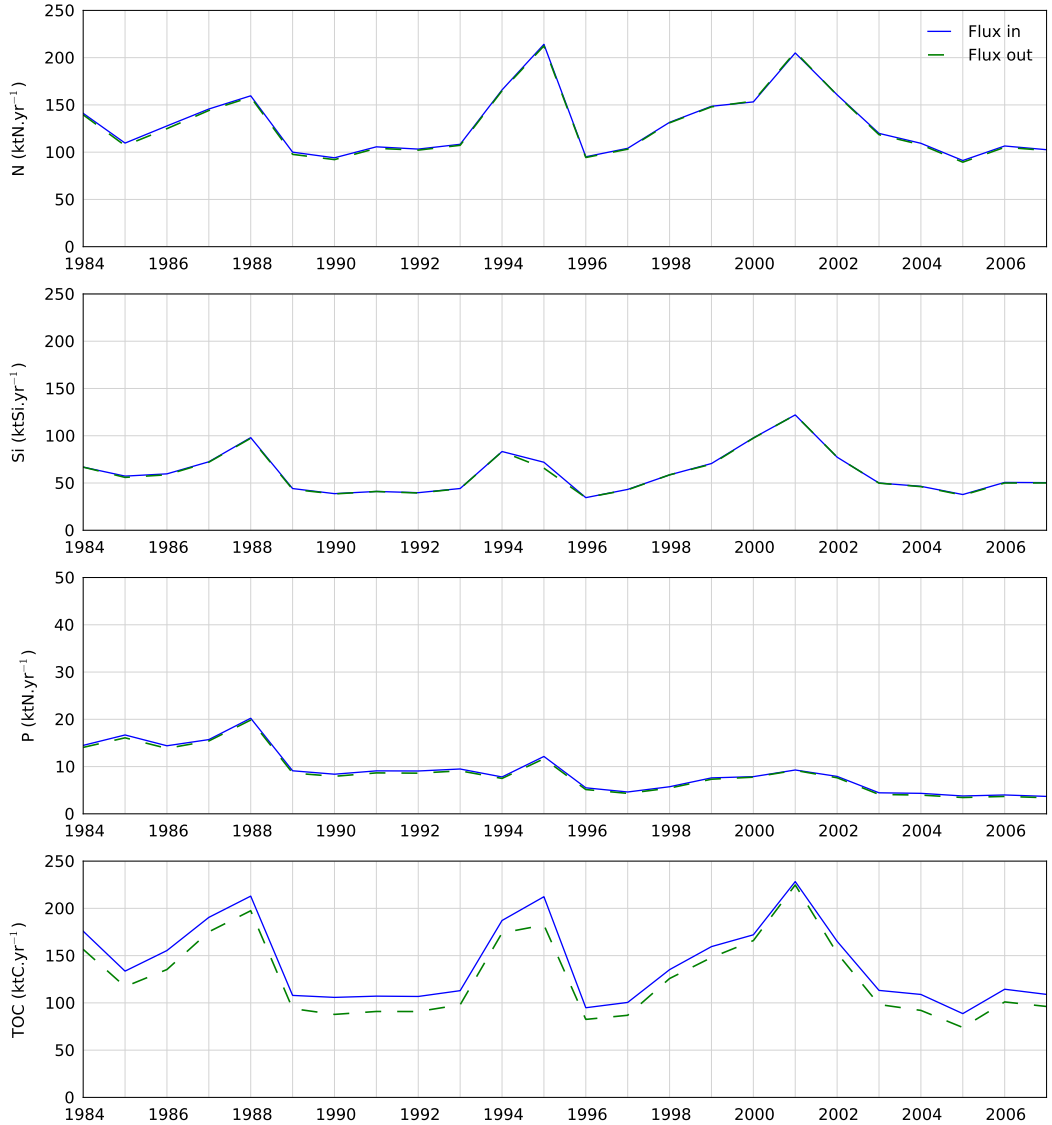

FIGURE 8.2 – Interannual variations, in yearly average, of total nitrogen, silicon, phosphorus and organic carbon fluxes entering the Seine saline estuary (Caudebec, in) and leaving the estuary Calculated values by the models (Riverstrahler –in- and LIFT –out-). The difference indicate the retention by the turbidity maximum zone of the Seine estuary.

Biogeochemical exchanges in estuaries (including their wetlands), but also on the continental shelves where intense transformations (e.g. inner and outer estuaries) may be impor-

tant for the N, P and Si fluxes reaching the open ocean (Nedwell et al., 2002; McKee et al., 2004). However many of large estuaries such as the Seine have been considerably modified for navigation (Cuvilliez et al., 2009). Decreasing the connectivity with saline and freshwater marshes have reduced the residence time of the water and particles, so that the transformation and retention/elimination of nutrients can be lowered due to the decreasing opportunity for exchanges across the interfaces (e.g. water/particle, particle/organisms), (Van Damme et al., 2009; Statham, 2012).

However, when looking at the seasonal scale, the LIFT calculations sometimes reveals significant nutrient retention of some nutrient for short period of time, which may affect the nutrient balance (N :P :Si) and temporarily modify the species succession and biomass amplitude at the coast (Garnier et al., 2010b). Figure 8.3 illustrates this with the case of two dry years (1989 and 2005) at the beginning and the end of the period studied, when phosphorus load in the river was respectively at its maximum and minimum, and one wet year, 2001, the wettest of the studied period.

At a seasonal scale, although a still low retention in the TMZ is evidenced, as a whole more in summer (May to September) that in winter (October to April) ; in average over the 24 years, total organic carbon shows the highest seasonal retention (22 % in summer vs. 11 % in winter), followed by phosphorus (10 % in summer vs. 4 % in winter) and nitrogen (4 % in summer vs. 1 % in winter), with no retention obtained for silicon (figure 8.3).

Interestingly, such slight transformations were found in summer period for a very short salinity gradient (3 km) of a small river entering the Arcachon bay (Canton et al., 2012), whereas the Humber UK estuary with a tidal length of 150 km, similar to the Seine, appeared a strong buffer for phosphates, removing 85 % of the load (Sanders et al., 1997). Too few studies are available for quantifying the buffer effect of estuaries, but their residence time is a good indicator for inferring retention (Nixon et al., 1996). Further combination of residence time with their geomorphology, on the basis of the world typology by Meybeck et al. (2007), would help refining the deliveries to coastal waters.

When plotting the average of the summer N, P, C retention of the Seine Estuary for each of the 24 years against the corresponding average discharge, a clearly inverse trend is shown, illustrating the role of residence time in favouring biogeochemical processes in the TMZ and its possible buffer role (figure 8.4). The wettest year in 2001 led to the lowest retention for all elements. Figure 8.4 also evidences the range of the summer retention, from 7 to 30 %, 0 to 6 % and 3 to 18 % for total carbon, nitrogen and phosphorus respectively.

The seasonal trend for silicon retention is not so clear, as silicon concentrations is related to the diatoms dynamics (uptake of silicon, grazing, sedimentation ...), with maximum growth in spring, from March to June, depending on the discharge, but also in autumn, when temperature decreases.

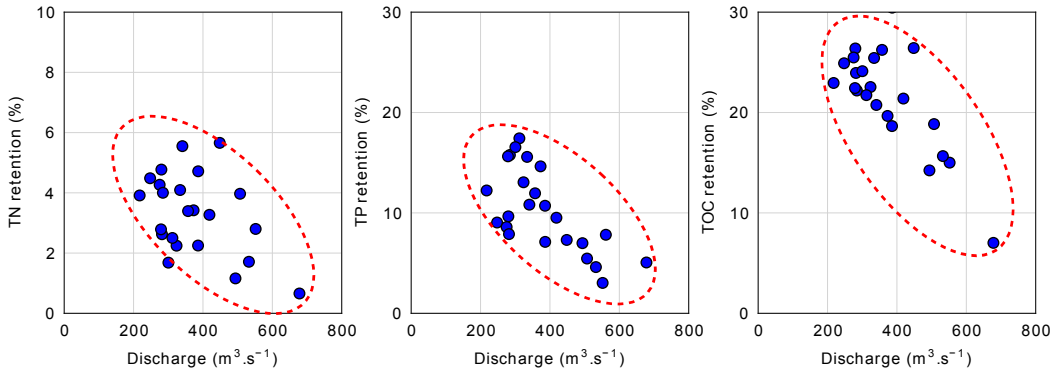

FIGURE 8.4 – Relationships between the percentages of total nitrogen, phosphorus and carbon retention and the associated discharges. Average summer values (May to September) for the 24 years.

8.4 Discussion

The Seine represents up to circa 80 - 85 % of the freshwater inflow in the Seine Bight and algal blooms are generally observed in the plume of the Seine River just downstream

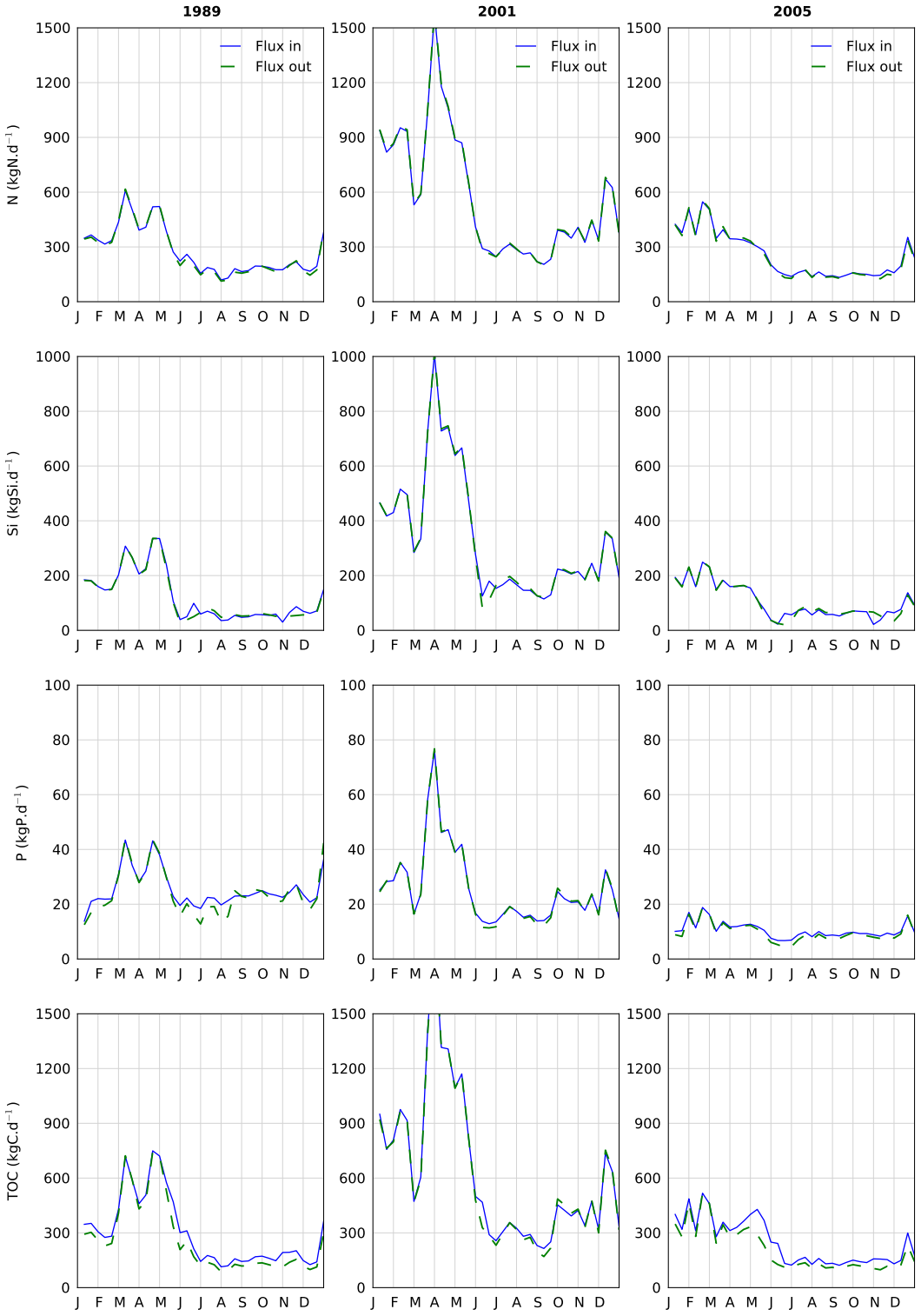

FIGURE 8.3 – Seasonal variations for two dry years (1989 and 2005) and one wet year (2001) of total nitrogen (TN), silicon (TSi), phosphorus (TP) and organic carbon (TOC) fluxes entering the Seine saline estuary (Caudebec, in) and leaving the estuary. Calculations by the models (Riverstrahler –in- and LIFT –out-). The difference indicates the retention by the turbidity maximum zone of the Seine estuary.

from the TMZ. The TMZ role of the Seine Estuary is rather low in its present geomorphology. The respective overall retentions in the Seine TMZ (in the order of 10 % P, nearly 0 % Si, 3 % N) cannot modify the Redfield ratios, nitrogen being presently largely in excess in regard to phosphorus and silicon.

The mechanistic model Seneque/Riverstrahler, LIFT coupled along the Seine continuum, does not describe the terrestrial processes controlling diffuse nutrient sources from agriculture. These are instead imposed as a forcing function or boundary conditions, obtained from other model results, observation surveys or literature data (Thieu et al., 2010). A challenge will be in the next few years to combine the Seneque/Riverstrahler drainage network model with a comprehensive, deterministic model of nutrient cycling in agricultural and semi-natural soils, such the public-domain model SWAT Model (Soil & Water Assessment Tool), (Srinivasan et al., 1998; Neitsch et al., 2005). This will allow to refine agriculture scenarios necessary to establish functional links with the adjoining terrestrial, freshwater and marine systems (Elliott and Whitfield, 2011). This is a major challenge for the next decade in order to combat eutrophication, to protect our freshwater resources, and to promote a sustainable agriculture. Our modeling tool could be a candidate at multiregional, continental to global scales, for in-stream nutrient transformation, retention and elimination within the drainage network as the result of biological and physical–chemical processes (Kroeze et al., 2012).

À retenir sur le filtre estuarien

- ⋆ Pour l'estuaire de l'Escaut, le modèle Seneque/Riverstrahler est capable de « nourrir » un modèle déterministe décrivant les processus biogéochimiques de la zone estuarienne.
- ⋆ Deux zones d'efflorescences algales ont été mises en évidence. La première, à l'amont de l'estuaire, en domaine d'eau douce, dominée par des *Diatomées* d'eau douce ; et la seconde en domaine marin, à l'aval de l'estuaire, dominée par des *Phaeocystis*.
- ⋆ Les zones de développement des bactéries sont étroitement liées aux rejets ponctuels le long de l'estuaire.
- ⋆ Les processus biologiques de transformation des nutriments se sont avérés moins importants que les processus physiques.
- ⋆ Pour l'estuaire de la Seine, le couple Seneque/Riverstrahler - LIFT a permis de quantifier la rétention de nutriments au sein de la zone estuarienne.
- ⋆ Au cours de la période 1984-2007, peu d'azote, de phosphore ou de silicium ont été retenus dans l'estuaire. Seul le carbone a subi une certaine rétention.
- ⋆ Le pouvoir rétentif de l'estuaire est lié aux conditions hydrologiques. En année sèche, la rétention est plus importante qu'en année humide. La rétention est donc liée au temps de séjour des masses d'eau dans l'estuaire.

Conclusions générales et perspectives

Ce que nous avons appris sur la cascade de nutriments

Dans un premier temps, nous avons replacé l'état de la cascade de nutriments actuelle au regard de son passé. Sur le petit bassin versant bien documenté de la Zenne (sous bassin de l'Escaut), nous avons pu reconstruire les flux de nutriments depuis la fin du 18ème siècle jusqu'à 2010. Grâce à une démarche originale alliant études de cartes anciennes et archives historiques, il a été possible de quantifier et de spatialiser les sources diffuses et ponctuelles, aux alentours de 1790 et de 1890. À ces périodes, les pollutions ponctuelles étaient nettement plus importantes que les pollutions diffuses. Parmi ces pollutions ponctuelles, celles d'origine industrielle prédominaient sur celles d'origine domestique.

L'étude de cartes de la fin du 18ème a permis de spatialiser et de quantifier les changements paysagers intervenus dans le bassin de la Zenne entre 1790 et le début du 21ème siècle. Le fait le plus marquant est une très forte urbanisation du bassin, due au développement de l'agglomération bruxelloise. Cette urbanisation s'est essentiellement faite au détriment des terres arables, des prairies et, dans une moindre mesure, de la forêt.

La présence de Bruxelles est responsable d'une ségrégation des pollutions aquatiques, avec un bassin amont moins touché par les pollutions industrielles et un secteur aval très perturbé par ces pollutions. Malgré la faible industrialisation de l'amont du bassin, les flux d'ammonium, de phosphore et de carbone apportés à la rivière ont tout de même augmenté entre 1790 et 1890.

Par contre, ces flux ont littéralement explosé à l'aval de Bruxelles entre ces deux dates. En revanche, Les nitrates, issus des pollutions diffuses ont été peu modifiés, l'agriculture étant resté de type rural traditionnel. De nos jours, les flux d'azote et de phosphore se sont rapprochés de ce qu'ils étaient en 1790, bien que les flux d'azote alors sous forme ammoniacale sont désormais essentiellement sous forme nitrique. Les flux de silicium, essentiellement liés à l'érosion du substrat et donc aux conditions climatiques, ont peu évolué dans le temps. Ainsi, nous avons mis en évidence trois phases temporelles d'évolution des flux, avec un pic de pollution à la fin du 19ème siècle.

Sur un temps moins long, mais à plus large échelle et avec des données plus précises, nous avons retracé, pour la première fois, l'évolution entre 1984 et 2007 à un pas de temps de 10 jours des flux de nutriments des 3S (Seine, Somme et Scheldt) ainsi que l'évolution de leurs impacts à la zone côtière adjacente en termes de développements algaux. Les trajectoires des régions agricoles de ces trois bassins en termes de rendement agricole et d'apports d'azote aux terres arables ont été établies depuis 1950. Certaines régions ont commencé à diminuer leurs fertilisations azotées dès le milieu des années 1980, notamment en Belgique, alors que d'autres les ont continuellement augmentées, notamment les régions de grandes cultures du bassin de la Seine. Ces trajectoires permettent la quantification des surplus azotés dans une perspective historique. Sur les terres arables, le surplus des apports d'azote au sol par rapport à son exportation par la récolte est pour l'essentiel lixivié vers l'hydrosystème. Au final, la contamination nitrique des nappes de ces trois bassins tend à atteindre le seuil fatidique des 11.3 $mgN.l^{-1}$, à ne pas dépasser pour la production de l'eau potable.

À Poses, à l'exutoire de la Seine, la concentration en nitrates n'a pas diminué au cours de cette période malgré les volontés politiques affichées. Elle a même eu tendance à légèrement augmenter, au mieux s'est stabilisée. Les nutriments issus des pollutions ponctuelles (NH_4^+ et PO_4^{3-}) ont, au contraire, largement diminué depuis le milieu des années 1980. La baisse a commencé au début des années 1990 et s'est poursuivie jusqu'à aujourd'hui. Le silicium, peu influencé par les activités anthropiques, n'a pas notablement évolué au cours de cette période. Son cycle reste très lié à celui du phytoplancton, qui, lui non plus, n'a pas franchement évolué en termes d'intensité des efflorescences.

À l'exutoire de l'Escaut, les tendances générales sont similaires mais avec quelques particularités. Les nitrates ont légèrement diminué, ce qui est à mettre en lien, vraisemblablement, avec une diminution des surplus azotés de certaines régions agricoles belges. La densité de population du bassin de l'Escaut (plus de 2 fois plus élevée que celle du bassin de la Seine) fait que les sources ponctuelles y restent plus importantes. Ainsi, l'ammonium et le phosphore n'ont drastiquement diminué qu'avec la mise en place des stations d'épuration de l'agglomération bruxelloise à la fin des années 2000.

Grâce à la spatialisation de Seneque/Riverstrahler, nous avons également pu étudier la qualité de l'eau du chevelu des rivières des hydrosystèmes. Concernant les pollutions phosphorées, la qualité s'est améliorée partout, passant de *moyenne* ou *mauvaise* à bonne, selon les critères du SEQ-Eau des Agences de Bassins français. Cependant, la pollution nitrique a augmenté à peu près dans toutes les rivières. En 1984, la situation était bonne dans les parties amont et *moyenne* à l'aval. En 2006, elle est *moyenne* ou *mauvaise* partout. Afin de tester les capacités de notre modèle à simuler une amélioration, nous avons construit deux scénarios de réduction des surplus agricoles azotés, de respectivement 25 % et 75 %. Selon le second scénario, un niveau de qualité *moyenne* serait atteignable sur l'ensemble des territoires étudiés, ce qui montre l'ampleur des efforts à fournir pour restaurer la qualité de l'eau.

Cette démarche a également permis de calculer les flux de nutriments annuels parvenant à la zone côtière pour les trois bassins. Il s'avère que les flux d'azote et de silicium sont très liés aux débits, faibles en année sèche et élevés en année humide. Les flux d'azote de la Seine n'ont pas diminué au cours de ces 24 dernières années. Par contre ils ont légèrement diminué dans le bassin de l'Escaut, grâce à la diminution des surplus agricoles, mais aussi suite à une amélioration des traitements en stations d'épuration.

Enfin, nous avons retracé les développements algaux en zone côtière au cours de la période de 25 ans. Il apparaît que les intensités ainsi que la durée des efflorescences algales ont nettement diminué au cours de cette période, en lien avec la forte diminution des apports de phosphore.

Afin de pénétrer plus en avant dans la cascade de l'azote, nous avons exploré le rôle de l'usage du sol et de la topographie sur les émissions de N_2O à l'échelle du bassin de l'Orgeval. D'un point de vue méthodologique, nous avons mis en évidence une différence certaine dans les représentations de l'usage du sol en fonction de la résolution de la base de données utilisée, ce qui est à prendre en compte lors des différents calculs basés sur les proportions de chaque usage du sol. Les émissions de N_2O par le réseau hydrographique se font préférentiellement aux ordres 1 et en été. Sur les bassins versants, elles ont essentiellement lieu en contexte de terres arables et de bas de pente.

En ce qui concerne l'abattement des nitrates dans les zones ripariennes, il est estimé de façon globale à environ 20 %. Cependant, il a été difficile de mettre cet abattement en relation avec des descripteurs environnementaux à l'échelle du bassin de la Seine. L'usage du sol, le paysage (au sens des petites régions agricoles) ou la largeur des zones ripariennes n'ont pas été perçus comme des facteurs essentiels. Le seul résultat, apparemment trivial, que nous avons mis en évidence est le rôle majeur joué par les zones ripariennes situées sur les ordres 1 ou 2. Toutefois, cette prédominance des petits ordres s'explique simplement par le fait qu'ils représentent plus de la moitié du linéaire fluvial et plus de la moitié de la surface drainée du bassin.

Outre celle des zones ripariennes, les transformations de l'azote au sein du réseau hydrographique sont importantes. De nombreuses études ont montré que les secteurs stagnants comme les lacs, les réservoirs ou les retenues d'eau sont des lieux propices à la dénitrification et donc à l'abattement des nitrates en raison de leur temps de séjour plus long. Des taux de rétention de 40 à plus de 80 % ont été relevés sur de nombreux plans d'eau dans de nombreuses régions (bassin de la Seine, Scandinavie, Amérique du Nord, Chine ...). Nous avons ainsi modélisé les effets d'une réintroduction d'étangs à l'échelle du bassin de la Seine. Afin de garder un aspect terroir, nous avons basé cette réintroduction fictive en s'appuyant sur le paysage tel qu'il était à la veille de l'ère industrielle. L'étude de la carte de Cassini, datant de la fin du 18ème siècle, nous a permis de réintroduire des étangs là où ils étaient dans le passé. Nous avons ainsi réalisé le premier recensement exhaustif et spatialisé des étangs de cette période, ce qui nous a permis de chiffrer la part du bassin consacré à l'époque aux étangs à 0.24 %. Ces étangs se situaient sur les ordres 1 essentiellement, et dans les régions à substrat imperméable. Nous avons d'abord montré que le modèle Seneque/Riverstrahler, conçu initialement pour décrire les processus biogéochimiques à l'échelle d'un bassin versant, pouvait tout à fait s'appliquer à un étang. Le modèle a été capable de reproduire la réten-

tion d'azote mesurée in-situ dans un étang à vocation agricole de Seine-et-Marne. A l'échelle d'un petit bassin comme l'Orgeval (100 km^2) les étangs peuvent conduire à un abattement d'azote, mais pas à l'échelle du bassin de la Seine dans son ensemble. Une diminution d'azote d'environ 10 % s'obtient en consacrant 1 % du bassin aux étangs. Avec une proportion de 5 %, une diminution d'azote de 30 % est envisageable. Au delà de 5 %, l'effet s'amortit.

Enfin, à la transition entre hydrosystème continental et zone côtière, nous avons lié Seneque/Riverstrahler à deux modèles estuariens. Les sorties de Seneque/Riverstrahler ont d'abord *nourri* un modèle mécaniste centré sur l'estuaire de l'Escaut. Les sorties fournies en termes de nutriments sont satisfaisantes pour reproduire les processus biogéochimiques qui se déroulent au sein de l'estuaire. Le modèle estuarien a permis de mettre en évidence deux zones privilégiées de développement du phytoplancton. La première, dans la partie amont, en domaine dulcicole, où se développent des efflorescences algales dominées par des Diatomées d'eau douce. La seconde, dans la partie marine de l'estuaire, voit plutôt se développer des algues non siliceuses. Ce lien entre un hydrosystème continental et un estuaire a également été exploré à l'embouchure de la Seine. Là, Seneque/Riverstrahler a *nourri* le modèle simplifié et non spatialisé LIFT. Ce modèle a permis de quantifier le rôle filtre de l'estuaire sur la période 1984-2007 et de le mettre en relation avec les années hydrologiques. Nous avons montré qu'au final, l'estuaire retient ou élimine assez peu les nutriments compte tenu des aménagements hydrauliques qu'il a subit depuis le $19^{ème}$ siècle, réduisant considérablement le temps de séjour des masses d'eau qui y transitent. Cependant, les années sèches, à faibles débits, sont plus propices à l'élimination des nutriments, notamment de l'azote. Le temps de séjour dans l'estuaire est donc un élément majeur dans la rétention des nutriments.

Les scénarios pour le futur co-construits avec les citoyens du programme AWARE

Les citoyens participants au programme AWARE ont tout d'abord reçu une information scientifique concernant la santé des systèmes fluviaux et des zones côtières adjacentes. Ils ont pris conscience qu'il existe deux types différents de pollution (en termes de nutriments). La première pollution, la plus facilement identifiable, est la pollution ponctuelle issue des activités industrielles et domestiques, produisant surtout du phosphore et de l'ammonium. La seconde, plus difficile à appréhender, est la pollution diffuse, agricole, à l'origine de la contamination par les nitrates du réseau hydrographique, mais aussi des aquifères. Leur première interrogation a été de connaître la part de chacune et leur évolution au cours du temps. Nos travaux de reconstruction des flux de nutriments depuis 1984 nous a permis de répondre à cette question. Partant de ce constat, ils nous ont demandé si nous étions arrivés au maximum des traitements possibles en station d'épuration et quels étaient les moyens de combattre les pollutions diffuses d'origine agricole. Les travaux sur les secteurs stagnants leur ont montré une des solutions curatives possibles d'atténuation des pollutions diffuses. Enfin, pour aller plus loin, nous avons construit avec eux quelques scénarios s'intéressant cette fois à des solutions préventives, de réduction des apports azotés aux cultures, présentés ci-dessous. Il est également intéressant de noter que, outre les nutriments, les citoyens s'interrogent aussi sur autres types de pollution (hydrocarbure, déchets toxiques, pesticides . . .), questions auxquelles notre modèle Seneque/Riverstrahler n'était pas adapté.

Quels scénarios pour la gestion future de la cascade de nutriments ?

Les scénarios présentés ci dessous sont également discutés dans le chapitre consacré au cas d'étude de la mer du Nord (Garnier et al., 2012) dans l'ouvrage consacré à la démarche AWARE :

> **The diseased southern North Sea : current status and possible solutions.**, dans *Bridging the Citizens-Science-Policy Gap, Connecting research, people and policy makers in Europe to achieve sustainable water ecosystems management*, Editor C. Sessa, European Water Research Series, 15 July 2012, ISBN : 9781780401140, signé par *Josette Garnier, Paul Passy, Véronique Rousseau, Nathalie Gypens, Julie Callens, Marie Silvestre, Gilles Billen, Christiane Lancelot.*

En accord avec l'intérêt des citoyens nous avons cherché à appréhender l'état de la qualité de l'eau lorsque la Directive Européenne sur les Eaux Résiduaires Urbaines (DERU) sera pleinement mise en application. Cette directive prévoit que toutes les stations d'épuration traitant plus de 2000 équivalents habitants abattent l'azote de 70 % et le phosphore de 90 %. Bien que l'application de cette directive soit bien avancée en France et en Belgique, nous avons construit le scénario correspondant à sa mise en œuvre complète. Les résultats attendus en termes de concentrations en nitrates au sein du réseau hydrographique ainsi qu'en termes d'efflorescences algales en zone côtière sont présentés figure 8.5.

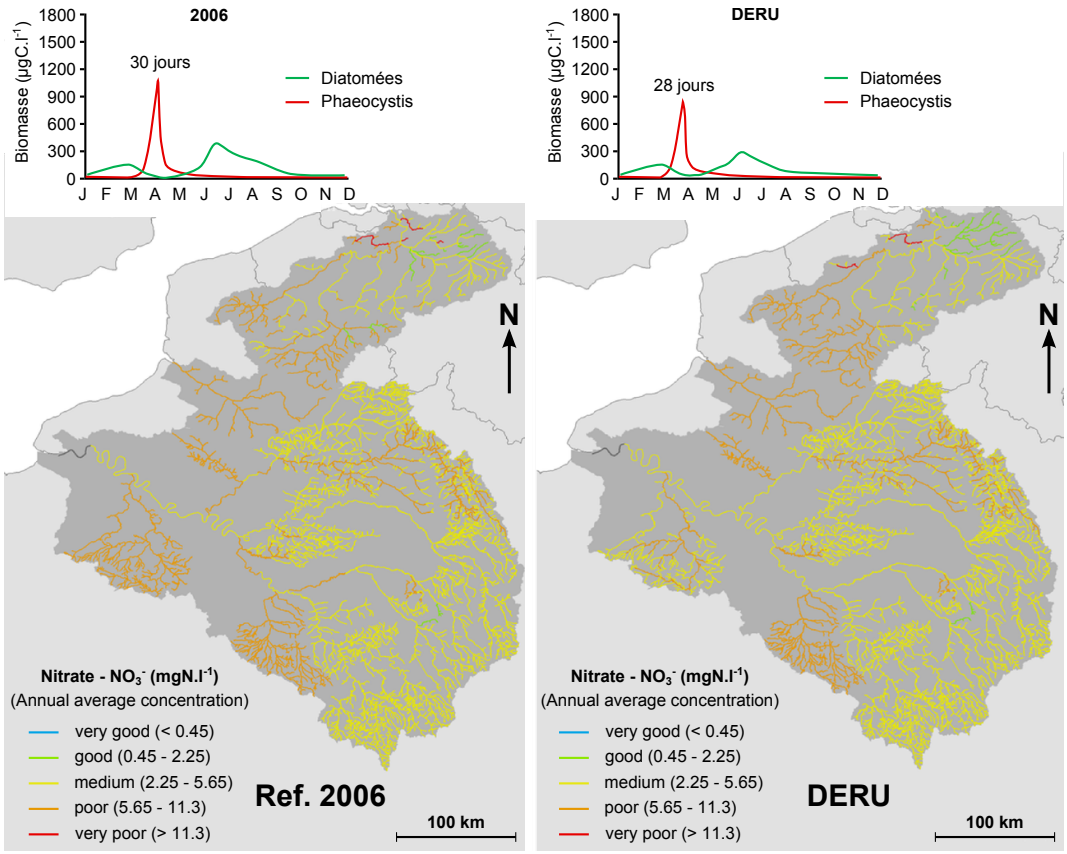

FIGURE 8.5 – Comparaison des concentrations en nitrates au sein du réseau hydrographique des 3S pour l'année 2006 et pour un scénario de mise en application de la « DERU » qui devrait être achevée en 2015. L'évolution des *Diatomées* et des *Phaeocystis* est indiquée ainsi que la durée et l'intensité des efflorescences.

Les nitrates étant en grande majorité issus des pollutions agricoles, leurs concentrations devraient peu changer avec l'application de cette directive. Seuls quelques tronçons de rivière dans les bassins de la Somme et de l'Escaut devraient voir leur situation s'améliorer. L'efflorescence algale pourrait diminuer de deux jours, passant de 30 à 28 jours.

Au vu de ces résultats limités de la mise aux normes DERU, un scénario visant à réduire la pollution diffuse agricole a été construit. Ce scénario s'inspire du « Grenelle de l'Environnement », un corpus français de lois voté à la fin des années 2000. Un des objectifs est de réduire les apports d'engrais, et donc d'azote, sur les bassins d'alimentation de captage d'eau potable les plus affectés par cette pollution. L'identification de ces captages prioritaires a été source de nombreux débats, et leur aire d'alimentation est encore en cours de délimitation pour une bonne partie d'entre eux. Cependant, nous avons pu proposer un scénario « Grenelle », consistant dans le passage à l'agriculture biologique de toutes les exploitations agricoles situées dans les aires d'alimentation des captages prioritaires. Nous avons défini arbitrairement ces aires sur base de la localisation des captages en sélectionnant tous les bassins élémentaires se trouvant à moins de 2 km de chaque captage. Par cette méthode arbitraire, nous parvenons à définir un tiers du bassin de la Seine comme prioritaire, valeur qui recoupe les estimations de l'Agence de l'Eau Seine-Normandie. Nous avons ensuite considéré, comme l'a fait Thieu et al. (2011) et comme les mesures réalisées depuis par notre laboratoire le confirment, que l'eau sous-racinaire issue des exploitations biologiques possède en moyenne une teneur en nitrate comprise entre 3 et 6 mgN^{-1}. Les résultats en termes de contamination nitrique de ce scénario exploratoire et idéalisé sont présentés dans la figure 8.6.

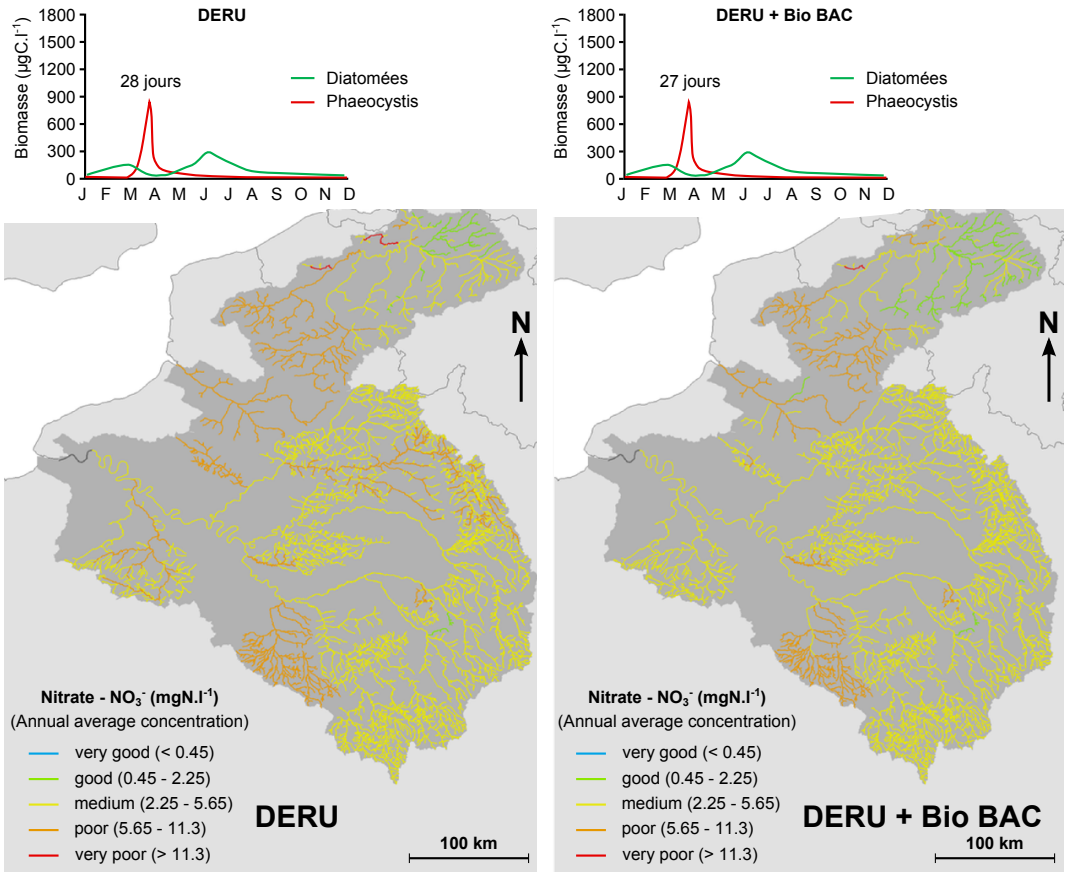

FIGURE 8.6 – Comparaison des concentrations en nitrates au sein du réseau hydrographique des 3S pour le scénario « DERU » (à gauche) et le scénario « Grenelle » (à droite). L'évolution des *Diatomées* et des *Phaeocystis* est indiquée ainsi que la durée et l'intensité des efflorescences.

La mise en application de ce scénario « Grenelle » permettrait donc une certaine amélioration dans les bassins de l'Oise, de la Somme ou de l'Eure. Cependant, la majeure partie du réseau ne verrait pas sa qualité sensiblement améliorée. Concernant la zone côtière, aucune diminution des efflorescences ne serait observée.

Enfin, afin de pousser les capacités des modèles à leur maximum et de tester quelle serait l'hypothétique meilleur résultat atteignable, nous avons effectué avec le modèle un scénario de conversion à l'agriculture biologique de toutes les zones agricoles des 3S, comme déjà exploré par Thieu et al. (2011). Bien que ce scénario soit totalement hypothétique, il était intéressant de montrer les meilleurs résultats qu'il est possible d'attendre d'une modification drastique des pratiques agricoles. Les résultats de ce scénario sont présentés dans la figure 8.7.

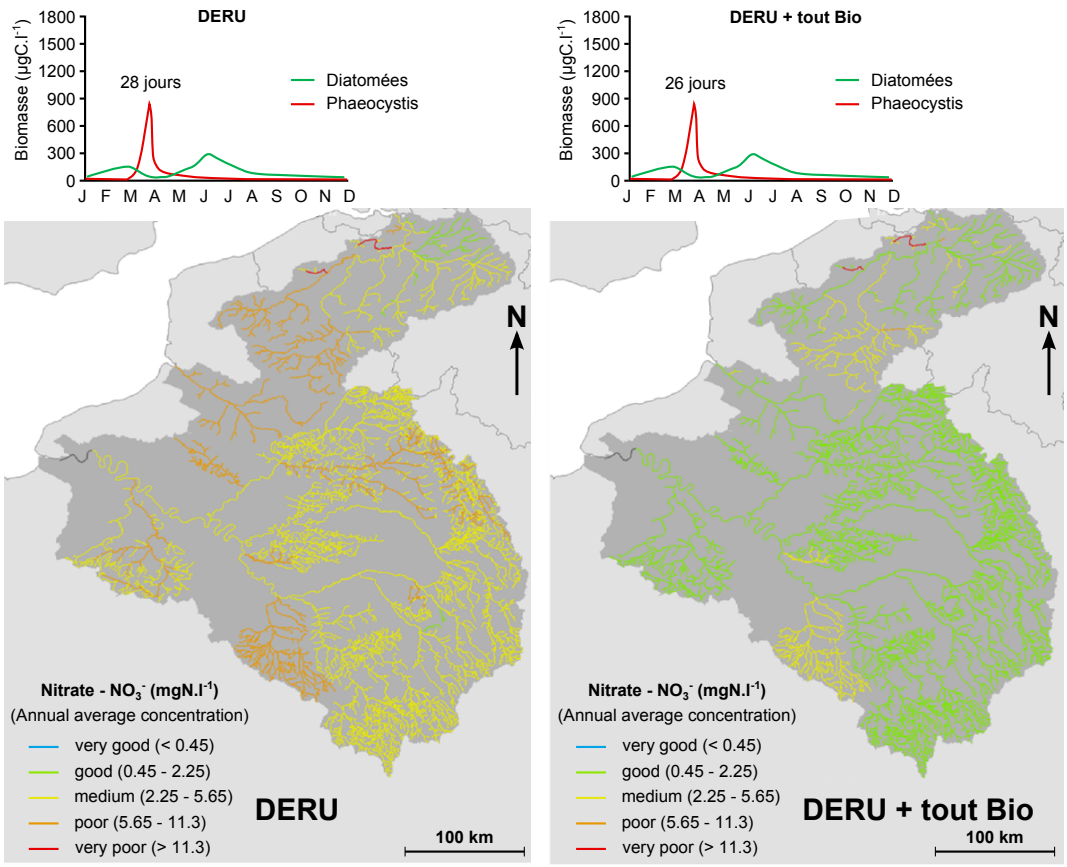

FIGURE 8.7 – Comparaison des concentrations en nitrates au sein du réseau hydrographique des 3S pour le scénario « DERU » (à gauche) et le scénario « tout bio » (à droite). L'évolution des *Diatomées* et des *Phaeocystis* est indiquée ainsi que la durée et l'intensité des efflorescences.

Le modèle montre que la qualité de l'eau au sein du réseau hydrographique s'améliorerait de façon spectaculaire avec une conversion totale à l'agriculture biologique. La quasi totalité des tronçons de rivière verraient leur qualité passer de moyenne à bonne. Cette amélioration des eaux continentales faciliterait grandement les processus de potabilisation. Par contre, paradoxalement, la qualité de la zone côtière ne s'en trouverait pas très sensiblement améliorée. La durée de l'efflorescence algale ne diminuerait que de deux jours, passant de 28 à 26 jours.

Les citoyens participants au projet ont donc pris conscience que seules des solutions préventives, visant à réduire drastiquement les apports diffus de l'agriculture, est en mesure de réellement diminuer les concentrations en nitrates du réseau hydrographique. L'agriculture biologique serait un moyen efficace d'y parvenir, mais nécessiterait un changement des habitudes commerciales et alimentaires de l'ensemble de la société. Sur le plan de l'alimentation, la part de protéines animales devrait être réduite au profit des protéines d'origine végétale. Le groupe de citoyens a bien pris conscience que chacun peut être un acteur majeur pour protéger, voire restaurer la qualité de l'eau. Toutefois la cohérence des politiques mises en œuvre par les pouvoirs publics en matière de lien entre une agriculture respectueuse de l'environnement et la protection des ressource en eau reste encore à trouver. D'autres formes d'agriculture, comme l'agriculture de précision, qui, sans remettre en cause les principes de l'agriculture industrielle, tentent de les mettre en oeuvre avec une parfaite maîtrise technique des processus, méritent également d'être explorées. Par ailleurs, des solutions curatives méritent également d'être explorées plus en détails tout en poursuivant une transformation profonde nécessaire des formes de production agricole.

Sensibilité des leviers d'action

Cette thèse a touché à plusieurs points de la cascade de nutriments en gardant l'objectif de réduire les flux de nutriments issus des bassins versants délivrés à la zone côtière. Lors de

notre démarche amont - aval, nous avons exploré les surplus azotés des terres arables, proposé des scénarios de conversion à l'agriculture biologique de quelques régions stratégiques du bassin ou de tout le bassin, mis en évidence le rôle de l'usage du sol et de la topographie sur les émissions de N_2O , tenté de mettre en relation la rétention riparienne avec des critères paysagers, montré le rôle des secteurs hydrographiques sur l'abattement de l'azote, mis en évidence les efforts portés sur les traitements des rejets ponctuels depuis le milieu des années 1980, quantifié l'effet filtre de l'estuaire vis-à-vis des nutriments et enfin retracé les efflorescences algales en zone côtière des 24 dernières années en simulant celles qui auraient lieu pour quelques scénarios futurs. Après cette exploration du continuum terre-mer, nous pouvons proposer une graduation quantitative de l'efficacité des mesures qui peuvent être prises pour réduire les flux de nutriments :

- **Changement des pratiques agricoles** (solution *préventive*). Ce changement pourrait s'appliquer à certaines régions sensibles du bassin, ou à sa totalité, ce qui maximiserait les effets. Évidemment, cette solution pose de nombreux enjeux d'ordre sociologique, économique et sociétal.
- **Aménagement des zones rippariennes** (solution *curative*). En l'état de nos connaissances, il est encore difficile de quantifier l'effet que nous pourrions en attendre à l'échelle du bassin de la Seine, mais il n'est sûrement pas négligeable. Cette solution serait également bénéfique au maintien d'une biodiversité forte le long des corridors fluviaux. Cependant, des enjeux fonciers pourraient entraver sa mise en place. Sur le plan des enjeux environnementaux il faudrait veiller à ce que les zones rippariennes ne soient pas à l'origine d'un déplacement de la pollution, à travers les émissions de N_2O.
- **Création / restauration de retenues au fil de l'eau** (solution *curative*). Cette solution ne réduirait que peu les flux d'azote à la mer mais permettrait d'améliorer localement la qualité de l'eau du réseau hydrographique. Ces aménagements devraient être localisés en tête de bassin, voire même en sortie de drains. Néanmoins, ce type de solution semble difficile à promouvoir dans un contexte de « continuité écologique », tel que prescrit par la loi sur l'eau et les milieux aquatiques (Melun, 2012). De plus, les effets négatifs sur le foncier, et peut-être encore sur la réduction concomitante du silicium ou sur l'accroissement des émissions de N_2O seraient des obstacles supplémentaires.
- **Amélioration du filtre estuarien** (solution *curative*). C'est sans doute sur ce point, que les moyens d'agir sont les plus compliqués. Il pourrait être envisageable de restituer quelques zones de divagation à l'estuaire ici ou là, afin d'augmenter le temps de séjour des masses d'eau et le potentiel de dénitrification benthique. Cependant, l'effet filtre de l'estuaire étant devenu tellement faible avec les aménagements, cette solution n'est pas forcément efficace.

Quelques perspectives

Plusieurs perspectives peuvent se dégager pour la suite de cette thèse. La première serait de mieux définir le rôle que jouent les zones ripariennes dans la rétention d'azote. Aucun autre facteur environnemental que les ordres de rivières n'a pu être clairement identifié par notre analyse à l'échelle du bassin du Grand Morin ou à celle du bassin de la Seine, comme gouvernant l'abattement de l'azote. Or, de nombreuses études mettent en avant une rétention variant selon la géologie, l'hydrogéologie ou l'usage du sol. Un premier travail pourrait être de revoir notre approche statistique en définissant plus finement les zones ripariennes. Il serait intéressant par exemple de mieux les discrétiser en se basant sur des photographies aériennes plutôt que sur la base de données Corine Land Cover ou de mieux prendre en compte la pédologie locale via les cartes de sols. Cette étude pourrait être menée dans un premier temps sur le bassin de l'Orgeval, voire du Grand Morin. Une deuxième perspective, en continuité de la précédente, serait d'explorer le rôle que joue l'ensemble du paysage à l'échelle du bassin versant élémentaire. Nous pouvons penser qu'un paysage présentant une topographie relativement variée avec des forêts en bas de pente retient mieux l'azote qu'un paysage avec une topographie uniforme et entièrement agricole. D'une manière plus générale, la caractérisation fine des paysages et de leur rôle sur la cascade de l'azote devrait faire l'objet de travaux, sur la base, notamment, des modélisations à l'échelle de paysages élémentaires telles que celles réalisées à l'aide de la plate forme de modélisation NitroScape (thèse de Sylvia Duretz, UMR SAS de Rennes) ou Casimod'N (thèse de Pierre Moreau, 2012, UMR SAS de Rennes). C'est précisément l'objectif du projet ANR Escapade qui va débuter l'an prochain et auquel l'UMR Sisyphe est associé.

Une troisième perspective serait d'affiner l'étude que nous avons menée sur les étangs. Nous avons vu que localement, la réintroduction de secteurs stagnants pouvait réduire significativement les concentrations en nitrates. Cependant, nous avons également montré que ces retenues influencent également les flux de phosphore et de silicium, ainsi que les dynamiques du phytoplancton et zooplancton. Or le problème de la qualité de l'eau n'est pas seulement une surabondance d'azote mais un déséquilibre entre azote, phosphore et silicium. Si les étangs retiennent plus le silicium que l'azote, dans un contexte de « pénurie » de silicium, leur ré-introduction pourrait avoir un effet contraire à celui recherché. Ainsi, il pourrait être judicieux de faire un bilan pour ces trois nutriments en différents points du réseau et pour certaines proportions d'étangs. Par ailleurs, les étangs pourraient modifier la continuité écologique des cours d"eau avec un impact négatif sur les communautés piscicoles.

Enfin, concernant les solutions préventives, deux dernières perspectives sont envisageables. La première serait de récupérer, lorsque les agences de l'eau auront achevé cette tâche, les délimitations de bassins d'alimentation de captage définitives et de recalculer notre scénario « Grenelle ». Nous aurions ainsi un résultat sans doute plus en accord avec ce que nous pourrions réellement obtenir. La seconde, qui intéresse également le scénario « Grenelle » serait de mieux préciser les concentrations sous-racinaires que nous utilisons dans nos simulations d'agriculture biologique. Elles sont actuellement fixées, suite à revue bibliographique, entre 3 et 6 $mgN.l^{-1}$. Or encore peu d'études s'intéressent à ces concentrations sous racinaires en contexte d'agriculture biologique. Une thèse en cours en partie sur ce sujet (de Marie Benoit) au laboratoire Sisyphe permettra de préciser ces valeurs dans des conditions variées (celles des rotations dans différents contextes pédoclimatiques. Il est également nécessaire de prendre l'aspect économique et sociétal d'une transformation des pratiques agricoles afin d'affiner nos scénarios. La thèse en cours de Juliette Anglade, également au laboratoire Sisyphe, vise justement à mieux préciser ces aspects.

« Le pessimisme de la connaissance n'empêche pas l'optimisme de la volonté. »

Antonio Gramsci

Bibliographie

Alexander, R., Smith, R., and Schwarz, G. (2000). Effect of stream channel size on the delivery of nitrogen to the Gulf of Mexico. *Nature*, 403(6771) :758–761.

Allen, J., Somerfield, P., and Gilbert, F. (2007). Quantifying uncertainty in high-resolution coupled hydrodynamic-ecosystem models. *Journal of Marine Systems*, 64(1-4) :3–14.

Allen, S. C., Jose, S., Nair, P., Brecke, B. J., Nkedi-Kizza, P., and Ramsey, C. L. (2004). Safety-net role of tree roots : evidence from a pecan (Carya illinoensis K. Koch)–cotton (Gossypium hirsutum L.) alley cropping system in the southern United States. *Forest Ecology and Management*, 192(2–3) :395–407.

Allen, T. F. H., Giampietro, M., and Little, A. M. (2003). Distinguishing ecological engineering from environmental engineering. *Ecological Engineering*, 20(5) :389–407.

Ambus, P. and Christensen, S. (1994). Measurement of N2O emission from a fertilized grassland : An analysis of spatial variability. *Journal of Geophysical Research*, 99(D8) :16549–16,555.

Amoros, C. and Roux, A. (1988). Interactions between water bodies within the floodplains of large rivers : function and development of connectivity. In *Connectivity in landscape Ecology*, volume 29, pages 125–130. K.F. Schreiber. Münst.Geogr, Münster.

Anderson, S., Udawatta, R., Seobi, T., and Garrett, H. (2009). Soil water content and infiltration in agroforestry buffer strips. *Agroforestry Systems*, 75(1) :5–16.

Appeltans, W., Hannouti, A., Damme, S. v., Soetaert, K., Vanthomme, R., and Tackx, M. (2003). Zooplankton in the Schelde estuary (Belgium/The Netherlands). The distribution of Eurytemora affinis : effect of oxygen ? *Journal of Plankton Research*, 25(11) :1441–1445.

Arheimer, B., Torstensson, G., and Wittgren, H. B. (2004). Landscape planning to reduce coastal eutrophication : agricultural practices and constructed wetlands. *Landscape and Urban Planning*, 67(1-4) :205–215.

Arndt, S., Lacroix, G., Gypens, N., Regnier, P., and Lancelot, C. (2011). Nutrient dynamics and phytoplankton development along an estuary–coastal zone continuum : A model study. *Journal of Marine Systems*, 84(3–4) :49–66.

Arndt, S., Vanderborght, J.-P., and Regnier, P. (2007). Diatom growth response to physical forcing in a macrotidal estuary : Coupling hydrodynamics, sediment transport, and biogeochemistry. *Journal of Geophysical Research*, 112(C5).

Attrill, M. and Rundle, S. (2002). Ecotone or Ecocline : Ecological Boundaries in Estuaries. *Estuarine, Coastal and Shelf Science*, 55(6) :929–936.

Avoine, J., Allen, G., Nichols, M., Salomon, J., and Larsonneur, C. (1981). Suspended-sediment transport in the Seine estuary, France : Effect of man-made modifications on estuary—shelf sedimentology. *Marine Geology*, 40(1–2) :119–137.

Bach, M., Breuer, L., Frede, H., Huisman, J., Otte, A., and Waldhardt, R. (2006). Accuracy and congruency of three different digital land-use maps. *Landscape and Urban Planning*, 78(4) :289–299.

Balestrini, R., Arese, C., Delconte, C., Lotti, A., and Salerno, F. (2011). Nitrogen removal in subsurface water by narrow buffer strips in the intensive farming landscape of the Po River watershed, Italy. *Ecological Engineering*, 37(2) :148–157.

Barles, S. (2007). Feeding the city : Food consumption and flow of nitrogen, Paris, 1801-1914. *Science of the Total Environment*, 375(1-3) :48–58.

Baron, J. S., Hall, E. K., Nolan, B. T., Finlay, J. C., Bernhardt, E. S., Harrison, J. A., Chan, F., and Boyer, E. W. (2012). The interactive effects of excess reactive nitrogen and climate change on aquatic ecosystems and water resources of the united states. *Biogeochemistry*.

Bartlett, K. B. and Harriss, R. C. (1993). Review and assessment of methane emissions from wetlands. *Chemosphere*, 26(1-4) :261–320.

Bartoli, F. and Souchier, B. (1978). Cycle et rôle du silicium d'origine végétale dans les écosystèmes forestiers tempérés. *Annales des Sciences Forestières*, 35(3) :187–202.

Bateman, E. J. and Baggs, E. M. (2005). Contributions of nitrification and denitrification to N2O emissions from soils at different water-filled pore space. *Biology and Fertility of Soils*, 41(6) :379–388.

Beaujouan, V., Durand, P., and Ruiz, L. (2001). Modelling the effect of the spatial distribution of agricultural practices on nitrogen fluxes in rural catchments. *Ecological Modelling*, 137(1) :93–105.

Beltrando, G. (2004). La répartition des climats du globe. In *Les climats : Processus, variabilité et risques*, Collection U, pages 137–165. Armand Colin, Paris, 1ère édition edition.

Beltrando, G. and Chémery, L. (1995). *Dictionnaire du climat*. Larousse.

Benoit, P. (2002). La carpe au Moyen-Âge. In *Dans l'eau, sous l'eau : le monde aquatique au Moyen âge*. Presses Paris Sorbonne.

Benoit, P. and Berthier, K. (2005). Approvisionnement en bois de Paris : le flottage en Morvan. In *Groupe d'Histoire des Forêts françaises*, pages 41–55.

Benoit, P., Berthier, K., Billen, G., and Garnier, J. (2002). Agriculture et aménagement du paysage hydrologique dans le bassin de la Seine au XIV-XVe siècle. Aix en Provence, France.

Benoit, P. and Mattéoni, O. (2005). Pêche et pisciculture en eau douce : la rivière et l'étang au Moyen Âge. Lille. Conseil Général du Nord.

Benoit, P., Passy, P., Rouillard, J., and Tigreat, P. (2010). Etudes historiques sur le bassin de la Seine avant le XIXe siècle. Technical report, PIREN-Seine, Paris.

Bérard, L. (1988). La consommation du Poisson en France : des prescriptions alimentaires à la prépondérance de la Carpe. *Anthropozoologica*, (spécial) :171–179.

Berthier, K. (2007). Usages, gestion et industrialisation de la bièvre dans le val-de-marne de l'Antiquite a nos jours. In *Actes des 18èmes Journées Scientifiques de l'Environnement 2007 : Environnement, Citoyenneté et Territoires Urbains*, volume 2007, page 18.

Beutel, M. W., Newton, C. D., Brouillard, E. S., and Watts, R. J. (2009). Nitrate removal in surface-flow constructed wetlands treating dilute agricultural runoff in the lower Yakima Basin, Washington. *Ecological Engineering*, 35(10) :1538–1546.

Beven, K. (2001). Rainfall-Runoff Modelling : The Primer. In *Rainfall-Runoff Modelling*, pages i–xxix. John Wiley & Sons, Ltd.

Beven, K. and Kirkby, M. (1979). A physically based, variable contributing area model of basin hydrology. *Hydrological Sciences Bulletin*, 24 :43–69.

Billen, C. and Duvosquel, J.-M. (2000). *Bruxelles*. Fonds Mercator, Bruxelles.

Billen, G., Barles, S., Chatzimpiros, P., and Garnier, J. (2012a). Grain, meat and vegetables to feed Paris : where did and do they come from ? Localising Paris food supply areas from the eighteenth to the twenty-first century. *Regional Environmental Change*, 12(2) :325–335.

Billen, G., Barles, S., Garnier, J., Rouillard, J., and Benoit, P. (2009a). The food-print of Paris : long-term reconstruction of the nitrogen flows imported into the city from its rural hinterland. *Regional Environmental Change*, 9(1) :13–24.

Billen, G., Beusen, A., Bouwman, L., and Garnier, J. (2010). Anthropogenic nitrogen autotrophy and heterotrophy of the world's watersheds : Past, present, and future trends. *Global Biogeochemical Cycles*, 24.

Billen, G. and Garnier, J. (1999). Nitrogen transfers through the Seine drainage network : a budget based on the application of theRiverstrahler'model. *Hydrobiologia*, 410 :139–150.

Billen, G. and Garnier, J. (2009). Eutrophisation des cours d'eau du bassin de la Seine, Comprendre comment l'activité de l'homme entraîne la prolifération des végétaux aquatiques. Technical Report 6, PIREN-Seine, Paris.

Billen, G., Garnier, J., and Barles, S. (2012b). History of the urban environmental imprint : introduction to a multidisciplinary approach to the long-term relationships between Western cities and their hinterland. *Regional Environmental Change*, 12(2) :249–253.

Billen, G., Garnier, J., Deligne, C., and Billen, C. (1999). Estimates of early-industrial inputs of nutrients to river systems : implication for coastal eutrophication. *Science of the Total Environment*, 244 :43–52.

Billen, G., Garnier, J., Ficht, A., and Cun, C. (2001). Modeling the response of water quality in the Seine river estuary to human activity in its watershed over the last 50 years. *Estuaries*, 24(6B) :977–993.

Billen, G., Garnier, J., and Hanset, P. (1994). Modeling phytoplankton development in whole drainage networks - the riverstrahler model applied to the seine river system. *Hydrobiologia*, 289(1-3) :119–137.

Billen, G., Garnier, J., and Meybeck, M. (1998). Les sels nutritifs : l'ouverture des cycles. In *La Seine en son bassin : Fonctionnement écologique d'un système fluvial anthropisé*, pages 531–566. Paris, elsevier edition.

Billen, G., Garnier, J., Mouchel, J., and Silvestre, M. (2007a). The Seine system : Introduction to a multidisciplinary approach of the functioning of a regional river system. *Science of the Total Environment*, 375(1-3) :1–12.

Billen, G., Garnier, J., Némery, J., Sebilo, M., Sferratore, A., Barles, S., Benoit, P., and Benoît, M. (2007b). A long-term view of nutrient transfers through the Seine river continuum. *Science of the Total Environment*, 375(1-3) :80–97.

Billen, G., Garnier, J., and Rousseau, V. (2005). Nutrient fluxes and water quality in the drainage network of the Scheldt basin over the last 50 years. *Hydrobiologia*, 540 :47–67.

Billen, G., Garnier, J., Thieu, V., Passy, P., Riousset, P., Silvestre, M., Théry, S., Vilain, G., and Billy, C. (2011a). La cascade de l'azote dans le bassin de la Seine, Comprendre les processus pour inverser les tendances. Technical Report 15, PIREN-Seine, Paris.

Billen, G., Garnier, J., Thieu, V., Silvestre, M., Barles, S., and Chatzimpiros, P. (2012c). Localising the nitrogen imprint of the Paris food supply : the potential of organic farming and changes in human diet. *Biogeosciences*, 9 :607–616.

Billen, G., Silvestre, M., Barles, S., Mouchel, J., Garnier, J., Curie, F., and Boët, P. (2009b). Le bassin de la Seine, Découvrir les fonctions et les services rendus par le système Seine. Technical Report 1, PIREN-Seine, Paris.

Billen, G., Silvestre, M., Leip, A., Garnier, J., Voss, M., Howarth, R. W., Bouraoui, F., Lepisto, A., Kortelainen, P., Johnes, P., Curtis, C., Humborg, C., Smedberg, E., Kaste, O., Ganeshram, R., Beusen, A., Lancelot, C., and Grizzetti, B. (2011b). Nitrogen flows from European regional watersheds to coastal marine waters. In *The European Nitrogen Assesment : Sources, Effects and Policy Perspectives*, pages 271–297. Cambridge University Press, Cambridge, UK, 1 edition.

Billen, G., Somville, M., Debecker, E., and Servais, P. (1985). A nitrogen budget of the scheldt hydrographical basin. *Netherlands Journal of Sea Research*, 19(3-4) :223–230.

Billen, G., Thieu, V., Garnier, J., and Silvestre, M. (2009c). Modelling the N cascade in regional watersheds : The case study of the Seine, Somme and Scheldt rivers. *Agriculture, Ecosystems & Environment*, 133(3-4) :234–246.

Bingham, M. A. and Biondini, M. (2010). Nitrate leaching as a function of plant community richness and composition, and the scaling of soil nutrients, in a restored temperate grassland. *Plant Ecology*, 212(3) :413–422.

Blomster, J., Bäck, S., Fewer, D. P., Kiirikki, M., Lehvo, A., Maggs, C. A., and Stanhope, M. J. (2002). Novel morphology in Enteromorpha (Ulvophyceae) forming green tides. *American Journal of Botany*, 89(11) :1756–1763.

Borges, A., Vanderborght, J., Schiettecatte, L., Gazeau, F., Ferrón-Smith, S., Delille, B., and Frankignoulle, M. (2004). Variability of the gas transfer velocity of CO2 in a macrotidal estuary (the Scheldt). *Estuaries and Coasts*, 27(4) :593–603.

Borja, A., Elliott, M., Carstensen, J., Heiskanen, A., and van de Bund, W. (2010). Marine management - Towards an integrated implementation of the European Marine Strategy Framework and the Water Framework Directives. *Marine Pollution Bulletin*, 60(12) :2175–2186.

Bouraoui, F. and Grizzetti, B. (2011). Long term change of nutrient concentrations of rivers discharging in European seas. *Science of the Total Environment*, 409(23) :4899–4916.

Bouvier, T. C. and Giorgio, P. A. d. (2002). Compositional Changes in Free-Living Bacterial Communities along a Salinity Gradient in Two Temperate Estuaries. *Limnology and Oceanography*, 47(2) :453–470.

Bouwman, A., Kram, T., and Goldewijk, K. (2006). *Integrated modelling of global environmental change. An overview of IMAGE 2.4*. Netherlands Environmental Assessment Agency, Bilthoven, The Netherlands.

Bouwman, A. F. (1996). Direct emission of nitrous oxide from agricultural soils. *Nutrient Cycling in Agroecosystems*, 46(1) :53–70.

Bouwman, A. F., Boumans, L. J. M., and Batjes, N. H. (2002a). Emissions of N2O and NO from fertilized fields : Summary of available measurement data. *Global Biogeochemical Cycles*, 16(4) :1058.

Bouwman, A. F., Boumans, L. J. M., and Batjes, N. H. (2002b). Modeling global annual N2O and NO emissions from fertilized fields. *Global Biogeochemical Cycles*, 16(4) :1080.

Braskerud, B. (2002). Factors affecting phosphorus retention in small constructed wetlands treating agricultural non-point source pollution. *Ecological Engineering*, 19(1) :41–61.

Bravard, J.-P., Provansal, M., Arnaud-Fassetta, G., Chabbert, S., Gaydou, P., Dufour, S., Richard, F., Valleteau, S., Melun, G., and Passy, P. (2008). Un atlas du paléo-environnement de la plaine alluviale du Rhône de la frontière suisse à la mer. *Edytem*, (6) :101–116.

Brenon, I. and Le Hir, P. (1999). Simulation du bouchon vaseux dans l'estuaire de la Seine : capacité et limites d'un modèle bidimensionnel horizontal. *Comptes Rendus de l'Académie des Sciences - Series IIA - Earth and Planetary Science*, 328(5) :327–332.

Brinson, M. M., Bradshaw, H. D., and Kane, E. S. (1984). Nutrient Assimilative Capacity of an Alluvial Floodplain Swamp. *Journal of Applied Ecology*, 21(3) :1041–1057.

Brisson, N., Gary, C., Justes, E., Roche, R., Mary, B., Ripoche, D., Zimmer, D., Sierra, J., Bertuzzi, P., Burger, P., Bussière, F., Cabidoche, Y., Cellier, P., Debaeke, P., Gaudillère, J., Hénault, C., Maraux, F., Seguin, B., and Sinoquet, H. (2003). An overview of the crop model stics. *European Journal of Agronomy*, 18(3–4) :309–332.

Brochier, J. E. (2002). Les sédiments anthropiques, Méthodes d'études et perspectives. In *Géologie de la préhistoire : méthodes, techniques, applications*, pages 453–477. Géopré.

Bryhn, A., Veidemane, K., Stålnacke, P., and Nagothu, U. S. (2012). The future of the Gulf of Riga : Pollution, Water Quality and Fish Production. In *Sustainable Water Ecosystems Management in Europe, Bridging the Knowledge of Citizens, Scientists and Policy Makers*, pages 53–66. Community research, Londres, IWA edition.

Brzezinski, M. and Nelson, D. (1995). The Annual Silica Cycle in the Sargasso Sea Near Bermuda. *Deep-Sea Research Part I-Oceanographic Research Papers*, 42(7) :1215–1237.

Burnett, C. D. (2005). The Edges of Empire and the Limits of Sovereignty : American Guano Islands. *American Quarterly*, 57(3) :779–803.

Burt, T. P. and Pinay, G. (2005). Linking hydrology and biogeochemistry in complex landscapes. *Progress in Physical Geography*, 29(3) :297 –316.

Canton, M., Anschutz, P., Poirier, D., Chassagne, R., Deborde, J., and Savoye, N. (2012). The buffering capacity of a small estuary on nutrient fluxes originating from its catchment (Leyre estuary, SW france). *Estuarine, Coastal and Shelf Science*, 99(0) :171–181.

Carré, C., de Gouvello, B., Deroubaix, J.-F., Deutsch, J.-C., and Hague, J. (2011). Les petites rivières urbaines d'Île-de-France, Découvrir leur fonctionnement pour comprendre les enjeux autour de leur gestion et de la reconquête de la qualité de l'eau. Technical Report 11, PIREN-Seine, Paris.

Casabianca, S., Penna, A., Pecchioli, E., Jordi, A., Basterretxea, G., and Vernesi, C. (2012). Population genetic structure and connectivity of the harmful dinoflagellate Alexandrium minutum in the Mediterranean Sea. *Proceedings of the Royal Society B-Biological Sciences*, 279(1726) :129–138.

Cassini, C.-F. and Cassini, J.-D. (1756). Carte de Cassini.

Cellier, P., Durand, P., Hutchings, H., Dragosits, U., Theobald, M., Drouet, J. L., Oenema, O., Bleeker, A., Breuer, L., Dalgaard, T., Duretz, S., Kros, J., Loubet, B., Olesen, J. E., Mérot, P., Viaud, V., de Vries, W., and Sutton, M. A. (2011). Nitrogen flows and fate in rural landscapes. In *The European Nitrogen Assesment : Sources, Effects and Policy Perspectives*, pages 229–248. Cambridge University Press, Cambridge, UK, 1 edition.

Cervetto, G., Gaudy, R., and Pagano, M. (1999). Influence of salinity on the distribution of Acartia tonsa (Copepoda, Calanoida). *Journal of Experimental Marine Biology and Ecology*, 239(1) :33–45.

Chapuis-Lardy, L., Wrage, N., Metay, A., Chotte, J.-L., and Bernoux, M. (2007). Soils, a sink for N2O ? A review. *Global Change Biology*, 13(1) :1–17.

Claval, P. (2011). Les Lumières et la Géographie. In *Histoire de la géographie*, number 65 in Que sais-je ?, page 126. Presses Universitaires de France - PUF, Paris, 3 edition.

Coeur, C. L. and Gautier, E. (2008). Les agents et les processus de l'érosion. In *Eléments de géographie physique*, pages 159–196. Bréal, Rosny, France, 2e édition edition.

Conley, D. J. (2002). Terrestrial ecosystems and the global biogeochemical silica cycle. *Global Biogeochemical Cycles*, 16(4).

Conley, D. J., Carstensen, J., Aigars, J., Axe, P., Bonsdorff, E., Eremina, T., Haahti, B., Humborg, C., Jonsson, P., Kotta, J., Lannegren, C., Larsson, U., Maximov, A., Medina, M. R., Lysiak-Pastuszak, E., Remeikaite-Nikiene, N., Walve, J., Wilhelms, S., and Zillen, L. (2011). Hypoxia Is Increasing in the Coastal Zone of the Baltic Sea. *Environmental Science & Technology*, 45(16) :6777–6783.

Coque, R. (2002). Les processus élémentaires de l'érosion. In *Géomorphologie*, pages 125–182. Armand Colin, Paris, sixième édition edition.

Corre, M. D., van Kessel, C., and Pennock, D. J. (1996). Landscape and Seasonal Patterns of Nitrous Oxide Emissions in a Semiarid Region. *Soil Science Society of America Journal*, 60(6) :1806–1815.

Corvol, A. (2007). *Forêt et eau : XIIIe-XXIe siècle*. Editions L'Harmattan.

Cozzi, S. and Giani, M. (2011). River water and nutrient discharges in the Northern Adriatic Sea : Current importance and long term changes. *Continental Shelf Research*, 31(18) :1881–1893.

Cugier, P., Billen, G., Guillaud, J., Garnier, J., and Ménesguen, A. (2005). Modelling the eutrophication of the Seine Bight (France) under historical, present and future riverine nutrient loading. *Journal of Hydrology*, 304(1-4) :381–396.

Curie, F., Ducharne, A., Bendjoudi, H., and Billen, G. (2011). Spatialization of denitrification by river corridors in regional-scale watersheds : Case study of the Seine river basin. *Physics and Chemistry of the Earth*, 36(12) :530–538.

Curie, F., Gaillard, S., Ducharne, A., and Bendjoudi, H. (2007). Geomorphological methods to characterise wetlands at the scale of the Seine watershed. *Science of the Total Environment*, 375(1-3) :59–68.

Cuvilliez, A., Deloffre, J., Lafite, R., and Bessineton, C. (2009). Morphological responses of an estuarine intertidal mudflat to constructions since 1978 to 2005 : The seine estuary (France). *Geomorphology*, 104(3–4) :165–174.

Czitrom, V. (1999). One-Factor-at-a-Time versus Designed Experiments. *The American Statistician*, 53(2) :126–131.

Dalu, J. and Ndamba, J. (2003). Duckweed based wastewater stabilization ponds for wastewater treatment (a low cost technology for small urban areas in Zimbabwe). *Physics and Chemistry of the Earth, Parts A/B/C*, 28(20–27) :1147–1160.

David, M. B., Wall, L. G., Royer, T. V., and Tank, J. L. (2006). Denitrification and the nitrogen budget of a reservoir in an agricultural landscape. *Ecological Applications*, 16(6) :2177–2190.

Davidson, E. A. and Schimel, J. P. (1995). Microbial processes of production and consumption of nitric oxide, nitrous oxide and methane. In *Biogenic Trace Gases : Measuring Emissions from Soil and Water*, pages 327–357. Wiley-Blackwell, 1 edition.

Davies, B. R., Biggs, J., Williams, P. J., Lee, J. T., and Thompson, S. (2007). A comparison of the catchment sizes of rivers, streams, ponds, ditches and lakes : implications for protecting aquatic biodiversity in an agricultural landscape. *Hydrobiologia*, 597(1) :7–17.

Davis, S. N. (1964). Silica in streams and ground water. *American Journal of Science*, 262(7) :870–891.

Dayssiols, J. (2009). Inquiétante marée verte sur le littoral breton. *L'Humanité*.

De Becker, E., Billen, G., Rousseau, V., and Stainier, E. (1985). Etude de la contamination azotée des eaux souterraines et de surface dans le bassin de la dyle à wavre. Etude pour le ministère de la région wallonne pour l'Eau, l'Environnement et la vie rurale, Ministère de la Région Wallonne pour l'Eau, l'Environnement et la vie rurale, Brussels, Belgium.

de Beule, M. (1994). Bruxelles, une ville industrielle méconnue. Impact urbanistique de l'industrialisation. Les dossiers de la Fonderies. Dossier, Bruxelles.

de Ferraris, J. (1770). Carte de Ferraris.

De Vries, F., Van Groenigen, J., Hoffland, E., and Bloem, J. (2011). Nitrogen losses from two grassland soils with different fungal biomass. *Soil Biology and Biochemistry*.

Deborde, J., Anschutz, P., Chaillou, G., Etcheber, H., Commarieu, M.-V., Lecroart, P., and Abril, G. (2007). The dynamics of phosphorus in turbid estuarine systems : Example of the gironde estuary (France). *Limnology and Oceanography*, 52(2) :862–872.

Décamps, H., Fortuné, M., Gazelle, F., and Pautou, G. (1988). Historical influence of man on the riparian dynamics of a fluvial landscape. *Landscape Ecology*, 1(3) :163–173.

Deemer, B. R., Harrison, J. A., and Whitling, E. W. (2011). Microbial dinitrogen and nitrous oxide production in a small eutrophic reservoir : An in situ approach to quantifying hypolimnetic process rates. *Limnology and Oceanography*, 56(4) :1189–1199.

DeFries, R. S., Asner, G. P., and Houghton, R. A. (2004). Ecosystems and Land Use Change. *Geophysical Monograph Series*, 153 :1–344.

Del Grosso, S. J., Parton, W. J., Mosier, A. R., Hartman, M. D., Brenner, J., Ojima, D. S., and Schimel, D. S. (2001). Simulated interaction of carbon dynamics and nitrogen trace gas fluxes using the DAYCENT model. In *Modeling Carbon and Nitrogen Dynamics for Soil Management*, pages 303–332. CRC Press Inc.

Delattre, B. (2011). La marée verte ne cesse de s'étendre. *La Libre Belgique*.

Deligne, C. (2003). *Bruxelles et sa rivière. Genèse d'un territoire urbain.* Turnhout, Bruxelles, brepols edition.

Deligne, C. (2012). *The rivers of Brussels, 1770-1880 : transformations of an urban landscape*. Pittsburgh University Press.

Demey, T. (1990). *Bruxelles. Chronique d'une capitale en chantier*, volume 1. Bruxelles, CFC editions edition.

Derex, J. (2001). Le décret du 14 frimaire an II sur l'assèchement des étangs : folles espérances et piètres résultats. L'application du décret en Brie. *Annales historiques de la Révolution française*, (325) :77–97.

Derruau, M. (2010). *Les formes du relief terrestre : Notions de géomorphologie*. Armand Colin, 8e édition edition.

Di, H. and Cameron, K. (2002). Nitrate leaching in temperate agroecosystems : sources, factors and mitigating strategies. *Nutrient Cycling in Agroecosystems*, 64(3) :237–256.

Diaz, R. J. and Rosenberg, R. (2008). Spreading dead zones and consequences for marine ecosystems. *Science*, 321(5891) :926–929.

Diderot, D. (1781). *Encyclopédie ou dictionnaire raisonné des sciences des arts et des métiers*. Sociétés Typographiques.

Dillon, P. and Molot, L. (1990). The role of ammonium and nitrate retention in the acidification of lakes and forested catchments. *Biogeochemistry*, 11(1) :23–43.

Dise, N., Ashmore, M., Belyazid, S., Bleeker, A., Bobbink, R., de Vries, W., Erisman, J., Spranger, T., Stevensand Leon van den Berg, C., Rivett, M., Reay, D., Curtis, C., Siemens, J., Maberly, S., Kaste, O., Humborg, C., Loeb, R., de Klein, J., Hejzlar, J., Skoulikidis, N., Kortelainen, P., Lepistö, A., and Wright, R. (2011). Nitrogen as a

threat to European terrestrial biodiversity. In *The European Nitrogen Assesment : Sources, Effects and Policy Perspectives*, pages 463–494. Cambridge University Press, Cambridge, UK, 1 edition.

Domingues, R. B., Barbosa, A. B., Sommer, U., and Galvao, H. M. (2011). Ammonium, nitrate and phytoplankton interactions in a freshwater tidal estuarine zone : potential effects of cultural eutrophication. *Aquatic Sciences*, 73(3) :331–343.

Dragosits, U., Theobald, M. R., Place, C. J., ApSimon, H. M., and Sutton, M. A. (2006). The potential for spatial planning at the landscape level to mitigate the effects of atmospheric ammonia deposition. *Environmental Science & Policy*, 9(7-8) :626–638.

Duché, S. and Beltrando, G. (2010). Spatio-temporal variability of ozone and nitrogen dioxide concentrations at background locations in the Paris area in 2007 and 2008. In *EGU General Assembly Conference Abstracts*, volume 12, page 587.

Dufourg, O. (2011). Jean-françois masselot, un dunkerquois engagé dans la gestion durable des eaux côtières. *La Voix du Nord*.

Durand, P., Breuer, L., Johnes, P., Billen, G., Butturini, A., Pinay, G., van Grinsven, H., Garnier, J., Rivett, M., Reay, D., Curtis, C., Siemens, J., Maberly, S., Kaste, O., Humborg, C., Loeb, R., de Klein, J., Hejzlar, J., Skoulikidis, N., Kortelainen, P., Lepistö, A., and Wright, R. (2011). Nitrogen processes in aquatic ecosystems. In *The European Nitrogen Assesment : Sources, Effects and Policy Perspectives*, pages 126–146. Cambridge University Press, Cambridge, UK, 1 edition.

Durandeau, S., Gabrielle, B., Godard, C., Jayet, P., and Le Bas, C. (2010). Coupling biophysical and micro-economic models to assess the effect of mitigation measures on greenhouse gas emissions from agriculture. *Climatic Change*, 98(1) :51–73.

Duretz, S., Drouet, J. L., Durand, P., Hutchings, N. J., Theobald, M. R., Salmon-Monviola, J., Dragosits, U., Maury, O., Sutton, M. A., and Cellier, P. (2011). NitroScape : A model to integrate nitrogen transfers and transformations in rural landscapes. *Environmental Pollution*, 159(11) :3162–3170.

Eckhardt, K. (2005). How to construct recursive digital filters for baseflow separation. *Hydrological Processes*, 19(2) :507–515.

Eckhardt, K. (2008). A comparison of baseflow indices, which were calculated with seven different baseflow separation methods. *Journal of Hydrology*, 352(1-2) :168–173.

Elliott, M. and Whitfield, A. (2011). Challenging paradigms in estuarine ecology and management. *Estuarine, Coastal and Shelf Science*, 94(4) :306–314.

Engstrom, L., Stenberg, M., Aronsson, H., and Linden, B. (2011). Reducing nitrate leaching after winter oilseed rape and peas in mild and cold winters. *Agronomy for Sustainable Development*, 31(2) :337–347.

Erisman, J., Bleeker, A., Galloway, J., and Sutton, M. (2007). Reduced nitrogen in ecology and the environment. *Environmental Pollution*, 150(1) :140–149.

Etcheber, H., Taillez, A., Abril, G., Garnier, J., Servais, P., Moatar, F., and Commarieu, M.-V. (2007). Particulate organic carbon in the estuarine turbidity maxima of the gironde, loire and seine estuaries : origin and lability. *Hydrobiologia*, 588(1) :245–259.

européen, P. (1991a). Directive 91/271/CEE du Conseil, du 21 mai 1991, relative au traitement des eaux urbaines résiduaires.

européen, P. (1991b). Directive n° 91/676/CEE du 12/12/91 concernant la protection des eaux contre la pollution par les nitrates à partir de sources agricoles.

européen, P. (2000). Directive 2000/60/EC of the European Parliament and of the Council establishing a framework for the Community action in the field of water policy.

européen, P. (2008). Directive cadre Stratégie pour le milieu marin.

Even, S., Billen, G., Bacq, N., Théry, S., Ruelland, D., Garnier, J., Cugier, P., Poulin, M., Blanc, S., Lamy, F., and Paffoni, C. (2007). New tools for modelling water quality of hydrosystems : An application in the Seine River basin in the frame of the Water Framework Directive. *Science of the Total Environment*, 375(1-3) :274–291.

Fardeau, J.-C. and Dorioz, J.-M. (2002). La dynamique du phosphore dans les zones humides. In *Fonctions et valeurs des zones humides*, pages 143–159. Dunod, Paris.

Favier, J. (1997). *Paris : Deux mille ans d'histoire*. Fayard.

Ferreira, J. G., Andersen, J. H., Borja, A., Bricker, S. B., Camp, J., da Silva, M. C., Garces, E., Heiskanen, A., Humborg, C., Ignatiades, L., Lancelot, C., Menesguen, A., Tett, P., Hoepffner, N., and Claussen, U. (2011). Overview of eutrophication indicators to assess environmental status within the European Marine Strategy Framework Directive RID C-5701-2011. *Estuarine Coastal and Shelf Science*, 93(2) :117–131.

Figuier, L. (1860). *Les merveilles de l'industrie, ou Description des principales industries modernes*. Furne, Jouvet et Cie.

Foden, J., Devlin, M. J., Mills, D. K., and Malcolm, S. J. (2010). Searching for undesirable disturbance : an application of the OSPAR eutrophication assessment method to marine waters of England and Wales. *Biogeochemistry*, 106 :157–175.

Foley, J. A., DeFries, R., Asner, G. P., Barford, C., Bonan, G., Carpenter, S. R., Chapin, F. S., Coe, M. T., Daily, G. C., Gibbs, H. K., Helkowski, J. H., Holloway, T., Howard, E. A., Kucharik, C. J., Monfreda, C., Patz, J. A., Prentice, I. C., Ramankutty, N., and Snyder, P. K. (2005). Global Consequences of Land Use. *Science*, 309(5734) :570–574.

Folorunso, O. A. and Rolston, D. E. (1985). Spatial and Spectral Relationships Between Field-measured Denitrification Gas Fluxes and Soil Properties. *Soil Science Society of America Journal*, 49(5) :1087–1093.

Forman, R. T. T. (1995a). *Land Mosaics : The Ecology of Landscapes and Regions*. Cambridge University Press.

Forman, R. T. T. (1995b). Some general principles of landscape and regional ecology. *Landscape Ecology*, 10(3) :133–142.

Forman, R. T. T. and Godron, M. (1981). Patches and Structural Components for a Landscape Ecology. *BioScience*, 31(10) :733.

Foucault, A. and Raoult, J.-F. (2010). *Dictionnaire de Géologie - 7e édition*. Dunod, 7e édition edition.

Freibauer, A. (2003). Regionalised inventory of biogenic greenhouse gas emissions from European agriculture. *European Journal of Agronomy*, 19(2) :135–160.

Fritz, M. (1994). Etude statistique de la contamination en nitrates des cours d'eau et des nappes principales du bassin de l'Yonne et de la seine en amont de montereau. Technical report, Université Pierre et Marie Curie, Paris, France.

Fustec, E., Greiner, I., Schanen, O., Gaillard, S., and Dzana, J.-G. (2000). Les zones humides riveraines : des milieux divers aux multiples fonctions. In *La Seine en son bassin : Fonctionnement écologique d'un système fluvial anthropisé*, pages 211–262. Elsevier France.

Gabrielle, B., Laville, P., Duval, O., Nicoullaud, B., Germon, J. C., and Hénault, C. (2006a). Process-based modeling of nitrous oxide emissions from wheat-cropped soils at the subregional scale. *Global Biogeochemical Cycles*, 20(4) :GB4018.

Gabrielle, B., Laville, P., Hénault, C., Nicoullaud, B., and Germon, J. (2006b). Simulation of Nitrous Oxide Emissions from Wheat-cropped Soils using CERES. *Nutrient Cycling in Agroecosystems*, 74(2) :133–146.

Gaillard, S., Abdou Dagga, N., Bendjoudi, H., and Billen, G. (2006). Exploitation de la base de données sur les corridors fluviaux du district seine-normandie. Technical report, PIREN-Seine, Paris.

Galloway, J. N., Townsend, A. R., Erisman, J. W., Bekunda, M., Cai, Z., Freney, J. R., Martinelli, L. A., Seitzinger, S. P., and Sutton, M. A. (2008). Transformation of the Nitrogen Cycle : Recent Trends, Questions, and Potential Solutions. *Science*, 320(5878) :889–892.

Garnier, J., Beusen, A., Thieu, V., Billen, G., and Bouwman, L. (2010a). N :P :Si nutrient export ratios and ecological consequences in coastal seas evaluated by the ICEP approach. *Global Biogeochemical Cycles*, 24 :12 PP.

Garnier, J. and Billen, G. (1994). Ecological interactions in a shallow sand-pit lake (lake Creteil, Parisian Basin, France) - a modeling approach. *Hydrobiologia*, 275 :97–114.

Garnier, J., Billen, G., Billen, C., Servais, P., and Onclincx, F. (1991). Bruxelles et sa rivière : le Prséent, le Passé et l'Avenir, Modélisation du fonctionnement de l'écosystème Senne. Technical report, Université Libre de Bruxelles, Groupe de Microbilologie des Milieux Aquatiques, Bruxelles.

Garnier, J., Billen, G., and Coste, M. (1995). Seasonal Succession of Diatoms and Chlorophyceae in the Drainage Network of the Seine River : Observations and Modeling. *Limnology and Oceanography*, 40(4) :750–765.

Garnier, J., Billen, G., Even, S., Etcheber, H., and Servais, P. (2008). Organic matter dynamics and budgets in the turbidity maximum zone of the seine estuary (France). *Estuarine, Coastal and Shelf Science*, 77(1) :150–162.

Garnier, J., Billen, G., Hannon, E., Fonbonne, S., Videnina, Y., and Soulie, M. (2002). Modelling the transfer and retention of nutrients in the drainage network of the Danube River. *Estuarine Coastal and Shelf Science*, 54(3) :285–308.

Garnier, J., Billen, G., Hanset, P., Testard, P., and Coste, G. (2000a). Développement algal et eutrophisation dans le réseau hydrographique de la seine. In *La Seine en son bassin : Fonctionnement écologique d'un système fluvial anthropisé*, pages 593–626. Elsevier France.

Garnier, J., Billen, G., and Levassor, A. (2000b). Réservoirs : fonctionnement et impacts écologiques. In *La Seine en son bassin : Fonctionnement écologique d'un système fluvial anthropisé*, pages 263–300. Elsevier France.

Garnier, J., Billen, G., Némery, J., and Sebilo, M. (2010b). Transformations of nutrients (N, p, si) in the turbidity maximum zone of the seine estuary and export to the sea. *Estuarine, Coastal and Shelf Science*, 90(3) :129–141.

Garnier, J., Billen, G., Passy, P., Rousseau, V., and Lancelot, C. (2009a). The North Sea-3S case Study : Inception Report. Synthèse 1.2.2, Bioforsk.

Garnier, J., Billen, G., Vilain, G., Martinez, A., Silvestre, M., Mounier, E., and Toche, F. (2009b). Nitrous oxide (N2O) in the Seine river and basin : Observations and budgets. *Agriculture, Ecosystems & Environment*, 133(3-4) :223–233.

Garnier, J., Laroche, L., and Pinault, S. (2006). Determining the domestic specific loads of two wastewater plants of the Paris conurbation (France) with contrasted treatments : A step for exploring the effects of the application of the European Directive. *Water Research*, 40(17) :3257–3266.

Garnier, J., Leporcq, B., Sanchez, N., and Philippon (1999). Biogeochemical mass-balances (C, N, P, Si) in three large reservoirs of the Seine basin (France). *Biogeochemistry*, 47(2) :119–146.

Garnier, J., Passy, P., Rousseau, V., Gypens, N., Callens, J., Silvestre, M., Billen, G., and Lancelot, C. (2012). The diseased southern North Sea : current status and possible solutions. In *Sustainable Water Ecosystems Management in Europe, Bridging the Knowledge of Citizens, Scientists and Policy Makers*, pages 67–82. Community research, Londres, IWA edition.

Garnier, J. A., Mounier, E. M., Laverman, A. M., and Billen, G. F. (2010c). Potential Denitrification and Nitrous Oxide Production in the Sediments of the Seine River Drainage Network (France). *Journal of Environmental Quality*, 39(2) :449–459.

Gazeau, F., Gattuso, J.-P., Middelburg, J., Brion, N., Schiettecatte, L.-S., Frankignoulle, M., and Borges, A. (2005). Planktonic and whole system metabolism in a nutrient-rich estuary (the Scheldt estuary). *Estuaries and Coasts*, 28(6) :868–883.

Giltrap, D. L., Li, C., and Saggar, S. (2010). DNDC : A process-based model of greenhouse gas fluxes from agricultural soils. *Agriculture, Ecosystems & Environment*, 136(3–4) :292–300.

Giordani, G., Mocenni, C., Bencivelli, S., and Viaroli, P. (2009). The Sacca di Goro Case Study : Inception Report. Synthèse 1.2.3, Bioforsk.

Girel, J. (1996). La prise en compte de l'histoire dans la gestion des corridors fluviaux : les enseignements des aménagements anciens. *Revue de géographie de Lyon*, 71(4) :341–352.

Gleize, F. and Mathieu, Y. (2012). The pilot experience with the AWARE citizens' panel. In *Sustainable Water Ecosystems Management in Europe, Bridging the Knowledge of Citizens, Scientists and Policy Makers*, pages 41–52. Community research, Londres, IWA edition.

Gopalakrishnan, G., Cristina Negri, M., and Salas, W. (2011). Modeling biogeochemical impacts of bioenergy buffers with perennial grasses for a row-crop field in Illinois. *GCB Bioenergy*, pages n/a–n/a.

Grataloup, A. M. (1998). *Précis de géographie*. Nathan.

Grizzetti, B., Bouraoui, F., and Aloe, A. (2012). Changes of nitrogen and phosphorus loads to European seas. *Global Change Biology*, 18(2) :769–782.

Grizzetti, B., Bouraoui, F., Billen, G., van Grinsven, H., Cardoso, A. C., Thieu, V., Garnier, J., Curtis, C., Howarth, R. W., and Johnes, P. (2011). Nitrogen as a threat to European water quality. In *The European Nitrogen Assesment : Sources, Effects and Policy Perspectives*, pages 379–404. Cambridge University Press, Cambridge, UK, 1 edition.

Groffman, P. M., Gold, A. J., and Simmons, R. C. (1992). Nitrate dynamics in riparian forests : Microbial studies. *Journal of Environmental Quality*, 21(4) :666–671.

Gruca-Rokosz, R. and Tomaszek, J. A. (2007). The effect of abiotic factors on denitrification rates in sediment of Solina Reservoir, Poland. *Environment Protection Engineering*, 33(2) :131–140.

Guerif, M., Houles, V., and Baret, F. (2007). Remote sensing and detection of nitrogen status in crops. Application to precise nitrogen fertilization. *Progress of Information Technology in Agriculture*, pages 593–601.

Guerrini, M., Mouchel, J., Meybeck, M., Penven, M., Hubert, G., and Muxart, T. (2000). Le bassin de la Seine : la confrontation du rural et de l'urbain. In *La Seine en son bassin : Fonctionnement écologique d'un système fluvial anthropisé*. Elsevier France.

Guézennec, L. (1999a). *1 - Seine-Aval : un estuaire et ses problèmes*. Editions Quae.

Guézennec, L. (1999b). Les estuaires : des systèmes complexes et particuliers. In *1 - Seine-Aval : un estuaire et ses problèmes*, pages 4–7. Editions Quae.

Guillerme, A. (1983). *Temps de L'eau*. Editions Champ Vallon.

Gypens, N., Lacroix, G., and Lancelot, C. (2007). Causes of variability in diatom and Phaeocystis blooms in Belgian coastal waters between 1989 and 2003 : A model study. *Journal of Sea Research*, 57(1) :19–35.

Gypens, N., Lacroix, G., Lancelot, C., and Borges, A. (2011). Seasonal and inter-annual variability of air–sea CO2 fluxes and seawater carbonate chemistry in the Southern North Sea. *Progress In Oceanography*, 88(1–4) :59–77.

Haag, D. and Kaupenjohann, M. (2001a). Landscape fate of nitrate fluxes and emissions in Central Europe - A critical review of concepts, data, and models for transport and retention. *Agriculture Ecosystems & Environment*, 86(1) :1–21.

Haag, D. and Kaupenjohann, M. (2001b). Parameters, prediction, post-normal science and the precautionary principle–a roadmap for modelling for decision-making. *Ecological Modelling*, 144(1) :45–60.

Hadas, A. and Rosenberg, R. (1992). Guano as a nitrogen source for fertigation in organic farming. *Nutrient Cycling in Agroecosystems*, 31(2) :209–214.

Hansson, L., Brönmark, C., Anders Nilsson, P., and Aabjoernsson, K. (2005). Conflicting demands on wetland ecosystem services : nutrient retention, biodiversity or both ? *Freshwater Biology*, 50(4) :705–714.

Hatch, D. J. (2004). *Controlling Nitrogen Flows And Losses*. Wageningen Academic Pub.

Haycock, N., Pinay, G., and Walker, C. (1993). Nitrogen-Retention in River Corridors - European Perspective. *Ambio*, 22(6) :340–346.

Haycock, N. E. and Burt, T. P. (1993). The sensitivity of rivers to nitrate leaching : the effectiveness of nearstream land as a nutrient retention zone.

Heckrath, G., Brookes, P. C., Poulton, P. R., and Goulding, K. W. T. (1995). Phosphorus Leaching from Soils Containing Different Phosphorus Concentrations in the Broadbalk Experiment. *Journal of Environmental Quality*, 24(5) :904–910.

Heller, R., Esnault, R., and Lance, C. (2004). *Physiologie végétale : Tome 1, Nutrition*. Dunod, 6e edition edition.

Hemond, H. and Eshleman, K. (1984). Neutralization of acid deposition by nitrate retention at bickford watershed, massachusetts. *Water Resources Research*, 20(11) :1718–1724.

Hénault, C., Bizouard, F., Laville, P., Gabrielle, B., Nicoullaud, B., Germon, J. C., and Cellier, P. (2005). Predicting in situ soil N2O emission using NOE algorithm and soil database. *Global Change Biology*, 11(1) :115–127.

Henriksen, A. and Wright, R. (1977). Effects of acid deposition on a small acid lake on southern Norway. *Nordic Hydrology*, 8 :1–10.

Hernandez, M. E. and Mitsch, W. J. (2007). Denitrification in created riverine wetlands : Influence of hydrology and season. *Ecological Engineering*, 30(1) :78–88.

Higounet, C. (1956). L'assolement triennal dans la plaine de France au XIIIe siècle. *Comptes-rendus des séances de l'Académie des Inscriptions et Belles-Lettres*, 100(4) :507–512.

Hill, A. (1996). Nitrate removal in stream riparian zones. *Journal of Environmental Quality*, 25(4) :743–755.

Hill, A. R. (1979). Denitrification in the nitrogen budget of a river ecosystem. *Nature*, 281(5729) :291–292.

Hir, P., Ficht, A., Jacinto, R., Lesueur, P., Dupont, J.-P., Lafite, R., Brenon, I., Thouvenin, B., and Cugier, P. (2001). Fine sediment transport and accumulations at the mouth of the seine estuary (France). *Estuaries and Coasts*, 24(6) :950–963.

Hirt, U., Venohr, M., Kreins, P., and Behrendt, H. (2008). Modelling nutrient emissions and the impact of nutrient reduction measures in the Weser river basin, Germany. *Water Science and Technology*, 58(11) :2251–2258.

Hofmann, A. F., Soetaert, K., Middelburg, J. J., et al. (2008). Present nitrogen and carbon dynamics in the Scheldt estuary using a novel 1-D model. *Biogeosciences*, 5(4).

Honisch, M., Hellmeier, C., and Weiss, K. (2002). Response of surface and subsurface water quality to land use changes. *Geoderma*, 105(3-4) :277–298.

Howardwilliams, C. (1985). Cycling and retention of nitrogen and phosphorus in wetlands : a theoretical and applied perspective. *Freshwater Biology*, 15(4) :391–431.

Howarth, R., Chan, F., Conley, D. J., Garnier, J., Doney, S. C., Marino, R., and Billen, G. (2011). Coupled biogeochemical cycles : eutrophication and hypoxia in temperate estuaries and coastal marine ecosystems. *Frontiers in Ecology and the Environment*, 9(1) :18–26.

Howarth, R. W. (2008). Coastal nitrogen pollution : A review of sources and trends globally and regionally. *Harmful Algae*, 8(1) :14–20.

Howarth, R. W., Billen, G., Swaney, D., Townsend, A., Jaworski, N., Lajtha, K., Downing, J. A., Elmgren, R., Caraco, N., Jordan, T., Berendse, F., Freney, J., Kudeyarov, V., Murdoch, P., and Zhao-Liang, Z. (1996). Regional nitrogen budgets and riverine N & P fluxes for the drainages to the North Atlantic Ocean : Natural and human influences. *Biogeochemistry*, 35 :75–139.

Howarth, R. W. and Marino, R. (2006). Nitrogen as the limiting nutrient for eutrophication in coastal marine ecosystems : Evolving views over three decades. *Limnology and Oceanography*, 51(1) :364–376.

Humborg, C., Conley, D. J., Rahm, L., Wulff, F., Cociasu, A., and Ittekkot, V. (2000). Silicon Retention in River Basins : Far-reaching Effects on Biogeochemistry and Aquatic Food Webs in Coastal Marine Environments. *AMBIO : A Journal of the Human Environment*, 29(1) :45–50.

Hutchinson, G. L. and Livingston, G. P. (1993). Use of chamber systems to measure trace gas fluxes. In *Agricultural Ecosystem Effects on Trace Gases and Global Climate Change : Proceedings of a Symposium Sponsored by Divisions A-3 and S-3 of the Americ*, pages 79–93. Amer Society of Agronomy.

Im, D., Kang, H., Kim, K., and Choi, S. (2011). Changes of river morphology and physical fish habitat following weir removal. *Ecological Engineering*, 37(6) :883–892.

Ionita, M., Lohmann, G., Rimbu, N., and Chelcea, S. (2012). Interannual variability of rhine river streamflow and its relationship with large-scale anomaly patterns in spring and autumn. *Journal of Hydrometeorology*, 13(1) :172–188.

Isenhart, T. M., Schultz, R. C., Mickelson, S. K., and Lee, K. (2000). Multispecies Riparian Buffers Trap Sediment and Nutrients during Rainfall Simulations. *Journal of Environmental Quality*, 29(4) :1200–1205.

Izaurralde, R. C., Lemke, R. L., Goddard, T. W., McConkey, B., and Zhang, Z. (2004). Nitrous Oxide Emissions from Agricultural Toposequences in Alberta and Saskatchewan. *Soil Science Society of America Journal*, 68(4) :1285.

Jähne, B., Huber, W., Dutzi, A., Wais, T., and Ilmberger, J. (1984). Wind/wave-tunnel experiment on the Schmidt number – and wave field dependence of air/water gas exchange. In *Gas Transfer at Water Surfaces*, pages 303–309. Springer, 1st ed. softcover of orig. ed. 1984 edition.

Jansson, M., Andersson, R., Berggren, H., and Leonardson, L. (1994). Wetlands and Lakes as Nitrogen Traps. *Ambio*, 23(6) :320–325.

Jaumain, S. (2011). *La région de Bruxelles-Capitale*. Racine edition.

Jensen, J., Kristensen, P., and Jeppesen, E. (1990). Relationships between nitrogen loading and in-lake nitrogen concentrations in shallow Danish lakes. *Internationale Vereinigung fuer Theoretische und Angewandte Limnologie*, 24(1) :201–204.

Johnston, C., Detenbeck, N., and Niemi, G. (1990). The cumulative effect of wetlands on stream water quality and quantity. A landscape approach. *Biogeochemistry*, 10.

Jones, M. N. (1984). Nitrate reduction by shaking with cadmium : Alternative to cadmium columns. *Water Research*, 18(5) :643–646.

Jose, S. (2009). Agroforestry for ecosystem services and environmental benefits : an overview. *Agroforestry Systems*, 76(1) :1–10.

Kaiser, E., Kohrs, K., Kücke, M., Schnug, E., Heinemeyer, O., and Munch, J. (1998). Nitrous oxide release from arable soil : Importance of N-fertilization, crops and temporal variation. *Soil Biology and Biochemistry*, 30(12) :1553–1563.

Kiernan, V. G. (1955). Foreign Interests in the War of the Pacific. *The Hispanic American Historical Review*, 35(1) :14.

Kirkby, M. J. (1975). Hydrograph modelling strategies. In *Process in Physical and Human Geography*, pages 69–90. Heinemann Educational Books.

Klein, C., Claquin, P., Bouchart, V., Le Roy, B., and Veron, B. (2010). Dynamics of Pseudo-nitzschia spp. and domoic acid production in a macrotidal ecosystem of the Eastern English Channel (Normandy, France). *Harmful Algae*, 9(2) :218–226.

Korsaeth, A. and Eltun, R. (2000). Nitrogen mass balances in conventional, integrated and ecological cropping systems and the relationship between balance calculations and nitrogen runoff in an 8-year field experiment in Norway. *Agriculture, Ecosystems & Environment*, 79(2-3) :199–214.

Koszelnik, P. and Tomaszek, J. (2008). Dissolved Silica Retention and Its Impact on Eutrophication in a Complex of Mountain Reservoirs. *Water, Air, & Soil Pollution*, 189(1) :189–198.

Koszelnik, P., Tomaszek, J. A., and Gruca-Rokosz, R. (2007). The significance of denitrification in relation to external loading and nitrogen retention in a mountain reservoir. *Marine and Freshwater Research*, 58(9) :818–826.

Krause, P., Boyle, D., and Bäse, F. (2005). Comparison of different efficiency criteria for hydrological model assessment. *Advances in Geosciences*, 5(89) :89–97.

Kreiling, R. M., Richardson, W. B., Cavanaugh, J. C., and Bartsch, L. A. (2011). Summer nitrate uptake and denitrification in an upper Mississippi River backwater lake : the role of rooted aquatic vegetation. *Biogeochemistry*, 104(1-3) :309–324.

Kroeze, C., Bouwman, L., and Seitzinger, S. (2012). Modeling global nutrient export from watersheds. *Current Opinion in Environmental Sustainability*, 4(2) :195–202.

Kromkamp, J. C. and Peene, J. (2005). Changes in phytoplankton biomass and primary production between 1991 and 2001 in the Westerschelde estuary (Belgium/The Netherlands). *Hydrobiologia*, 540(1) :117–126.

Kromkamp, J. C. and Van Engeland, T. (2010). Changes in Phytoplankton Biomass in the Western Scheldt Estuary During the Period 1978-2006. *Estuaries and Coasts*, 33(2) :270–285.

Kuusemets, V. and Mander, U. (2002). Nutrient flows and management of a small watershed. *Landscape Ecology*, 17 :59–68.

Lacoste, Y. (2000). *Atlas 2000. La France et le Monde*. Nathan, nouv. éd. 1996 edition.

Lacroix, G., Ruddick, K., Gypens, N., and Lancelot, C. (2007a). Modelling the relative impact of rivers (Scheldt/Rhine/Seine) and western channel waters on the nutrient and diatoms/Phaeocystis distributions in belgian waters (southern north sea). *Continental Shelf Research*, 27(10–11) :1422–1446.

Lacroix, G., Ruddick, K., Ozer, J., and Lancelot, C. (2004). Modelling the impact of the Scheldt and Rhine/Meuse plumes on the salinity distribution in Belgian waters (southern North Sea). *Journal of Sea Research*, 52(3) :149–163.

Lacroix, G., Ruddick, K., Park, Y., Gypens, N., and Lancelot, C. (2007b). Validation of the 3D biogeochemical model MIRO&CO with field nutrient and phytoplankton data and MERIS-derived surface chlorophyll a images. *Journal of Marine Systems*, 64(1–4) :66–88.

Lancelot, C. (1995). The mucilage phenomenon in the continental coastal waters of the North Sea. *Science of the Total Environment*, 165(1-3) :83–102.

Lancelot, C., Billen, G., Sournia, A., Weisse, T., Colijn, F., Veldhuis, M., Davies, A., and Wassman, P. (1987). Phaeocystis blooms and nutrient enrichment in the continental coastal zones of the North Sea. *Ambio*, 16(1) :38–46.

Lancelot, C., Gypens, N., Billen, G., Garnier, J., and Roubeix, V. (2007). Testing an integrated river-ocean mathematical tool for linking marine eutrophication to land use : The Phaeocystis-dominated Belgian coastal zone (Southern North Sea) over the past 50 years. *Journal of Marine Systems*, 64(1-4) :216–228.

Lancelot, C. and Mathot, S. (1987). Dynamics of a phaeocystis-dominated spring bloom in belgian coastal waters .1. phytoplanktonic activities and related parameters. *Marine Ecology-Progress Series*, 37(2-3) :239–248.

Lancelot, C. and Muylaert, K. (2012). Trends in Estuarine Phytoplankton Ecology. In *Treatise on Coastal and Estuarine Science*, Biogeochemistry.

Lancelot, C., Rousseau, V., and Gypens, N. (2009). Ecologically based indicators for Phaeocystis disturbance in eutrophied Belgian coastal waters (Southern North Sea) based on field observations and ecological modelling. *Journal of Sea Research*, 61(1-2) :44–49.

Lancelot, C., Spitz, Y., Gypens, N., Ruddick, K., Becquevort, S., Rousseau, V., Lacroix, G., and Billen, G. (2005). Modelling diatom and Phaeocystis blooms and nutrient cycles in the Southern Bight of the North Sea : the MIRO model. *Marine Ecology-Progress Series*, 289 :63–78.

Lancelot, C., Thieu, V., Polard, A., Garnier, J., Billen, G., Hecq, W., and Gypens, N. (2011). Cost assessment and ecological effectiveness of nutrient reduction options for mitigating Phaeocystis colony blooms in the Southern North Sea : An integrated modeling approach. *Science of the Total Environment*, 409(11) :2179–2191.

Lancelot, C., Veth, C., and Mathot, S. (1991). Modelling ice-edge phytoplankton bloom in the Scotia-Weddell sea sector of the Southern Ocean during spring 1988. *Journal of Marine Systems*, 2(3–4) :333–346.

Lascoumes, P. (2007). Gouverner par les cartes. *Genèses*, n° 68(3) :2–3.

Lassaletta, L., Garcia-Gomez, H., Gimeno, B. S., and Rovira, J. V. (2009). Agriculture-induced increase in nitrate concentrations in stream waters of a large Mediterranean catchment over 25 years (1981-2005). *Science of the Total Environment*, 407(23) :6034–6043.

Lassaletta, L., Romero, E., Billen, G., Garnier, J., García-Gómez, H., and Rovira, J. V. (2012). Spatialized N budgets in a large agricultural Mediterranean watershed : high loading and low transfer. *Biogeosciences*, 9 :57–70.

Laursen, A. and Seitzinger, S. (2002). Measurement of denitrification in rivers : an integrated, whole reach approach. *Hydrobiologia*, 485(1-3) :67–81.

Le, T., Garnier, J., Billen, G., Théry, S., Duong, T., and Chau, V. (2007). La qualité des eaux du Fleuve Rouge (Vietnam) : observation et modélisation. In *Actes des JSIRAUF*, page 6, Hanoi, Vietnam.

Lecolle, F. (1987). *La Seine aux temps glaciaires.* Musée archéologique départemental du Val d'Oise, Guiry-en-Vexin.

Lee, K. H., Isenhart, T. M., and Schultz, R. C. (2003). Sediment and nutrient removal in an established multi-species riparian buffer. *Journal of Soil and Water Conservation*, 58(1) :1–8.

Lefeuvre, J.-C., Fustec, E., and Barnaud, G. (2002). De l'élimination à la reconquête des zones humides. In *Fonctions et valeurs des zones humides*, pages 1–16. Dunod, Paris.

Lehuger, S. (2009). *Modelling greenhouse gas balance of agro-ecosystems iin Europe.* PhD thesis, AgroParisTech, Thiverval-Grignon, France.

Levasseur, O. (2004). Brève histoire de la consommation des produits de la mer (XVIème - XIXème siècles). In *Actes de l'AISLF*, page 13, Tours, France.

Li, C. (1996). The DNDC model. *NATO ASI Series*, 38 :263–268.

Li, X., Jongman, R. H., Hu, Y., Bu, R., Harms, B., Bregt, A. K., and He, H. S. (2005). Relationship between landscape structure metrics and wetland nutrient retention function : A case study of Liaohe Delta, China. *Ecological Indicators*, 5(4) :339–349.

Linn, D. M. and Doran, J. W. (1984). Effect of Water-Filled Pore Space on Carbon Dioxide and Nitrous Oxide Production in Tilled and Nontilled Soils. *Soil Science Society of America Journal*, 48(6) :1267–1272.

Lionard, M., Muylaert, K., Gansbeke, D. V., and Vyverman, W. (2005). Influence of changes in salinity and light intensity on growth of phytoplankton communities from the Schelde river and estuary (Belgium/The Netherlands). *Hydrobiologia*, 540(1) :105–115.

Lionard, M., Muylaert, K., Hanoutti, A., Maris, T., Tackx, M., and Vyverman, W. (2008a). Inter-annual variability in phytoplankton summer blooms in the freshwater tidal reaches of the Schelde estuary (Belgium). *Estuarine, Coastal and Shelf Science*, 79(4) :694–700.

Lionard, M., Muylaert, K., Tackx, M., and Vyverman, W. (2008b). Evaluation of the performance of HPLC–CHEMTAX analysis for determining phytoplankton biomass and composition in a turbid estuary (Schelde, Belgium). *Estuarine, Coastal and Shelf Science*, 76(4) :809–817.

Livingston, G. P. and Hutchinson, G. L. (1995). Enclosure-based measurement of trace gas exchange. In *Biogenic Trace Gases : Measuring Emissions from Soil and Water*. Blackwell Science Ltd.

Ludwig, W., Bouwman, A. F., Dumont, E., and Lespinas, F. (2010). Water and nutrient fluxes from major Mediterranean and Black Sea rivers : Past and future trends and their implications for the basin-scale budgets. *Global Biogeochemical Cycles*, 24.

Luu, T., Garnier, J., Billen, G., Le, T., Nemery, J., Orange, D., and Le, L. (2012). N, P, Si budgets for the Red River Delta (northern Vietnam) : how the delta affects river nutrient delivery to the sea. *Biogeochemistry*, 107(1) :241–259.

Maes, F., Schrijvers, J., and Vanhulle, A. (2005). *A Flood of Space. Towards a Spatial structure Plan for the Sustainable Management of the North Sea*. Belgian Science Policy.

Maguire, R. O. and Sims, J. T. (2002). Soil Testing to Predict Phosphorus Leaching. *Journal of Environment Quality*, 31(5) :1601.

Manassaram, D., Backer, L., and Moll, D. (2006). A review of nitrates in drinking water : Maternal exposure and adverse reproductive and developmental outcomes. *Environmental Health Perspectives*, 114(3) :320–327.

Maréchal, D. (2004). *A soil-based approach to rainfall-runoff modelling in ungauged catchments for England and Wales*. PhD thesis, Cranfield University, Cranfield, United Kingdom.

Marsh, T. J. (2001). Climate change and hydrological stability : A look at long-term trends in south-eastern britain. *Weather*, 56(10) :319–326.

Martin-Jézéquel, V., Hildebrand, M., and Brzezinski, M. A. (2000). Silicon metabolism in diatoms : implications for growth. *Journal of Phycology*, 36(5) :821–840.

Massei, N., Laignel, B., Deloffre, J., Mesquita, J., Motelay, A., Lafite, R., and Durand, A. (2010). Long-term hydrological changes of the seine river flow (france) and their relation to the north atlantic oscillation over the period 1950–2008. *International Journal of Climatology*, 30(14) :2146–2154.

Matthews, R., Wassmann, R., and Arah, J. (2000). Using a Crop/Soil Simulation Model and GIS Techniques to Assess Methane Emissions from Rice Fields in Asia. I. Model Development. *Nutrient Cycling in Agroecosystems*, 58(1) :141–159.

McClain, M. E., Boyer, E. W., Dent, C. L., Gergel, S. E., Grimm, N. B., Groffman, P. M., Hart, S. C., Harvey, J. W., Johnston, C. A., Mayorga, E., McDowell, W. H., and Pinay, G. (2003). Biogeochemical hot spots and hot moments at the interface of terrestrial and aquatic ecosystems. *Ecosystems*, 6(4) :301–312.

McKee, B., Aller, R., Allison, M., Bianchi, T., and Kineke, G. (2004). Transport and transformation of dissolved and particulate materials on continental margins influenced by major rivers : benthic boundary layer and seabed processes. *Continental Shelf Research*, 24(7–8) :899–926.

Mégnien, C. (1979). *Hydrogéologie du centre du bassin de Paris : contribution à l'étude de quelques aquifères principaux*. Mémoires du BRGM (Paris), ISSN 0071-8246 ; 98. Éditions du B.R.G.M., [Paris.

Meire, P., Ysebaert, T., Damme, S. V., Bergh, E. V. d., Maris, T., and Struyf, E. (2005). The Scheldt estuary : a description of a changing ecosystem. *Hydrobiologia*, 540(1) :1–11.

Melun, G. (2012). *Évaluation des impacts hydromorphologiques du rétablissement de la continuité hydro-sédimentaire et écologique sur l'Yerres aval*. PhD thesis, Université Paris 7 Denis Diderot, Paris.

Ménesguen, A. (2001). L'eutrophisation des eaux marines et saumâtres en Europe, en particulier en France. Technical Report DEL/EC/01.02, IFREMER.

Ménesguen, A. (2003). Les "marées vertes" en Bretagne, la responsabilité du nitrate. Synthèse, IFREMER, Plouzané, Bretagne, France.

Merot, P., Squividant, H., Aurousseau, P., Hefting, M., Burt, T., Maitre, V., Kruk, M., Butturini, A., Thenail, C., and Viaud, V. (2003). Testing a climato-topographic index for predicting wetlands distribution along an European climate gradient. *Ecological Modelling*, 163(1-2) :51–71.

Meybeck, M., Dürr, H., Roussennac, S., and Ludwig, W. (2007). Regional seas and their interception of riverine fluxes to oceans. *Marine Chemistry*, 106(1–2) :301–325.

Meyer, S., Reeb, C., and Bosdeveix, R. (2008). *Botanique : Biologie et physiologie végétales*. Maloine, 2e édition edition.

Mialet, B., Gouzou, J., Azémar, F., Maris, T., Sossou, C., Toumi, N., Van Damme, S., Meire, P., and Tackx, M. (2011). Response of zooplankton to improving water quality in the Scheldt estuary (Belgium). *Estuarine, Coastal and Shelf Science*, 93(1) :47–57.

Mignolet, C., Schott, C., and Benoît, M. (2007). Spatial dynamics of farming practices in the Seine basin : Methods for agronomic approaches on a regional scale. *Science of the Total Environment*, 375(1-3) :13–32.

Mitsch, W., Day, J., Zhang, L., and Lane, R. (2005a). Nitrate-nitrogen retention in wetlands in the Mississippi river basin. *Ecological Engineering*, 24(4) :267–278.

Mitsch, W. J. and Gosselink, J. G. (2000). The value of wetlands : importance of scale and landscape setting. *Ecological Economics*, 35(1) :25–33.

Mitsch, W. J., Zhang, L., Anderson, C. J., Altor, A. E., and Hernandez, M. E. (2005b). Creating riverine wetlands : Ecological succession, nutrient retention, and pulsing effects. *Ecological Engineering*, 25(5) :510–527.

Montagnini, F. and Nair, P. (2004). Carbon sequestration : An underexploited environmental benefit of agroforestry systems. *Agroforestry Systems*, 61-62(1) :281–295.

Moriasi, D. N., Arnold, J. G., Van Liew, M. W., Bingner, R. L., Harmel, R. D., and Veith, T. L. (2007). Model evaluation guidelines for systematic quantification of accuracy in watershed simulations.

Mouchel, J., Boêt, P., Hubert, G., and Guerrini, M. (2000). Un bassin et des hommes : une histoire tourmentée. In *La Seine en son bassin : Fonctionnement écologique d'un système fluvial anthropisé*, pages 77–125. Elsevier France.

Muller-Karulis, B. and Aigars, J. (2011). Modeling the long-term dynamics of nutrients and phytoplankton in the Gulf of Riga. *Journal of Marine Systems*, 87(3-4) :161–176.

Muscutt, A., Harris, G., Bailey, S., and Davies, D. (1993). Buffer zones to improve water quality : a review of their potential use in UK agriculture. *Agriculture, Ecosystems & Environment*, 45(1–2) :59–77.

Muylaert, K., Sabbe, K., and Vyverman, W. (2000). Spatial and Temporal Dynamics of Phytoplankton Communities in a Freshwater Tidal Estuary (Schelde, Belgium). *Estuarine, Coastal and Shelf Science*, 50(5) :673–687.

Muylaert, K., Sabbe, K., and Vyverman, W. (2009). Changes in phytoplankton diversity and community composition along the salinity gradient of the Schelde estuary (Belgium/The Netherlands). *Estuarine, Coastal and Shelf Science*, 82(2) :335–340.

Nahlik, A. M. and Mitsch, W. J. (2010). Methane Emissions From Created Riverine Wetlands. *Wetlands*, 30(4) :783–793.

Nedwell, D., Dong, L., Sage, A., and Underwood, G. (2002). Variations of the nutrients loads to the mainland U.K. estuaries : Correlation with catchment areas, urbanization and coastal eutrophication. *Estuarine, Coastal and Shelf Science*, 54(6) :951–970.

Neitsch, S. L., Arnold, J. G., Kiniry, J. R., and Williams, J. R. (2005). *Soil and Water Assessment Tool (SWAT), Theoretical Documentation.* Blackland Research Center, Grassland. Soil and Water Research Laboratory, Agricultural Research Service, Temple.

Nelson, W. M., Gold, A. J., and Groffman, P. M. (1995). Spatial and temporal variation in groundwater nitrate removal in a riparian forest. *Journal of Environmental Quality*, 24(4) :691–699.

Nielsen, D. L., Brock, M. A., Rees, G. N., and Baldwin, D. S. (2003). Effects of increasing salinity on freshwater ecosystems in Australia. *Aust. J. Bot.*, 51(6) :655–665.

Nixon, S., Ammerman, J., Atkinson, L., Berounsky, V., Billen, G., Boicourt, W., Boynton, W., Church, T., Ditoro, D., Elmgren, R., Garber, J., Giblin, A., Jahnke, R., Owens, N., Pilson, M., and Seitzinger, S. (1996). The fate of nitrogen and phosphorus at the land-sea margin of the north atlantic ocean. *Biogeochemistry*, 35(1) :141–180.

Nixon, S. and Buckley, B. (2002). A strikingly rich zone — Nutrient enrichment and secondary production in coastal marine ecosystems. *Estuaries and Coasts*, 25(4) :782–796.

Némery, J. and Garnier, J. (2007). Origin and fate of phosphorus in the Seine watershed (France) : Agricultural and hydrographic P budgets. *Journal of Geophysical Research-Biogeosciences*, 112(G3).

Oertli, B., Joye, D. A., Castella, E., Juge, R., Cambin, D., and Lachavanne, J. B. (2002). Does size matter ? The relationship between pond area and biodiversity. *Biological Conservation*, 104(1) :59–70.

Officer, C. B. and Ryther, J. H. (1980). The possible importance of silicon in marine eutrophication. *Marine Ecology*, 3 :83–91.

Onclincx, F. (1991). Les entreprises de Blanchiment, de teinture et d'impression sur étoffe à Anderlecht, Forest et Uccle entre 1830 et 1870. Mémoire, Université Libre de Bruxelles, Bruxelles.

Ouattara, N. K., de Brauwere, A., Billen, G., and Servais, P. (2012). Modelling faecal contamination in the scheldt land–sea continuum. part i. the scheldt drainage network. *Journal of Marine Systems*, (0).

Paerl, H. W., Valdes, L. M., Peierls, B. L., Adolf, J. E., and Harding, L. W. (2006). Anthropogenic and Climatic Influences on the Eutrophication of Large Estuarine Ecosystems. *Limnology and Oceanography*, 51(1) :448–462.

Palone, R. and Todd, A. (1998). *Chesapeake Bay Riparian Handbook : A Guide for Establishing and Maintaining Riparian Forest Buffers.*

Parton, W. J., Hartman, M., Ojima, D., and Schimel, D. (1998). DAYCENT and its land surface submodel : description and testing. *Global and Planetary Change*, 19(1–4) :35–48.

Parton, W. J., Holland, E. A., Grosso, S. J. D., Hartman, M. D., Martin, R. E., Mosier, A. R., Ojima, D. S., and Schimel, D. S. (2001). Generalized model for NO x and N2O emissions from soils. *Journal of Geophysical Research*, 106(D15) :17403–17,419.

Parton, W. J., Mosier, A. R., Ojima, D. S., Valentine, D. W., Schimel, D. S., Weier, K., and Kulmala, A. E. (1996). Generalized model for N2 and N2O production from nitrification and denitrification. *Global Biogeochemical Cycles*, 10(3) :401–412.

Passy, P., Garnier, J., Billen, G., Fesneau, C., and Tournebize, J. (2012). Restoration of ponds in rural landscapes : Modelling the effect on nitrate contamination of surface water (the Seine River Basin, France). *Science of the Total Environment.*

Pedersen, M., Kristensen, E., Kronvang, B., and Thodsen, H. (2009). Ecological effects of re-introduction of salmonid spawning gravel in lowland danish streams. *River Research and Applications*, 25(5) :626–638.

Pelletier, M. (1990). *La carte de Cassini : L'extraordinaire aventure de la carte de France.* Presses de l'École Nationale des Ponts et Chaussées.

Penna, N., Capellacci, S., and Ricci, F. (2004). The influence of the Po River discharge on phytoplankton bloom dynamics along the coastline of Pesaro (Italy) in the Adriatic Sea. *Marine Pollution Bulletin*, 48(3-4) :321–326.

Pennock, D., Zebarth, B., and De Jong, E. (1987). Landform classification and soil distribution in hummocky terrain, Saskatchewan, Canada. *Geoderma*, 40(3–4) :297–315.

Pennock, D. J. (2005). Precision conservation for co-management of carbon and nitrogen on the Canadian prairies. *Journal of Soil and Water Conservation*, 60(6) :396–401.

Pennock, D. J., Farrell, R. E., Sutherland, R. A., and van Kessel, C. (1992). Landscape-Scale Variations in Denitrification. *Soil Science Society of America Journal*, 56(3) :770–776.

Pennock, D. J., van Kessel, C., and Farrell, R. E. (1993). Seasonal Variations in Denitrification and Nitrous Oxide Evolution at the Landscape Scale. *Soil Science Society of America Journal*, 57(4) :988–995.

Penven, M.-J., Muxart, T., Bartoli, F., Bonté, P., Brunstein, D., Cosandey, C., Gouy, V., Irace, S., Leviandier, T., and Sogon, S. (2000). Petits bassins ruraux et pollutions diffuses. In *La Seine en son bassin : Fonctionnement écologique d'un système fluvial anthropisé*, pages 159–210. Elsevier France.

Peperzak, L. (2002). *The wax and wane of Phaeocystis globosa blooms*. PhD thesis, University of Groninge, Groninge, the Netherlands.

Pichon, C. L., Gorges, G., Boët, P., Baudry, J., Goreaud, F., and Faure, T. (2006). A Spatially Explicit Resource-Based Approach for Managing Stream Fishes in Riverscapes. *Environmental Management*, 37(3) :322–335.

Pinay, G., Black, V., Planty-Tabacchi, A., Gumiero, B., and Decamps, H. (2000). Geomorphic control of denitrification in large river floodplain soils. *Biogeochemistry*, 50(2) :163–182.

Pinay, G., CL&#x000C9 ;MENT, J. C., and Naiman, R. J. (2002). Basic Principles and Ecological Consequences of Changing Water Regimes on Nitrogen Cycling in Fluvial Systems. *Environmental Management*, 30 :481–491.

Pinay, G., Decamps, H., Arles, C., and Lacassinseres, M. (1989). Topographic Influence on Carbon and Nitrogen Dynamics in Riverine Woods. *Archiv Fur Hydrobiologie*, 114(3) :401–414.

Pinay, G. and Trémolières, E. (2002). La rétention et l'élimination de l'azote. In *Fonctions et valeurs des zones humides*, pages 129–142. Dunod, Paris.

Pinckney, J. L., Paerl, H. W., and Harrington, M. B. (1999). Responses of the phytoplankton community growth rate to nutrient pulses in variable estuarine environments. *Journal of Phycology*, 35(6) :1455–1463.

Pitte, J.-R. (2012). *Histoire du paysage français : De la préhistoire à nos jours*. Tallandier, 5e édition edition.

Plant, R. (1999). *Effects of land use on regional nitrous oxide emissions in the humid tropics of Costa Rica*. PhD thesis, Department of Environmental Sciences, Wageningen Agricultural University, Wageningen, The Netherlands.

Poitevin, J. (1997). Les contrats de nappes : Une nouvelle approche de la gestion des eaux souterraines pour un développement durable. Technical report, Institut d'Aménagement et d'Urbanisme de la région Ile de France, Paris, France.

Pomerol, C. (1986). *Guides géologiques : Bassin de Paris - Ile-de-France, Pays de Bray*. Masson.

Pomerol, C. (2000). *Découverte géologique de Paris et de l'Île-de-France*. Editions du BRGM.

Prigent, C., Papa, F., Aires, F., Jimenez, C., Rossow, W. B., and Matthews, E. (2012). Changes in land surface water dynamics since the 1990s and relation to population pressure. *Geophysical Research Letters*, 39(8) :L08403.

Privat-Deschanel, A. and Focillon, A. J. (1880). *Dictionnaire général des sciences théoriques et appliquées ...* C. Delagrave.

Puissant, J. and de Beule, M. (1989). La première région industrielle belge. In *La Région de Bruxelles : des villages d'autrefois à la ville d'aujourd'hui*, pages 262–291. Crédit Communal, Bruxelles.

Quinlan, E. L. and Phlips, E. J. (2007). Phytoplankton assemblages across the marine to low-salinity transition zone in a blackwater dominated estuary. *Journal of Plankton Research*, 29(5) :401–416.

Quynh, L. T. P. (2005). *Fonctionnement biogéochimique du Fleuve Rouge (Nord-Vietnam) : Bilans et modélisation*. PhD thesis, Université Pierre et Marie Curie & Académie de la Science et de la technologie du Vietnam, Paris.

Quynh, L. T. P., Billen, G., Garnier, J., Théry, S., Fézard, C., and Minh, C. V. (2005). Nutrient (N, P) budgets for the Red River basin (Vietnam and China). *Global Biogeochemical Cycles*, 19(2) :GB2022.

Rabalais, N. N., Diaz, R. J., Levin, L. A., Turner, R. E., Gilbert, D., and Zhang, J. (2010). Dynamics and distribution of natural and human-caused hypoxia. *Biogeosciences*, 7(2) :585–619.

Redfield, A. C., Ketchum, B. H., and Richards, F. A. (1963). The influence of organisms on the composition of sea-water. In *The sea*, pages 12–37. M. N. Hill, New York.

Regnier, P., Wollast, R., and Steefel, C. (1997). Long-term fluxes of reactive species in macrotidal estuaries : Estimates from a fully transient, multicomponent reaction-transport model. *Marine Chemistry*, 58(1–2) :127–145.

Roberts, G. and Marsh, T. (1987). The effects of agricultural practices on the nitrate concentrations in the surface water domestic supply sources of western europe. *Institute for Agronomical and Hydrological Studies Publication*, (164) :365–380.

Rolston, D. E. and Folorunso, O. A. (1984). Spatial Variability of Field-Measured Denitrification Gas Fluxes. *Soil Science Society of America Journal*, 48(6) :1214–1219.

Roubeix, V. and Lancelot, C. (2008). Effect of salinity on growth, cell size and silicification of an euryhaline freshwater diatom Cyclotella Meneghiniana Kutz. *Transitional waters Bulletin*, 1 :31–38.

Roubeix, V., Rousseau, V., and Lancelot, C. (2008). Diatom succession and silicon removal from freshwater in estuarine mixing zones : From experiment to modelling. *Estuarine, Coastal and Shelf Science*, 78(1) :14–26.

Rouillard, J., Benoit, P., and Morera, R. (2011). L'eau dans les campagnes du bassin de la Seine avant l'ère industrielle, Comprendre les paysages d'aujourd'hui. Technical Report 10, PIREN-Seine, Paris.

Rousseau, V., Billen, E., and De Becker, E. (1986). Etude de la contamination azotée des eaux souterraines et de surface dans le bassin de la dyle à wavre. Etude pour le ministère de la région wallonne pour l'Eau, l'Environnement et la vie rurale, Ministère de la Région Wallonne pour l'Eau, l'Environnement et la vie rurale, Brussels, Belgium.

Rousseau, V., Lancelot, C., and Cox, D. (2006). *Current Status of Eutrophication of the Belgian Coastal Zone*. Presses Universitaires de Bruxelles, Bruxelles.

Rousseau, V., Leynaert, A., Daoud, N., and Lancelot, C. (2002). Diatom succession, silicification and silicic acid availability in Belgian coastal waters (Southern North Sea) RID A-4211-2010. *Marine Ecology-Progress Series*, 236 :61–73.

Rousseau, V., Vaulot, D., Casotti, R., Cariou, V., Lenz, J., Gunkel, J., and Baumann, M. (1994). The life cycle of Phaeocystis (Prymnesiophycaea) : evidence and hypotheses. *Journal of Marine Systems*, 5(1) :23–39.

Ruddick, K. and Lacroix, G. (2006). Hydrodynamics and meteorology of the Belgian Coastal Zone. In *Current Status of Eutrophication in the Belgian Coastal Zone*, pages 1–16. Presses Universitaires de Bruxelles.

Ruelland, D., Billen, G., Brunstein, D., and Garnier, J. (2007). SENEQUE : A multi-scaling GIS interface to the Riverstrahler model of the biogeochemical functioning of river systems. *Science of the Total Environment*, 375(1-3) :257–273.

Ruiz-Ramos, M., Gabriel, J. L., Vazquez, N., and Quemada, M. (2011). Evaluation of nitrate leaching in a vulnerable zone : effect of irrigation water and organic manure application. *Spanish Journal of Agricultural Research*, 9(3) :924–937.

Sabater, S., Butturini, A., Clement, J.-C., Burt, T., Dowrick, D., Hefting, M., Matre, V., Pinay, G., Postolache, C., Rzepecki, M., and Sabater, F. (2003). Nitrogen Removal by Riparian Buffers along a European Climatic Gradient : Patterns and Factors of Variation. *Ecosystems*, 6 :20–30.

Sanchez, N. and Garnier, J. (1997). *Le processus de dénitrification dans les sédiments du barrage-réservoir de la Marne : Etude de sa cinetique et modélisation = The denitrification process in sédiments of the Marne Reservoir : Study of its kinetic and modelling*. Text, Pierre et Marie Curie, Paris.

Sanders, R., Jickells, T., Malcolm, S., Brown, J., Kirkwood, D., Reeve, A., Taylor, J., Horrobin, T., and Ashcroft, C. (1997). Nutrient fluxes through the humber estuary. *Journal of Sea Research*, 37(1–2) :3–23.

Saunders, D. and Kalff, J. (2001). Nitrogen retention in wetlands, lakes and rivers. *Hydrobiologia*, 443(1-3) :205–212.

Schimel, D. S. and Potter, C. S. (1995). Process modelling and spatial extrapolation. In *Biogenic Trace Gases : Measuring Emissions from Soil and Water*, pages 358–384. Blackwell Science Ltd.

Schmit, C., Rounsevell, M., and La Jeunesse, I. (2006). The limitations of spatial land use data in environmental analysis. *Environmental Science & Policy*, 9(2) :174–188.

Schott, C., Mignolet, C., and Benoît, M. (2009). Agriculture du bassin de la Seine, Découvrir l'agriculture du bassin de la Seine pour comprendre les enjeux de la gestion de l'eau. Technical Report 5, PIREN-Seine, Paris.

Schultz, R. C., Isenhart, T. M., Colletti, J. P., Simpkins, W. W., Udawatta, R. P., and Schultz, P. L. (2009). Riparian and upland buffer practices. In *North American Agroforestry : An Integrated Science & Practice*, pages 163–218. Amer Society of Agronomy.

Sebilo, M. (2003). *Utilisation du traçage isotopique naturel pour caractériser et quantifier les processus de nitrification et de dénitrification à l'échelle du réseau hydrographique de la Seine*. PhD thesis, Paris VI, Paris.

Sebilo, M., Billen, G., Grably, M., and Mariotti, A. (2003). Isotopic composition of nitrate-nitrogen as a marker of riparian and benthic denitrification at the scale of the whole Seine River system. *Biogeochemistry*, 63(1) :35–51.

Seitzinger, S. P. (1988). Denitrification in Freshwater and Coastal Marine Ecosystems : Ecological and Geochemical Significance. *Limnology and Oceanography*, 33(4) :702–724.

Seitzinger, S. P., Mayorga, E., Bouwman, A. F., Kroeze, C., Beusen, A. H. W., Billen, G., Van Drecht, G., Dumont, E., Fekete, B. M., Garnier, J., and Harrison, J. A. (2010). Global river nutrient export : A scenario analysis of past and future trends RID F-2280-2011. *Global Biogeochemical Cycles*, 24.

Servais, P., Garnier, J., Demarteau, N., Brion, N., and Billen, G. (1999). Supply of organic matter and bacteria to aquatic ecosystems through waste water effluents. *Water Research*, 33(16) :3521–3531.

Sessa, C. (2012a). Building a new Science - Citizens - Policy interface : theoretical foundations. In *Sustainable Water Ecosystems Management in Europe, Bridging the Knowledge of Citizens, Scientists and Policy Makers*, pages 31–40. Community research, Londres, IWA edition.

Sessa, C. (2012b). *Sustainable Water Ecosystems Management in Europe, Bridging the Knowledge of Citizens, Scientists and Policy Makers*. Community research, Londres, IWA edition.

Sferratore, A., Garnier, J., Billen, G., Conley, D. J., and Pinault, S. (2006). Diffuse and point sources of silica in the seine river watershed. *Environmental Science & Technology*, 40(21) :6630–6635.

Sha, C., Wang, T., and Lu, J. (2010). Relative Sensitivity of Wetland Plants to SO(2) Pollution. *Wetlands*, 30(6) :1023–1030.

Shen, L., Xu, H., Guo, X., and Wu, P. (2012). Oceanography of Skeletonema costatum harmful algal blooms in the East China Sea using MODIS and QuickSCAT satellite data. *Journal of Applied Remote Sensing*, 6.

Silvestre, M., Billen, G., and Garnier, J. (2012). Amstram, une application de webmapping basée sur les statistiques de transport et de production permettant d'évaluer la provenance des marchandises.

Skaloud, P., Rezacova, M., and Ellegaard, M. (2006). Spatial distribution of Phytoplankton in spring 2004 along a transect in the eastern part of the North Sea. *Journal of Oceanography*, 62(5) :717–729.

Skiba, U., Sheppard, L., Macdonald, J., and Fowler, D. (1998). Some key environmental variables controlling nitrous oxide emissions from agricultural and semi-natural soils in Scotland. *Atmospheric Environment*, 32(19) :3311–3320.

Slawyk, G. and MacIsaac, J. J. (1972). Comparison of two automated ammonium methods in a region of coastal upwelling. *Deep Sea Research and Oceanographic Abstracts*, 19(7) :521–524.

Smil, V. (2004). *Enriching the Earth : Fritz Haber, Carl Bosch, and the Transformation of World Food Production*. MIT Press.

Smith, K., Thomson, P., Clayton, H., Mctaggart, I., and Conen, F. (1998). Effects of temperature, water content and nitrogen fertilisation on emissions of nitrous oxide by soils. *Atmospheric Environment*, 32(19) :3301–3309.

Smith, S. V., Renwick, W. H., Bartley, J. D., and Buddemeier, R. W. (2002). Distribution and significance of small, artificial water bodies across the United States landscape. *The Science of The Total Environment*, 299(1-3) :21–36.

Soetaert, K. and Herman, P. (1995). Nitrogen dynamics in the Westerschelde estuary (SW Netherlands) estimated by means of the ecosystem model MOSES. *Hydrobiologia*, 311(1) :225–246.

Soetaert, K., Middelburg, J. J., Heip, C., Meire, P., Van Damme, S., and Maris, T. (2006). Long-term change in dissolved inorganic nutrients in the heterotrophic Scheldt estuary (Belgium, The Netherlands). *Limnology and Oceanography*, 51(1) :409–423.

Soyer, R. and Cailleux, A. (1964). *Géologie de la Région Parisienne*. Number 854 in Que sais-je ? Presses Universitaires de France, Paris, 2e éd. edition.

Spinelli, R., Nati, C., and Magagnotti, N. (2006). Biomass harvesting from buffer strips in Italy : three options compared. *Agroforestry Systems*, 68(2) :113–121.

Srinivasan, R., Arnold, J. G., and Jones, C. A. (1998). Hydrologic modelling of the united states with the soil and water assessment tool. *International Journal of Water Resources Development*, 14(3) :315–325.

Stålnacke, P., Bryhn, A., Håkanson, L., Nagothu, U. S., and Veidemane, K. (2009). The Gulf of Riga Case Study : Inception Report. Synthèse 1.2.1, Bioforsk.

Stålnacke, P., Nagothu, U. S., and Quevauviller, C. (2012). Developping the science - policy interface to integrate water research and management. In *Sustainable Water Ecosystems Management in Europe, Bridging the Knowledge of Citizens, Scientists and Policy Makers*, pages 7–14. Community research, Londres, IWA edition.

Statham, P. J. (2012). Nutrients in estuaries — an overview and the potential impacts of climate change. *Science of The Total Environment*, 434(0) :213–227.

Strahler, A. (1957). Quantitative analysis of watershed geomorphology. *Transactions, American Geophysical Union*, 38(6) :913–920.

Strebel, O., Duynisveld, W., and Böttcher, J. (1989). Nitrate pollution of groundwater in western europe. *Agriculture, Ecosystems & Environment*, 26(3–4) :189–214.

Sutton, M. A., Howard, C. M., Willem Erisman, J., Billen, G., Bleeker, A., Grennfelt, P., van Grinsven, H., and Grizzetti, B. (2011). *The European Nitrogen Assessment : Sources, Effects and Policy Perspectives*. Cambridge University Press, Cambridge, UK.

Taylor, T. and Longo, A. (2010). Valuing algal bloom in the Black Sea Coast of Bulgaria : A choice experiments approach. *Journal of Environmental Management*, 91(10) :1963–1971.

Theobald, M. R., Bealey, W. J., Tang, Y. S., Vallejo, A., and Sutton, M. A. (2009). A simple model for screening the local impacts of atmospheric ammonia. *Science of the Total Environment*, 407(23) :6024–6033.

Thieu, V. (2009). *Modélisation spatialisée des flux de nutriments (N, P, Si) des bassins de la Seine, de la Somme et de l'Escaut : impact sur l'eutrophisation de la Manche et de la Mer du Nord*. PhD thesis, Université Pierre et Marie Curie.

Thieu, V., Billen, G., and Garnier, J. (2009). Nutrient transfer in three contrasting NW European watersheds : The Seine, Somme, and Scheldt Rivers. A comparative application of the Seneque/Riverstrahler model. *Water Research*, 43(6) :1740–1754.

Thieu, V., Billen, G., Garnier, J., and Benoît, M. (2011). Nitrogen cycling in a hypothetical scenario of generalised organic agriculture in the Seine, Somme and Scheldt watersheds. *Regional Environmental Change*, 11(2) :359–370.

Thieu, V., Garnier, J., and Billen, G. (2010). Assessing the effect of nutrient mitigation measures in the watersheds of the Southern Bight of the North Sea. *Science of the Total Environment*, 408(6) :1245–1255.

Thouvenot, M., Billen, G., and Garnier, J. (2007). Modelling nutrient exchange at the sediment-water interface of river systems. *Journal of Hydrology*, 341(1-2) :55–78.

Thouvenot, M., Karvonen, T., and Granlund, K. (2006). Modelling various forms of nitrogen and their behaviour in a small agricultural catchment in Southern Finland - Part II : Nitrogen processes in rivers. In Jones, J., editor, *International Association of Theoretical and Applied Limnology, Vol 29, Pt 4, Proceedings*, volume 29, pages 2006–2008. E Schweizerbart'sche Verlagsbuchhandlung, Stuttgart.

Tilman, D., Cassman, K. G., Matson, P. A., Naylor, R., and Polasky, S. (2002). Agricultural sustainability and intensive production practices. *Nature*, 418(6898) :671–677.

Tomaszek, J. A. and Czerwieniec, E. (2000). In situ chamber denitrification measurements in reservoir sediments : an example from southeast Poland. *Ecological Engineering*, 16(1) :61–71.

Tournebize, J., Arlot, M., Billy, C., Birgand, F., Gillet, J., and Dutertre, A. (2008). Quantification et maîtrise des flux de nitrates : de la parcelle drainée au bassin versant. *Ingénieries EAT spécial Azote, phosphates et pesticides. Stratégies et perspectives de réduction des flux*.

Touzery, M. (1998). *Atlas de la généralité de Paris au XVIIIe siècle : Un paysage retrouvé*. Comité pour l'Histoire Economique et Financière de la France - CHEEF.

Trainer, V. L., Bates, S. S., Lundholm, N., Thessen, A. E., Cochlan, W. P., Adams, N. G., and Trick, C. G. (2012). Pseudo-nitzschia physiological ecology, phylogeny, toxicity, monitoring and impacts on ecosystem health. *Harmful Algae*, 14 :271–300.

Turner, R., Rabalais, N., Swenson, E., Kasprzak, M., and Romaire, T. (2005). Summer hypoxia in the northern Gulf of Mexico and its prediction from 1978 to 1995. *Marine Environmental Research*, 59(1) :65–77.

Turrell, W., Henderson, E., Slesser, G., Payne, R., and Adams, R. (1992). Seasonal changes in the circulation of the northern North Sea. *Continental Shelf Research*, 12(2-3) :257–286.

Udawatta, R. P., Krstansky, J. J., Henderson, G. S., and Garrett, H. E. (2002). Agroforestry Practices, Runoff, and Nutrient Loss. *Journal of Environment Quality*, 31(4) :1214.

Uitz, J., Stramski, D., Gentili, B., D'Ortenzio, F., and Claustre, H. (2012). Estimates of phytoplankton class-specific and total primary production in the Mediterranean Sea from satellite ocean color observations. *Global Biogeochemical Cycles*, 26.

Van Damme, S., Frank, D., Micky, T., Olivier, B., Eric, S., Britta, G., Oswald, V. C., and Patrick, M. (2009). Tidal exchange between a freshwater tidal marsh and an impacted estuary : the scheldt estuary, belgium. *Estuarine, Coastal and Shelf Science*, 85(2) :197–207.

Van Damme, S., Struyf, E., Maris, T., Ysebaert, T., Dehairs, F., Tackx, M., Heip, C., and Meire, P. (2005). Spatial and temporal patterns of water quality along the estuarine salinity gradient of the Scheldt estuary (Belgium and The Netherlands) : results of an integrated monitoring approach. *Hydrobiologia*, 540(1) :29–45.

van den Heuvel, R., Hefting, M., Tan, N., Jetten, M., and Verhoeven, J. (2009). N2O emission hotspots at different spatial scales and governing factors for small scale hotspots. *Science of The Total Environment*, 407(7) :2325–2332.

Van Noordwijk, M., Lawson, G., Soumare, A., Groot, J. J. R., and Hairiah, K. (1996). Root distribution of trees and crops : competition and/or complimentarity. In *Tree-Crop Interactions : A Physiological Approach*, pages 319–364. CABI Publishing.

Vandenberghe, C. (2010). Mise en relation de l'évolution de l'agriculture et de la qualité de l'eau entre 1950 et 2000. *Biotechnology Agronomy Society Environment*, 14(S1) :9–16.

Vanderborght, J., Wollast, R., Loijens, M., and Regnier, P. (2002). Application of a transport-reaction model to the estimation of biogas fluxes in the Scheldt estuary. *Biogeochemistry*, 59(1) :207–237.

Vanderborght, J.-P., Folmer, I. M., Aguilera, D. R., Uhrenholdt, T., and Regnier, P. (2007). Reactive-transport modelling of C, N, and O2 in a river–estuarine–coastal zone system : Application to the Scheldt estuary. *Marine Chemistry*, 106(1–2) :92–110.

vanOostrom, A. (1995). Nitrogen removal in constructed wetlands treating nitrified meat processing effluent. *Water Science and Technology*, 32(3) :137–147.

Verbanck, M., Vanderborght, J., and Wollast, R. (1994). Major ion content of urban wastewater : assessment of per capita loading. *Journal (Water Pollution Control Federation)*, 61 :1722–1728.

Verburg, P., van Bodegom, P., van der Gon, H., Bergsma, A., and van Breemen, N. (2006). Upscaling Regional Emissions of Greenhouse Gases from Rice Cultivation : Methods and Sources of Uncertainty. *Plant Ecology*, 182(1) :89–106.

Verhoff, F. H., Yaksich, S. M., and Melfi, D. A. (1980). River nutrient and chemical transport estimation. *Journal of the Environmental Engineering Division*, 106 :591–608.

Vervaeck, S., Vermeersch, A., Prevenier, W., Petit, R., Joosen, H., Hélin, E., Dumont, M. E., Roo, R. D., Bruwier, M., Bovesse, J., Scufflaire, A., and Dhondt, J. (1960). Bibliographie de l'histoire de Belgique — Bibliografie van de geschiedenis van België. 1959. *Revue belge de philologie et d'histoire*, 38(4) :1082–1186.

Viaroli, P., Giordani, G., Mocenni, C., Sparacino, E., Lovo, S., and Bencivelli, S. (2012). The Sacca di Goro : a cooperative decision making experiment for a sustainable lagoon exploitation. In *Sustainable Water Ecosystems Management in Europe, Bridging the Knowledge of Citizens, Scientists and Policy Makers*, pages 83–96. Community research, Londres, IWA edition.

Vidon, P. G. F. and Hill, A. R. (2004). Landscape controls on nitrate removal in stream riparian zones. *Water Resources Research*, 40 :14 PP.

Viennot, P., Ducharne, A., Habets, F., Lamy, F., and Ledoux, E. (2009a). Hydrogéologie du bassin de la Seine, Comprendre et anticiper le fonctionnement hydrodynamique du bassin pour une gestion durable de la ressource. Technical Report 2, PIREN-Seine, Paris.

Viennot, P., Ledoux, E., Monget, J.-M., Schott, C., Garnier, C., and Beaudoin, N. (2009b). La pollution du bassin de la Seine par les nitrates. Technical Report 3, PIREN-Seine, Paris.

Vilain, G., Garnier, J., Roose-Amsaleg, C., and Laville, P. (2012). Potential of denitrification and nitrous oxide production from agricultural soil profiles (Seine Basin, France). *Nutrient Cycling in Agroecosystems*, 92(1) :35–50.

Vilain, G., Garnier, J., Tallec, G., and Cellier, P. (2010). Effect of slope position and land use on nitrous oxide (N2O) emissions (Seine Basin, France). *Agricultural and Forest Meteorology*, 150(9) :1192–1202.

Vilain, G., Garnier, J., Tallec, G., and Tournebize, J. (2011). Indirect N2O emissions from shallow groundwater in an agricultural catchment (Seine Basin, France). *Biogeochemistry*, pages 1–19.

Völker, S. and Kistemann, T. (2011). The impact of blue space on human health and well-being - Salutogenetic health effects of inland surface waters : a review. *International journal of hygiene and environmental health*, 214(6) :449–460. PMID : 21665536.

Vollenweider, R. (1969). Possibilities and limits of elementary models concerning budget of substances in lakes. *Archiv fur Hydrobiologie*, 66(1) :1–12.

Vörösmarty, C. J., McIntyre, P. B., Gessner, M. O., Dudgeon, D., Prusevich, A., Green, P., Glidden, S., Bunn, S. E., Sullivan, C. A., Liermann, C. R., and Davies, P. M. (2010). Global threats to human water security and river biodiversity. *Nature*, 467(7315) :555–561.

Vymazal, J. (2011). Constructed Wetlands for Wastewater Treatment : Five Decades of Experience †. *Environmental Science & Technology*, 45(1) :61–69.

Wang, X. H., Yin, C. Q., and Shan, B. Q. (2005). The role of diversified landscape buffer structures for water quality improvement in an agricultural watershed, North China. *Agriculture, ecosystems & environment*, 107(4) :381–396.

Wanninkhof, R. (1992). Relationship Between Wind Speed and Gas Exchange Over the Ocean. *Journal of Geophysical Research*, 97(C5) :7373–7382.

Williams, P., Whitfield, M., Biggs, J., Bray, S., Fox, G., Nicolet, P., and Sear, D. (2004). Comparative biodiversity of rivers, streams, ditches and ponds in an agricultural landscape in Southern England. *Biological Conservation*, 115(2) :329–341.

Wollast, R. (1983). Interactions in estuaries and coastal waters. In *The major biogeochemical cycles and their interactions*, SCOPE 21, pages 385–407. Wiley-interscience edition.

Wollast, R. (1988). The Scheldt estuary. In *Pollution of the North Sea : an assessment*, pages 185–193. Springer.

Wright, R. F. (1983). Input-output budgets at Langtjern, a small acidified lake in southern Norway. *Hydrobiologia*, 101(1-2) :1–12.

Yan, W., Yin, C., and Tang, H. (1997). Nutrient Retention by Multipond Systems : Mechanisms for the Control of Nonpoint Source Pollution. *Journal of Environmental Quality*, 27(5) :1009–1017.

Zewei, C. (2007). Ces milliards perdus à cause de la pollution. *Courrier International*.

Zhu, Z., Zhang, J., Wu, Y., Zhang, Y., Lin, J., and Liu, S. (2011). Hypoxia off the Changjiang (Yangtze River) Estuary : Oxygen depletion and organic matter decomposition. *Marine Chemistry*, 125(1-4) :108–116.

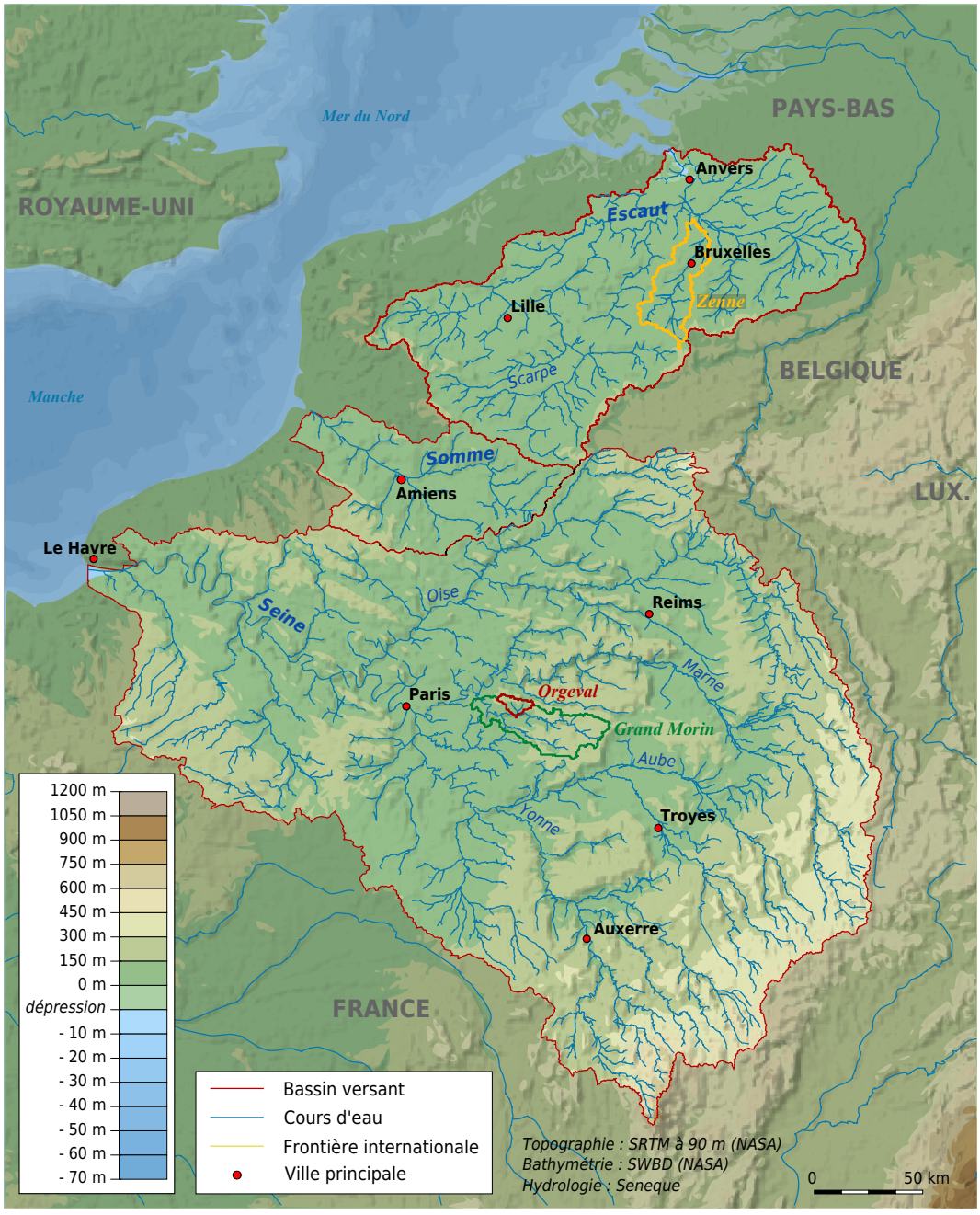

FIGURE 8.8 – Localisation des bassins du Grand Morin, de l'Orgeval et de la Zenne au sein des « 3S ».